Organometallic Reaction Mechanisms: Olefin Polymerization Catalysis and C-H Bond Activation by Early Transition Metal Bisphenolate Complexes and Protonolysis of Bipyrimidine Platinum Methyl Complexes

Thesis by
Suzanne R. Golisz

In Partial Fulfillment of the Requirements for the Degree of Doctor of Philosophy

Division of Chemistry and Chemical Engineering

California Institute of Technology
Pasadena, California
2010
(Defended May 24, 2010)

© 2010
Suzanne R. Golisz
All Rights Reserved

Dedicated to the memory of my grandparents,

Kathleen Pitterman
Joseph Pitterman
Mary Goliszewski
Joseph “Smiles” Goliszewski

Acknowledgements

I must first thank all of the lovely ladies who made the administrative aspects of graduate school very easy; Dian Buchness, Laura Howe, Agnes Tong, Anne Penney, Cece Manoochehri, and especially Pat Anderson who not only reminded me how to use the fax machine every time I forgot but also chatted with me about pencil skirts, pumps, and Ann Taylor.

Cora Carriedo, Carlos Rodriguez, Joseph Drew, Steven Gould, and Ronald Koen helped to ensure that I had all the chemicals and supplies I need to be successful.

Thank you to the two Mr. Fix-Its in the department, Thomas Dunn and Richard Gerhart, for always coming when called to Mead or Noyes and repairing all the J. Young NMR tubes I broke over the years.

The following people were instrumental in acquiring data; Mona Shahgholi and Naseem Torian for HRMS, David VanderVelde and Scott Ross for NMR, Scott Virgil for the Symyx robot, and Michael Day and Lawrence Henling for X-ray crystallography.

Thank you to my committee Harry Gray (Chair), David Tirrell, and Brian Stoltz for challenging me to be thorough in my ideas and research.

The former members of the Bercaw Group were incredibly helpful throughout my time at Caltech, especially Theodor Agapie for starting the bisphenolate project; Jeffery Byers for being my lab partner and teaching me high vacuum line techniques, olefin polymerization, and how to shoot a basketball; George Chen; Paul Elowe; Nilay Hazari; Sara Klamo for polymer analysis; Bo-Lin Lin; Josef Meier; Susan Schofer for initiating the Symyx collaboration; Travis Williams; Aaron Wilson; Jeffery Yoder; David

Weinberg for teaching me disc golf and oxygen diffusion rates; and Melanie Zimmerman.

My contemporaries in the Bercaw Group made my time in graduate school enjoyable and intellectually rewarding, especially Steven Baldwin for knowing the location of every piece of glassware in the lab and being the biggest Steeler fan in Pasadena; Ross Fu; Amaruka Hazari; Rachel Klet, my new lab partner and knitting circle member, for graciously washing my dishes and willingly discussing my personal and chemical problems; Valerie Scott Kristof; Yan Choi Lam; Taylor Lenton, knitting circle member, for indulging my political aspirations; Alex Miller for keeping me safe by keeping everyone else in line; Paul Oblad; Ian Tonks for taking over the Beamer Box; Ted Weintrob; Nathan West for helpful discussions on platinum chemistry; Matt Winston, knitting circle member, for getting me Peet's; and Sze-Man Yu.

My two advisors, Jay Labinger and John Bercaw, have been excellent to me throughout the years. I want to thank them for allowing me the freedom to explore the topics that interest me and giving brilliant advice when I got confused.

To my family, Mom, Dad, and Paul, for supporting me through all the years of my schooling, helping me to decide to come to Caltech, and understanding when I don't return phone calls.

None of this would have been possible without my future husband, Shane Arney. His love and support guided me through the ups and downs of graduate school.

Abstract

Mechanistic aspects of organometallic transformations such as polymerization, C-H activation, and protonolysis have been examined. Relationships between catalyst geometry and polymer microstructure were defined. The mechanism of an intramolecular C-H activation process was found to involve two competing pathways. The protonolysis of platinum methyl complexes was investigated for kinetic isotope effects and observation of intermediates.

Bisphenolate ligands with pyridine- and benzene-diyl linkers were synthesized and metalated with group 4 and 5 transition metals. The solid state structures of some of the group 4 complexes were solved. The titanium, zirconium, hafnium, and vanadium complexes were tested for propylene, 1-hexene, and ethylene/1-octene polymerization activities with methylaluminoxane as co-catalyst. Titanium and zirconium (IV) precatalysts with pyridine-diyl linkers provided mixtures of isotactic and atactic polypropylene while titanium (IV) precatalysts with benzene-diyl linkers gave atactic polypropylene only. The hafnium (IV) precatalyst with a pyridine-diyl linker generated moderately isotactic polypropylene.

A titanium dibenzyl complex featuring a ligand with two phenolates linked by a benzene-diyl was found to undergo thermal decomposition to give toluene and a cyclometalated dimeric complex. The thermal decomposition followed first order kinetics and was studied at a number of temperatures to determine the activation parameters. Deuterated isotopologs were synthesized to measure the kinetic isotope effects. The complexes with deuterium in the benzyl methylene positions decomposed slower than the protio analogs. Isotopologs of toluene with multiple deuteration positions

were observed in the product mixtures. These data are consistent with competing α-abstraction and σ-bond metathesis.

The protonolysis of bipyrimidine-ligated platinum (II) complexes was explored. The bipyrimidine platinum dimethyl complex (bpm)$PtMe_2$ was shown to undergo protonation at the metal upon addition of trifluoroacetic acid (tfa) to give a platinum (IV) hydride intermediate which reductively eliminated methane to give (bpm)PtMe(tfa). Using a mixture of deutero- and protio-acid, all isotopologs of methane were observed. The protonation of (bpm)PtMe(tfa) was less straightforward as no intermediates were found, and CH_4, CH_3D, and CH_2D_2 were observed upon addition of a mixture of deutero- and protio-acid. The protonation of a nitrogen of the bpm ligand was also examined and determined improbable under the present conditions.

Table of Contents

Introduction

The synthetic chemist thrives on the ability to take a seemingly simple molecule and create something more complex and more valuable. In general, substances which are readily available and highly abundant serve as the starting materials while the identity of the product is left to the imagination of the chemist (or market demands). Hydrocarbon feedstocks such as petroleum and natural gas have dominated the chemical industry for the last 50 years; not only because they have dramatic implications for the energy sector, but also because they represent plentiful precursors which the synthetic chemist can transform into value-added products.

Petroleum resources are primarily used for transportation;[1] however, energy intensive (700 °C) catalytic cracking of petroleum generates olefins such as ethylene and propylene. In the presence of a metal catalyst (or free radical initiator for ethylene) these olefins can be converted to polymers. Billions of pounds of polymer are produced each year for applications in every market sector of the economy. However, as the need for new materials emerges, new polymers must be created. In this direction, the synthetic chemist applies decades of knowledge[2-3] about the relationship between catalyst and polymer (Figure 1) to design new catalyst frameworks for the desired polymer architecture.

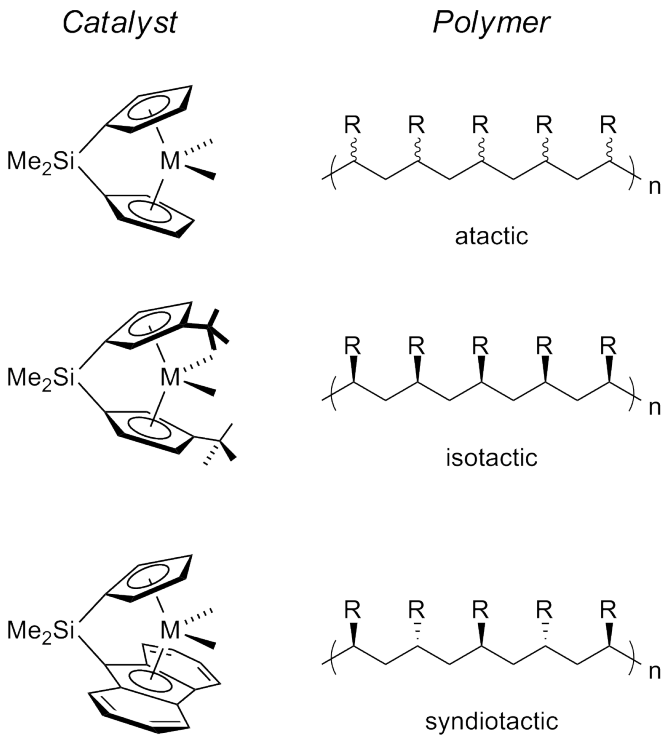

Figure 1. An illustration of the relationship between catalyst framework and polymer microstructure for generic metallocene catalysts and α-olefin polymers.

Non-metallocene ligands[4-11] (Figure 2) on early transition metals have been explored as new catalyst frameworks for the production of new types of polymers. The non-metallocene ligand described in Chapter One features two donating phenolate moieties connected by sp^2-sp^2 bonds *via* a central linker which could include a third donor group. Sterically diverse phenolates were synthesized along with two different central groups (2,6-pyridyl and benzene-1,3-diyl). These new catalysts were investigated at a fundamental level to understand how the geometry of the catalyst influenced the resulting polymer microstructure.

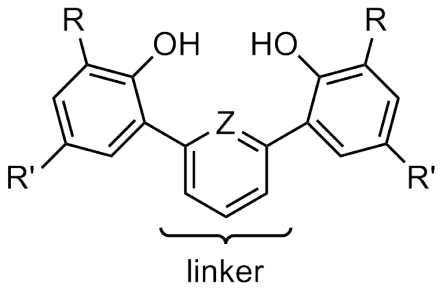

Figure 2. A schematic of the neutral non-metallocene bisphenolate ligand where R and R' = alkyl or aryl; linker = 2,6-pyridyl or benzene-1,3-diyl; Z = N (neutral) or C (neutral or anionic).

During the examination of the bisphenolate(benzene-1,3-diyl) titanium catalyst, an interesting cyclometalation reaction was discovered which involved the activation of the 2-C-H bond of the benzene-1,3-diyl linker. Similar reactivity has been observed with tantalum[5-6] and molybdenum[12] complexes. The mechanism of the titanium reaction was carefully studied to determine the elementary steps of the transformation. The findings of this research are described in Chapter Two.

As mentioned in the first paragraph, olefinic feedstocks for the production of polymers are not the only hydrocarbon of interest. Methane, a byproduct of the catalytic cracking of petroleum and the major component of natural gas, represents a chemical source which can be used in its natural form or converted to more useful products. Commercially, methane is combined with water in a steam reforming process to generate synthesis gas, a mixture of CO and H_2 (Eq 1). Synthesis gas can be converted to a variety of products including methanol (Eq 2). The ability to directly convert methane to methanol (Eq 3) is a highly desirable process not only because it eliminates the formation of synthesis gas but also because methanol is more easily transported than methane.

$$CH_4\ (g) + H_2O\ (g) \xrightarrow[\text{heat}]{[Ni]} CO\ (g) + 3\ H_2\ (g) \qquad \Delta H° = +49.3\ \text{kcal/mol} \qquad (1)$$

$$CO\ (g) + 2\ H_2\ (g) \xrightarrow[80\ \text{atm, } 250\ °C]{[Cu/ZnO/Al_2O_3]} CH_3OH\ (g) \qquad \Delta H° = -21.7\ \text{kcal/mol} \qquad (2)$$

$$CH_4\ (g) + 1/2\ O_2\ (g) \xrightarrow{catalyst?} CH_3OH\ (g) \qquad \Delta H° = -30.7\ \text{kcal/mol} \qquad (3)$$

Currently, no chemical company practices direct conversion of methane to methanol (Eq 3) due to the economic considerations of both the catalyst and the oxidant. The original report of a homogenous system for the partial oxidation of methane uses a platinum (II) catalyst and platinum (IV) oxidant (Eq 4).[13]

$$CH_4 + [PtCl_6]^{2-} + H_2O\ (Cl^-) \xrightarrow[H_2O,\ 120°C]{[PtCl_4]^{2-}} CH_3OH\ (CH_3Cl) + [PtCl_4]^{2-} + 2\ HCl \qquad (4)$$

The best system discovered to date, representing an improved catalyst and a less expensive oxidant, involves a bipyrimidine platinum dichloride ((bpm)$PtCl_2$) precatalyst that operates in fuming sulfuric acid with SO_3 as the oxidant (Eq 5). This system exhibits 90% conversion of methane to methyl bisulfate with 81% selectivity.[14]

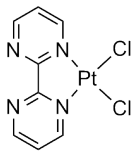

$$CH_4 + 2\ H_2SO_4 \xrightarrow[220°C]{} CH_3OSO_3H + 2\ H_2O + SO_2 \qquad (5)$$

Unfortunately, the mechanism of this system is poorly understood. Experiments designed to better comprehend how (bpm)$PtCl_2$ achieves partial oxidation of methane are described in Chapter Three.

The work featured in this thesis combines synthetic and mechanistic chemistry to address issues relevant to the utilization of olefins and methane. New catalysts have been

synthesized and tested for the polymerization of α-olefins. The resulting polymer was analyzed to provide insight on the relationship between non-metallocene catalyst geometry and polymer microstructure. The reactivity of the bisphenolate(benzene-1,3-diyl) titanium catalyst was closely examined to determine the mechanism of the C-H activation. The mechanism of (bpm)$PtCl_2$ catalyzed partial oxidation of methane was studied to understand the success of the bipyrimidine ligand.

References

1. *Transportation Energy Data Book*. 28 ed.; Department of Energy: 2009.

2. Coates, G. W. *Chem. Rev.* **2000,** *100*, 1223-1252.

3. Resconi, L.; Cavallo, L.; Fait, A.; Piemontesi, F. *Chem. Rev.* **2000,** *100*, 1253-1345.

4. Agapie, T.; Golisz, S. R.; Tofan, D.; Bercaw, J. E. US Pat. Appl. Pub. 11/859,089, 2007.

5. Agapie, T.; Bercaw, J. E. *Organometallics* **2007,** *26*, 2957-2959.

6. Agapie, T.; Day, M. W.; Bercaw, J. E. *Organometallics* **2008,** *27*, 6123-6142.

7. Agapie, T.; Henling, L. M.; DiPasquale, A. G.; Rheingold, A. L.; Bercaw, J. E. *Organometallics* **2008,** *27*, 6245-6256.

8. Tonks, I. A.; Henling, L. M.; Day, M. W.; Bercaw, J. E. *Inorg. Chem.* **2009,** *48*, 5096-5105.

9. Chan, M. C. W.; Tam, K.-H.; Pui, Y.-L.; Zhu, N. *J. Chem. Soc., Dalton Trans.* **2002**, 3085-3087.

10. Chan, M. C.-W.; Tam, K.-H. US Pat. 2003191015, 2003.

11. Chan, M. C. W.; Tam, K.-H.; Zhu, N.; Chiu, P.; Matsui, S. *Organometallics* **2006,** *25*, 785-792.

12. Sarkar, S.; Carlson, A. R.; Veige, M. K.; Falkowski, J. M.; Abboud, K. A.; Veige, A. S. *J. Am. Chem. Soc.* **2008,** *130*, 1116-1117.

13. Gol'dshleger, N. F.; Es'kova, V. V.; Shilov, A. E.; Shteinman, A. A. *Zh. Fiz. Khim.* **1972,** *46*, 785-786.

14. Periana, R. A.; Taube, D. J.; Gamble, S.; Taube, H.; Satoh, T.; Fujii, H. *Science* **1998,** *280*, 560-564.

Chapter One

Synthesis of Early Transition Metal Bisphenolate Complexes and their Use as Olefin Polymerization Catalysts

Reproduced in part from Golisz, S.R.; Bercaw, J.E. *Macromolecules* **2009**, *42*, 8751-8762.

Abstract

Bisphenolate ligands with pyridine- and benzene-diyl linkers have been synthesized and metalated with group 4 and 5 transition metals. The solid state structures of some of the group 4 complexes have been solved. The titanium, zirconium, hafnium, and vanadium complexes were tested for propylene polymerization and ethylene/1-octene copolymerization activities with methylaluminoxane as co-catalyst. The vanadium (III) precatalyst is the most active for propylene polymerization and shows the highest 1-octene incorporation for ethylene/1-octene copolymerization. The zirconium (IV) precatalyst was the most active for propylene polymerization of the group 4 precatalysts. Titanium and zirconium (IV) precatalysts with pyridine-diyl linkers provided mixtures of isotactic and atactic polypropylene while titanium (IV) precatalysts with benzene-diyl linkers gave atactic polypropylene only. The hafnium (IV) precatalyst with a pyridine-diyl linker generated moderately isotactic polypropylene.

Introduction

Polymers are ubiquitous materials with applications in household products, biomedicine and transportation. The polymerizations of ethylene, propylene, and styrene with Ziegler-Natta catalysts represent important processes that have grown to a worldwide production exceeding 100 billion pounds per year.[1] Understanding the influence of catalyst structure on polymer composition and microstructure allows for the development of polymer architectures with various applications.[2-7] Single-site catalysts are amenable to these types of studies such that an enormous number of metallocene and non-metallocene catalysts have been synthesized in the last thirty years.[2, 6] Metallocene

catalysts are well understood with respect to the relationship between catalyst symmetry and polymer microstructure (Figure 1).[4] However, non-metallocene catalysts represent a less understood sector of polymerization catalysts with respect to catalyst symmetry-polymer microstructure relationships.[3, 5]

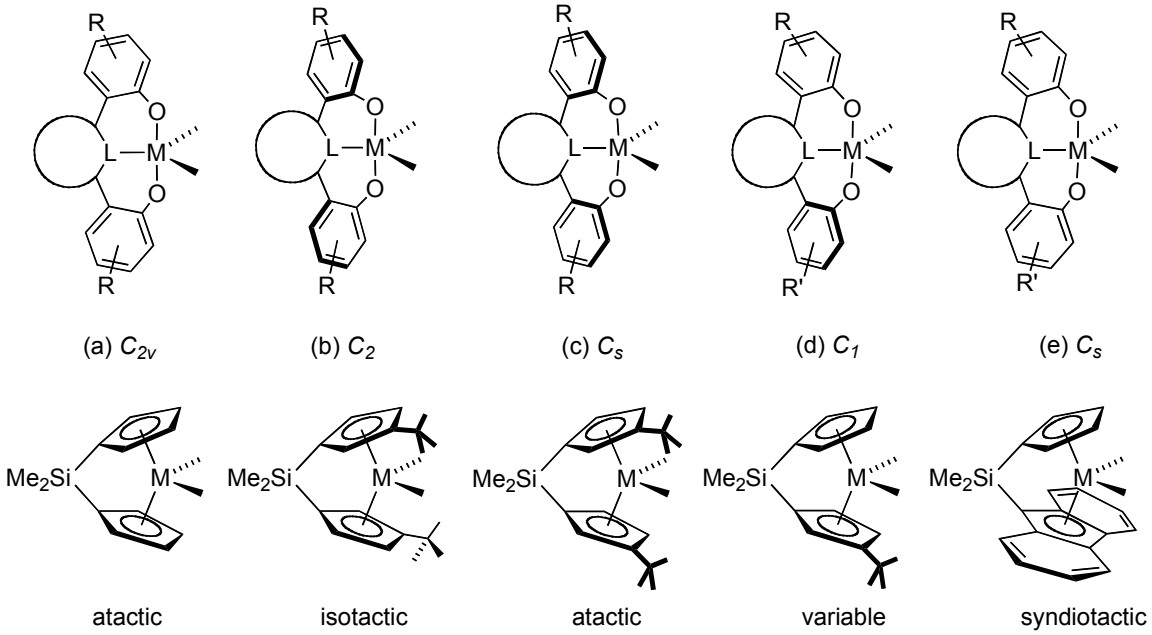

Figure 1. The relationship between catalyst geometry and anticipated polymer microstructure where R = alkyl; linker = pyridine-diyl or benzene-diyl, and L = N (neutral) or C (neutral or anionic).

Given the promising ability of non-metallocene catalysts to control polymer tacticity, we found it desirable to synthesize a new type of ligand for detailed study. This non-metallocene ligand framework features a bidentate or tridentate moiety with two anionic donors positioned around a central atom or donor connected at the *ortho* position *via* semi-rigid sp^2-sp^2 linkages (see Figure 1). We and others have begun to explore the

polymerization activities and selectivities of group 4 complexes with these ligands.[8-12] Herein we disclose the synthesis of bisphenolate pyridine- and benzene-diyl linked ligands. Group 4 and 5 complexes supported by these ligands have been prepared and their utility as polymerization catalysts has been examined, including their influence on molecular weight and ability to control polymer tacticity.

Results and Discussion

Ligand Synthesis. The ligands (**1-H$_2$**, **2-H$_2$**, **3-H$_2$**, and **4-H$_2$**) were synthesized with overall yields ranging from 20% to 60% (Scheme 1). The acid-promoted alkylation of *p*-cresol with 1-adamantanol was previously reported.[13] Both o*rtho*-bromination and deprotonation with sodium hydride followed by protection with chloromethyl methylether (MOM-Cl) occur in high yield. In the case of the adamantyl substituted species, the deprotonation/protection reaction produced an unidentifiable byproduct which was removed by Kugleröhr distillation. The coupling reaction of the protected bromo-phenol with either 2,6-dibromopyridine or 1,3-dibromobenzene was achieved through lithium-halogen exchange followed by transmetalation using $ZnCl_2$ and palladium-catalyzed Negishi cross-coupling.[14] The protecting group (MOM) was removed by treatment with acidic methanol at 65°C. Simple filtration of the methanol solution afforded the adamantyl substituted ligands (**1-H$_2$** and **3-H$_2$**). The *t*-butyl substituted ligands (**2-H$_2$** and **4-H$_2$**) were obtained by solvent removal. The identity of the ligands was confirmed by ^{1}H NMR spectroscopy, ^{13}C NMR spectroscopy, and HRMS.

Scheme 1

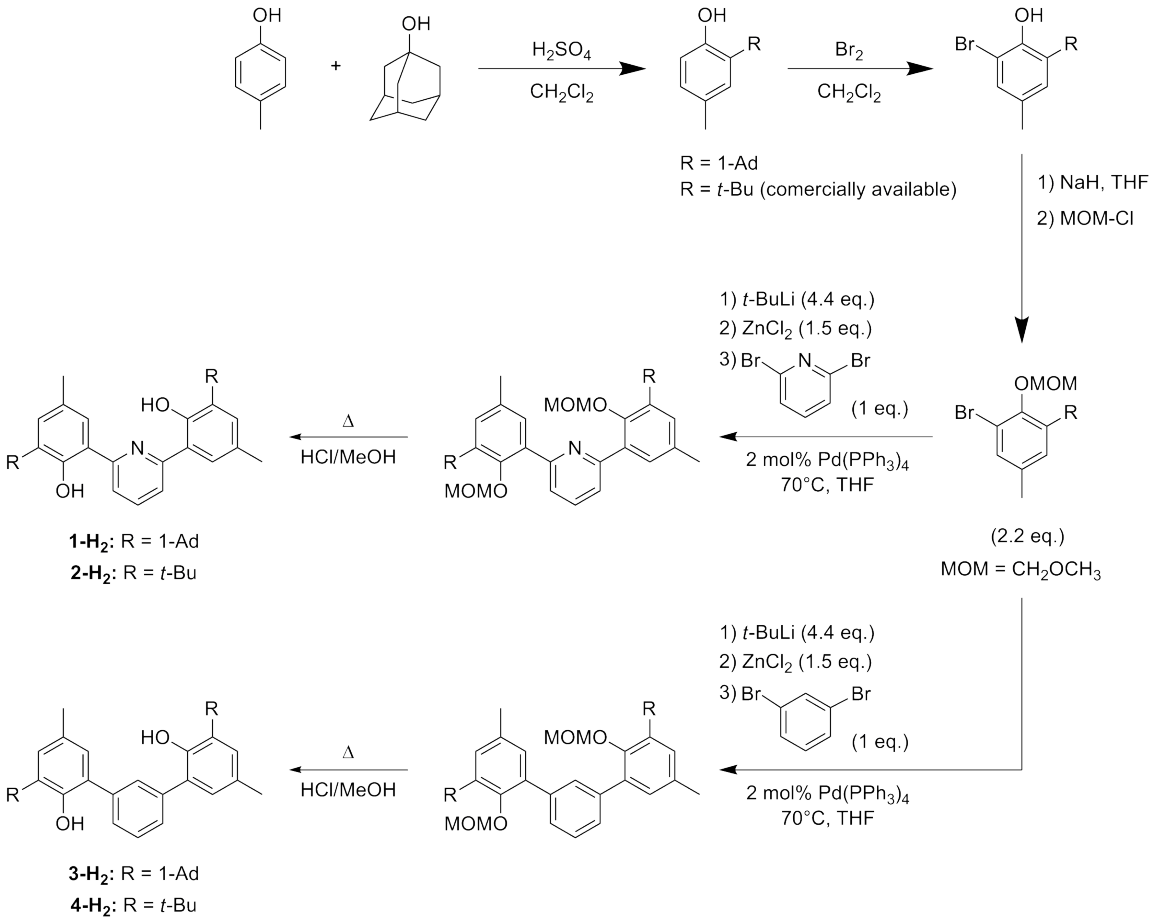

Preparation of Metal Complexes. The ligands (or their dianions) were treated with the appropriate early transition metal precursors ($TiCl_4(THF)_2$, $Ti(OCH(CH_3)_2)_4$, $Ti(CH_2C_6H_5)_4$, $Zr(CH_2C_6H_5)_4$, $Hf(CH_2C_6H_5)_4$, or $VCl_3(THF)_3$ where $OCH(CH_3)_2$ = O^{i}Pr and $CH_2C_6H_5$ = Bn) to give the desired products (Scheme 2 and Scheme 3). The salt metathesis reaction with $TiCl_4(THF)_2$ or $VCl_3(THF)_3$ involved initial deprotonation of the ligand with potassium benzyl. The KCl byproduct was removed by filtration. Repeated attempts using the salt metathesis routes with $ZrCl_4(THF)_2$ or $HfCl_4(THF)_2$ proved unsuccessful because substantial amounts of the bis-ligated species formed under

a variety of conditions. (The bis-ligated species was identified by ^{1}H NMR spectroscopy data from independent synthesis using an excess of ligand with $ZrBn_4$.[8]) The alcohol elimination reaction with $Ti(O^iPr)_4$ lead to the desired product only when heated at 80°C overnight. Alkane elimination reactions were successfully employed with the tetrabenzyl derivatives of the entire group 4 series. All metal complexes were characterized by NMR spectroscopy with the exception of the paramagnetic vanadium complex (vide infra). Further confirmation was obtained through elemental analysis, and in some cases, X-ray quality crystals were grown.

As shown previously, these complexes display different solution-state geometries (C_{2v}, C_s, C_2, or C_1) that may, in principle, be assigned by ^{1}H NMR spectroscopy through analysis of the benzyl [CH_2] protons: (1) C_{2v} geometry is expected to lead to a singlet, (2) C_s geometry should give two singlets, (3) C_2 geometry makes the [CH_2] protons diastereotopic, which should lead to two doublets, and (4) C_1 geometry would make all four benzylic protons different, appearing as four doublets.[8] All complexes with pyridine-diyl linkers (**1-TiBn$_2$**, **2-TiBn$_2$**, **1-ZrBn$_2$**, and **1-HfBn$_2$**) featured one singlet between 3.1 and 4.1 ppm integrating as four benzyl protons, implying either a C_{2v} geometry or dynamic equilibration of methylene hydrogens for a lower symmetry structure to give a singlet on the NMR timescale. The complexes with benzene-diyl linkers (**3-TiBn$_2$** and **4-TiBn$_2$**) showed two singlets between 1.9 and 3.7 ppm with each signal attributed to two benzyl protons, indicating (time-averaged) C_s geometry. These geometry assignments were corroborated by X-ray crystallography data.

The orange/brown solid of **1-VCl(THF)$_2$** was paramagnetic and showed very broad peaks in the ^{1}H NMR spectrum. The solution magnetic susceptibility was

determined using the Evans Method to give a μ_{eff} = 2.90(2) μ_B.[15] This matches the predicted value (μ_{eff}(spin only) = 2.82) for two unpaired electrons in trivalent vanadium complexes. The presence of two coordinated THF molecules was confirmed by elemental analysis.

Scheme 2

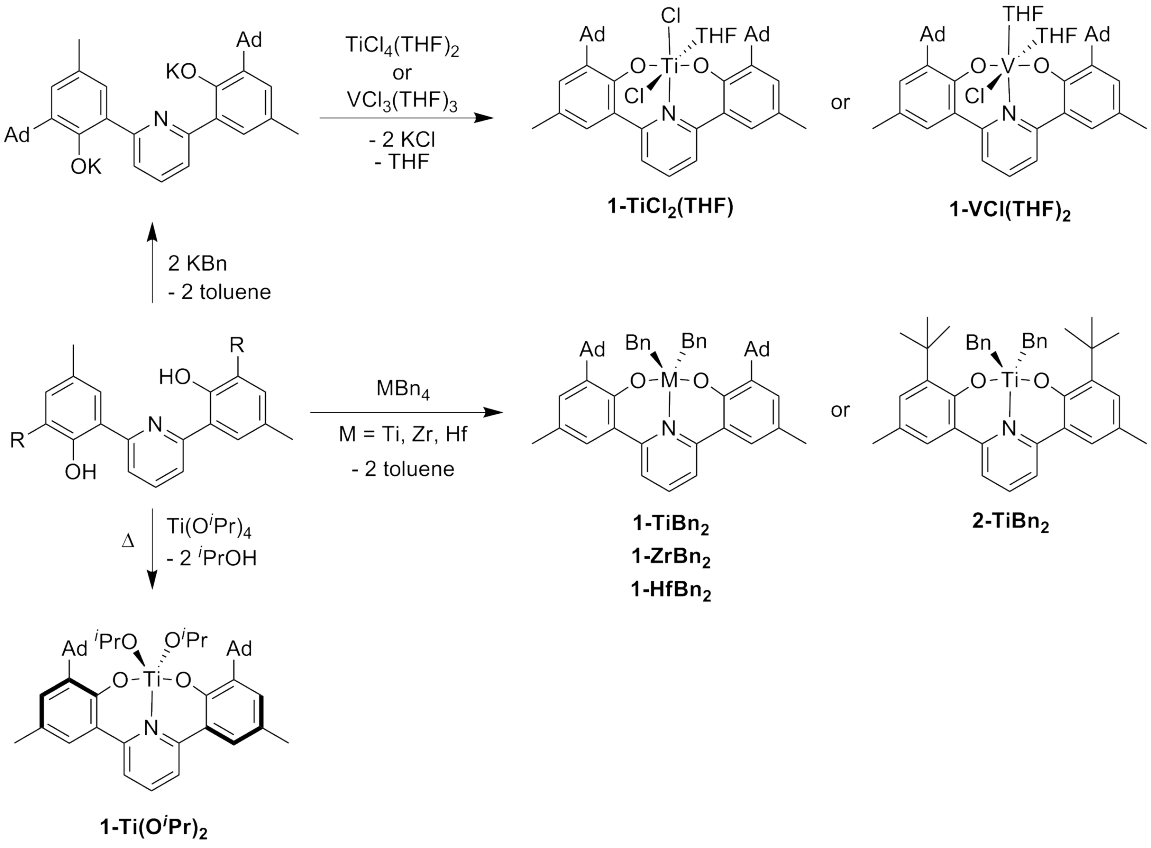

Scheme 3

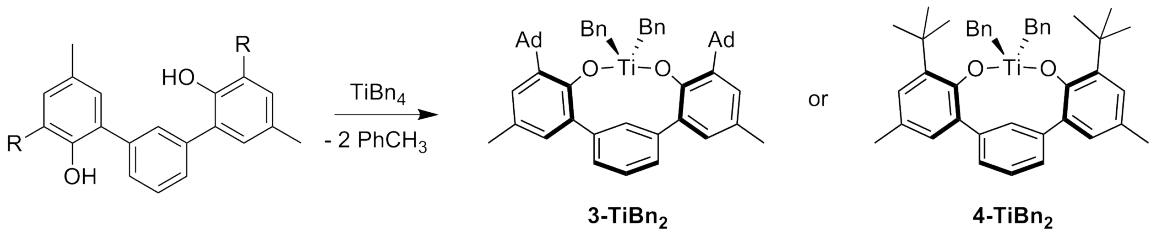

3-TiBn$_2$ **4-TiBn$_2$**

X-Ray Crystal Structures. Colorless single-crystals suitable for X-ray diffraction of **1-Ti(O^{i}Pr)$_2$** were serendipitously obtained from a benzene-d_6 solution in a J. Young NMR tube (Figure 2). The complex shows C_2-symmetry around the metal center with *pseudo*-trigonal bipyramidal geometry (crystal and refinement data can be found in Table 1). The bond lengths of Ti1-O1 and Ti1-O2 (the oxygens of the phenolate moieties) are essentially identical to each other at 1.92 Å. The Ti1-O3 and Ti1-O4 bonds (where the oxygens are from the alkoxides) are also identical at 1.75 Å. The twist angle (defined as the angle between the Ti-O$_{phenolate}$ bond and the N-C$_{ortho}$ bond) of **1-Ti(O^{i}Pr)$_2$** is 36°.

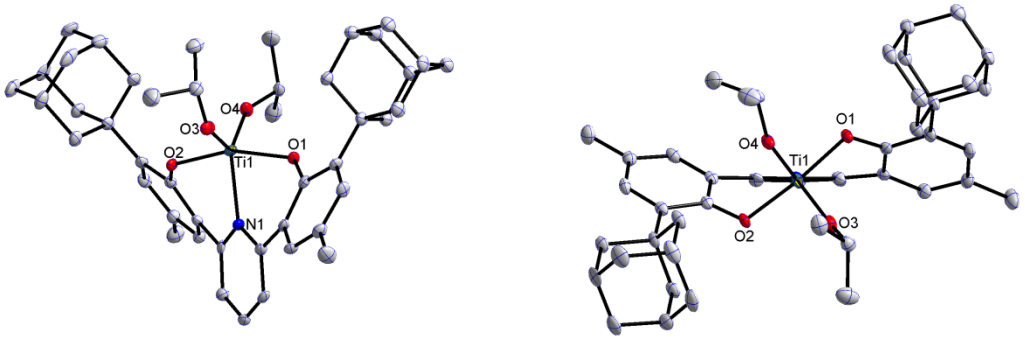

Figure 2. The solid state structure of **1-Ti(O^{i}Pr)$_2$**. The top view is shown on the right, looking down the Ti1-N1 bond. Hydrogens have been omitted for clarity. Selected bond

lengths (Å) and angles (°): Ti1-N1 2.169(2), Ti1-O1 1.92(19), Ti1-O2 1.92(18), Ti1-O3 1.758(2), Ti1-O4 1.75(18), O1-Ti1-O2 159.79(8), N1-Ti1-O1 79.53(8), N1-Ti1-O2 80.84(8).

Single crystals of **1-ZrBn$_2$(Et$_2$O)** were obtained by cooling a diethyl ether (Et_2O) solution of **1-ZrBn$_2$** to -35°C (Figure 3). The complex adopts a *pseudo*-octahedral geometry at zirconium due to the coordinated diethyl ether with C_s-symmetry (crystal and refinement data can be found in Table 1). The pyridine ring is canted approximately 42° from either of the planes of the phenolate rings, similar to previous observations for tantalum and zirconium complexes with closely related ligands.[8, 16-17] This canting allows one of the benzyl groups (C40, C41) to sit in the space vacated by the pyridine. The presence of a coordinated diethyl ether appeared to be an effect of crystallization only. When the synthesis of **1-ZrBn$_2$** was carried out in diethyl ether followed by removal of the solvent to give a solid, which was dissolved in benzene-d_6, no coordinated diethyl ether was observed in the ^{1}H NMR.

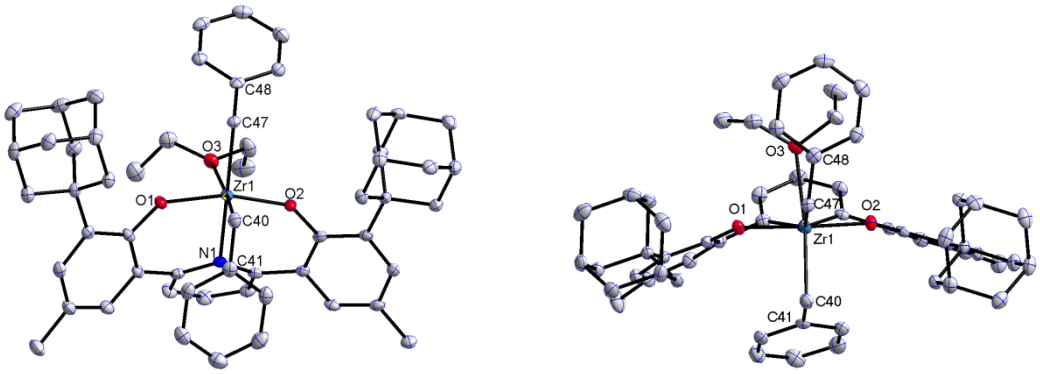

Figure 3. The solid state structure of **1-ZrBn$_2$(Et$_2$O)**. The top view is shown on the right, looking down the Zr1-N1 bond. Hydrogens have been omitted for clarity. Selected bond lengths (Å) and angles (°): Zr1-N1 2.47(13), Zr1-O1 1.98(11), Zr1-O2 1.98(12), Zr1-C40 2.29(16), Zr1-C47 2.32(16), Zr1-O3 2.39(11), O1-Zr1-O2 158.53(4), C48-C47-Zr1 120.6(11), C41-C40-Zr1 98.3(10).

Dark red crystals of **4-TiBn$_2$** were obtained by cooling a concentrated solution in petroleum ether to -35°C overnight (Figure 4). The geometry about titanium is *pseudo*-tetrahedral as the closest carbon from the benzene-diyl linker (C18) is greater than 2.9 Å from Ti1 (crystal and refinement data can be found in Table 1). The ligand is arranged in a nearly C_s-fashion, while the overall symmetry of the complex is C_1 due to the asymmetry in the placement of the benzyl groups. This geometry creates a large void on the backside of the complex (below C36 and behind C18). The plane of the benzene-diyl linker is canted further (approximately 48°) from the plane of the phenolates than in the case of **1-ZrBn$_2$(Et$_2$O)**. This is mostly likely a result of the fact that there is no bond between Ti1 and C18 (vide supra). The observation of separate singlets for the two benzyl methylene protons in the ^{1}H NMR spectrum at room temperature (vide supra) indicates that interconversion of benzyls via pivoting of the benzene-diyl about the *ipso* $C_{benzene\text{-}diyl}$-$C_{phenolate}$ linkages has a substantial barrier.

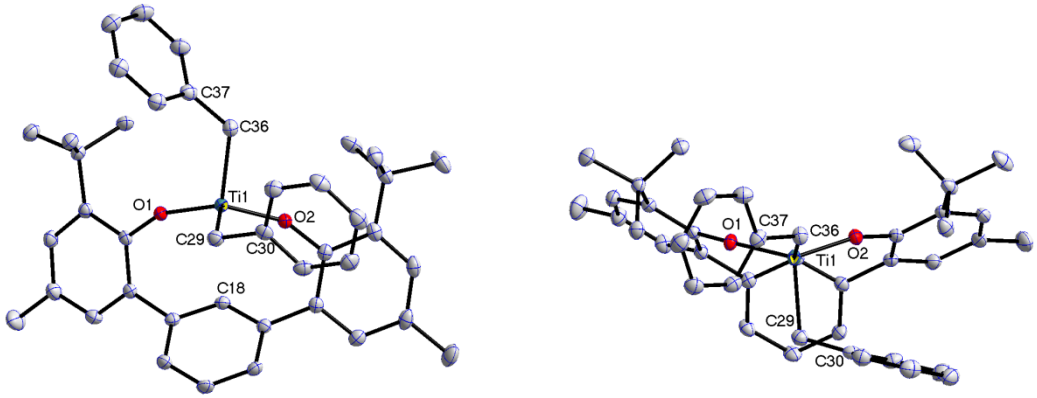

Figure 4. The solid state structure of **4-TiBn$_2$**. The top view is shown on the right, looking down the Ti1-C18 vector. Hydrogens have been omitted for clarity. Selected bond lengths (Å) and angles (°): Ti1-O1 1.812(7), Ti1-O2 1.805(7), Ti1-C29 2.10(11), Ti1-C36 2.09(11), O1-Ti1-O2 129.27(3), C29-Ti1-C36 101.46(4), Ti1-C36-C37 125.80(7), Ti1-C29-C30 110.53(7).

Table 1. Crystal and Refinement Data for **1-Ti(O^{i}Pr)$_2$**, **1-ZrBn$_2$(Et$_2$O)**, and **4-TiBn$_2$**.

	1-Ti(O^{i}Pr)$_2$	**1-ZrBn$_2$(Et$_2$O)**	**4-TiBn$_2$**
Empirical formula	$C_{45}H_{57}NO_4Ti \cdot 2.5 (C_6H_6)$	$C_{57}H_{67}NO_3Zr \cdot C_4H_{10}O$	$C_{42}H_{46}O_2Ti$
Formula weight	919.09	979.46	630.69
Crystal size (mm^3)	0.33 x 0.26 x 0.05	0.27 x 0.21 x 0.07	0.37 x 0.18 x 0.12
Temperature (K)	100(2)	100(2)	100(2)
a (Å)	13.206(3)	9.971(5)	11.811(6)
b (Å)	13.234(3)	11.280(6)	12.473(7)
c (Å)	15.814(3)	23.361(13)	13.659(7)

α(°)	80.36(4)	97.9(10)	100.57(3)
β(°)	67.61(4)	101.8(10)	100.81(3)
γ(°)	74.12(4)	95.2(10)	102.04(3)
Volume (Å^3)	2451.7(8)	2528.6(2)	1880.5(17)
Z	2	2	2
Crystal system	Triclinic	Triclinic	Triclinic
Space group	P-1 (#2)	P-1 (#2)	P-1 (#2)
d_{calc} (Mg/m^3)	1.245	1.286	1.114
θ range (°)	1.71 to 28.36	1.80 to 33.76	1.81 to 37.31
μ (mm^{-1})	0.224	0.266	0.259
Abs. correction	None	None	None
GOF	1.17	1.15	2.28
R_1,[a] wR_2[b] $[I>2\sigma(I)]$	0.056, 0.099	0.044, 0.073	0.050, 0.088

[a] $R_1 = \Sigma||F_o| - |F_c||/\Sigma|F_o|$. [b] $wR_2 = [\Sigma[w(F_o^2 - F_c^2)^2]/\Sigma[w(F_o^2)^2]]^{1/2}$.

Propylene Polymerization with Ti, Zr, Hf and V Precatalysts. Propylene polymerizations have been performed in the presence of methylaluminoxane (MAO) as co-catalyst for all group 4 and 5 precatalysts herein synthesized. The sole exception was **1-Ti(O^{i}Pr)$_2$**, which could not be activated by MAO, possibly due to the relative strength of Ti-O$_{iso\text{-propoxide}}$ vs. Al-O bonds. All polymerizations were performed at 0°C for 30 minutes[18] in 2 mL of toluene with a minimum of 1000 equivalents of MAO and essentially liquid propylene, [C_3H_6] = 12 M.[19] The effect of precatalyst on activity,

molecular weight, and tacticity has been investigated (Table 2). The polypropylenes (PP) were analyzed by gel permeation chromatography (GPC) and ^{13}C NMR.

Table 2. Propylene Polymerization Results.[a]

Catalyst	Catalyst Loading (mg)	MAO (eq)	Yield (mg)	Activity[b]	M_W	M_N	PDI
1-VCl(THF)$_2$	4.0	3000	2040	803	1117000	578000	2.03
1-TiCl$_2$(THF)	4.0	1000	44	17	576000	125000	4.60
1-TiBn$_2$	3.9	1000	23	9	2432000/ 11000	754000/ 6810	3.22/ 1.62
2-TiBn$_2$	30.0	1000	90	4	2468000	77500	31.8
1-ZrBn$_2$	6.2	1000	635	212	3630000/ 2600	513000/ 630	7.08/ 4.26
1-HfBn$_2$[c]	5.0	1000	17	3			
3-TiBn$_2$	30.0	1000	1600	72	11500	5960	1.94
4-TiBn$_2$	30.0	1000	1200	41	7500	3660	2.06
1-Ti(O^{i}Pr)$_2$	Not activated by MAO						

[a]Conditions: Propylene (5 atm, approx. 30 mL), toluene (2 mL), 0°C, 30 m. [b]Activity = kg PP · mol cat $^{-1}$ · h^{-1}. [c]The omission of data indicated that an insufficient amount of material was available for analysis.

The vanadium precatalyst is the most active. The activity of the vanadium precatalyst varied with different amounts of MAO while the molecular weight remained constant (Table 3). Molecular weight analysis of the resulting PP shows narrow polydispersity with a number average molecular weight greater than 500,000 g/mol. The ^{13}C NMR spectrum shows slight syndiotactic enrichment with a large amount of the 2,1-erythro regioerror common to many vanadium polymerization catalysts (Figure 5).[20] This polymer is rather insoluble with blue/green particles (residual vanadium) dispersed amid the white polymeric mass. The insolubility is possibly due, in part, to the high molecular weight. The PDI of approximately two indicates only one active catalytic species. It is difficult to conclusively determine the active species because vanadium can access a variety of oxidation states. Current theories suggest that V(II), V(III), V(IV), and V(V) may all be catalytically active oxidation states in olefin polymerization.[21] A few vanadium (III) precatalysts have been examined for their activity for olefin polymerization; while most of these precatalysts are active for ethylene polymerization or oligomerization,[22] those same precatalysts show little or no activity for propylene.[23] A tris(2-methyl-1,3-butanedionato)vanadium precatalyst showed activity of 470 kg PP · mol cat $^{-1}$ · h^{-1} at 0°C with an [Al]/[V] ratio of 400 where the co-catalyst was $Al(C_2H_5)_2Cl$.[24]

Table 3. The results of varying the amount of MAO with **1-VCl(THF)$_2$** for propylene polymerization.[a]

Entry	Catalyst Loading (μmol)	MAO (eq)	Yield (mg)	Activity[b]	M_W[c]	M_N	PDI
1	5.0	500	210	84.0			
2	5.1	500	313	122.7	1147347	497142	2.31
3	5.0	1000	478	191.2			
4	6.3	1000	559	177.5	1446521	641472	2.26
5	5.1	2000	698	273.7			
6	5.1	2000	894	350.6	1170922	578123	2.03
7	5.1	3000	1753	687.5			
8	5.1	3000	2038	803.1			
9	5.1	4000	1546	606.3			
10	5.1	4000	1606	629.8			

[a]Conditions: Propylene (5 atm, approx. 30 mL), toluene (2 mL), 0°C, 30 m. [b]Activity = kg PP · mol cat $^{-1}$ · h^{-1}. [c]The omission of data indicated that the analysis was not performed.

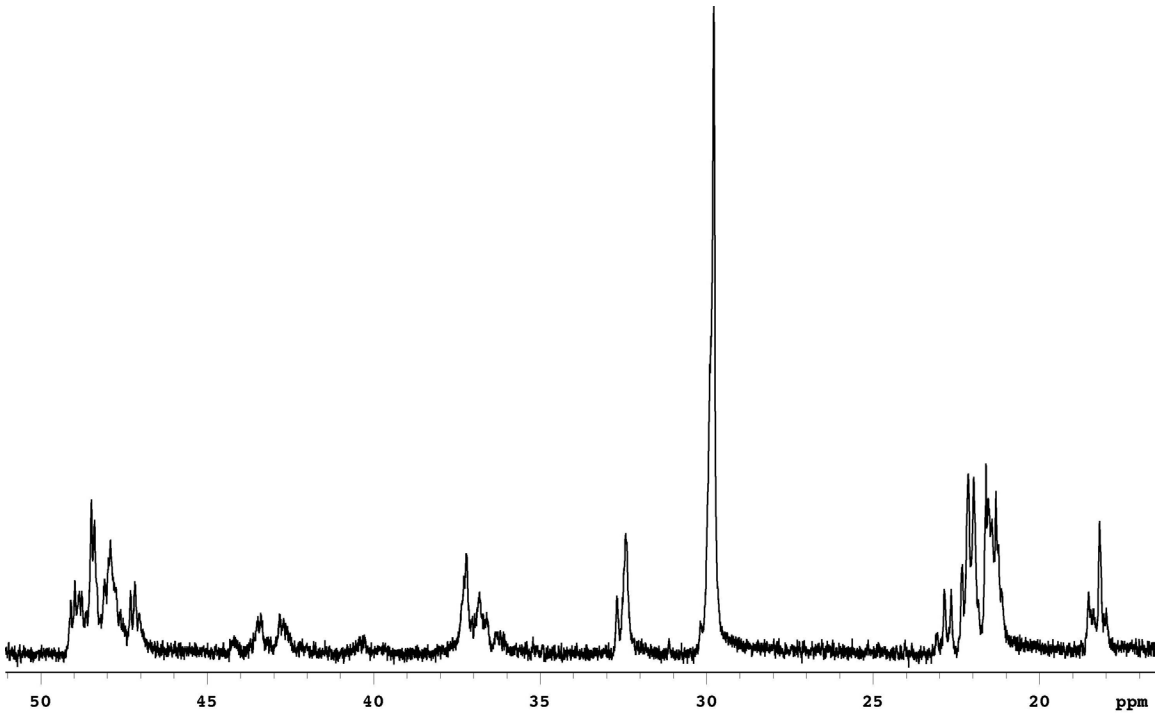

Figure 5. The ^{13}C NMR spectrum of polypropylene produced with **1-VCl(THF)$_2$** in $C_2D_2Cl_4$.

Comparing the linking groups, there is a marked increase in activity going from the pyridine-diyl linker to the benzene-diyl linker (compare **1-TiBn$_2$** to **3-TiBn$_2$**); however, both of these linking groups are less active than the furan-diyl or thiophene-diyl linking groups which generate propylene oligomers.[8] A zirconium dibenzyl precatalyst featuring a tetradentate [ONNO]-type ligand was found to be two orders of magnitude more active for propylene polymerization (11,500 kg PP · mol^{-1} · h^{-1} at 50°C) than **1-ZrBn$_2$**.[25] The more interesting observation is the difference in molecular weight depending on the linking group. For all group 4 precatalysts with pyridine-diyl linked bisphenolate ligands, the molecular weight distribution is very broad and in some cases bimodal, indicating the presence of more than one catalytically active species. On the

contrary, the precatalysts with benzene-diyl linked bisphenolate ligands feature narrow PDI (approximately 2) suggesting that only one species is responsible for polymer formation.

Most of the PPs generated were quite insoluble and required heating above 120°C in $C_2D_2Cl_4$ or $C_6D_4Cl_2$ to reach the concentration necessary for acceptable ^{13}C NMR data. ^{13}C NMR for PP generated from **1-TiCl$_2$(THF)** is typical for group 4 precatalysts and is shown in Figure 6. Group 4 precatalysts generate mostly regioregular PP with minimal amounts of the 2,1-erythro error.[26] Further analysis of the methyl region revealed an interesting motif where the *mmmm* pentad was enhanced relative to the other pentads. The other pentads resembled statistically atactic polypropylene (aPP). This motif appeared in the PP from titanium and zirconium precatalysts with pyridine-diyl linkers (Figure 7 and Table 4). On the other hand, the benzene-diyl linked precatalysts generated only aPP, and the hafnium precatalyst produced moderately (*mmmm* = 40%) isotactic polypropylene (iPP).

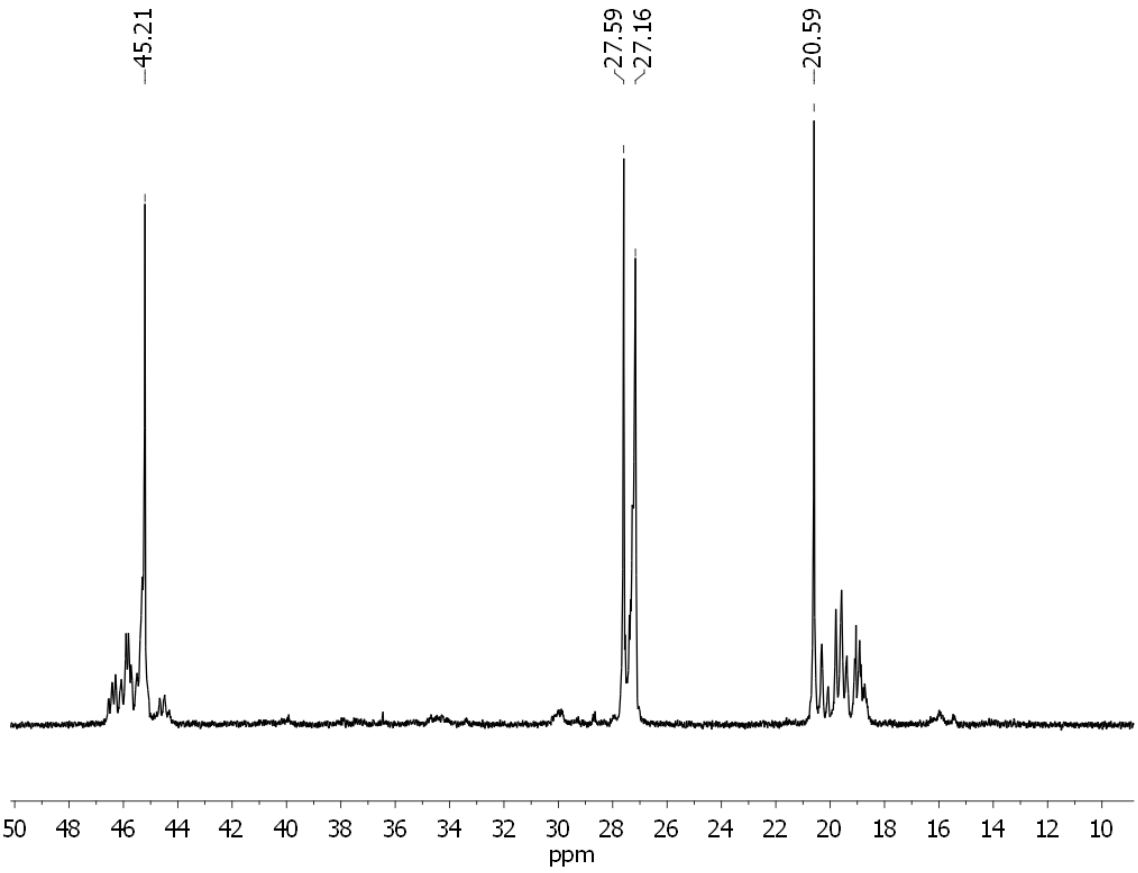

Figure 6. The ^{13}C NMR spectrum of polypropylene produced with **1-TiCl$_2$(THF)** in $C_6D_4Cl_2$.

a)

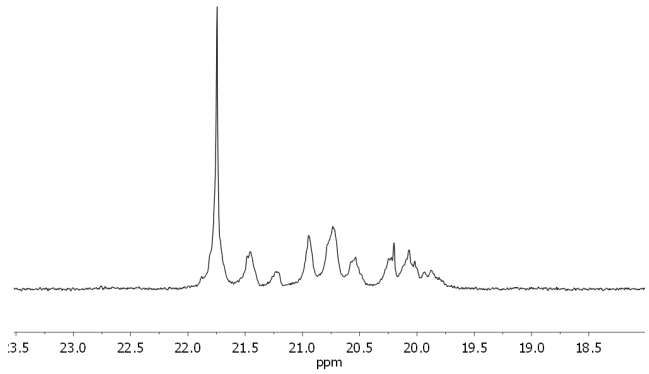
23.0
22.5
22.0
21.5
21.0
20.5
20.0
19.5
19.0
18.5
ppm

b)

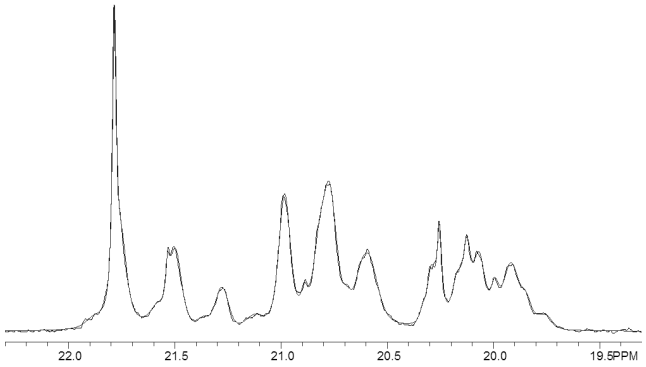
22.0
21.5
21.0
20.5
20.0
19.5PPM

c)

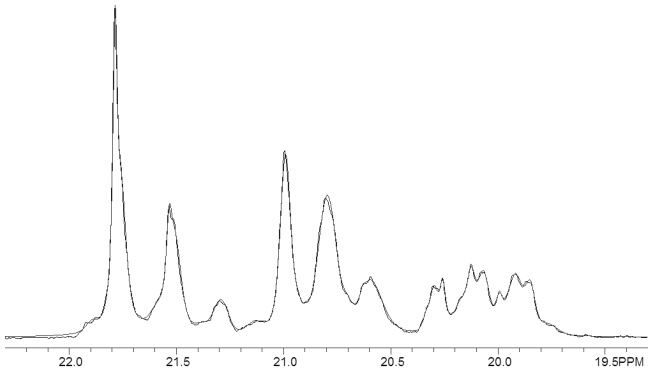
22.0
21.5
21.0
20.5
20.0
19.5PPM

d)

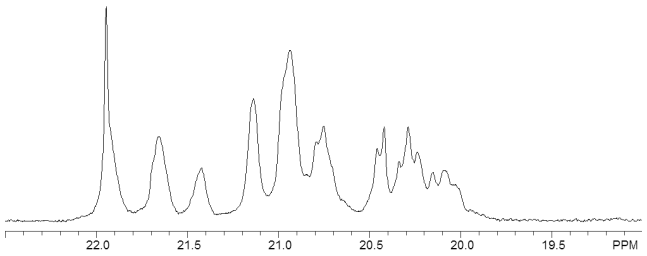
22.0
21.5
21.0
20.5
20.0
19.5
PPM

e)

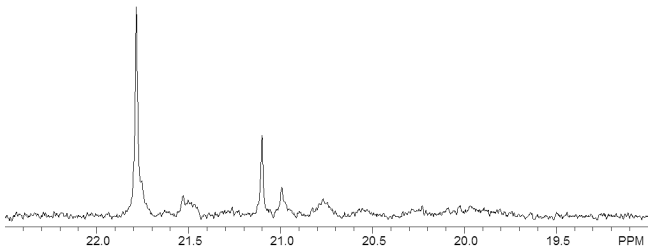
22.0
21.5
21.0
20.5
20.0
19.5
PPM

f)

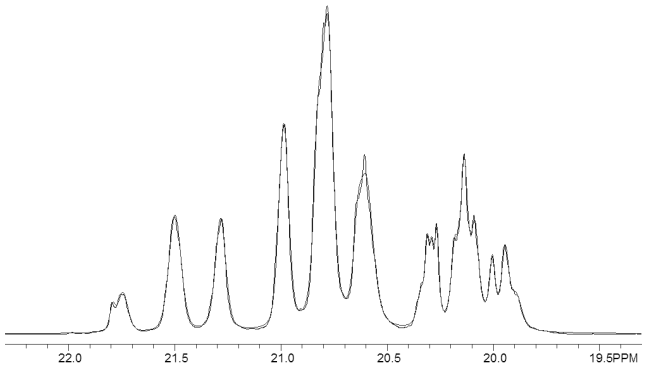
22.0
21.5
21.0
20.5
20.0
19.5PPM

g)

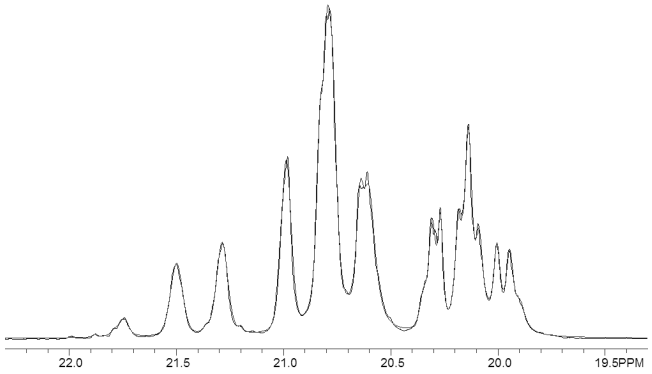

Figure 7. An expansion of the methyl region of the ^{13}C NMR (tetrachloroethane-d_2/*o*-dichlorobenzene-d_4 (1:4, v:v)) spectra of polypropylene produced with the following precatalysts: a) **1-TiCl$_2$(THF)**, b) **1-TiBn$_2$**, c) **2-TiBn$_2$**, d) **1-ZrBn$_2$**, e) **1-HfBn$_2$**, f) **3-TiBn$_2$**, g) **4-TiBn$_2$**.

Table 4. Stereo-sequence distribution (at the pentad level) of PPs.

Pentad	1-VCl $(THF)_2$	1-$TiCl_2$ (THF)	1-$TiBn_2$	2-$TiBn_2$	1-$ZrBn_2$	1-$HfBn_2$	3-$TiBn_2$	4-$TiBn_2$
mmmm	0.036	0.471	0.165	0.197	0.131	0.40	0.030	0.015
mmmr	0.066	0.089	0.094	0.124	0.092	0.13	0.079	0.049
rmmr	0.062	0.029	0.035	0.034	0.045	0.07	0.068	0.065
mmrr	0.087	0.078	0.115	0.148	0.102	0.11	0.111	0.095
mmrm/ rmrr	0.186	0.096	0.188	0.154	0.214	0.11	0.263	0.275
rmrm	0.172	0.054	0.105	0.091	0.126	0.04	0.147	0.157
rrrr	0.126	0.071	0.068	0.048	0.074	0.03	0.073	0.087
mrrr	0.142	0.060	0.120	0.096	0.126	0.04	0.150	0.172
mrrm	0.123	0.053	0.111	0.109	0.092	0.06	0.080	0.087

Note: the uncertainty is ± 0.004

Fractionation of Polypropylene Produced by 1-$TiCl_2$(THF). To determine whether the motif observed with **1-$TiCl_2$(THF)**, **1-$TiBn_2$**, **2-$TiBn_2$**, and **1-$ZrBn_2$** (Figure 7a, 7b, 7c, and 7d) was a new type of polymer or a result of multiple polymers, a PP sample produced with **1-$TiCl_2$(THF)** was extracted from a paper thimble by a series of refluxing solvents (diethyl ether, hexanes, and heptanes) such that the polymer was separated on the basis of difference in tacticity.[27] About half of the polymer (by weight) dissolved in diethyl ether (Table 5). Very little of the polymer was soluble in either hexanes or heptanes. The other half of the polymer (by weight) was insoluble in all solvents tested. ^{13}C NMR was obtained for both major fractions (Figure 8). The diethyl ether soluble fraction is essentially low molecular weight aPP. The insoluble fraction had

a significant amount of residual aluminum, most likely from inefficient removal of the MAO (this was confirmed by elemental analysis: C: 2.44; H: 3.22; Al: 32.7) which made initial attempts to obtain ^{13}C NMR data quite difficult. Prolonged stirring in acidified methanol removed enough aluminum such that a very dilute sample of the polymer component remained. ^{13}C NMR analysis of a dilute sample indicated iPP; however, due to the poor signal to noise ratio in that spectrum, triad analysis for mechanism of stereocontrol was not reliable.[28-31] The fractionation experiment confirmed that group 4 pyridine-diyl linked precatalysts[32] generated two different types of polymer (iPP and aPP), most likely from two catalytically active species.

Table 5. The results of the fractionation of polypropylene made from **1-TiCl$_2$(THF)**.

Solvent	Amount (g)	^{13}C NMR	M_W	M_N	PDI
Initial	3.28	Mixture			
Diethyl ether soluble	1.50	aPP	21000	9180	2.29
Hexanes soluble	0.10				
Heptanes soluble	0.10				
Insoluble	1.58	iPP			

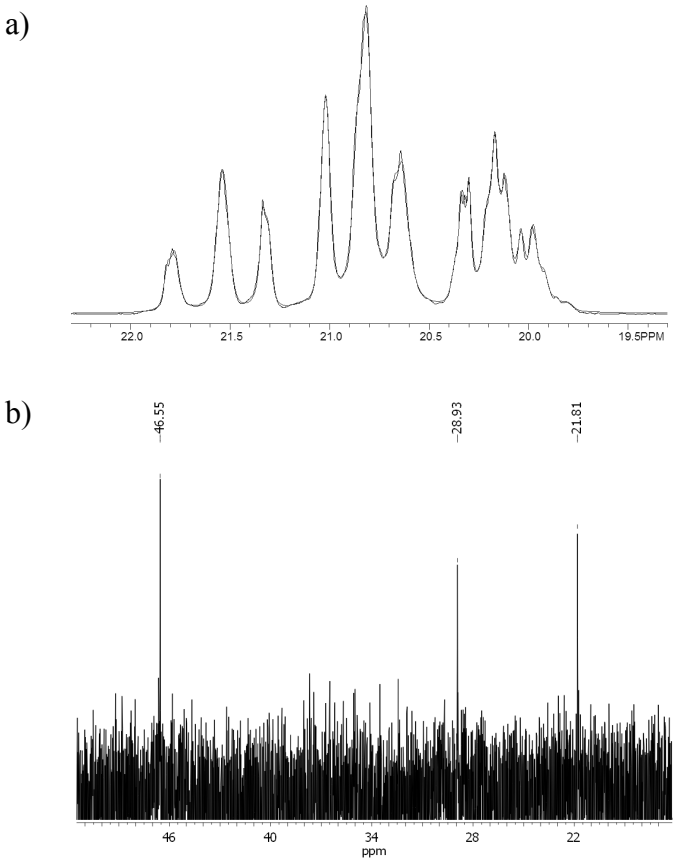

Figure 8. The ^{13}C NMR spectra of the polypropylene produced by **1-TiCl$_2$(THF)** after fractionation: a) an expansion of the methyl region for the diethyl ether soluble fraction and b) insoluble fraction.

Stoichiometric Activation. In most cases, stoichiometric activation of the dibenzyl complexes with $[C_6H_5NH(CH_3)_2][B(C_6F_5)_4]$ or $[(C_6H_5)_3C][B(C_6F_5)_4]$ in the presence of propylene gave no polymer. For one experiment in which tri(*iso*-butyl)aluminum (TIBA, 50 eq.) was added as an air and moisture scavenger, a small amount of polymer was obtained (10 mg polymer for 5 mg precatalyst). Due to the low activity, this polymer was not analyzed.

Treating the benzene-diyl linked precatalyst **4-TiBn$_2$** with less than one equivalent of activator (approximately 13 mol%) gave toluene and the benzene-diyl metalated dimeric species **[4-TiBn]$_2$** with the formula $\{Ti(CH_2C_6H_5)[(OC_6H_2\text{-}2\text{-}C(CH_3)_3\text{-}4\text{-}CH_3)C_6H_3(2\text{-}C(CH_3)_3\text{-}4\text{-}CH_3C_6H_2\text{-}\square^2\text{-}O]\}_2$ where a phenolate from one titanium bridges to the other titanium (this complex has been fully characterized and will be described in Chapter 2; see Figure 9).[33]

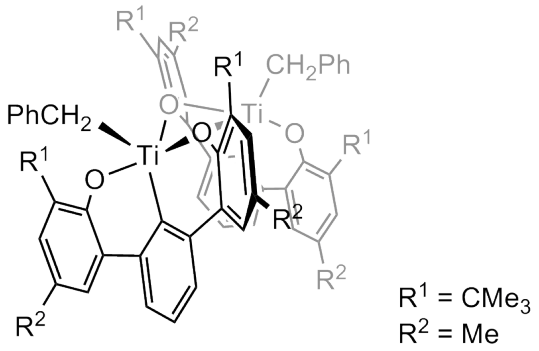

Figure 9. A schematic of the dimer obtained from **4-TiBn$_2$** in the presence of a sub-stoichiometric amount of activator.

We considered the possibility that this dimeric complex, which, surprisingly, contains a C_2-symmetric cyclometalated tridentate ligand, could act as an olefin polymerization catalyst without the addition of co-catalyst (MAO). To test this idea, the dimeric species **[4-TiBn]$_2$** was introduced to an atmosphere of ethylene in a J. Young NMR tube and, in a separate experiment, was subjected to the standard propylene polymerization conditions. Neither experiment showed polymer production. It was therefore concluded that the C_2-symmetric species was not active for olefin polymerization. By extension, the only benzene-diyl linked catalyst which is active for

olefin polymerization is the C_s-symmetric Ti-benzyl cationic species derived from **4-TiBn$_2$** (Scheme 4).

Scheme 4

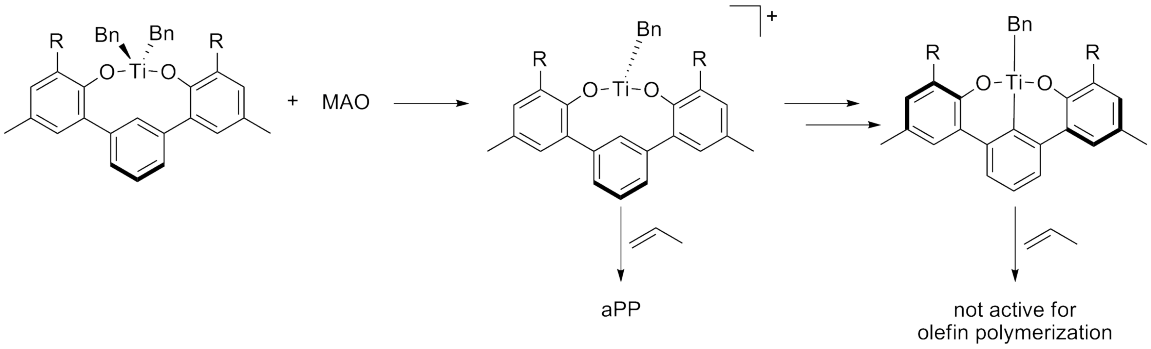

The Role of Aluminum. It was previously observed that the ratio of low molecular weight PP to high molecular weight PP and thus aPP to iPP (produced from **2'-ZrBn$_2$** where the *para* methyl group has been replaced by a *t*-butyl group) changed with the number of equivalents of MAO, where an increased amount of MAO favored the low molecular weight aPP.[8] This implied that the MAO may be interacting in such a way to influence the relative concentrations of the active catalytic species. Possibilities include transmetalation to generate an aluminum catalyst and modification of the ligand by aluminum. To test the first hypothesis, control reactions were performed to show that bisphenolate ligated aluminum methyl species were not competent catalysts for propylene polymerization.[34] Regarding the second possibility, aluminum has been shown to reduce C=N bonds to the amide functionalities and phenoxy-imine ligands to phenoxy-amines.[35-37] Additional experiments were performed on the bisphenolate system to determine whether MAO reacted irreversibly with the ligand.[38] Neither free

pyridine-diyl linked ligand nor the complementary group 4 dibenzyl complex showed ligand modification with MAO at room temperature or upon heating.

It has become clear that group 4 pyridine-diyl linked precatalysts generate both low molecular weight aPP and high molecular weight iPP, benzene-diyl linked precatalysts generate only low molecular weight aPP from a C_s-symmetric active species, and bisphenolate ligated aluminum species are not competent olefin polymerization catalysts. Drawing from experience with metallocenes where the geometry of the precatalyst dictates the polymer tacticity,[4] an analogous mechanism is possibly in operation here. The benzene-diyl linked precatalysts were shown to be C_s-symmetric in the solution, solid, and (probably) active states; C_s-symmetric catalysts are expected to give aPP as observed herein (Figure 1). The group 4 pyridine-diyl linked precatalysts exhibited a variety of different geometries; averaged C_{2v}-symmetric in solution, and either C_2- or C_s-symmetric in the solid state depending on the coordination environment of the metal. We speculate that the group 4 pyridine-diyl linked precatalysts can access two different geometries in solution upon activation with MAO; a C_2-symmetric species which generates the iPP and a C_s-symmetric species which produces the aPP. Possibly, an interaction between the MAO and the nitrogen of the pyridine ring breaks the metal-nitrogen bond to give a C_s-symmetric species, while maintaining the M-N bond gives a C_2-symmetric species. Looking at the solid state structure of C_s-symmetric **4-TiBn$_2$** (Figure 4), there is a large vacancy under the benzyl group (C36 and C37) and behind the benzene-diyl linker. The canting of the pyridine ring in **1-ZrBn$_2$(Et$_2$O)** (Figure 3) sets up the nitrogen so that it points away from the metal and into that space.

This void would be properly arranged for an aluminum species to interact with the nitrogen on the pyridine ring thus generating a C_s-symmetric species.

1-Hexene Polymerization. A stock solution of **1-TiCl$_2$(THF)** in toluene was prepared and injected into a flask containing MAO, 1-hexene, and, in some cases, toluene. The polymerizations were monitored by GC for 1-hexene conversion, and the generated polymer was isolated and analyzed (Table 6). In general, activity increased with increasing 1-hexene concentration, a result of the increased amount of monomer available for polymerization. However, increasing 1-hexene concentration decreased conversion such that a plot of 1-hexene conversion versus time approaches an asymptote.

Table 6. 1-Hexene Polymerization Data for **1-$TiCl_2$(THF)**.[a]

Entry	MAO (eq)	[1-Hexene]	Time (h)	Yield (mg)	% Conversion	Activity[b]
1	500	1.98	6	352	64.6	11
2	500	5.63	2	266	27.5	25
3	500	5.84	2	136	10.8	13
4	500	6.15	0.5	63	4.4	24
5	500	neat	0.5	286		108
6	500	neat	0.5	502	12	189
7	1000	2.50	1.5	291	25.6	37
8	1000	2.70	3.08	384	36.9	24
9	1000	6.84	1.5	522	23.6	66
10	1000	8.00	2.25	384	23.5	32
11	1000	neat	0.75	1004	19.1	253

[a]Conditions: 5.3 μmol catalyst loading, 22°C, toluene, constant volume of 4 mL.

[b]activity = kg poly · mol cat $^{-1}$ · h^{-1}.

The resulting homo(1-hexene) polymers were analyzed by ^{13}C NMR (Figures 10 and 11). As with polypropylene, the ^{13}C NMR provided insight on the microstructure of the polymer. Carbons $3B_4$, $4B_4$, the methine, and αα can couple and change chemical shift due to the stereochemistry of the inserted monomer.[39] Since all four of these carbons had broad resonances in the ^{13}C NMR, it was appropriate to conclude that the poly(1-hexene) was atactic.

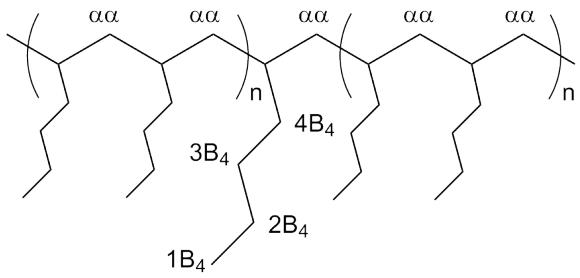

Figure 10. A schematic of poly(1-hexene).

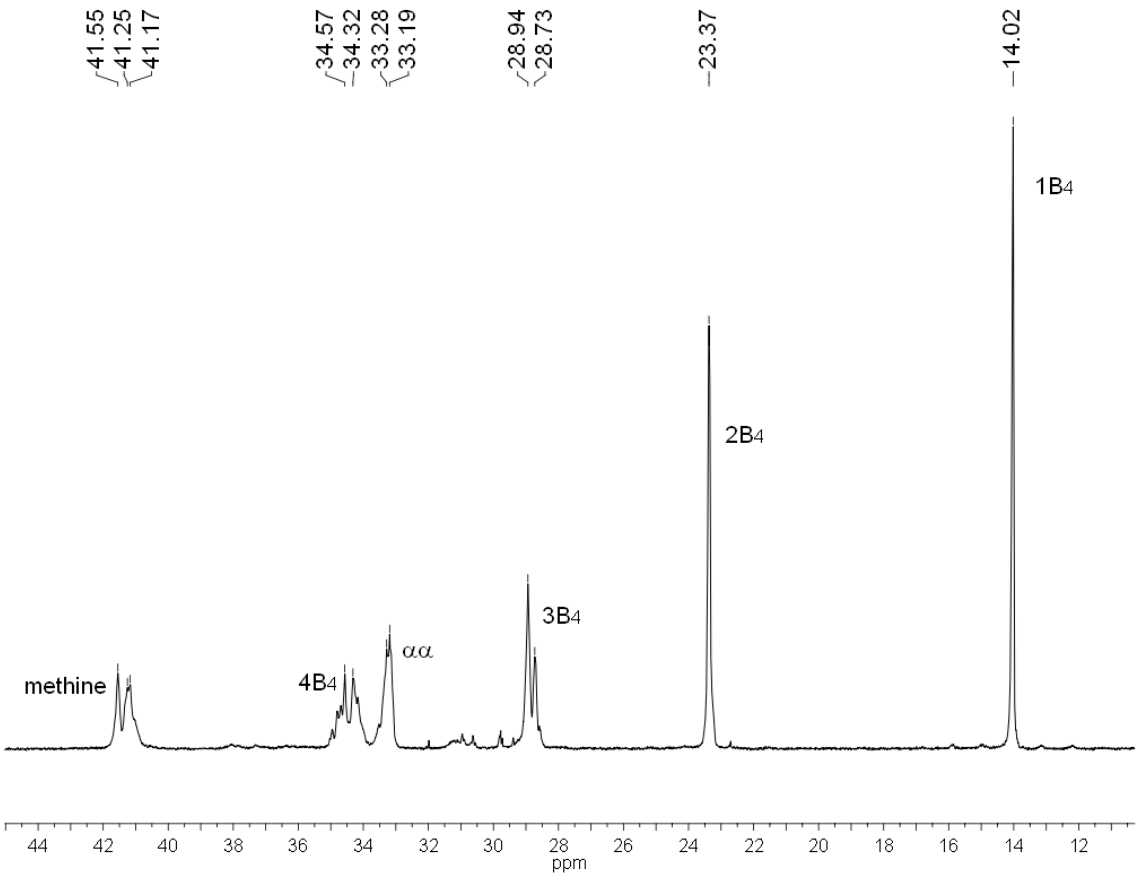

Figure 11. The ^{13}C NMR spectra of poly(1-hexene) produced with **1-TiCl$_2$(THF)**.

Ethylene/1-Octene Copolymerization. The non-metallocene catalysts, **1-TiCl$_2$(THF)**, **1-ZrBn$_2$**, and **1-VCl(THF)$_2$**, were investigated to establish whether they

are capable of producing ethylene/1-octene copolymers. In the presence of ethylene (1 atm) and 1-octene (ca. 50% by volume) in toluene with MAO as co-catalyst, all three precatalysts produced polymer (Table 7). The titanium catalyst had very low activity, and the resulting polymer could not be characterized. Both the zirconium and vanadium catalysts produced enough polymer for characterization.

Table 7. Ethylene/1-Octene Copolymerization Data.[a]

Catalyst	Yield (mg)	Activity[b]	Comonomer Incorporation (mol %)
1-$TiCl_2(THF)$[c]	20	3	
1-$ZrBn_2$	1200	160	0.5
1-$VCl(THF)_2$	374	50	6.6

[a]Conditions: Ethylene (1 atm), 1-octene (2 mL), toluene (2 mL), MAO (1000 eq.), rt. [b]activity = kg poly · mol cat $^{-1}$ · h^{-1}. [c]The omission of data indicated that an insufficient amount of material was available for analysis.

The copolymers were analyzed by ^{13}C NMR (Figure 12 and 13) for the amount of comonomer incorporation (mol %).[40] The zirconium catalyst showed a large preference for ethylene over 1-octene. The vanadium catalyst was slightly more efficient at incorporating 1-octene into the growing polyethylene chain. Neither catalyst is capable of incorporating the amount of 1-octene necessary to produce an elastomer. Although no research group has disclosed the generation of ethylene/1-octene copolymers via vanadium precatalysts, a number of groups have reported ethylene/propylene copolymers.[24, 41] There is also one known example of ethylene/1-hexene

copolymerization where tridentate salicylaldiminato ligands on vanadium (III) in the presence of $Al(C_2H_5)_2Cl$ could incorporate up to 13 mol% 1-hexene.[42]

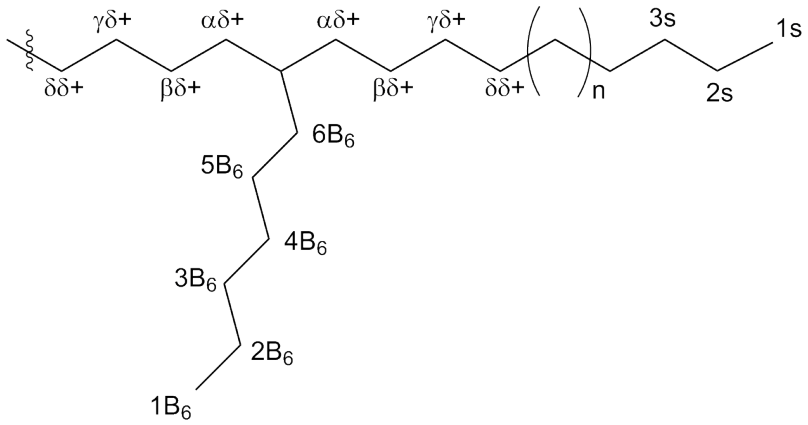

Figure 12. A schematic of an ethylene/1-octene copolymer.

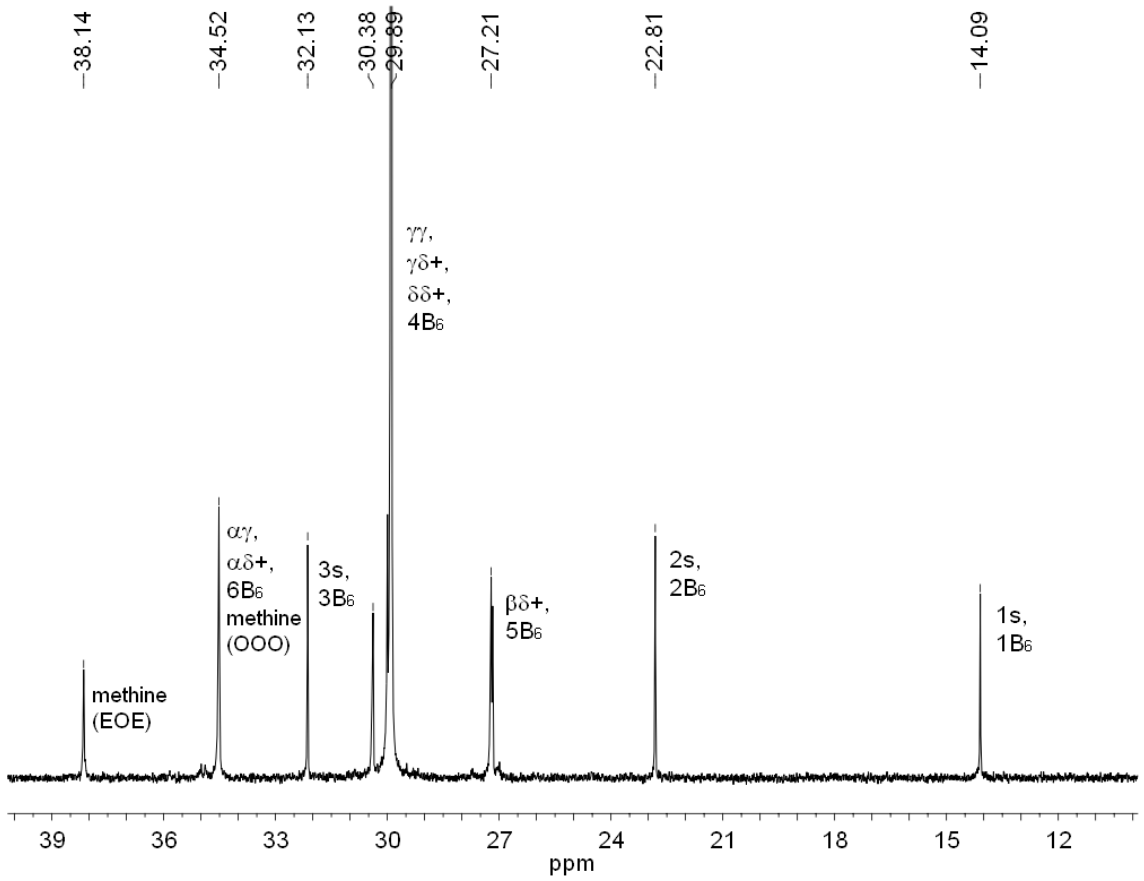

Figure 13. The ^{13}C NMR of the polymer produced by **1-VCl(THF)** in the presence of ethylene and 1-octene.

Conclusion

The bisphenolate ligands with both pyridine- and benzene-diyl linkers were metalated with group 4 and 5 metal precursors to give the desired complexes. These complexes were then found to be capable of olefin polymerization when activated with MAO. For the vanadium precatalyst, the activity for polypropylene was one of the highest of known V(III) olefin polymerization catalysts. Vanadium was also the most efficient at incorporating 1-octene into the ethylene/1-octene copolymer. In the case of

group 4 pyridine-diyl linked bisphenolates, two different types of polymer were obtained: high molecular weight iPP and low molecular weight aPP. Conversely, benzene-diyl linked precatalysts generated only low molecular weight aPP. We speculate that the benzene-diyl linked precatalyst can access only a C_s-symmetric cationic catalyst species. The pyridine-diyl linked precatalyst can access two cationic catalyst species, a C_2-symmetric species which generates iPP and a C_s-symmetric species which produces aPP; the latter might arise from the coordination of aluminum (from MAO) to the pyridine.

Experimental

General Considerations. All air- and moisture-sensitive compounds were manipulated under argon or nitrogen using standard glovebox, Schlenk, and high-vacuum line techniques.[43] Argon and ethylene were purified and dried by passage through columns of MnO on vermiculite and activated 4 Å molecular sieves. Solvents were dried over sodium benzophenone ketyl or titanocene.[44] All organic chemicals, $ZrCl_4$, and VCl_3 were purchased and used as received from Aldrich. The metal precursors $TiCl_4$ and $Ti(O^iPr)_4$ were purchased from Strem and used as received. The $HfCl_4$ (99%) was purchased from Cerac and used as received. The activators methylaluminoxane (MAO), $[Ph_3C][B(C_6F_5)_4]$, and $[C_6H_5NH(CH_3)_2][B(C_6F_5)_4]$ were purchased from Albemarle. The MAO was dried *in vacuo* at 150°C overnight to remove free trimethylaluminum before use. Propylene was dried by passage through a Matheson 2110 drying system equipped with an OXISORB column. The concentration of propylene in toluene solutions was calculated according to literature data.[19] NMR spectra of ligands and

precatalysts were recorded on a Varian Unity Inova 500 (499.852 MHz for ^{1}H) or Varian Mercury (300 MHz for ^{1}H) spectrometer. NMR solvents were purchased from Cambridge Isotope. Chemical shifts were reported using the residual solvent signal. Analysis by GC-MS was carried out on an HP 5890 Series II gas chromatograph connected to an HP 5972 mass spectrometric detector. A 60 m x 0.32 μm internal diameter column was used which was coated with a 5 μm thick 100% methylsiloxane film. High resolution mass spectra (HRMS) were obtained from the California Institute of Technology Mass Spectrometry Facility. X-ray quality crystals were mounted on a glass fiber with Paratone-N oil. Data were collected on a Bruker KAPPA APEX II instrument. Structures were determined using direct methods or, in some cases, Patterson maps with standard Fourier techniques using the Bruker AXS software package. GPC data were generated on Symyx HT-GPC's using an IR4 detector, calibrated with narrow PS standards and adjusted for PP alpha and K's. 2-Adamantyl-4-methylphenol;[13] $TiCl_4(THF)_2$, $ZrCl_4(THF)_2$, $HfCl_4(THF)_2$, and $VCl_3(THF)_3$;[45] and tetrabenzyl complexes of group 4[46] were prepared according to literature procedures.

Synthesis of 2-adamantyl-4-methyl-5-bromophenol. 2-Adamantyl-4-methylphenol (9.9 g, 40.9 mmol) was dissolved in CH_2Cl_2 (200 mL). Bromine (2.09 mL, 40.9 mmol) was added dropwise to the solution. After 20 m, GC-MS showed a single peak corresponding to the product. The crude mixture was washed with H_2O, dried over $MgSO_4$, filtered, and dried with a rotary evaporator to give a pale yellow solid: 10.6 g, 80%. ^{1}H NMR (300 MHz, $CDCl_3$): δ 1.78 (s, 6H, Ad), 2.11 (s, 9H, Ad), 2.26 (s, 3H, C*H*$_3$), 5.64 (s, 1H, O*H*), 6.96 (s, 1H, C$_6$*H*$_2$), 7.16 (s, 1H, C$_6$*H*$_2$).

Synthesis of 2-*t*-butyl-4-methyl-5-bromophenol. 2-*t*-Butyl-4-methylphenol (16 g, 97.4 mmol) was dissolved in CH_2Cl_2 (200 mL). Bromine (5.0 mL, 97.4 mmol) was added dropwise to the solution. After 1.5 h, GC-MS showed a single peak corresponding to the product. The crude mixture was washed with H_2O, dried over $MgSO_4$, filtered, and dried with a rotary evaporator to give golden yellow oil: 22.7 g, 96%. ^{1}H NMR (500 MHz, $CDCl_3$): δ 1.40 (s, 9H, C(C*H*$_3$)$_3$), 2.27 (s, 3H, C*H*$_3$), 5.64 (s, 1H, O*H*), 7.02 (s, 1H, C$_6$*H*$_2$), 7.17 (s, 1H, C$_6$*H*$_2$). ^{13}C NMR (125 MHz, $CDCl_3$): δ 20.55, 29.37, 35.26, 111.87, 127.35, 129.59, 130.21, 137.17, 148.13. HRMS (FAB+) obsd (M+H)-H_2 241.0236, calcd for $C_{11}H_{14}BrO$, 241.0228.

Protection of 2-adamantyl-4-methyl-5-bromophenol. Sodium hydride (574 mg, 23.9 mmol) was suspended in anhydrous THF (10 mL). 2-Adamantyl-4-methyl-5-bromophenol (6.4 g, 19.9 mmol) was dissolved in anhydrous THF (100 mL) and transferred by cannula onto the sodium hydride suspension. The mixture became blue in color and hydrogen gas was evolved. After 30 m, chloromethyl methylether (1.7 mL, 21.9 mmol) was syringed into the reaction flask. The mixture was stirred for 14 h. The mixture was concentrated, extracted in H_2O, washed with diethyl ether (50 mL, 3x), dried over $MgSO_4$, filtered and dried with a rotary evaporator. The crude product was purified by Kugelröhr distillation to give a white solid: 5.2 g, 71%. ^{1}H NMR (300 MHz, $CDCl_3$): δ 1.78 (s, 6H, Ad), 2.11 (s, 9H, Ad), 2.28 (s, 3H, C*H*$_3$), 3.72 (s, 3H, CH_2OCH_3), 5.22 (s, 2H, C*H*$_2$OCH$_3$), 7.05 (s, 1H, C$_6$*H*$_2$), 7.24 (s, 1H, C$_6$*H*$_2$).

Protection of 2-*t*-butyl-4-methyl-5-bromophenol. Sodium hydride (2.7 g, 112.2 mmol) was suspended in anhydrous THF (25 mL). 2-*t*-Butyl-4-methyl-5-bromophenol

(22.73 g, 93.4 mmol) was dissolved in anhydrous THF (200 mL) and transferred by cannula onto the sodium hydride suspension. The mixture became magenta in color and hydrogen gas was evolved. After 4 h, the mixture turned dark blue in color and chloromethyl methylether (7.8 mL, 102.8 mmol) was syringed into the reaction flask. The mixture was stirred for 14 h. The mixture was quenched with water, concentrated, extracted in diethyl ether, washed with water (50 mL, 3x), dried over $MgSO_4$, filtered and dried with a rotary evaporator to give a brownish red oil: 25.1 g, 94%. ^{1}H NMR (500 MHz, $CDCl_3$): δ 1.42 (s, 9H, C(CH_3)$_3$), 2.28 (s, 3H, CH_3), 3.69 (s, 3H, CH_2OCH_3), 5.21 (s, 2H, CH_2OCH$_3$), 7.09 (s, 1H, C_6H_2), 7.25 (s, 1H, C_6H_2). ^{13}C NMR (125 MHz, $CDCl_3$): δ 20.71, 30.79, 35.56, 57.73, 99.32, 117.58, 127.58, 132.07, 134.39, 144.92, 150.66. HRMS (FAB+) obsd (M+H)-H_2 285.0502, calcd for $C_{13}H_{18}BrO_2$, 285.0490.

General Procedure for the Ligand Coupling Reaction. The protected bromophenol (3.3 mmol) was dissolved in THF (30 mL) in a glass vessel with a Köntes valve and cooled to just above its freezing point (-100°C). *t*-Butyl lithium (6.6 mmol) was added dropwise and the reaction was stirred for 30 m to give a cloudy, light brown mixture. Zinc chloride (2.2 mmol) was added to the reaction mixture and stirred for 30 m to give a transparent orange solution. The dibromo-linker (1.5 mmol) and tetrakis(triphenylphosphine)palladium (0.03 mmol) were added to the reaction mixture which was sealed and placed in an oil bath. The mixture was heated at 70°C overnight. The reaction was quenched with H_2O and concentrated under reduced pressure. The remaining aqueous sludge was extracted in diethyl ether or CH_2Cl_2, dried over $MgSO_4$, filtered, and dried with a rotary evaporator. The crude product was suspended in acidified methanol and heated to reflux to remove both impurities and the protecting

group. After cooling to rt, filtration or removal of volatiles with a rotary evaporator of the neutralized suspension gave the desired product. If necessary, further purification was achieved by column chromatography (9:1, Hexanes: CH_2Cl_2) or Kugelröhr distillation.

1-H₂. Pale yellow solid: 507 mg, 60%. ^{1}H NMR (500 MHz, $CDCl_3$): δ 1.79 (s, 12H, Ad), 2.09 (s, 6H, Ad), 2.23 (s, 12H, Ad), 2.37 (s, 6H, C*H*$_3$), 7.15 (s, 2H, C_6H_2), 7.29 (s, 2H, C_6H_2) 7.62 (d, 2H, *m*-C_5H_3N, J = 8 Hz), 7.96 (t, 1H, *p*-C_5H_3N, J = 8 Hz), 10.51 (bs, 2H, O*H*). ^{13}C NMR (125 MHz, $CDCl_3$): δ 21.22, 29.37, 37.39, 40.57, 120.55, 121.99, 126.47, 128.31, 129.89, 138.25, 139.94, 153.56, 157.25. HRMS (FAB+) obsd (M+H)-H_2 558.3345, calcd for $C_{39}H_{44}NO_2$, 558.3372.

2-H₂. Pale yellow solid: 730 mg, 42%. ^{1}H NMR (500 MHz, $CDCl_3$): δ 1.49 (s, 18H, C(C*H*$_3$)$_3$), 2.39 (s, 6H, C*H*$_3$), 7.23 (s, 2H, C_6H_2), 7.33 (s, 2H, C_6H_2) 7.64 (d, 2H, *m*-C_5H_3N, J = 8 Hz), 7.97 (t, 1H, *p*-C_5H_3N, J = 8 Hz), 10.58 (s, 2H, O*H*). ^{13}C NMR (125 MHz, $CDCl_3$): δ 21.19, 29.75, 35.26, 120.48, 121.81, 126.64, 128.16, 129.95, 138.03, 139.95, 153.42, 157.24. HRMS (FAB+) obsd M+ 403.2507, calcd for $C_{27}H_{33}NO_2$, 403.2511.

3-H₂. Beige solid: 13.2 g, 36%. ^{1}H NMR (500 MHz, $CDCl_3$): δ 1.79 (s, 12H, Ad), 2.09 (s, 6H, Ad), 2.18 (s, 12H, Ad), 2.33 (s, 6H, C*H*$_3$), 5.29 (s, 2H, O*H*), 6.94 (s, 2H, C_6H_2), 7.07 (s, 2H, C_6H_2), 7.49 (d, 2H, *m*-C_6H_4, J = 7.5 Hz), 7.58 (s, 1H, C_6H_4), 7.59 (t, 1H, *p*-C_6H_4, J = 7.5 Hz). ^{13}C NMR (125 MHz, $CDCl_3$): δ 21.05, 29.31, 37.21, 40.73, 127.72, 128.29, 129.04, 129.31, 130.41, 131.05, 136.69, 139.10, 149.05. HRMS (FAB+) obsd M+ 558.3486, calcd for $C_{40}H_{46}O_2$, 558.3498.

4-H_2. Pale yellow crystalline solid: 1.9 g, 67%. ^{1}H NMR (500 MHz, $CDCl_3$): δ 1.47 (s, 18H, C(CH_3)$_3$), 2.35 (s, 6H, CH_3), 5.33 (s, 2H, O*H*), 6.97 (s, 2H, C_6H_2), 7.15 (s, 2H, C_6H_2), 7.52 (d, 2H, *m*-C_6H_4, J = 7.5 Hz), 7.58 (s, 1H, C_6H_4), 7.63 (t, 1H, *p*-C_6H_4, J = 7.5 Hz). ^{13}C NMR (125 MHz, $CDCl_3$): δ 21.02, 29.91, 35.08, 127.82, 128.26, 128.53, 129.00, 129.19, 130.47, 130.96, 136.45, 139.12, 148.91. HRMS (FAB+) obsd M+ 402.2555, calcd for $C_{28}H_{34}O_2$, 402.2559.

Synthesis of 1-$TiCl_2$(THF). Potassium benzyl (47 mg, 0.357 mmol) and **1-H_2** (100 mg, 0.178 mmol) were dissolved in THF (15 mL) and stirred for 30 m. This solution was added to $TiCl_4(THF)_2$ (60 mg, 0.178 mmol) and allowed to stir for 30 m. The THF was removed *in vacuuo*. The resulting solid was suspended in diethyl ether and filtered. The filtrate was dried under vacuum to give a dark red crystalline solid: 77 mg, 58%. ^{1}H NMR (300 MHz, C_6D_6): δ 0.81 (m, 4H, THF), 2.01 (dd, 18H, Ad), 2.25 (s, 6H, CH_3), 2.61 (s, 12H, Ad), 3.39 (m, 4H, THF), 6.89 (d, 2H, *m*-C_5H_3N), 7.00 (t, 1H, *p*-C_5H_3N), 7.16 (s, 2H, C_6H_2), 7.28 (s, 2H, C_6H_2). Analysis: Calculated (Found) C: 69.05 (68.44); H: 6.74 (7.14); N: 1.87 (1.93); Ti: 6.40 (5.94).

Synthesis of 1-Ti(O^{i}Pr)$_2$. Titanium tetra-*iso*-propoxide (100 mg, 0.35 mmol) was dissolved in benzene (10 mL). **1-H_2** (200 mg, 0.35 mmol) predissolved in benzene (10 mL) was added to the titanium. The reaction was heated overnight at 80°C. After cooling, the solvent was removed *in vacuuo* to give a yellow solid: 142 mg, 56%. ^{1}H NMR (300 MHz, C_6D_6): δ 1.10 (s, 12H, CH(CH_3)$_2$), 1.95 (dd, 12H, Ad), 2.23 (s, 6H, Ad), 2.35 (s, 6H, CH_3), 2.56 (s, 12H, Ad), 5.04 (m, 2H, C*H*(CH_3)$_2$), 7.00 (t, 1H, *p*-C_5H_3N), 7.10 (d, 2H, *m*-C_5H_3N), 7.21 (s, 2H, C_6H_2), 7.35 (s, 2H, C_6H_2).

Synthesis of 1-VCl(THF)$_2$. Potassium benzyl (93 mg, 0.714 mmol) and **1-H$_2$** (200 mg, 0.357 mmol) were dissolved in THF (15 mL) and stirred for 30 m. This solution was added to $VCl_3(THF)_3$ (133 mg, 0.357 mmol) and allowed to stir for 30 m. The THF was removed *in vacuuo*. The resulting solid was suspended in diethyl ether and filtered. The filtrate was dried under vacuum to give an orange/brown solid: 166 mg, 59%. ^{1}H NMR (C_6D_6): paramagnetic. Magnetic moment: $\mu_{eff} = 2.90(2)\ \mu_B$. Analysis: Calculated (Found) C: 71.37 (72.04); H: 6.92 (7.53); N: 1.85 (1.70); Cl: 4.68 (4.6).

General Procedure for the Synthesis of Dibenzyl Complexes. The tetrabenzyl complex of titanium, zirconium, or hafnium (0.357 mmol) was dissolved in toluene, pentane, petroleum ether or diethyl ether (10 mL). The ligand (0.357 mmol) predissolved in the same solvent (10 mL) was added to the metal. The reaction was stirred for 1 h. The solvent was removed *in vacuuo*. Recrystallization was achieved by dissolving in pentane or petroleum ether and cooling to -35°C for a few days.

1-TiBn$_2$. Orange solid: 136 mg, 71%. ^{1}H NMR (300 MHz, C_6D_6): δ 1.88 (dd, 12H, Ad), 2.25 (s, 6H, Ad), 2.33 (s, 6H, CH_3), 2.87 (s, 12H, Ad), 4.05 (s, 4H, CH_2), 6.30 (t, 2H, C$_6H_5$), 6.47 (t, 4H, C$_6H_5$), 6.71 (t, 1H, *p*-C$_5H_3$N), 6.87 (m; 2H, *m*-C$_5H_3$N; 4H, C$_6H_5$; 2H, C$_6H_2$), 7.38 (s, 2H, C$_6H_2$). Analysis: Calculated (Found) C: 80.79 (80.57); H: 7.29 (7.18); N: 1.78 (1.76).

2-TiBn$_2$. Orange solid: 137 mg, 86%. ^{1}H NMR (500 MHz, C_6D_6): δ 2.27 (s, 18H, C(CH_3)$_3$), 2.57 (s, 6H, CH_3), 4.13 (s, 4H, CH_2), 6.59 (t, 2H, C$_6H_5$, J = 7 Hz), 6.76 (t, 4H, C$_6H_5$, J = 8 Hz), 6.99 (t, 1H, *p*-C$_5H_3$N, J = 8 Hz), 6.80 (d, 4H, C$_6H_5$, J = 7.5 Hz), 7.14 (s, 2H, C$_6H_2$), 7.42 (s 2H, C$_6H_2$), 7.73 (d, 2H, *m*-C$_5H_3$N, J = 2 Hz). ^{13}C NMR (125

MHz, C_6D_6): δ 21.65, 31.68, 36.00, 85.53, 123.15, 123.68, 129.72, 129.93, 130.84, 137.02, 137.76, 139.02, 156.96, 157.11.

3-TiBn$_2$. Berry red solid: 131 mg, 69%. ^{1}H NMR (300 MHz, C_6D_6): δ 1.84 (dd, 12H, Ad), 2.20 (s, 6H, Ad), 2.27 (s, 6H, CH_3), 2.80 (s, 12H, Ad), 3.71 (s, 2H, CH_2), 4.19 (s, 2H, CH_2), 6.44 (t, 1H, *p*-C$_6H_4$), 6.56 (d, 2H, *m*-C$_6H_4$), 6.62 (s, 1H, C$_6H_4$), 6.65 (d, 2H, C$_6H_5$), 6.67 (d, 2H, C$_6H_5$), 6.86 (s, 2H, C$_6H_2$), 6.94 (t, 4H, C$_6H_5$), 7.28 (s, 2H, C$_6H_2$), 7.38 (d, 2H, C$_6H_5$).

4-TiBn$_2$. Dark red crystals: 219 mg, 55%. ^{1}H NMR (500 MHz, C_6D_6): δ 1.65 (s, 18H, C(CH_3)$_3$), 2.02 (s, 2H, CH_2), 2.26 (s, 6H, CH_3), 3.49 (s, 2H, CH_2), 6.65 (s, 1H, C$_6H_4$), 6.67 (d, 2H, J = 7 Hz, C$_6H_5$), 6.75 (t, 1H, J = 7.5 Hz, C$_6H_5$), 6.90 (m, 3H, J = 7.5 Hz, C$_6H_5$), 7.03 (d, 2H, J = 8 Hz, C$_6H_5$), 7.06 (bs, 2H, C$_6H_2$), 7.10 (m, 5H, J = 8.5 Hz, C$_6H_4$ and C$_6H_5$), 7.28 (d, 2H, J = 2 Hz, C$_6H_2$). ^{13}C NMR (125 MHz, C_6D_6): δ 21.54, 30.72, 35.92, 94.85, 96.99, 124.14, 124.34, 127.22, 127.92, 128.01, 128.09, 128.14, 128.29, 128.84, 128.91, 131.84, 131.99, 135.84, 138.28, 142.30, 145.06, 146.41, 161.75.

1-ZrBn$_2$. Yellow solid: 147 mg, 99%. ^{1}H NMR (500 MHz, C_6D_6): δ 1.92 (dd, 12H, Ad, J = 12 Hz, J = 60 Hz), 2.22 (s, 6H, Ad), 2.28 (s, 6H, CH_3), 2.62 (s, 12H, Ad), 3.42 (s, 4H, CH_2), 6.27 (t, 2H, C$_6H_5$, J = 7.5 Hz), 6.46 (t, 4H, C$_6H_5$, J = 8 Hz), 6.71 (s, 2H, C$_6H_2$), 6.81 (t, 1H, *p*-C$_5H_3$N, J = 8.5 Hz), 6.87 (d, 2H, *m*-C$_5H_3$N, J = 7.5 Hz), 6.98 (d, 4H, C$_6H_5$, J = 7 Hz), 7.25 (s, 2H, C$_6H_2$). ^{13}C NMR (125 MHz, C_6D_6): δ 21.61, 30.07, 38.01, 42.29, 63.04, 122.91, 125.16, 126.03, 129.13, 129.39, 129.67, 130.11, 130.40, 130.56, 137.72, 138.59, 154.81, 159.75.

1-HfBn$_2$. Tan solid: 81 mg, 98%. ^{1}H NMR (500 MHz, C_6D_6): δ 1.92 (dd, 12H, Ad, J = 12 Hz, J = 62 Hz), 2.22 (s, 6H, Ad), 2.29 (s, 6H, CH_3), 2.65 (s, 12H, Ad), 3.16 (s,

4H, CH_2), 6.32 (t, 2H, C_6H_5, J = 7 Hz), 6.49 (t, 4H, C_6H_5, J = 8 Hz), 6.70 (s, 2H, C_6H_2), 6.74 (t, 1H, *p*-C_5H_3N, J = 8 Hz), 6.84 (d, 2H, *m*-C_5H_3N, J = 8 Hz), 6.98 (d, 4H, C_6H_5, J = 11 Hz), 7.28 (s, 2H, C_6H_2). ^{13}C NMR (125 MHz, C_6D_6): δ 21.59, 30.08, 38.04, 42.22, 69.81, 123.06, 124.96, 126.03, 128.89, 129.049, 129.67, 130.02, 130.28, 130.67, 138.27, 138.89, 155.34, 159.44.

Propylene Polymerization. An Andrews Glass Co. vessel was charged with MAO and toluene and fitted with a pressure regulator with a Swagelok quick-connect valve and septum. The vessel was cooled to 0°C and propylene was condensed (30 mL). The catalyst was dissolved in toluene and injected into the vessel. After the polymerization was complete, the system was vented and the residue was quenched with acidified methanol. The polymers were filtered and dried under vacuum prior to analysis.

Fractionation. A Kumagawa extractor was used for the fractionation experiment. Each solvent (diethyl ether, hexanes, and heptanes) was refluxed for 36 hours. The solvent was transferred to a round bottom flask and dried with a rotary evaporator. The polymers were dried on the high vacuum line prior to analysis.

1-Hexene Polymerization. Specially made 15 mL Schlenk flasks that fit septa on the side arm were charged with MAO and tetradecane (internal standard). Toluene and monomer were vacuum transferred into the reaction vessels in the desired amounts. While purging with argon, an aliquot was removed and quenched with butanol for the initial GC trace. The catalyst was dissolved in toluene and injected into the vessels. At intervals during the polymerization, aliquots were removed and quenched for GC analysis. When the polymerization had proceeded to the desired completion, the vessels

were vented and the residue was quenched with acidified methanol. The polymers were filtered and dried under vacuum prior to analysis.

Ethylene/1-Octene Polymerization. Specially made 15 mL Schlenk flasks that fit septa on the side arm were charged with MAO (1000 eq.) and 1-octene. Toluene was vacuum transferred into the reaction vessels in the desired amount after degassing the 1-octene. An atmosphere of ethylene was introduced after the reaction vessel warmed to rt. A catalyst solution in toluene was injected through the side arm while ethylene was flowing. The reaction vessels were left open to the ethylene source such that a constant atmosphere of ethylene was always present. The polymerizations were quenched with acidified methanol. The polymers were filtered and dried under vacuum prior to analysis.

Polymer ^{13}C NMR Analysis. All samples were dissolved in 10 mm NMR tubes in a mixture of solvent (tetrachloroethane-d_2/*o*-dichlorobenzene-d_4 (1/4 v/v)) with typical concentrations of 0.1 g/mL. The tubes were then heated in a heating block set at 150ºC. The sample tubes were repeatedly vortexed and heated to achieve a homogeneous flowing fluid. Finally the sample tubes were left in the heat block for 12 hours. The ^{13}C NMR spectra were taken on a Varian Inova Unity 400 MHz spectrometer. The following acquisition parameters were used: 1.4 seconds relaxation delay, 2.6 seconds acquisition time, 90 degree pulse of 14.5 μs, full NOE with Waltz decoupling, 2000-8000 scans. All measurements were taken without sample spinning and at 126 ± 1°C, calibrated by ethylene glycol. The ^{13}C NMR spectra were referenced at 74.24 ppm for the center peak of tetrachloroethane-d_2.

References

1. *Chem. Eng. News* **1998,** *76*, 1.

2. Brintzinger, H. H.; Fischer, D.; Mulhaupt, R.; Rieger, B.; Waymouth, R. M. *Angew. Chem. Int. Ed. Eng.* **1995,** *34*, 1143-1170.

3. Britovsek, G. J. P.; Gibson, V. C.; Wass, D. F. *Angew. Chem. Int. Ed.* **1999,** *38*, 428-447.

4. Coates, G. W. *Chem. Rev.* **2000,** *100*, 1223-1252.

5. Coates, G. W.; Hustad, P. D.; Reinartz, S. *Angew. Chem. Int. Ed.* **2002,** *41*, 2236-2257.

6. Gibson, V. C.; Spitzmesser, S. K. *Chem. Rev.* **2003,** *103*, 283-315.

7. Resconi, L.; Cavallo, L.; Fait, A.; Piemontesi, F. *Chem. Rev.* **2000,** *100*, 1253-1345.

8. Agapie, T.; Henling, L. M.; DiPasquale, A. G.; Rheingold, A. L.; Bercaw, J. E. *Organometallics* **2008,** *27*, 6245-6256.

9. Chan, M. C. W.; Tam, K.-H.; Pui, Y.-L.; Zhu, N. *J. Chem. Soc., Dalton Trans.* **2002**, 3085-3087.

10. Chan, M. C. W.; Kui, S. C. F.; Cole, J. M.; McIntyre, G. J.; Matsui, S.; Zhu, N.; Tam, K.-H. *Chem. Eur. J.* **2006,** *12*, 2607-2619.

11. Chan, M. C. W.; Tam, K.-H.; Zhu, N.; Chiu, P.; Matsui, S. *Organometallics* **2006,** *25*, 785-792.

12. Tam, K.-H.; Lo, J. C. Y.; Guo, Z.; Chan, M. C. W. *J. Organomet. Chem.* **2007,** *692*, 4750-4759.

13. Gademann, K.; Chavez, D. E.; Jacobsen, E. N. *Angew. Chem. Int. Ed.* **2002,** *41*, 3059-3061.

14. Milne, J. E.; Buchwald, S. L. *J. Am. Chem. Soc.* **2004,** *126*, 13028-13032.

15. Evans, D. F. *J. Chem. Soc.* **1959**, 2003-2005.

16. Agapie, T.; Day, M. W.; Bercaw, J. E. *Organometallics* **2008,** *27*, 6123-6142.

17. Tonks, I. A.; Henling, L. M.; Day, M. W.; Bercaw, J. E. *Inorg. Chem.* **2009,** *48*, 5096-5105.

18. The catalysts appeared to be active for at least two hours, although all polymerizations reported here were quenched after 30 minutes.

19. Frank, H. *Oster. Chem. Zeit.* **1967,** *68*, 360-361.

20. Zambelli, A.; Sessa, I.; Grisi, F.; Fusco, R.; Accomazzi, P. *Macromol. Rapid Commun.* **2001,** *22*, 297-310.

21. Gambarotta, S. *Coord. Chem. Rev.* **2003,** *237*, 229-243.

22. Schmidt, R.; Welch, M. B.; Knudsen, R. D.; Gottfried, S.; Alt, H. G. *J. Mol. Catal. A: Chem.* **2004,** *222*, 17-25.

23. Sato, Y.; Nakayama, Y.; Yasuda, H. *J. Appl. Polym. Sci.* **2003,** *89*, 1659-1662.

24. Doi, Y.; Suzuki, S.; Soga, K. *Macromolecules* **1986,** *19*, 2896-2900.

25. Groysman, S.; Tshuva, E. Y.; Reshef, D.; Gendler, S.; Goldberg, I.; Kol, M.; Goldschmidt, Z.; Shuster, M.; Lidor, G. *Isr. J. Chem.* **2002,** *42*, 373-381.

26. Lin, S.; Waymouth, R. M. *Macromolecules* **1999,** *32*, 8283-8290.

27. De Rosa, C.; Auriemma, F.; Spera, C.; Talarico, G.; Tarallo, O. *Macromolecules* **2004,** *37*, 1441-1454.

28. Bovey, F. A.; Tiers, G. V. D. *J. Polym. Sci.* **1960,** *44*, 173-182.

29. Doi, Y.; Asakura, T. *Makromol. Chem.* **1975,** *176*, 507-509.

30. Doi, Y.; Suzuki, E.; Keii, T. *Makromol. Chem., Rapid Commun.* **1981,** *2*, 293-297.

31. Sheldon, R. A.; Rueno, T.; Tsunetsugu, T.; Furakawa, J. *J. Polym. Sci.* **1965,** *3*, 23-26.

32. Similar results were expected for **1-TiCl$_2$(THF)**, **1-TiBn$_2$**, **2-TiBn$_2$**, and **1-ZrBn$_2$** because the ^{13}C NMR spectra for crude polymer are comparable; implying that the coordinated THF does not influence the type of polymer produced.

33. Golisz, S. R.; Bercaw, J. E. *Manuscript in preparation*.

34. Trimethylaluminum was added to the ligands **1-H$_2$** and **2-H$_2$** to form bisphenolate aluminum methyl complexes (**1-AlMe** and **2-AlMe**). Both of these aluminum species were subjected to standard propylene polymerization conditions, and in neither case was any PP observed. Additional reactions where only ligand was subjected to standard propylene polymerization conditions were also performed in the hope that an aluminum species which was capable of polymerizing propylene might form in situ. Again, no polymer was observed.

35. Makio, H.; Kashiwa, N.; Fujita, T. *Adv. Synth. Catal.* **2002,** *344*, 477-493.

36. Mitani, M.; Saito, J.; Ishii, S.-I.; Nakayama, Y.; Makio, H.; Matsukawa, N.; Matsui, S.; Mohri, J.-I.; Furuyama, R.; Terao, H.; Bando, H.; Tanaka, H.; Fujita, T. *Chem. Rec.* **2004,** *4*, 137-158.

37. Calderazzo, F.; Englert, U.; Pampaloni, G.; Santi, R.; Sommazzi, A.; Zinna, M. *J. Chem. Soc., Dalton Trans.* **2005**, 914-922.

38. NMR scale reactions were performed using **1-H$_2$** or **1-TiCl$_2$(THF)** in bendene-d_6 to show no reaction upon mixing at room temperature, nor was there a reaction at 90°C.

39. Murray, M. C.; Baird, M. C. *Can. J. Chem.* **2001,** *79*, 1012-1018.

40. Randall, J. C. *J. Macromol. Sci., Rev. Macromol. Chem. Phys.* **1989,** *C29*, 201-317.

41. Hagen, H.; Boersma, J.; Lutz, M.; Spek, A. L.; van Koten, G. *Eur. J. Inorg. Chem.* **2001**, 117-123.

42. Wu, J.-Q.; Pan, L.; Li, Y.-G.; Liu, S.-R.; Li, Y.-S. *Organometallics* **2009,** *28*, 1817-1825.

43. Burger, B. J.; Bercaw, J. E. *ACS Symp. Ser.* **1987,** *357*, 79-98.

44. Marvich, R. H.; Brintzinger, H. H. *J. Am. Chem. Soc.* **1971,** *93*, 2046-2048.

45. Manzer, L. *Inorg. Syn.* **1982,** *21*, 135-140.

46. Zucchini, U.; Giannini, U.; Albizzat, E.; Dangelo, R. *J. Chem. Soc., Chem. Commun.* **1969**, 1174-1175.

Chapter Two

Intramolecular C-H Activation of a Bisphenolate(benzene) Ligated Titanium Dibenzyl Complex. Competing Pathways Involving α-Hydrogen Abstraction and σ-Bond Metathesis.

Abstract

A titanium dibenzyl complex featuring a ligand with two phenolates linked by a benzene-1,3-diyl was found to undergo thermal decomposition to give toluene and a cyclometalated dimeric complex. The thermal decomposition followed first-order kinetics and was studied at a number of temperatures to determine the activation parameters ($\Delta H^{\ddagger}$ = 27.2(5) kcal/mol and $\Delta S^{\ddagger}$ = -6.2(14) cal/mol·K). Deuterated isotopologs were synthesized to measure the kinetic isotope effects. The complexes with deuterium in the benzyl methylene positions decomposed slower than the protio analogs. Isotopologs of toluene with multiple deuteration positions were observed in the product mixtures. These data are consistent with competing α-abstraction and σ-bond metathesis.

Introduction

Metal-benzyl linkages are common in the field of olefin polymerization as they can be activated by methylaluminaoxane (MAO) or stoichiometric activators (e.g. $[Ph_3C][BF_4]$). Tetrabenzyl titanium has been known to polymerize ethylene and α-olefins since 1968.[1] More recently, metal-benzyl linkages have received attention in the field of C-H bond activation.[2-12] Fundamental transformations such as C-H bond activation are usually invoked as elementary steps of higher order catalytic reactions such as polymerization, dehydrogenation, or alkane functionalization.[13]

We have recently reported group 4 dibenzyl complexes having two phenolates linked by 2,6-pyridyl, 2,5-pyrazolyl, 2,5-furanyl, 2,5-thiophenyl, or benzene-1,3-diyl groups that are active for olefin polymerization.[14-15] Attempts to activate the titanium dibenzyl complex having the bisphenolate(benzene-1,3-diyl) ligand by treatment with

substoichiometric amounts of reagents that remove one benzide group gave instead a cyclometalated dimeric product bridged by two phenolate oxygens where activation of the 2-C-H bond of the benzene-1,3-diyl linker resulted in cyclometalation and loss of toluene. This same product could also be obtained by simply heating the neutral dibenzyl complex. Chromium,[16] tantalum,[17-18] and molybdenum[19] complexes having similar ligands show an analogous propensity for C-H activation; although, the resulting products remain monomeric. The mechanism(s) for thermal loss of toluene from the bisphenolate(benzene-1,3-diyl) titanium dibenzyl complex has been examined, and an interesting and unusual process involving parallel pathways has been identified.

Results

Synthesis of $Ti(CH_2C_6H_5)_2[(OC_6H_2\text{-}2\text{-}CMe_3\text{-}4\text{-}CH_3)_2C_6H_3]$ (1) and Its Conversion to Dimer 2. As described in an earlier publication,[15] a bisphenolate(benzene-1,3-diyl) ligand featuring *tert*-butyl groups in the *ortho* positions and methyl groups in the *para* positions has been prepared and metalated using titanium tetrabenzyl ($TiBn_4$) *via* toluene elimination to give a ligated dibenzyl complex (**1**). Heating a solution of **1** in an aromatic solvent facilitates C-H bond activation to give toluene and a cyclometalated complex that readily dimerizes (**2**, see Scheme 1). The dimer was quite asymmetric showing two peaks for the *tert*-butyl groups, two peaks for the methyl groups, and two doublets for the benzyl protons in the ^{1}H NMR spectrum. This evidence alone does not prove dimeric speciation in solution because a monomeric complex featuring a C_2-symmetric ligand with a single benzyl group on the same metal would exhibit identical ^{1}H NMR coupling; however, the monomeric cyclometalated

complex is coordinatively unsaturated and sterically unencumbered due to the tridentate ligand thus making dimerization favorable. A single crystal X-ray structure determination of **2** (Figure 1, Table 1) reveals that each titanium is five-coordinate, bound by the two phenolates of the bisphenolate(benzene-1,3-diyl) ligand, one bridging phenolate oxygen from the ligand on the other titanium, one benzyl group positioned away from the dimer core and bent toward the linker of the ligand, and one phenyl linkage from the now metalated ligand. The reaction forming the dimer is very clean with no detectable amounts of other decomposition or side products, thus amenable to mechanistic study.

Scheme 1

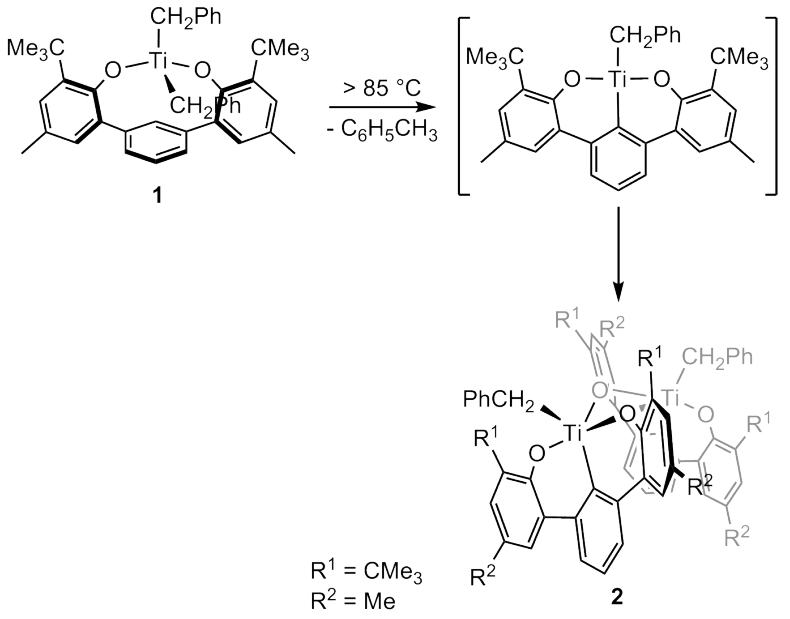

{Ti(CH$_2$C$_6$H$_5$)[(OC$_6$H$_2$-2-CMe$_3$-4-CH$_3$)C$_6$H$_3$(μ_2-OC$_6$H$_2$-2-CMe$_3$-4-CH$_3$]}$_2$

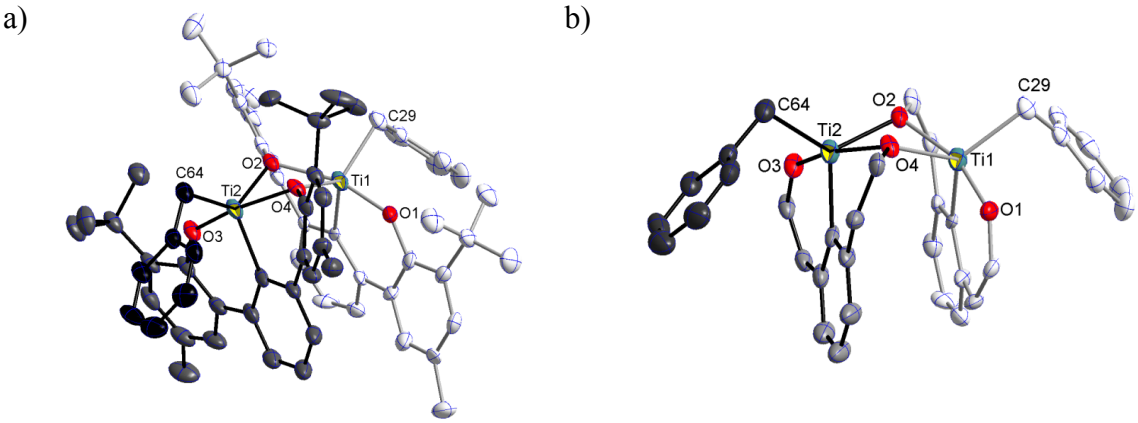

Figure 1. The solid state structure of **2**. Hydrogens have been omitted for clarity: a) side view; b) skeletal view with ligand framework atoms (only) and residual benzyl ligand for each titanium. Selected bond lengths (Å) and angles (°) for **2**: Ti1-O2 2.038(3), Ti1-O4 2.042(3), Ti2-O2 2.049(3), Ti2-O4 2.025(2), O2-Ti1-O4 70.20(11), O2-Ti2-O4 70.34(11), Ti1-C29-C30 105.1(2), Ti2-C64-C65 106.2(2).

Table 1. Crystal and Refinement Data for **2**.

	2
Empirical formula	$C_{70}H_{76}O_4Ti_2$
Formula weight	1077.11
Crystal size (mm^3)	0.15 x 0.12 x 0.01
Temperature (K)	100(2)
a (Å)	14.018(8)
b (Å)	14.480(8)
c (Å)	14.732(10)
α (°)	99.37(3)
β (°)	104.86(4)
γ (°)	92.77(3)
Volume ($Å^3$)	2838.9(3)
Z	2
Crystal system	Triclinic
Space group	P-1
d_{calc} (Mg/m^3)	1.260
θ range (°)	1.79 to 23.31
μ (mm^{-1})	0.331
Abs. correction	Semi-empirical from equivalents
GOF	1.22
R_1,[a] wR_2[b] [$I>2\sigma(I)$]	0.061, 0.064

[a] $R_1 = \Sigma||F_o| - |F_c||/\Sigma|F_o|$. [b] $wR_2 = [\Sigma[w(F_o^2 - F_c^2)^2]/\Sigma[w(F_o^2)^2]]^{1/2}$.

Determination of the Activation Parameters for Conversion of 1 to 2. The transformation of **1** to **2** in *o*-xylene-d_{10} was monitored over a temperature range of 30 K (368-398 K) with first order behavior observed over two half-lives for all temperatures. The rates for the temperature study are reported in Table 2 and the Eyring plot is shown in Figure 2. The activation parameters so derived ($\Delta H^{\ddagger}$ = 27.2(5) kcal/mol and $\Delta S^{\ddagger}$ = -6.1(2) cal/mol·K) are similar to those observed for the thermal decomposition of $Cp^*_2Ti(CH_3)_2$ ($\Delta H^{\ddagger}$ = 27.6(3) kcal/mol and $\Delta S^{\ddagger}$ = -2.9(7) cal/mol·K),[20] (η^5-$C_5H_4CMe_2Ph$)$TiBn_3$ ($\Delta H^{\ddagger}$ = 24(2) kcal/mol and $\Delta S^{\ddagger}$ = -5(5) cal/mol·K),[21] and $Cp^*_2HfBn_2$ ($\Delta H^{\ddagger}$ = 34(1) kcal/mol and $\Delta S^{\ddagger}$ = 1(3) cal/mol·K),[22] where α-hydrogen abstraction has been proposed as the rate determining step. The other commonly proposed mechanism for transformations of early transition metal alkyls is σ-bond metathesis. The reaction between $Cp^*_2ScCH_3$ and 4-methylstyrene in hydrocarbon solvent at elevated temperature results in $Cp^*_2ScCH{=}CH(p\text{-}C_6H_4CH_3)$ and methane with $\Delta H^{\ddagger}$ = 12 kcal/mol and $\Delta S^{\ddagger}$ = -36 cal/mol·K via a σ-bond metathesis process.[23]

Figure 2. The Eyring plot for the formation of **2**.

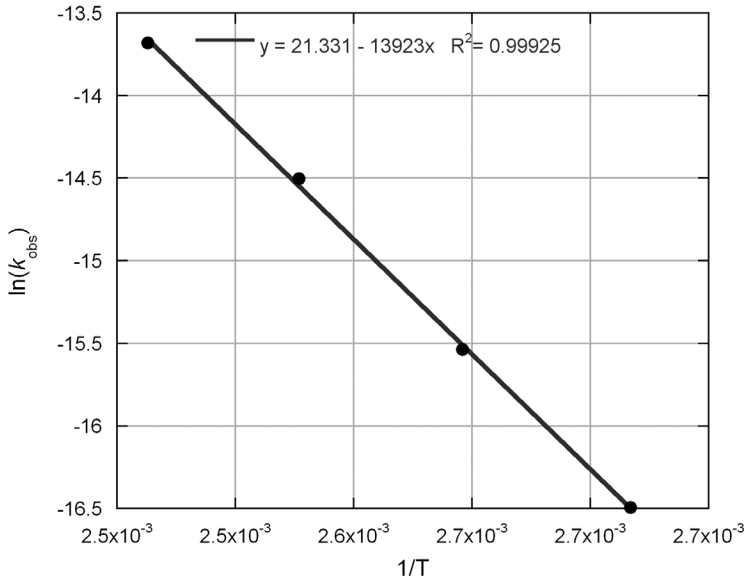

Table 2. Rate data and activation parameters for the formation of **2**.

T (K)	k_{obs} (s^{-1})
368	2.27(5) x 10^{-5}
378	6.62(3) x 10^{-5}
388	1.7(1) x 10^{-4}
398	4.0(5) x 10^{-4}
$\Delta H^{\ddagger}$ = 27.2(5) kcal/mol	
$\Delta S^{\ddagger}$ = -6.2(14) cal/mol·K	

Kinetic Isotope Effects Associated with Conversion of 1 to 2. A number of complexes suitable for kinetic isotope experimentation have been prepared by selectively incorporating deuterium in the ligand or the benzyl groups (Figure 3). The synthesis of

an analogous version of the ligand having a partially deuterated benzene-1,3-diyl linker has been reported.[17-18] As such, it was straightforward to synthesize the ligand-deuterated titanium dibenzyl complex **1-*d*$_3$** by using perdeuterated aniline to generate the partially deuterated 1,3-dibromobenzene-d_3 prior to the coupling with the two phenolates. The procedure used for the synthesis of benzyl groups deuterated at either the methylene or phenyl positions is shown in Scheme 2. Benzoic acid (or benzoic acid-d_5) was reduced with $LiAlD_4$ (or $LiAlH_4$) to give the partially deuterated benzyl alcohol. The benzyl alcohol was converted to the benzyl chloride with $SOCl_2$ in the presence of benzotriazole. Addition of magnesium turnings to freshly distilled benzyl chloride in dry diethyl ether afforded the benzyl magnesium chloride Grignard, which was readily metalated with titanium tetrachloride. The deuterated tetrabenzyl titanium complexes were crystallized from petroleum ether. Mixing the protio-ligand with the deuterated tetrabenzyl titanium complexes gave the isotopologs **1-*d*$_4$**, **1-*d*$_{10}$**, and **1-*d*$_{14}$** shown in Figure 3. The reaction rates of the isotopologs were monitored at 388 K in *o*-xylene-d_{10} and showed first-order behavior over at least two half-lives (Figure 4 and Table 3).

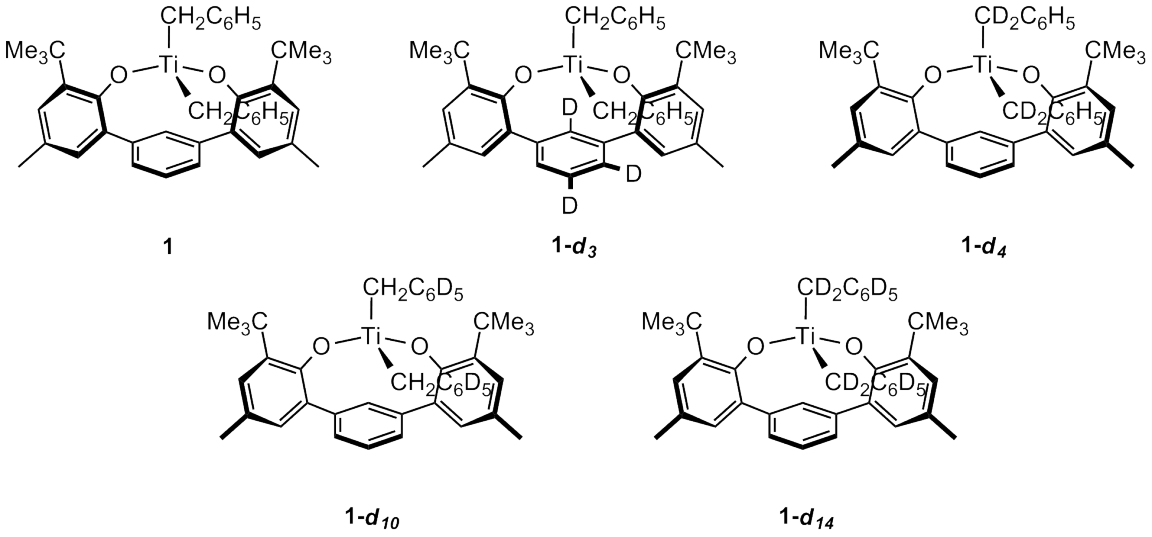

Figure 3. The isotopologs of **1**.

Scheme 2

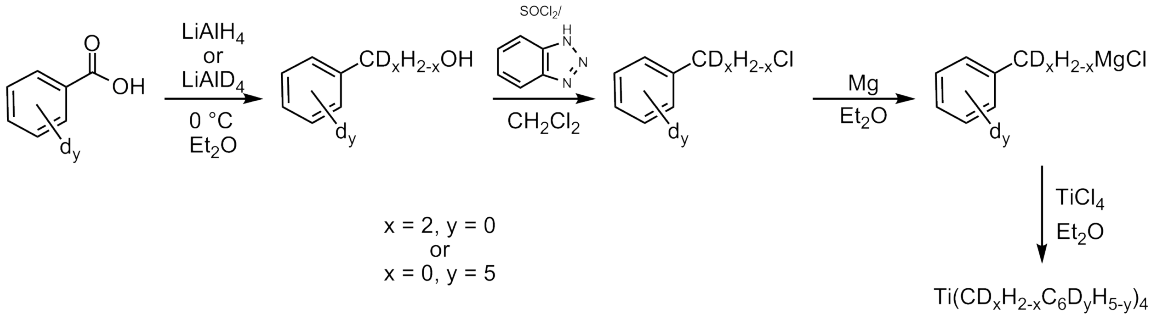

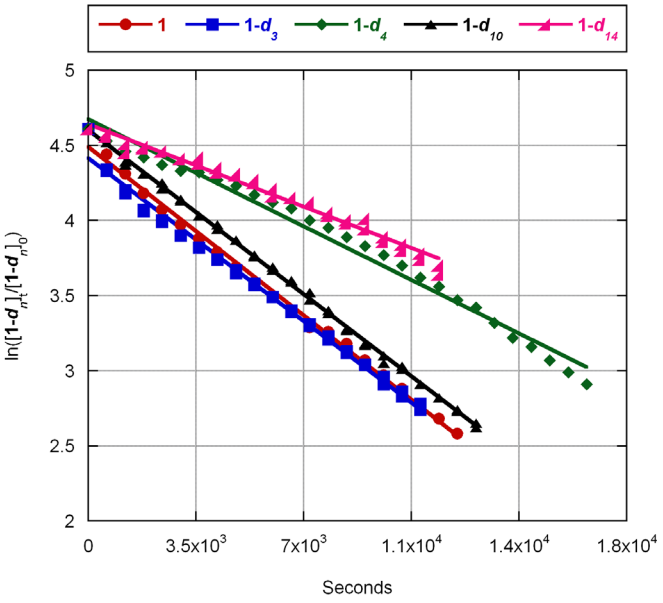

Figure 4. A plot of the rates of the thermolysis of **1** and its isotopologs in *o*-xylene-d_{10} at 388 K.

Table 3. The rates of the thermolysis of **1** and its isotopologs in *o*-xylene-d_{10} at 388 K.

Isotopolog	k_{obs} (s^{-1})	H/D labeling of the evolved toluenes[a]		H/D labeling of methylene for the residual benzyl of **2**[b]	
1	1.7(1) x 10^{-4}	100%	$C_6H_5CH_3$	100%	[Ti-CH_2-Ph]
1-*d*$_3$	1.55(2) x 10^{-4}	56%	$C_6H_5CH_3$	54%	[Ti-CHD-Ph]
		44%	$C_6H_5CH_2D$	46%	[Ti-CH_2-Ph]
1-*d*$_4$	9.5(7) x 10^{-5}	84%	$C_6H_5CHD_2$		[Ti-CD_2-Ph]
		16%	$C_6H_5CD_3$	15%	[Ti-CHD-Ph]
1-*d*$_{10}$	1.58(2) x 10^{-4}	100%	$C_6D_5CH_3$	100%	[Ti-CH_2-Ph]
1-*d*$_{14}$	7.8(2) x 10^{-5}	78%	$C_6D_5CHD_2$		[Ti-CD_2-Ph]
		22%	$C_6D_5CD_3$	13%	[Ti-CHD-Ph]

[a]Approximate ratio of labeled toluenes were determined by ^{1}H NMR analysis of the product toluene methyl resonance for **1**, **1-*d*$_3$**, and **1-*d*$_{10}$** and ^{2}H NMR analysis of the product toluene methyl resonance for **1-*d*$_4$**, and **1-*d*$_{14}$**. [b]Approximate amount of labeled methylene groups were determined by ^{1}H NMR analysis of the product methylene resonance.

The rates of **1**, **1-*d*$_3$**, and **1-*d*$_{10}$** were approximately the same while the rates for **1-*d*$_4$** and **1-*d*$_{14}$** were similar to each other but slower than the other three complexes, suggesting that rate-limiting α-H abstraction from one benzyl group, generating one equivalent of toluene and a titanium benzylidene, is an important step in the overall conversion. However, the most interesting and revealing outcomes are the isotopic compositions of the toluenes liberated from some of the isotopologs (Table 3) which

imply that α-abstraction is not the only process. For complexes **1** and **1-*d*$_{10}$** only protons were observed in the methyl group of the toluene. However, for **1-*d*$_3$**, a roughly equal molar mixture of $C_6H_5CH_3$ and $C_6H_5CH_2D$ was found, and for **1-*d*$_4$** (or **1-*d*$_{14}$**), two isotopologs of toluene, a major component, $C_6H_5CHD_2$ (or $C_6D_5CHD_2$), and a minor component, $C_6H_5CD_3$ (or $C_6D_5CD_3$), were observed. Concomitant with the observed toluene isotopolog ratios, two isotopologs were observed in the benzyl methylene groups of the products of **1-*d*$_3$**, **1-*d*$_4$**, and **1-*d*$_{14}$** whose ratios were roughly complementary with those for the toluene (Table 3). In the ^{1}H NMR spectrum for **2** (obtained from thermolysis of **1** or **1-*d*$_{10}$**), the [Ti-C*H*$_2$-Ph] of the benzyl appeared as two doublets at 2.97 and 4.02 ppm with a coupling constant of 10 Hz. The products of thermolysis of **1-*d*$_3$**, **1-*d*$_4$**, and **1-*d*$_{14}$** contain, in addition to these two doublets attributable to [Ti-C*H*$_2$-Ph], two additional singlets at 2.94 and 3.97 ppm due to [Ti-C*H*D-Ph], shifted slightly upfield because of the heavy isotope shift (Figure 5). The H-D coupling for the latter was not resolved; however, this H-D coupling is not always resolved, e.g. for [Ti-C*H*D-Ph] in a monomeric tucked-in cyclopentadienyl complex (η^5:η^1-$C_5H_4CMe_2C_6D_4$)Ti(CH_2Ph)(CHDPh).[21]

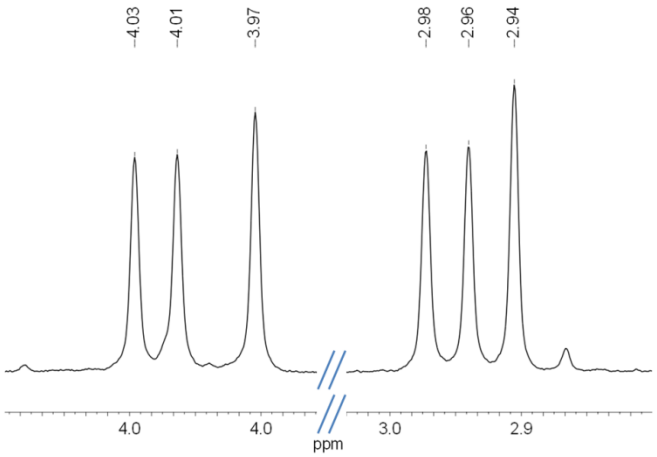

Figure 5. The ^{1}H NMR (C_6D_6) spectrum of the methylene of the residual benzyl of **2**, synthesized from **1-*d*$_3$**.

Other Metals. The rates for the analogous per-protio complexes with zirconium and hafnium were qualitatively different than **1**. The thermal decomposition of the zirconium complex was significantly faster than **1** while the hafnium complex was considerably slower than **1**. Both the zirconium and hafnium complexes generated the analogous dimeric product (**2**). These observations may suggest that the mechanism for either zirconium or hafnium is different than titanium; however, the data is too preliminary.

Discussion

The enthalpy and entropy of activation are similar to systems which are known to undergo C-H activation *via* rate determining α-abstraction,[20-22] and the kinetic isotope effect (KIE) for each isotopolog also implied α-abstraction was the rate determining step—the rates for **1-*d*$_4$** and **1-*d*$_{14}$** which have deuterium in the benzyl methylene

positions are approximately half those for **1**, **1-*d*$_3$**, and **1-*d*$_{10}$** which have protons in those positions. On the other hand, the toluene distribution (Table 3) cannot be explained by simple α-abstraction. We considered the possibility that the α-abstraction step is reversible, such that the eliminated toluene can reinsert into the benzylidene intermediate thus accounting for the isotope distribution. However, when **1** was heated in the presence of toluene-d_8, only $C_6H_5CH_3$ and toluene-d_8 were observed. An alternate explanation for the toluene distribution is a bimetallic process. When equimolar amounts of **1** and **1-*d*$_{14}$** were heated together, neither $C_6H_5CH_2D$ nor $C_6D_5CH_2D$ were observed. Therefore, the mechanism most consistent with the data is two competing pathways: α-abstraction and σ-bond metathesis (Scheme 4).[24]

Scheme 4

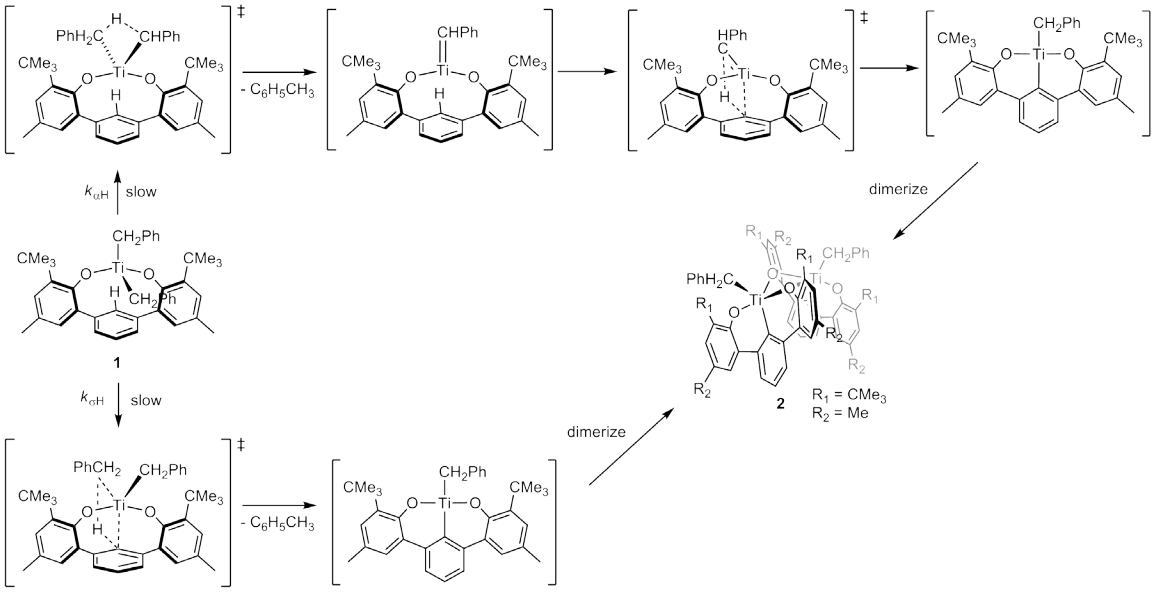

The α-abstraction process involves one benzyl group abstracting a methylene hydrogen from the other benzyl group to form a benzylidene and toluene. The C-H bond of the benzene-diyl linker undergoes 1,2-insertion into the Ti-C bond of the benzylidene to form the four-coordinate cyclometalated species. The σ-bond metathesis involves the C-H bond of the benzene-diyl linker approaching the metal-benzyl linkage to form a four-center transition state. A concerted event leads to the formation of the new Ti-C bond and release of toluene. In the case of **1**, the two mechanisms cannot be differentiated because the toluene product is the same under either mechanism. The same is true for the **1-*d*$_{10}$** example as only $C_6D_5CH_3$ toluene was observed in the ^{1}H NMR spectrum. In the case of **1-*d*$_3$**, α-abstraction leads to $C_6H_5CH_3$ while σ-bond metathesis leads to $C_6H_5CH_2D$. Comparing the amounts of toluene allows for the determination of the relative rates of protio α-abstraction ($k_{\alpha H}$) versus deutero σ-bond metathesis ($k_{\sigma D}$). The isotopologs which have deuterium in the methylene position of the benzyl groups (**1-*d*$_4$** or **1-*d*$_{14}$**) lead to $C_6H_5CD_3$ or $C_6D_5CD_3$ when the reaction proceeds via α-abstraction and $C_6H_5CHD_2$ or $C_6D_5CHD_2$ when the reaction proceeds via σ-bond metathesis. Comparing the toluene ratios using ^{2}H NMR leads to the relative rates of deutero α-abstraction ($k_{\alpha D}$) versus protio σ-bond metathesis ($k_{\sigma H}$). A system of equations can be used to determine the individual rates from the k_{obs} and toluene ratios (see Figure 6). From these equations, the rates and KIE for each process were determined (see Table 5).

$$k_{obs}(\bar{x}[\mathbf{1}, \mathbf{1\text{-}d_{10}}]) = k_{\alpha H} + k_{\sigma H}$$

$$k_{obs}(\mathbf{1\text{-}d_3}) = k_{\alpha H} + k_{\sigma D}$$

$$k_{obs}(\bar{x}[\mathbf{1\text{-}d_4}, \mathbf{1\text{-}d_{14}}]) = k_{\alpha D} + k_{\sigma H}$$

$$44\ k_{\alpha H} = 56\ k_{\sigma D}$$

$$\bar{x}[16, 22]\ k_{\sigma H} = \bar{x}[84, 78]\ k_{\alpha D}$$

Figure 6. The system of equations used to determine the rates.

Table 5. The rates and kinetic isotope effects for both α-abstraction and σ-bond metathesis at 388 K.

α-abstraction		σ-bond metathesis	
$k_{\alpha H}$	= 8.75(2) x 10^{-5}	$k_{\sigma H}$	= 7.04(5) x 10^{-5}
$k_{\alpha D}$	= 1.60(5) x 10^{-5}	$k_{\sigma D}$	= 6.74(2) x 10^{-5}
KIE	= 5.5(3)	KIE	= 1.0(1)

The data show that the kinetic isotope effect is more pronounced for the α-abstraction mechanism. At first, this may seem counterintuitive because σ-bond metathesis processes generally have large KIE (the elimination of CH_4 from $Cp_2Zr(Me)(SCH_2R)$ has a KIE of 5.2(0.2) at 353 K[25] and the reaction of $(Cp^*\text{-}d_{15})_2ScCH_3$ with C_6Y_6 (Y = H or D) at 353 K has a KIE of 2.8(2)),[23] and α-abstraction processes usually have smaller KIE (the thermal decomposition of $(\eta^5\text{-}C_5H_4CMe_2Ph)TiBn_3$ has a KIE of 1.23(0.05) at 338 K[21] and the thermal decomposition of $Cp^*_2HfBn_2$ has KIE of 3.1(2) at 413 K).[22] However, in related systems which undergo α-abstraction (albeit

different due to the heteroatom), (^{t}Bu$_3$SiO)$_2$Ti(Bn)(^{t}Bu$_3$SiNH)[26] and (^{t}Bu$_3$SiNH)$_3$Zr(Bn)[27] release toluene to form metal-imido species with KIEs of 5.6(2) at 363 K and 7.1(6) at 370 K, respectively. These data show that the value of the KIE is more a result of the geometry of the transition state rather than the mode of the chemical transformation. In the present case, we can interpret the KIEs to mean that the transition state for the α-abstraction process is highly symmetrical with a large amount of bond breaking. The transition state for the σ-bond metathesis process is likely unsymmetrical with the bonds between the C-H of the linker mostly intact. Furthermore, a large amount of rearrangement must occur so that the complex aligns properly for the σ-bond metathesis transition state. This process does not influence the value of the KIE as no bonds have been broken. Instead, the rearrangement manifests as the moderately negative $\Delta S^{\ddagger}$.

Conclusion

The thermal decomposition of **1** generates the cyclometalated dimer **2** and toluene. Both the activation parameters and kinetic isotope effects are consistent with an α-abstraction mechanism. However, the toluene isotopologs and the isotope distribution in **2** suggested that σ-bond metathesis was competitive with α-abstraction. The transition state for the α-abstraction process was very late while the transition state for the σ-bond metathesis was very early as evidenced by the KIEs of 5.5(3) and 1.0(1), respectively.

Experimental

General Considerations. All air- and moisture-sensitive compounds were manipulated under argon or nitrogen using standard glovebox, Schlenk, and high-vacuum line techniques.[28] Argon was purified and dried by passage through columns of MnO on vermiculite and activated 4 Å molecular sieves. Solvents were dried over sodium benzophenone ketyl or titanocene.[29] All organic chemicals were purchased and used as received from Aldrich. The metal precursor $TiCl_4$ was purchased from Strem and used as received. All deuterated compounds were purchased from Cambridge Isotopes. NMR spectra of ligands and metal complexes were recorded on a Varian Unity Inova 500 (499.852 MHz for ^1H) spectrometer. HRMS was obtained from the California Institute of Technology Mass Spectrometry Facility. X-ray quality crystals were mounted on a glass fiber with Paratone-N oil. Data were collected on a Bruker KAPPA APEX II instrument. Structures were determined using direct methods or, in some cases, Patterson maps with standard Fourier techniques using the Bruker AXS software package. The tetrabenzyl titanium[30] was prepared according to a literature procedure. 1,3-Dibromobenzene-d_3[17] and the bisphenolate ligand[15] were prepared as reported previously. All errors are standard deviations.

Ligand-d_3. The protected 2-*tert*-butyl-4-methyl-5-bromophenol[15] (534 mg, 1.9 mmol) was dissolved in THF (30 mL) in a glass vessel with a Kontes valve and cooled to just above its freezing point (-100°C). *tert*-Butyl lithium (3.9 mmol) was added dropwise and the reaction was stirred for 30 m to give a cloudy, light brown mixture. Zinc chloride (177 mg, 1.3 mmol) was added to the reaction mixture and stirred for 30 m to give a transparent orange solution. 1,3-Dibromobenzene-d_3 (200 mg, 0.8 mmol) and

tetrakis(triphenylphosphine) palladium (22 mg, 0.02 mmol) were added to the reaction mixture which was sealed and placed in an oil bath. The mixture was heated at 70°C overnight. The reaction was quenched with H_2O and concentrated under reduced pressure. The remaining aqueous sludge was extracted in CH_2Cl_2, dried over $MgSO_4$, filtered, and dried by rotary evaporation. The crude product was suspended in acidified methanol and heated to reflux to remove both impurities and the protecting group. After cooling to rt, rotary evaporation of the neutralized suspension gave the desired product. Further purification was achieved by column chromatography (Hexanes/CH_2Cl_2, 9:1) to give a pale yellow crystalline solid: 195 mg, 57% yield. ^{1}H NMR (500 MHz, $CDCl_3$): δ 1.47 (s, 18H, C(C*H*$_3$)$_3$), 2.35 (s, 6H, C*H*$_3$), 5.33 (s, 2H, O*H*), 6.97 (s, 2H, C$_6$*H*$_2$), 7.15 (s, 2H, C$_6$*H*$_2$), 7.53 (s, 1H, C$_6$D$_3$*H*). ^{13}C NMR (125 MHz, $CDCl_3$): δ 21.02, 29.91, 35.08, 127.82, 128.21, 128.24, 128.53, 128.89, 129.20, 136.45, 138.94, 139.02, 148.91. HRMS (FAB+) obsd M+ 405.2763, calcd for $C_{28}H_{31}O_2D_3$, 405.2747.

Benzyl Alcohol-*d*$_2$. This compound was synthesized from a modified literature preparation[31] to give a colorless oil: 1.1 g, 84% yield. ^{1}H NMR (500 MHz, $CDCl_3$): δ 1.74 (s, 1H, O*H*), 7.31 (m, 1H, *p*-C$_6$*H*$_5$), 7.38 (d, 4H, $^3J_{H\text{-}H}$ = 4.4 Hz, C$_6$*H*$_5$). ^{13}C NMR (125 MHz, $CDCl_3$): δ 64.91, 127.24, 127.89, 128.77, 140.96. HRMS (EI+) obsd M+ 110.0700, calcd for $C_7H_6OD_2$, 110.0701.

Benzyl Alcohol-*d*$_5$. This compound was synthesized from a modified literature preparation[31] to give a colorless oil: 0.9 g, 98% yield. ^{1}H NMR (500 MHz, $CDCl_3$): δ 1.85 (t, 1H, $^3J_{H\text{-}H}$ = 5.6 Hz, O*H*), 4.68 (d, 2H, $^3J_{H\text{-}H}$ = 5.4 Hz, C*H*$_2$). ^{13}C NMR (125 MHz, $CDCl_3$): δ 65.48, 126.75 (t, $^1J_{C\text{-}D}$ = 24 Hz), 127.33 (t, $^1J_{C\text{-}D}$ = 24 Hz), 128.24 (t, $^1J_{C\text{-}D}$ = 24 Hz), 140.88. HRMS (EI+) obsd M+ 113.0892, calcd for $C_7H_3OD_5$, 113.0889.

Benzyl Chloride-*d_2*. This compound was synthesized from a modified literature preparation[32] to give a yellow oil. The crude mixture was distilled under vacuum to give a colorless oil: 0.6 g, 46% yield. ^{1}H NMR (500 MHz, $CDCl_3$): δ 7.37 (m, 5H, C_6H_5). ^{13}C NMR (125 MHz, $CDCl_3$): δ (*C*D_2 in baseline), 128.40, 128.57, 128.73, 137.36. HRMS (EI+) obsd M+ 128.0379, calcd for $C_7H_5ClD_2$, 128.0362.

Benzyl Chloride-*d_5*. This compound was synthesized from a modified literature preparation[32] to give a brown oil. The crude mixture was distilled under vacuum to give a colorless oil: 0.9 g, 84% yield. ^{1}H NMR (500 MHz, $CDCl_3$): δ 4.61 (s, 2H, CH_2). ^{13}C NMR (125 MHz, $CDCl_3$): δ 46.41, 128.36 (t, $^1J_{C\text{-}D}$ = 24 Hz), 128.44 (t, $^1J_{C\text{-}D}$ = 24 Hz), 137.53. HRMS (EI+) obsd M+ 131.0554, calcd for $C_7H_2ClD_5$, 131.0550.

General Procedure for the Synthesis of the Isotopologs of Tetrabenzyl Titanium. In the glovebox, benzyl chloride (4.6 mmol) was dissolved in diethyl ether. Magnesium turnings (6.9 mmol) were added to the solution. The reaction was monitored by GC/MS. The resulting Grignard was filtered. Titanium tetrachloride (1.1 mmol) was added to the Grignard solution. The reaction was allowed stir at room temperature overnight. The crude mixture was filtered through celite and washed with diethyl ether. The diethyl ether was removed *in vacuuo*. The dark brown sludge was suspended in petroleum ether and filtered to give a dark red solution. Storing the dark red solution in the freezer at -35°C overnight gave dark red crystals of the desired tetrabenzyl titanium isotopolog.

Tetrabenzyl titanium-*d_{28}*. 474 mg, 26% yield. ^{13}C NMR (125 MHz, C_6D_6): δ 96.93 (qn, $^1J_{C\text{-}D}$ = 20 Hz), 124.59 (t, $^1J_{C\text{-}D}$ = 24 Hz), 129.29 (t, $^1J_{C\text{-}D}$ = 24 Hz), 129.56 (t, $^1J_{C\text{-}D}$ = 24 Hz), 142.38.

Tetrabenzyl titanium-*d_{20}*. 250 mg, 30% yield. ^{1}H NMR (500 MHz, C_6D_6): δ 2.81 (s, 8H, C*H*$_2$C$_6$D$_5$). ^{13}C NMR (125 MHz, C_6D_6): δ 98.46, 124.56 (t, $^{1}J_{C\text{-}D}$ = 24 Hz), 129.22 (t, $^{1}J_{C\text{-}D}$ = 24 Hz), 129.53 (t, $^{1}J_{C\text{-}D}$ = 24 Hz), 142.51.

Tetrabenzyl titanium-*d_8*. 132 mg, 29% yield. ^{1}H NMR (500 MHz, C_6D_6): δ 6.60 (dd, 8H, *J* = 1 Hz, *J* = 8 Hz, C$_6$*H*$_5$), 6.95 (tt, 4H, *J* = 1 Hz, *J* = 8 Hz, C$_6$*H*$_5$), 7.09 (tt, 8H, *J* = 1 Hz, *J* = 8 Hz, C$_6$*H*$_5$). ^{13}C NMR (125 MHz, C_6D_6): δ 97.11 (qn, $^{1}J_{C\text{-}D}$ = 20 Hz), 125.10, 129.72, 130.09, 142.59.

General Procedure for the Synthesis of Ligated Titanium Dibenzyl Complexes. Tetrabenzyl titanium (0.357 mmol) was dissolved in toluene (10 mL). The ligand (0.357 mmol) predissolved in the same solvent (10 mL) was added to the metal. The reaction was stirred for 1 h. The solvent was removed *in vacuuo*. Recrystallization was achieved by dissolving in pentane or petroleum ether, filtering, and cooling to -35°C for a few days.

1. Dark red crystals: 220 mg, 55% yield. ^{1}H NMR (500 MHz, C_6D_6): δ 1.65 (s, 18H, C(C*H*$_3$)$_3$), 2.02 (s, 2H, C*H*$_2$C$_6$H$_5$), 2.26 (s, 6H, C*H*$_3$), 3.49 (s, 2H, C*H*$_2$C$_6$H$_5$), 6.65 (s, 1H, C$_6$*H*$_4$), 6.67 (d, 2H, *J* = 7 Hz, CH$_2$C$_6$*H*$_5$), 6.75 (t, 1H, *J* = 7.5 Hz, CH$_2$C$_6$*H*$_5$), 6.90 (m, 3H, *J* = 7.5 Hz, CH$_2$C$_6$*H*$_5$), 7.03 (d, 2H, *J* = 8 Hz, CH$_2$C$_6$*H*$_5$), 7.06 (bs, 2H, C$_6$*H*$_2$), 7.10 (m, 5H, *J* = 8.5 Hz, C$_6$*H*$_4$ and CH$_2$C$_6$*H*$_5$), 7.28 (d, 2H, *J* = 2 Hz, C$_6$*H*$_2$). ^{13}C NMR (125 MHz, C_6D_6): δ 21.54, 30.71, 35.91, 94.85, 96.99, 124.14, 124.34, 127.21, 127.92, 128.01, 128.09, 128.14, 128.28, 128.84, 128.91, 131.83, 131.99, 135.84, 138.27, 142.30, 145.07, 146.41, 161.74.

1-*d_3*. Dark red crystals: 81 mg, 47% yield. ^{1}H NMR (500 MHz, C_6D_6): δ 1.65 (s, 18H, C(C*H*$_3$)$_3$), 2.01 (s, 2H, C*H*$_2$C$_6$H$_5$), 2.25 (s, 6H, C*H*$_3$), 3.49 (s, 2H, C*H*$_2$C$_6$H$_5$), 6.67

(d, 2H, J = 7 Hz, $CH_2C_6H_5$), 6.75 (t, 1H, J = 7.5 Hz, $CH_2C_6H_5$), 6.90 (m, 3H, J = 7.5 Hz, $CH_2C_6H_5$), 7.03 (d, 2H, J = 7 Hz, $CH_2C_6H_5$), 7.06 (bs, 2H, C_6H_2), 7.08 (s, 1H, C_6D_3H), 7.10 (d, 2H, J = 7 Hz, $CH_2C_6H_5$), 7.27 (d, 2H, J = 2 Hz, C_6H_2). ^{13}C NMR (125 MHz, C_6D_6): δ 21.53, 30.69, 35.91, 94.86, 96.99, 124.14, 124.34, 127.91, 128.00, 128.09, 128.27, 128.84, 128.91, 128.92, 131.85, 135.81, 135.84, 138.28, 142.11, 142.18, 145.09, 146.45, 161.75.

1-*d*$_4$. Dark red crystals: 40 mg, 24% yield. ^{1}H NMR (500 MHz, C_6D_6): δ 1.63 (s, 18H, $C(CH_3)_3$), 2.22 (s, 6H, CH_3), 6.57 (t, 1H, J = 1.5 Hz, C_6H_4), 6.63 (dd, 2H, J = 8 Hz, J = 1.5 Hz, C_6H_5), 6.72 (tt, 1H, J = 7 Hz, J = 1.5 Hz, C_6H_5), 6.86 (m, 3H, C_6H_5), 6.99 (d, 1H, J = 1 Hz, C_6H_5), 7.01 (d, 1H, J = 1.5 Hz, C_6H_5), 7.03 (d, 2H, J = 2 Hz, C_6H_2), 7.05 (d, 2H, J = 1 Hz, C_6H_5), 7.09 (s, 1H, C_6H_4), 7.10 (d, 2H, J = 3 Hz, C_6H_4), 7.24 (d, 2H, J = 2 Hz, C_6H_2). ^{13}C NMR (125 Hz, C_6D_6): δ 21.53, 30.74, 35.93, 105.73, 124.14, 124.34, 126.92, 127.98, 128.03, 128.10, 128.15, 128.33, 128.49, 128.83, 128.92, 131.82, 131.99, 135.83, 138.25, 142.34, 144.84, 146.23, 161.71.

1-*d*$_{10}$. Dark red crystals: 61 mg, 41% yield. ^{1}H NMR (500 MHz, C_6D_6): δ 1.63 (s, 18H, $C(CH_3)_3$), 2.00 (s, 2H, $CH_2C_6D_5$), 2.23 (s, 6H, CH_3), 3.46 (s, 2H, $CH_2C_6D_5$), 6.60 (t, 1H, J = 1.5 Hz, C_6H_4), 7.03 (d, 2H, J = 2 Hz, C_6H_2), 7.07 (t, 1H, J = 2.5 Hz, C_6H_4), 7.08 (d, 2H, J = 2 Hz, C_6H_4), 7.24 (d, 2H, J = 2 Hz, C_6H_2). ^{13}C NMR (126 MHz, C_6D_6): δ 21.54, 30.72, 35.92, 94.68, 96.89, 123.72, 124.66, 127.09, 127.69, 127.88, 128.02, 128.09, 128.12, 129.23, 129.53, 131.81, 131.99, 135.82, 138.26, 142.32, 144.76, 146.12, 161.73.

1-*d*$_{14}$. Dark red crystals: 36 mg, 25% yield. ^{1}H NMR (500 MHz, C_6D_6): δ 1.64 (s, 18H, $C(CH_3)_3$), 2.23 (s, 6H, CH_3), 6.55 (t, 1H, J = 1.5 Hz, C_6H_4), 7.03 (d, 2H, J = 2

Hz, C_6H_2), 7.07 (t, 1H, J = 2.5 Hz, C_6H_4), 7.08 (d, 2H, J = 2 Hz, C_6H_4), 7.25 (d, 2H, J = 2 Hz, C_6H_2). ^{13}C NMR (126 MHz, C_6D_6): δ 21.54, 30.75, 35.93, 93.21 (m, 1C, CD_2), 95.70 (m, 1C, CD_2), 123.72, 126.76, 127.38, 127.56, 127.74, 127.87, 128.03 128.10, 128.15, 128.68, 131.79, 131.99, 135.80, 138.22, 142.35, 144.52, 145.92, 161.69.

General Procedure for Monitoring Decomposition. Bisphenolate(benzene-1,3-diyl) titanium dibenzyl complexes (20-25 mg) were dissolved in *o*-xylene-d_{10} (0.5 mL, b.p. 143-145°C) with a small amount of ferrocene (3-5 mg) as the internal standard in a sealed J. Young NMR tube. An initial ^{1}H NMR spectrum was acquired at room temperature. The tube was submerged in an oil bath for regular time intervals where the oil level reached the bottom of the Teflon cap. ^{1}H NMR spectra were recorded at room temperature for each regular time interval. The disappearance of the *tert*-butyl peak was monitored against the ferrocene.

2. Dark brown solution in benzene. ^{1}H NMR (500 MHz, C_6D_6) δ 1.29 (s, 18H, $C(CH_3)_3$), 1.88 (s, 18H, $C(CH_3)_3$), 2.21 (s, 6H, CH_3), 2.27 (s, 6H, CH_3), 2.98 (d, 4H, CH_2, J = 9.7 Hz), 4.02 (d, 4H, CH_2, J = 9.7 Hz), 6.36 (d, 2H, J = 7.4 Hz), 6.42 (m, 6H), 6.53 (t, 4H, J = 7.5 Hz), 6.61 (t, 2H, J = 7.7 Hz), 6.69 (s, 2H), 7.05 (d, 4H, J = 7.1 Hz), 7.24 (s, 2H), 7.27 (s, 2H). ^{13}C NMR (126 MHz, C_6D_6) δ 21.44, 21.71, 30.62, 33.02, 35.23, 35.83, 98.39, 105.39, 124.26, 125.21, 126.13, 126.55, 126.72, 129.00, 130.06, 130.24, 131.59, 132.94, 133.85, 135.55, 136.33, 136.42, 136.78, 138.13, 140.84, 155.17, 158.58.

References

1. Giannini, U.; Zucchini, U. *Chem. Commun.* **1968**, 940.

2. Cleary, B. P.; Eisenberg, R. *Organometallics* **1992,** *11*, 2335-2337.

3. Cleary, B. P.; Eisenberg, R. *J. Am. Chem. Soc.* **1995,** *117*, 3510-3521.

4. Kataoka, Y.; Imanishi, M.; Yamagata, T.; Tani, K. *Organometallics* **1999,** *18*, 3563-3565.

5. Kataoka, Y.; Shizuma, K.; Yamagata, T.; Tani, K. *Chem. Lett.* **2001**, 300-301.

6. Sjövall, S.; Andersson, C.; Wendt, O. F. *Organometallics* **2001,** *20*, 4919-4926.

7. Sjövall, S.; Johansson, M.; Andersson, C. *Organometallics* **1999,** *18*, 2198-2205.

8. Sjövall, S.; Kloo, L.; Nikitidis, A.; Andersson, C. *Organometallics* **1998,** *17*, 579-583.

9. Sjövall, S.; Svensson, P. H.; Andersson, C. *Organometallics* **1999,** *18*, 5412-5415.

10. Tejel, C.; Bravi, R.; Ciriano, M. A.; Oro, L. A.; Bordonaba, M.; Graiff, C.; Tiripicchio, A.; Burini, A. *Organometallics* **2000,** *19*, 3115-3119.

11. Tejel, C.; Ciriano, M. A.; Jiménez, S.; Oro, L. A.; Graiff, C.; Tiripicchio, A. *Organometallics* **2005,** *24*, 1105-1111.

12. Zhu, Y. J.; Fan, L.; Chen, C. H.; Finnell, S. R.; Foxman, B. M.; Ozerov, O. V. *Organometallics* **2007,** *26*, 6701-6703.

13. Labinger, J. A.; Bercaw, J. E. *Nature* **2002,** *417*, 507-514.

14. Agapie, T.; Henling, L. M.; DiPasquale, A. G.; Rheingold, A. L.; Bercaw, J. E. *Organometallics* **2008,** *27*, 6245-6256.

15. Golisz, S. R.; Bercaw, J. E. *Macromolecules* **2009,** *42*, 8751-8762.

16. O'Reilly, M.; Falkowski, J. M.; Ramachandran, V.; Pati, M.; Abboud, K. A.; Dalal, N. S.; Gray, T. G.; Veige, A. S. *Inorg. Chem.* **2009,** *48*, 10901-10903.

17. Agapie, T.; Bercaw, J. E. *Organometallics* **2007,** *26*, 2957-2959.

18. Agapie, T.; Day, M. W.; Bercaw, J. E. *Organometallics* **2008,** *27*, 6123-6142.

19. Sarkar, S.; Carlson, A. R.; Veige, M. K.; Falkowski, J. M.; Abboud, K. A.; Veige, A. S. *J. Am. Chem. Soc.* **2008,** *130*, 1116-1117.

20. McDade, C.; Green, J. C.; Bercaw, J. E. *Organometallics* **1982,** *1*, 1629-1634.

21. Deckers, P. J. W.; Hessen, B. *Organometallics* **2002,** *21*, 5564-5575.

22. Bulls, A. R.; Schaefer, W. P.; Serfas, M.; Bercaw, J. E. *Organometallics* **1987,** *6*, 1219-1226.

23. Thompson, M. E.; Baxter, S. M.; Bulls, A. R.; Burger, B. J.; Nolan, M. C.; Santarsiero, B. D.; Schaefer, W. P.; Bercaw, J. E. *J. Am. Chem. Soc.* **1987,** *109*, 203-219.

24. The involvement of the oxygens as a shuttle for the hydrogen atoms cannot be excluded.

25. Buchwald, S. L.; Nielsen, R. B. *J. Am. Chem. Soc.* **1988,** *110*, 3171-3175.

26. Bennett, J. L.; Wolczanski, P. T. *J. Am. Chem. Soc.* **1997,** *119*, 10696-10719.

27. Schaller, C. P.; Cummins, C. C.; Wolczanski, P. T. *J. Am. Chem. Soc.* **1996,** *118*, 591-611.

28. Burger, B. J.; Bercaw, J. E. *ACS Symp. Ser.* **1987,** *357*, 79-98.

29. Marvich, R. H.; Brintzinger, H. H. *J. Am. Chem. Soc.* **1971,** *93*, 2046-2048.

30. Zucchini, U.; Giannini, U.; Albizzat, E.; Dangelo, R. *J. Chem. Soc., Chem. Commun.* **1969**, 1174-1175.

31. Bialecki, J. B.; Ruzicka, J.; Attygalle, A. B. *J. Labelled Compd. Radiopharm.* **2007,** *50*, 711-715.

32. Chaudhari, S. S.; Akamanchi, K. G. *Synlett* **1999**, 1763-1765.

Chapter Three

Protonolysis of Bipyrimidine Platinum Methyl Complexes

Abstract

The protonolysis of bipyrimidine-ligated platinum (II) complexes was explored. The bipyrimidine platinum dimethyl complex (bpm)$PtMe_2$ was shown to undergo protonation at the metal upon addition of trifluoroacetic acid (tfa) to give a platinum (IV) hydride intermediate which reductively eliminated methane to give (bpm)PtMe(tfa). Using a mixture of deutero- and protio-acid, all isotopologs of methane were observed. The protonation of (bpm)PtMe(tfa) was less straightforward as no intermediates were found, and CH_4, CH_3D, and CH_2D_2 were observed upon addition of a mixture of deutero- and protio-acid. The protonation of a nitrogen of the bpm ligand was also examined and determined improbable under the present conditions. The correlation between kinetic isotope effect and mechanism was discussed.

Introduction

Partial oxidation of alkanes, specifically methane, continues to be an active research area for organometallic chemistry. In 1972, Shilov developed a system for the conversion of methane to methanol using a platinum (II) catalyst and platinum (IV) oxidant under mild conditions with reasonable selectivity (Eq 1).[1] Although not commercially viable due to the expensive oxidant, the discovery sparked an interest in homogeneous, ligated platinum (II) catalysts[2-44] for direct methane conversion.

$$CH_4 + [PtCl_6]^{2-} + H_2O\,(Cl^-) \xrightarrow[H_2O,\ 120°C]{[PtCl_4]^{2-}} CH_3OH\,(CH_3Cl) + [PtCl_4]^{2-} + 2\,HCl \qquad (1)$$

The best system discovered to date involves a bipyrimidine platinum dichloride ((bpm)$PtCl_2$) precatalyst that operates in fuming sulfuric acid with SO_3 as the oxidant (Eq

2). This system exhibits 90% conversion of methane to methyl bisulfate with 81% selectivity.[45]

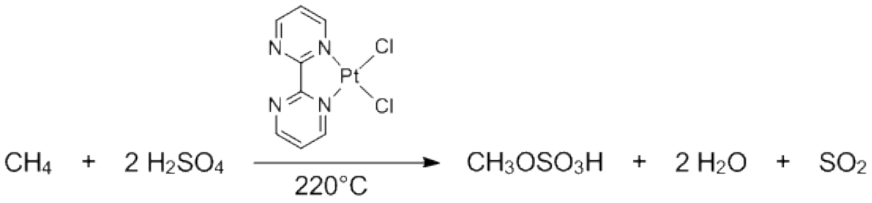

The commonly accepted mechanism for Shilov-type chemistry is a three step catalytic cycle involving a) C-H activation, b) oxidation, and c) reductive elimination (Figure 1).[46] It was subsequently shown by multiple groups that the rate and selectivity determining step was the C-H activation step which could proceed *via* an oxidative addition with a platinum (IV) hydride intermediate or an electrophilic substitution with no change in oxidation state.[47] For the specific case of (bpm)$PtCl_2$, the nature of the C-H activation step is unclear as no experiments have been reported and computational studies indicate that either mechanism is possible.[48-56]

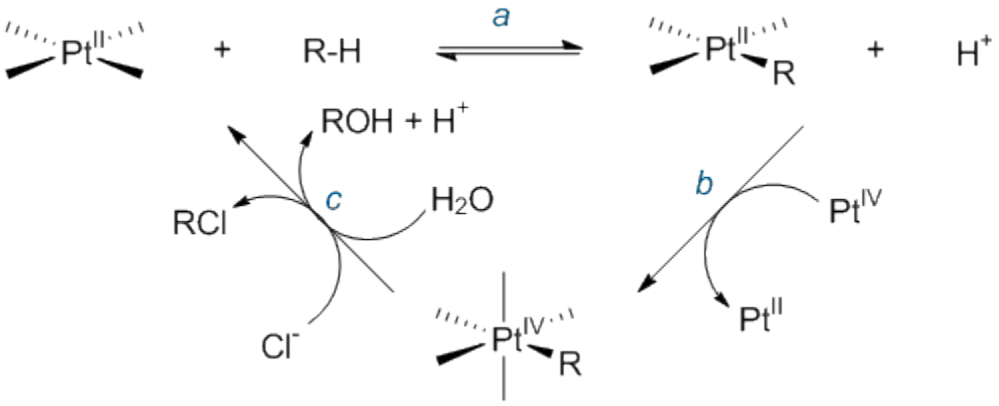

Figure 1. The Shilov Cycle.

In general, C-H activation is difficult to monitor, so the microscopic reverse (protonolysis) is studied. The microscopic reverse of oxidative addition is protonation at the metal, and the microscopic reverse of electrophilic substitution is protonation at the alkyl. Using platinum alkyl complexes which can be protonated with acid, kinetic isotope effects (KIEs) and direct observation of intermediate(s) provide evidence for the mechanism. Experiments directed at elucidating the mechanism of C-H activation by (bpm)$PtCl_2$ have been performed using (bpm)$PtMe_2$ and (bpm)PtMe(tfa).

Results and Discussion

Protonolysis of (bpm)$PtMe_2$. The synthesis of (bpm)$PtMe_2$ (**1**) from bipyrimidine and $[Me_2Pt(\mu\text{-}SMe_2)]_2$ was first reported by Puddephatt in 1986.[57] To ensure that the product was monometallic, a large excess of bipyrimidine was used. The desired product was separated from the remaining ligand by column chromatography with basified silica and crystallized from acetone (Figure 2, crystal and refinement data can be found in Table 1).

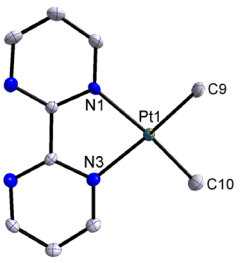

Figure 2. The solid state structure of **1**. Hydrogens have been omitted for clarity. Selected Bond Distances (Å): Pt1-C9 2.038(4), Pt1-C10 2.037(4), Pt1-N1 2.095(3), Pt1-N3 2.092(3).

Table 1. Crystal and Refinement Data.

	1	**2**	**4**	**5**
Empirical formula	$C_{10}H_{12}N_4Pt$	$C_{11}H_9F_3N_4O_2Pt$ • CH_2Cl_2	3.52 ($C_9H_9ClN_4Pt$) 0.48 ($C_8H_6Cl_2N_4Pt$)	$C_{12}H_6F_6N_4O_4Pt$
Formula weight	383.33	566.24	406.29	579.30
Crystal size (mm^3)	0.09 x 0.02 x 0.02	0.22 x 0.07 x 0.03	0.17 x 0.15 x 0.10	0.24 x 0.09 x 0.04
Temperature (K)	100(2)	100(2)	100(2)	160(2)
a (Å)	13.482(5)	8.948(4)	9.547(4)	8.193(4)
b (Å)	15.497(6)	23.271(10)	33.042(13)	20.254(10)
c (Å)	10.185(4)	7.755(3)	13.419(6)	9.733(5)
α (°)	90	90	90	90
β (°)	100.62(2)	96.86(2)	105.51(2)	99.91(3)
γ (°)	90	90	90	90
Volume ($Å^3$)	2091.3(14)	1603.2(12)	4078.6(3)	1590.9(14)
Z	8	4	16	4
Crystal system	Monoclinic	Monoclinic	Monoclinic	Monoclinic
Space group	$P2_1/c$	$P\ 2_1/c$	$P\ 2_1/c$	$P\ 2_1$

d_{calc} (Mg/m^3)	2.44	2.35	2.65	2.42
θ range (°)	2.02 to 32.07	1.75 to 43.07	1.69 to 37.45	2.01 to 33.20
μ (mm^{-1})	13.39	9.13	14.02	8.92
Abs. correction	Semi-empirical from equivalents	Semi-empirical from equivalents	Semi-empirical from equivalents	Gaussian
GOF	1.25	2.07	1.76	1.67
R_1,[a] wR_2[b] [$I>2\sigma(I)$]	0.029, 0.037	0.029, 0.051	0.031, 0.046	0.052, 0.089

[a] $R_1 = \Sigma||F_o| - |F_c||/\Sigma|F_o|$. [b] $wR_2 = [\Sigma[w(F_o^2 - F_c^2)^2]/\Sigma[w(F_o^2)^2]]^{1/2}$.

The protonolysis of **1** was investigated using 25 equivalents of trifluoroacetic acid (10:1 tfa-d_1 to tfa) to determine the KIE (Scheme 1).[58] The reaction occurs immediately as evidenced by the color change from red to golden yellow to give (bpm)PtMe(tfa) (**2**, Figure 3, crystal and refinement data can be found in Table 1). The methane generated from the reaction and the methyl group of **2** were examined to determine the isotope distribution (Table 2). The ^{1}H NMR of the methane region (Figure 4a) clearly shows CH_4, CH_3D, CH_2D_2, and CHD_3 while the Pt-Me region has resonances for Pt-CH_3, Pt-CH_2D, and Pt-CHD_2 (Figure 4b). This abundance of isotopologs indicates that protonation is reversible but does not specify the site of protonation.

Scheme 1

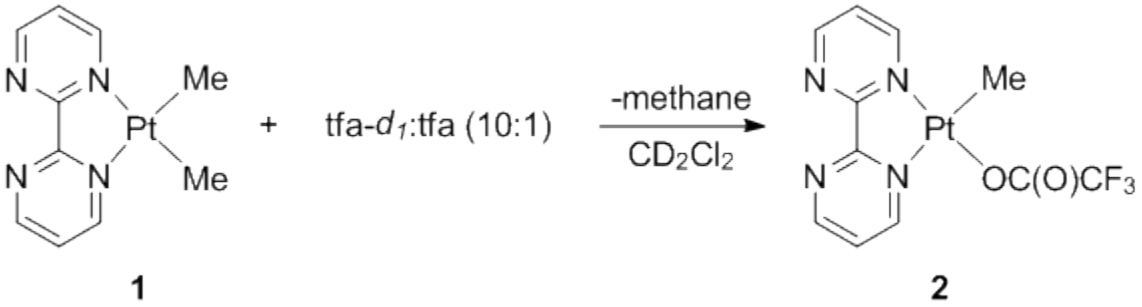

1 **2**

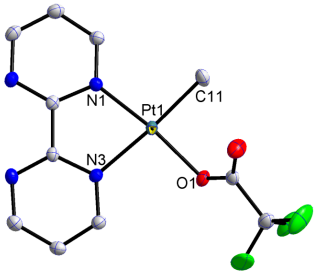

Figure 3. The solid state structure of **2**. Hydrogens have been omitted for clarity. Selected Bond Distances (Å): Pt1-C11 2.033(2), Pt1-O1 2.016(15), Pt1-N1 1.986(16), Pt1-N3 2.095(16).

Table 2. The methane and methyl group isotopolog distribution in the reaction of **1** and 25 equiv. tfa-d_1 to tfa (10:1) to give **2**.[a]

Methane	ppm	% (std dev)	Methyl	ppm	% (std dev)
CH_4	0.21	43.4(5.7)	Pt-CH_3	1.16	50.6 (4.0)
CH_3D	0.19	25.4(0.8)	Pt-CH_2D	1.14	23.8 (1.0)
CH_2D_2	0.18	17.7(1.6)	Pt-CHD_2	1.12	25.7 (3.1)
CHD_3	0.16	13.6(4.8)			

[a]Neither CD_4 nor Pt-CD_3 were quantified as it is impossible to observe these species in the ^{1}H NMR spectrum; however, it is likely that they are present in the reaction mixture.

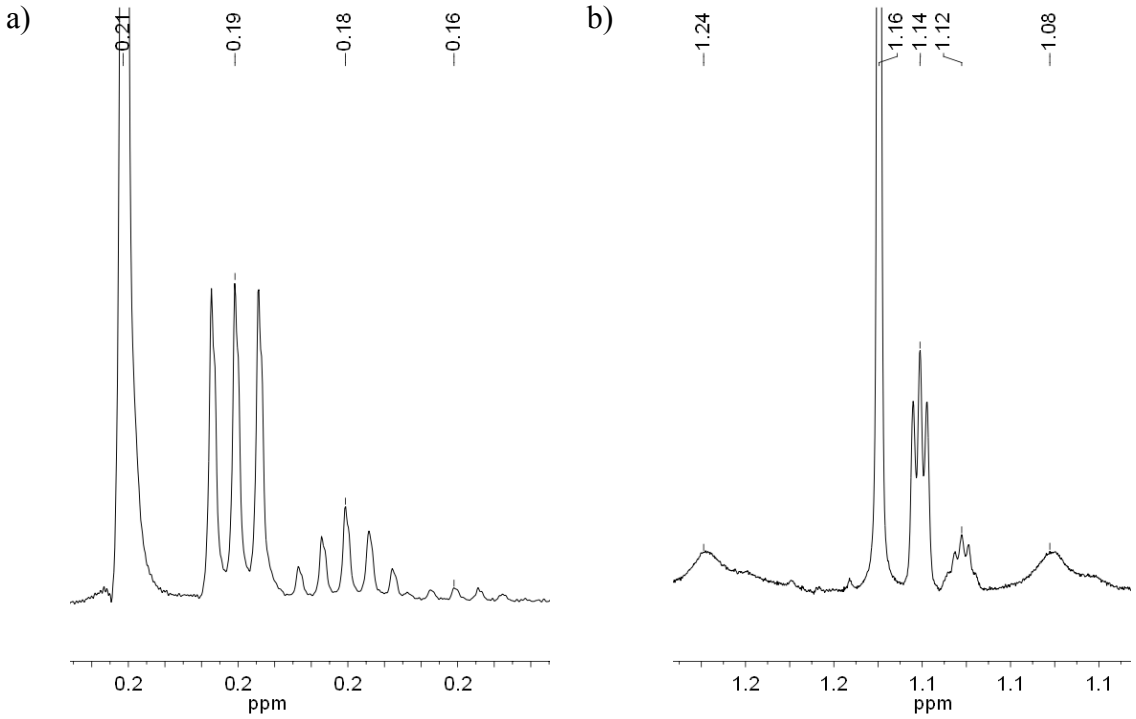

Figure 4. The ^{1}H NMR spectra (CD_2Cl_2) of the methane (a) and methyl (b) regions in the reaction of **1** with 25 equiv. tfa-d_1 to tfa (10:1) to give **2**. Both CH_4 and Pt-CH_3 are off scale.

Observation of Intermediates during the Protonolysis of (bpm)PtMe$_2$. Due to the fast reaction rate, cooling the protonation to -80 °C might allow for the observation of intermediates. As such, tfa was added to a solution of **1** in CD_2Cl_2 at -80 °C and the ^{1}H NMR spectrum was recorded. Under all conditions examined (different amounts of tfa, different order of addition, and colder reaction temperatures using $CDCl_2F$[59]), two platinum (IV) hydrides which accounted for approximately 10% of the species in solution were observed. To circumvent this problem, different acid sources were examined. Hydrochloric acid (12 M) was added to **1** in CD_2Cl_2 at -80 °C giving quantitative

conversion to (bpm)Pt(H)Me_2(Cl) (**3**). The observation of a platinum hydride intermediate suggests that protonation occurs at the metal. Upon warming to room temperature, **3** looses methane to generate (bpm)PtMe(Cl) (**4**, Figure 5, crystal and refinement data can be found in Table 1), the chloride analog of **2**. This implies that both tfa and HCl protonate **1** *via* the same mechanism. The proposed mechanism for the protonolysis of **1** is shown in Scheme 2. The acid reversibly protonates the metal to generate the observed platinum hydride intermediate (**A**). Reductive coupling to form a σ-adduct (**B**) is rapid and reversible, thus explaining the observed isotope distribution. Methane loss from **B** is rate-determining and irreversible.

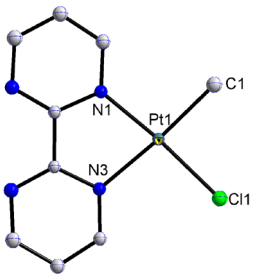

Figure 5. The solid state structure of **4**. Hydrogens have been omitted for clarity.

Scheme 2

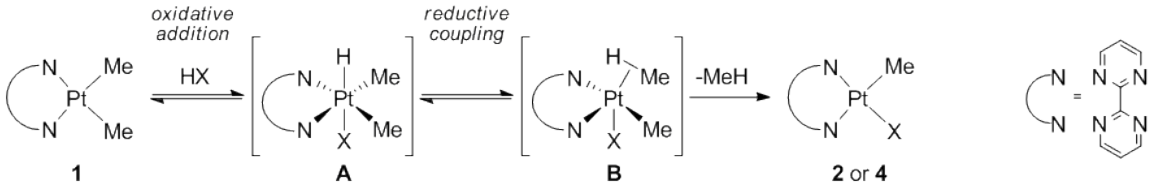

Protonolysis of (bpm)PtMe(tfa). To investigate the actual microscopic reverse of C-H activation by (bpm)$PtCl_2$, the protonolysis of **2** was examined. Addition of tfa to

2 (Scheme 3) results in the formation of methane and (bpm)Pt(tfa)$_2$ (**5**, Figure 6, crystal and refinement data can be found in Table 1). The protonolysis of **2** was slower than **1** and dependent on the amount of acid such that the reaction with 25 equivalents of tfa occurred over a number of hours, and the reaction with 100 equivalents of tfa was complete within minutes. No intermediates were observed during the course of the reaction at room temperature or when a large excess of tfa was used at -40 °C.[60] To gain insight on the mechanism, the KIE was investigated using 25 equivalents tfa-d_1 to tfa (10:1) in dichloroethane-d_4. Analysis of the methane region in the ^{1}H NMR spectrum (Figure 7) revealed that mostly CH_4 and CH_3D were generated along with a small amount of CH_2D_2 (less than 9%). The presence of CH_2D_2 clearly indicates that protonolysis of **2** is reversible; however, the site of protonation remains unclear.

Scheme 3

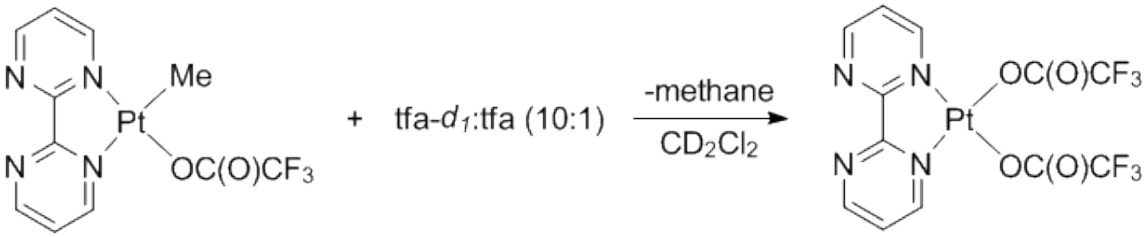

2 **5**

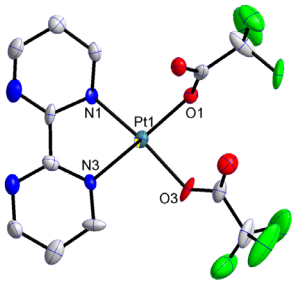

Figure 6. The solid state structure of **5**. Hydrogens have been omitted for clarity. Selected Bond Distances (Å): Pt1-O1 1.996(7), Pt1-O3 2.046(8), Pt1-N1 1.987(10), Pt1-N3 2.008(8).

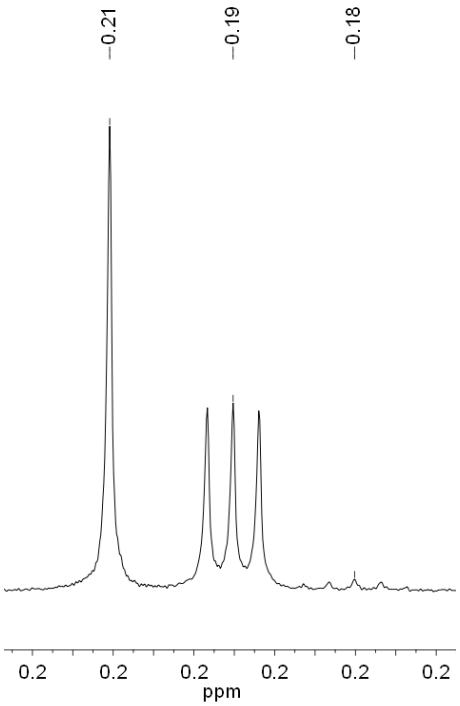

Figure 7. The ^{1}H NMR spectrum ($C_2D_4Cl_2$) of the methane region in the reaction of **2** with 25 equiv. tfa-d_1 to tfa (10:1) at 65 °C to give **5**.

To determine the site of protonation, the temperature dependent KIE was monitored from -30 °C to 65 °C. The KIE was calculated by comparing the amount of CH_4 to the total deuterium containing methane isotopologs (CH_3D and CH_2D_2) and correcting for the 10:1 tfa-d_1 to tfa mixture. As anticipated, the KIE decreased with increasing temperature (Table 3). The reported values are near the upper limit of what is

considered semi-classical;[61-63] however, the Arrhenius parameters which can be derived from the plot of ln(KIE) versus 1/T (Figure 8) imply that the tunneling contribution is negligible as A_H/A_D (1.0(6)) is close to the calculated range of 0.7-1.2[64] and E_a^D-E_a^H (1.0(3)) is less than 1.2 kcal/mol.[36] The numbers reported here compare well to the KIEs and the Arrhenius parameters derived for the protonolysis of (tmeda)PtMe(Cl) with a mixture of tfa-d_1 and tfa (2:1) to give (tmeda)$PtCl_2$ where KIE = 4.4 (21 °C), A_H/A_D = 1.1, and E_a^D-E_a^H = 0.8 kcal /mol (tmeda = tetramethylethylenediamine).[65] Addition of an excess of HCl to (tmeda)PtMe(Cl) at -78 °C results in the formation of (tmeda)Pt(H)Me(Cl)(Cl), clearly demonstrating protonation at the metal.[4]

Table 3. The temperature dependent KIE values for the protonation of **2** with 25 equiv. tfa-d_1 to tfa (10:1) to give **5.**

T (K)	KIE
243	8.2
273	7.3
298	6.9
318	4.4
338	4.9

$A_H/A_D = 1.0(6)$

$E_a^D - E_a^H = 1.0(3)$ kcal/mol

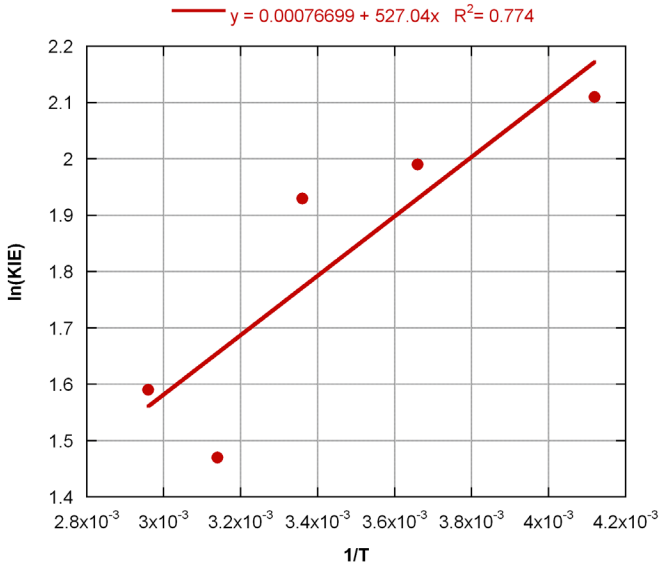

Figure 8. A plot of the ln(KIE) versus 1/T for the protonation of **2** with 25 equiv. tfa-d_1 to tfa (10:1) to give **5**.

The Correlation between KIE and Mechanism. Within the semi-classical limits, normal KIEs (1.3-5.0) have been assigned to protonation at the alkyl while inverse KIEs (0.3-0.7) have been found for systems which involve a hydride.[30, 66] The KIE for the protonolysis of **2** is similar to those found for protonation at the alkyl and for (tmeda)PtMe(Cl) which undergoes protonation at the metal. The KIEs obtained for protonolysis reactions describe the overall reaction and not the individual elementary steps. For systems in which a hydride is observed, the elementary steps might have normal KIEs but the overall KIE is inverse because the individual normal KIEs are in opposition.[66] Therefore small differences in the KIEs for the elementary steps may have significant consequences for the overall KIE. There is at least one example for which the trend does not hold. When (tmeda)Pt(CH_2Ph)(Cl) is protonated with a mixture of HCl and DCl, the KIE for the reversible protonation is 0.51(5) while the overall KIE is 1.55(10).[3] Recent combined experimental and theoretical work suggests that abnormally large KIEs (> 10 at room temperature) are indicative of protonation at the alkyl.[36] Therefore, without the observation of an intermediate, it is impossible to determine the site of protonation.

Mechanism of the Protonolysis of (bpm)PtMe(tfa). The isotopolog distribution for the protonation of **2** requires that protonation is reversible such that a second deuterium can be incorporated into the methane. The protonation of **2** might follow the same mechanism as the protonation of **1** where reversible oxidative addition of HX results in a platinum hydride intermediate which is in equilibrium with the σ-adduct and methane loss is both irreversible and rate-determining (Scheme 2). If this is true, the hydride should have been visible when the reaction was cooled in the presence of a large

amount of acid. However if the rate of oxidative addition is similar to the rate of methane loss and the rate of reductive coupling is very fast then as soon as the hydride forms it will quickly go on to product. These relative rates would explain the absence of hydride intermediate, and as long as the first two steps are reversible, the formation of CH_2D_2 is consistent with the proposal. Alternatively, if reversible protonation of **2** occurs at the methyl to form a σ-adduct (**C**) followed by rate-determining methane loss, this would also account for the observed methane isotopologs (Scheme 4). The data presented favors neither mechanism.

Scheme 4

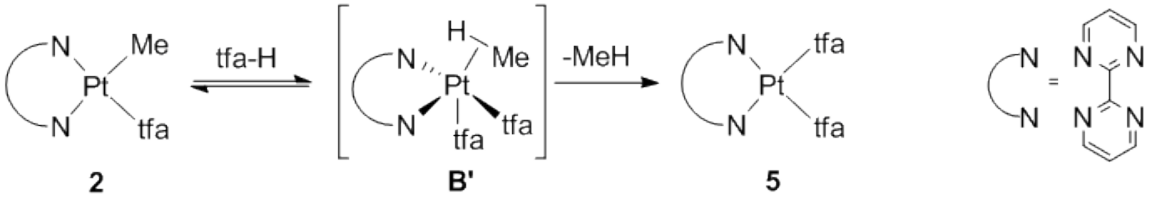

Protonation at Nitrogen. Computational studies have indicated the stability and likely involvement of $[(bpmH)PtCl_2]^+$ where one of the nitrogens not-bound to platinum is protonated prior to the C-H activation event in the catalytic system.[48-49, 52, 54, 56] Due to the highly acidic media necessary for catalysis, the proposed $[(bpmH)PtCl_2]^+$ is reasonable. To test whether a nitrogen of bpm was protonated prior to protonation of the methyl group one equivalent of tfa was added to either **1** or **2**. In the case of **1**, an immediate reaction to give **2** was observed. For **2**, the reaction was much slower. Initially small changes in chemical shift were observed for **2** with more dramatic movement observed for the aryl protons than the aliphatic protons. Over time, **2** converts

to **5** and methane with no other species observed in solution. This data suggests that although tfa might coordinate to **2** initially either as an acid-base pair with the bpm or in some other fashion, the adduct is less stable than **5**. Furthermore, in the presence of excess tfa (100 equivalents), there is no evidence in the ^{1}H NMR, HRMS, or X-ray crystal structure that is consistent with a proton on the nitrogen of the bpm in **5**. Therefore under the conditions examined, a species where a nitrogen of bpm is protonated does not appear long-lived or stable.

Conclusion

The protonolysis of (bpm)$PtMe_2$ (**1**) and (bpm)PtMe(tfa) (**2**) was found to be reversible due to the methane isotopolog distribution upon addition of a mixture of deutero- and protio-acid which included at least one dideutero isotopolog for each platinum species. The protonolysis of **1** was shown to proceed through an oxidative addition mechanism to give a platinum (IV) hydride intermediate. No intermediates were observed in the protonolysis of **2**. Reversible protonation at either the metal or the methyl of **2** is consistent with the observed isotopologs. The temperature-dependent KIE for this process could also be consistent with either mechanism. As more data becomes available regarding KIEs for protonolysis reactions, the correlation between KIE value and mechanism becomes ambiguous.

Experimental

General Considerations. All air- and moisture-sensitive compounds were manipulated under argon or nitrogen using standard glovebox, Schlenk, and high-vacuum line techniques.[67] Argon was purified and dried by passage through columns of MnO on vermiculite and activated 4 Å molecular sieves. Solvents were dried over activated alumina. All organic chemicals were purchased and used as received from Aldrich. The metal precursor $K_2[PtCl_4]$ was purchased from Strem and used as received. All deuterated materials were purchased from Cambridge Isotopes. NMR spectra of ligands and metal complexes were recorded on a Varian Unity Inova 500 or 600 spectrometer. HRMS was obtained from the California Institute of Technology Mass Spectrometry Facility. X-ray quality crystals were mounted on a glass fiber with Paratone-N oil. Data were collected on a Bruker KAPPA APEX II instrument. All errors are standard deviations.

(bpm)PtMe$_2$ (1). This compound was synthesized *via* the method of Puddephatt.[57] Purification was achieved by column chromatography with triethylamine-treated silica and methylene chloride as the eluent to give a red solid which could be recrystalized from acetone (320 mg, 27%). ^{1}H NMR (500 MHz, CD_2Cl_2): δ 1.05 (s, 6H, C*H*$_3$, $^2J_{Pt\text{-}H}$ = 87.5 Hz), 7.64 (dd, 2H, bpm, *J* = 5.5, 4.8 Hz), 9.28 (dd, 2H, bpm, *J* = 4.7, 2.2 Hz), 9.40 (dd, 2H, bpm, *J* = 5.5, 2.2 Hz). ^{13}C NMR (126 MHz, CD_2Cl_2): δ -16.90 ($^1J_{Pt\text{-}C}$ = 829 Hz), 124.64, 153.59, 157.02, 163.23. HRMS (ESI+) obsd (M+H)-H_2 382.0639, calcd for $C_{10}H_{11}N_4Pt$, 382.0632.

(bpm)PtMe(tfa) (2). (Bipyrimidine)$PtMe_2$ (100 mg, 0.26 mmol) was dissolved in dry CH_2Cl_2 (50 mL). Trifluoroacetic acid (20 μL, 0.26 mmol) was added dropwise

under an argon flow. The solvent was removed *in vacuuo* after 30 m of stirring to give a yellow-orange solid which was recrystalized from hot methanol (119 mg, 79%). ^{1}H NMR (500 MHz, CD_2Cl_2): δ 1.08 (s, 3H, CH_3, $^{2}J_{Pt\text{-}H}$ = 79 Hz), 7.58 (dd, 1H, bpm, *J* = 5.9, 4.8 Hz), 7.79 (dd, 1H, bpm, *J* = 5.0, 0.5 Hz), 8.90 (dd, 1H, bpm, *J* = 5.4, 2.2 Hz), 9.24 (dd, 1H, bpm, *J* = 4.7, 2.0 Hz), 9.27 (dd, 1H, bpm, *J* = 4.8, 2.2 Hz), 9.30 (dd, 1H, bpm, *J* = 5.9, 2.1 Hz). ^{13}C NMR (126 MHz, CD_2Cl_2): δ -13.61 ($^{1}J_{Pt\text{-}C}$ = 790.9 Hz), 114.54 (q, CF_3, *J* = 290 Hz), 124.27, 125.15, 154.25, 156.84, 157.89, 159.54, 160.66, 162.45 (q, *C*=O, *J* = 36 Hz), 164.08. HRMS (FAB+) obsd M+ 481.0341, calcd for $C_{11}H_9N_4O_2F_3Pt$, 481.0326.

(bpm)Pt(H)Me$_2$(Cl) (3). (Bipyrimidine)$PtMe_2$ (5 mg, 13.0 μmol) was dissolved in CD_2Cl_2 (0.5 mL). Hydrochloric acid (12 *M*, 1.1 μL, 13.0 μmol) was added at -80 °C. ^{1}H NMR (500 MHz, CD_2Cl_2, -80 °C): δ -20.90 (s, H, Pt-*H*, $^{1}J_{Pt\text{-}H}$ = 1569.5 Hz), 1.35 (s, 6H, C*H*$_3$, $^{2}J_{Pt\text{-}H}$ = 69 Hz), 7.84 (t, 2H, bpm, *J* = 10 Hz), 9.14 (d, 2H, bpm, *J* = 3.8 Hz), 9.22 (d, 2H, bpm, *J* = 2.5 Hz).

(bpm)PtMe(Cl) (4). (Bipyrimidine)$PtMe_2$ (111 mg, 0.29 mmol) was dissolved in CH_2Cl_2 (50 mL). Hydrochloric acid (12 *M*, 24 μL, 0.29 mmol) was added. The solvent was removed *in vacuuo* after 30 m of stirring to give a yellow-orange solid (88 mg, 75%). ^{1}H NMR (600 MHz, CD_2Cl_2): δ 1.20 (s, 3H, C*H*$_3$, $^{2}J_{Pt\text{-}H}$ = 78 Hz), 7.64 (dd, 1H, bpm, *J* = 5.9, 4.7 Hz), 7.81 (dd, 1H, bpm, *J* = 5.4, 4.8 Hz), 9.26 (dd, 1H, bpm, *J* = 4.8, 2.2 Hz), 9.31 (dd, 1H, bpm, *J* = 4.7, 2.1 Hz), 9.43 (dd, 1H, bpm, *J* = 5.9, 2.0 Hz), 9.77 (dd, 1H, bpm, *J* = 5.4, 2.3 Hz). ^{13}C NMR (151 MHz, CD_2Cl_2): δ -15.63 ($^{1}J_{Pt\text{-}C}$ = 732.8 Hz), 124.83, 125.08, 154.81, 155.17, 157.42, 159.27, 161.44, 163.99. HRMS (ESI+) obsd M+H 405.0240, calcd for $C_9H_{10}N_4ClPt$, 405.0232.

(bpm)Pt(tfa)$_2$ (5). An excess of trifluoroacetic acid was added to **2**. ^{1}H NMR (500 MHz, CD_2Cl_2): δ 7.84 (dd, 2H, bpm, *J* = 5.9, 4.9 Hz), 8.84 (dd, 2H, bpm, *J* = 5.9, 2.0 Hz), 9.34 (dd, 2H, bpm, *J* = 4.9, 2.0 Hz). ^{13}C NMR (126 MHz, CD_2Cl_2): δ 115.26 (q, *C*F_3, *J* = 284.9 Hz) 125.06, 156.48, 158.84 (q, *C*=O, *J* = 41.9 Hz), 161.19. HRMS (FAB+) obsd M-$C_2O_2F_3$ 466.0091, calcd for $C_{10}H_6N_4O_2F_3Pt$-$C_2O_2F_3$, 466.0091.

Conditions of Protonolysis. An excess of trifluoroacetic acid (25 equiv. tfa-d_1 to tfa, 10:1) was added to a stock solution of **1** or **2** in CD_2Cl_2 or $C_2D_4Cl_2$ (5 mg per 0.6 mL) in a J. Young NMR tube. The tube was placed in a bath (oil or ethylene glycol) at the proper temperature. The residual methane and platinum methyl were analyzed by ^{1}H NMR upon completion of the reaction.

References

1. Gol'dshleger, N. F.; Es'kova, V. V.; Shilov, A. E.; Shteinman, A. A. *Zh. Fiz. Khim.* **1972,** *46*, 785-786.

2. Hill, G. S.; Rendina, L. M.; Puddephatt, R. J. *Organometallics* **1995,** *14*, 4966-4968.

3. Stahl, S. S.; Labinger, J. A.; Bercaw, J. E. *J. Am. Chem. Soc.* **1995,** *117*, 9371-9372.

4. Stahl, S. S.; Labinger, J. A.; Bercaw, J. E. *J. Am. Chem. Soc.* **1996,** *118*, 5961-5976.

5. Falvello, L. R.; Garde, R.; Miqueleiz, E. M.; Tomas, M.; Urriolabeitia, E. P. *Inorg. Chim. Acta* **1997,** *264*, 297-303.

6. Holtcamp, M. W.; Labinger, J. A.; Bercaw, J. E. *J. Am. Chem. Soc.* **1997,** *119*, 848-849.

7. Romeo, R.; Plutino, M. R.; Elding, L. I. *Inorg. Chem.* **1997,** *36*, 5909-5916.

8. Wick, D. D.; Goldberg, K. I. *J. Am. Chem. Soc.* **1997,** *119*, 10235-10236.

9. Holtcamp, M. W.; Henling, L. M.; Day, M. W.; Labinger, J. A.; Bercaw, J. E. *Inorg. Chim. Acta* **1998,** *270*, 467-478.

10. Johansson, L.; Ryan, O. B.; Tilset, M. *J. Am. Chem. Soc.* **1999,** *121*, 1974-1975.

11. Heiberg, H.; Johansson, L.; Gropen, O.; Ryan, O. B.; Swang, O.; Tilset, M. *J. Am. Chem. Soc.* **2000,** *122*, 10831-10845.

12. Johansson, L.; Tilset, M.; Labinger, J. A.; Bercaw, J. E. *J. Am. Chem. Soc.* **2000,** *122*, 10846-10855.

13. Johansson, L.; Ryan, O. B.; Romming, C.; Tilset, M. *J. Am. Chem. Soc.* **2001,** *123*, 6579-6590.

14. Johansson, L.; Tilset, M. *J. Am. Chem. Soc.* **2001,** *123*, 739-740.

15. Thomas, J. C.; Peters, J. C. *J. Am. Chem. Soc.* **2001,** *123*, 5100-5101.

16. Konze, W. V.; Scott, B. L.; Kubas, G. J. *J. Am. Chem. Soc.* **2002,** *124*, 12550-12556.

17. Wik, B. J.; Lersch, M.; Tilset, M. *J. Am. Chem. Soc.* **2002,** *124*, 12116-12117.

18. Wong-Foy, A. G.; Henling, L. M.; Day, M.; Labinger, J. A.; Bercaw, J. E. *J. Mol. Catal. A: Chem.* **2002,** *189*, 3-16.

19. Song, D.; Wang, S. *Organometallics* **2003,** *22*, 2187-2189.

20. Thomas, J. C.; Peters, J. C. *J. Am. Chem. Soc.* **2003,** *125*, 8870-8888.

21. Gerdes, G.; Chen, P. *Organometallics* **2004,** *23*, 3031-3036.

22. Heyduk, A. F.; Zhong, H. A.; Labinger, J. A.; Bercaw, J. E. *ACS Symp. Ser.* **2004,** *885*, 250-263.

23. Tilset, M.; Johansson, L.; Lersch, M.; Wik, B. J. *ACS Symp. Ser.* **2004,** *885*, 264-282.

24. Driver, T. G.; Day, M. W.; Labinger, J. A.; Bercaw, J. E. *Organometallics* **2005,** *24*, 3644-3654.

25. Liang, L.-C.; Lin, J.-M.; Lee, W.-Y. *Chem. Commun.* **2005**, 2462-2464.

26. Romeo, R.; Plutino, M. R.; Romeo, A. *Helv. Chim. Acta* **2005,** *88*, 507-522.

27. Khaskin, E.; Zavalij, P. Y.; Vedernikov, A. N. *J. Am. Chem. Soc.* **2006,** *128*, 13054-13055.

28. MacDonald, M. G.; Kostelansky, C. N.; White, P. S.; Templeton, J. L. *Organometallics* **2006,** *25*, 4560-4570.

29. Owen, J. S.; Labinger, J. A.; Bercaw, J. E. *J. Am. Chem. Soc.* **2006,** *128*, 2005-2016.

30. Romeo, R.; D'Amico, G. *Organometallics* **2006,** *25*, 3435-3446.

31. Wik, B. J.; Ivanovic-Burmazovic, I.; Tilset, M.; Van Eldik, R. *Inorg. Chem.* **2006,** *45*, 3613-3621.

32. Wik, B. J.; Lersch, M.; Krivokapic, A.; Tilset, M. *J. Am. Chem. Soc.* **2006,** *128*, 2682-2696.

33. Driver, T. G.; Williams, T. J.; Labinger, J. A.; Bercaw, J. E. *Organometallics* **2007,** *26*, 294-301.

34. Kloek, S. M.; Goldberg, K. I. *J. Am. Chem. Soc.* **2007,** *129*, 3460-3461.

35. Williams, T. J.; Labinger, J. A.; Bercaw, J. E. *Organometallics* **2007,** *26*, 281-287.

36. Bercaw, J. E.; Chen, G. S.; Labinger, J. A.; Lin, B.-L. *J. Am. Chem. Soc.* **2008,** *130*, 17654-17655.

37. McKeown, B. A.; Foley, N. A.; Lee, J. P.; Gunnoe, T. B. *Organometallics* **2008,** *27*, 4031-4033.

38. West, N. M.; White, P. S.; Templeton, J. L. *Organometallics* **2008,** *27*, 5252-5262.

39. Williams, T. J.; Caffyn, A. J. M.; Hazari, N.; Oblad, P. F.; Labinger, J. A.; Bercaw, J. E. *J. Am. Chem. Soc.* **2008,** *130*, 2418-2419.

40. Netland, K. A.; Graziani, O.; Krivokapic, A.; Heyn, R. H.; Tilset, M. *J. Coord. Chem.* **2009,** *62*, 3085-3097.

41. Parmene, J.; Ivanovic-Burmazovic, I.; Tilset, M.; van Eldik, R. *Inorg. Chem.* **2009,** *48*, 9092-9103.

42. Fortman, G. C.; Scott, N. M.; Linden, A.; Stevens, E. D.; Dorta, R.; Nolan, S. P. *Chem. Commun.* **2010,** *46*, 1050-1052.

43. Oblad, P. F.; Bercaw, J. E.; Hazari, N.; Labinger, J. A. *Organometallics* **2010,** *29*, 789-794.

44. Villalobos, J. M.; Hickman, A. J.; Sanford, M. S. *Organometallics* **2010,** *29*, 257-262.

45. Periana, R. A.; Taube, D. J.; Gamble, S.; Taube, H.; Satoh, T.; Fujii, H. *Science* **1998,** *280*, 560-564.

46. Kushch, L. A.; Lavrushko, V. V.; Misharin, Y. S.; Moravsky, A. E.; Shilov, A. E. *Nouv. J. Chim.* **1983,** *7*, 729-733.

47. Stahl, S. S.; Labinger, J. A.; Bercaw, J. E. *Angew. Chem. Int. Ed.* **1998,** *37*, 2180-2192.

48. Ahlquist, M.; Nielsen, R. J.; Periana, R. A.; Goddard, W. A. *J. Am. Chem. Soc.* **2009,** *131*, 17110-17115.

49. Ahlquist, M.; Periana, R. A.; Goddard, W. A., III *Chem. Commun.* **2009**, 2373-2375.

50. Gilbert, T. M.; Hristov, I.; Ziegler, T. *Organometallics* **2001,** *20*, 1183-1189.

51. Hristov, I. H.; Ziegler, T. *Organometallics* **2003,** *22*, 1668-1674.

52. Kua, J.; Xu, X.; Periana, R. A.; Goddard, W. A., III *Organometallics* **2002,** *21*, 511-525.

53. Mylvaganam, K.; Bacskay, G. B.; Hush, N. S. *J. Am. Chem. Soc.* **1999,** *121*, 4633-4639.

54. Paul, A.; Musgrave, C. B. *Organometallics* **2007,** *26*, 793-809.

55. Xu, X.; Fu, G.; Goddard, W. A., III; Periana, R. A. *Stud. Surf. Sci. Catal.* **2004,** *147*, 499-504.

56. Xu, X.; Kua, J.; Periana, R. A.; Goddard, W. A., III *Organometallics* **2003,** *22*, 2057-2068.

57. Scott, J. D.; Puddephatt, R. J. *Organometallics* **1986,** *5*, 1538-1544.

58. The large excess of tfa was employed to mitigate the effects of the protons on the glass of the NMR tube.

59. Siegel, J. S.; Anet, F. A. L. *J. Org. Chem.* **1988,** *53*, 2629-2630.

60. The mixture of **2**, tfa and CD_2Cl_2 was solid at temperatures below -40 °C.

61. Bell, R. P., *The Proton in Chemistry*. 2nd ed.; 1973.

62. Bell, R. P. *Chem. Soc. Rev.* **1974,** *3*, 513-44.

63. Bell, R. P., *The Tunnel Effect in Chemistry*. 1980.

64. Schneider, M. E.; Stern, M. J. *J. Am. Chem. Soc.* **1972,** *94*, 1517-1522.

65. Chen, G. S. *Mechanisms of C-H Bond Activation by Platinum(II).* California Institute of Technology, Pasadena, CA, 2010.

66. Jones, W. D. *Acc. Chem. Res.* **2003,** *36*, 140-146.

67. Burger, B. J.; Bercaw, J. E. *ACS Symp. Ser.* **1987,** *357*, 79-98.

Appendix A

Robotic Lepidoptery: Structural Characterization of (Mostly) Unexpected Palladium Complexes Obtained from High-Throughput Catalyst Screening

Reproduced from Bercaw, J.E.; Day, M.W.; Golisz, S.R.; Hazari, N.; Henling, L.M.; Labinger, J.A.; Schofer, S.J.; Virgil, S. *Organometallics* **2009**, *28*, 5017-5024.

Abstract

In the course of a high-throughput search for optimal combinations of bidentate ligands with Pd(II) carboxylates to generate oxidation catalysts, we obtained and crystallographically characterized a number of crystalline products. While some combinations afforded the anticipated (L-L)Pd(OC(O)R)$_2$ structures (L-L = bipyridine, tmeda; R = CH_3, CF_3), many gave unusual oligometallic complexes resulting from reactions such as C-H activation (L-L = sparteine), P-C bond cleavage (L-L = 1,2-bis(diphenylphosphino)ethane, and C-C bond formation between solvent (acetone) and ligand (L-L = 1,4-bis(2,6-diisopropylphenyl)-1,4-diaza-1,3-butadiene). These findings illustrate potential pitfalls of screening procedures based on assuming uniform, *in situ* catalyst self-assembly.

Introduction

The role of automated high-throughput experimentation (HTE) in homogeneous catalysis is steadily increasing.[1-2] Efficient application of such methods virtually requires some degree of catalyst self-assembly; having to pre-synthesize all the candidates to be tested will almost always be far too time-consuming. Most commonly members of a ligand library are allowed to react *in situ* with a suitable metal complex, which acts as the catalyst precursor. While this is often successful, there is an obvious concern: in any given case, the targeted species might <u>not</u> form, so that a negative result in catalytic performance could reflect that failure rather than the actual properties of the desired catalyst.

On the other hand, in HTE, reactions are often carried out in multi-well plates, with the individual containers more or less open to the environment, thus permitting gradual concentration by solvent evaporation; variations of relative and absolute concentrations, solvent, and temperature may also be included in the screening regime. These constitute excellent conditions for the serendipitous generation of crystals—of the intended product or something else—without much (or any) additional effort. Long ago, Cotton summed up the then-state-of-the-art in characterizing metal cluster structures: "Thus the student of cluster chemistry is in somewhat the position of the collector of lepidoptera or meteorites, skipping observantly over the countryside and exclaiming with delight when fortunate enough to encounter a new specimen."[3] In this sense, one potential role of an HTE robot may be as an extremely effective butterfly net.

We have recently reported the palladium-catalyzed oxidative aromatization of cycloolefins, using molecular oxygen as the terminal oxidant: cyclohexene can be oxidized to benzene, and 1,2-dihydronaphthalene to naphthalene, at room temperature in the presence of palladium(II) trifluoroacetate (tfa) and O_2 (Eq 1).[4] Palladium complexes with diimine ligands have also been found to oxidatively aromatize cyclohexene to benzene, at elevated temperatures.[5] For both of these systems, C-H bond activation from an η^2-olefinic intermediate is proposed.

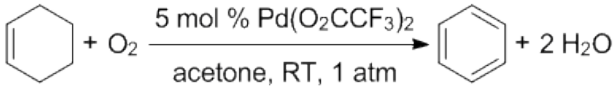

(1)

We wanted to extend these promising results to the oxidation of more useful substrates such as linear alkenes and alkanes, for which no examples of reaction were found under the above conditions. While the ligand-free $Pd(tfa)_2$ catalyst system is more

active than those of the diimine-ligated complexes, it is also considerably less stable, decomposing to Pd metal at temperatures much above ambient. Conceivably an appropriately ligated catalyst, even if inherently less reactive, could be operated at sufficiently high temperature to overcome the differential and activate more difficult substrates. To explore this possibility, we initiated a high-throughput study involving a variety of Pd(II) precursors, chelating ligands, solvents, and reaction conditions. While no effective metal-ligand combination was detected, the study did generate a number of crystalline species. Some of these displayed solid state structures quite different from those expected for simple coordination of ligand to Pd (which may be why catalytically active species were not formed), often resulting from unexpected and unusual reactivity. We report here on these findings.

Results and Discussion

HTE Methodology. The robot was used to generate solutions of a wide range of combinations of catalyst precursor ($Pd(tfa)_2$ or $Pd(OAc)_2$), ligand, and substrate (cyclohexene or 1,2-dihydronaphthalene) in acetone ($Pd(tfa)_2$ and $Pd(OAc)_2$ have limited solubility in many other solvents and the control reaction described in Eq 1 shows significant solvent dependence, so the choice of solvent was not varied in this work). The following N- and P-centered bidentate ligands were expected to react according to Eq 2: 2,2'-bipyridine (bpy), N,N,N',N'-tetramethylethylenediamine (tmeda), (-)-sparteine, 1,2-bis(diphenylphosphino)ethane (dp), and 1,4-bis(2,6-diisopropylphenyl)-1,4-diaza-1,3-butadiene (diimine). 2-Phenylpyridine was

also included in the study, anticipating that a chelate product would result from C-H activation as shown in Eq 3.

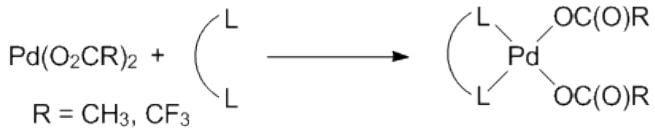

(2)

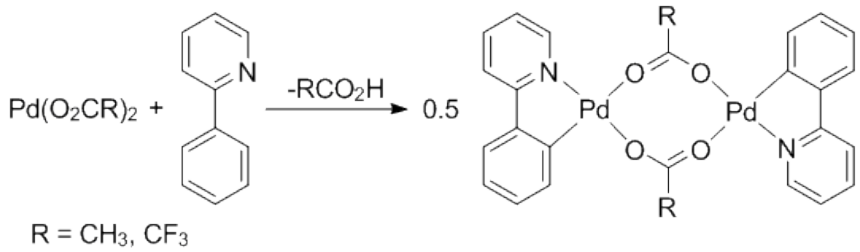

(3)

When cyclohexene was used as substrate, control samples (without substrate) were found to contain substantial amounts of both cyclohexene and benzene, indicating considerable cross-contamination by volatile components. Although we expect this problem could have been largely eliminated by improving the experimental set-up (which employed a porous rubber mat held flush to the glass vials with a metal plate affixed by screws), instead we simply restricted screening to the less volatile 1,2-dihydronaphthalene, for which no such transfer could be detected. Most ligand-Pd combinations resulted in no oxidation activity whatsoever; a couple of cases gave low activity, substantially less than that found for the ligand-free catalysts. (We believe incomplete complexation is probably responsible for these low conversions; another possibility is that some ligated palladium complexes are active, although inherently less active than their ligand-free counterparts.) Hence, this survey was abandoned.

A parallel set of substrate-free samples was generated, using the robot, to investigate whether the desired catalysts assemble properly. In many of these cases, solvent evaporation in air directly provided X-ray quality crystals. All such reactions

were scaled up in the laboratory, to determine by NMR spectroscopy whether the crystalline material was identical to the main product generated in solution. Some of the products were also examined by mass spectrometry.

Bipyridine Complexes. Both $Pd(tfa)_2$ and $Pd(OAc)_2$ react with bpy according to Eq. 2, as confirmed by ^1H NMR spectroscopy. From the HTE screening, $(bpy)Pd(tfa)_2$ (**1**) was obtained as pale yellow needles (crystal and refinement data are shown in Table 1). The inner coordination sphere of **1** (Figure 1) appears entirely unexceptional, with the bipyridine lying in the Pd coordination plane, and the two monodentate trifluoroacetate groups bent out of the plane, both in the same direction, very similar to the orientation found in an earlier structure of a $(bpy)Pd(carboxylate)_2$.[6] The crystal packing of **1** reveals intermolecular Pd-Pd and π-stacking interactions between adjacent molecules (Figure 2) and the separations fall within the expected range: Pd-Pd distances are between 3.0 and 3.2 Å, and all spacings between the bpy rings are less than 3.8 Å, with the closest contact being approximately 3.4 Å. Each complex participates in a Pd-Pd interaction with another complex directly above (or below), and a π-stacking interaction between bpy rings with the complex directly below (or above). These two interactions combine to create a columnar structure comprised of alternating d^8-d^8 and π-stacking interactions. While both π-stacking between adjacent bpy rings[7] and d^8-d^8 interactions between metal centers[8-9] are well established, to the best of our knowledge, **1** is the first example of a structure which contains *both* of these interactions in the same crystal.

A second polymorph of **1** (**1'**) was also obtained. Although these crystals were not of high enough quality to obtain quantitative data, an overlay of the two molecules shows clear differences (Figure 3). In particular, the trifluoroacetate groups are no longer

oriented in the same direction with respect to the square plane as in **1**. This allows the molecules to align in the unit cell so that π-stacking is the predominant interaction, with no short Pd-Pd contacts. For **1**, it appears that such an alignment, with only π-stacking (or only d^8-d^8 interactions) is prevented by steric repulsions between the parallel-oriented tfa groups. Clearly there is only a small energetic difference between **1** and **1'**, and the exact conditions for crystallization influence which polymorph is obtained.

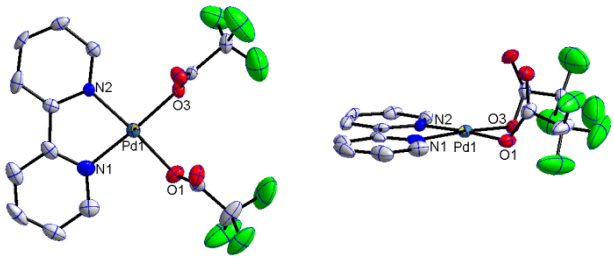

Figure 1. The solid state structure of **1**. Hydrogens have been omitted for clarity. Selected bond distances of **1** (Å): Pd1-N1 2.004(1), Pd1-N2 1.993(1), Pd1-O1 2.016(1), Pd1-O3 2.007(1).

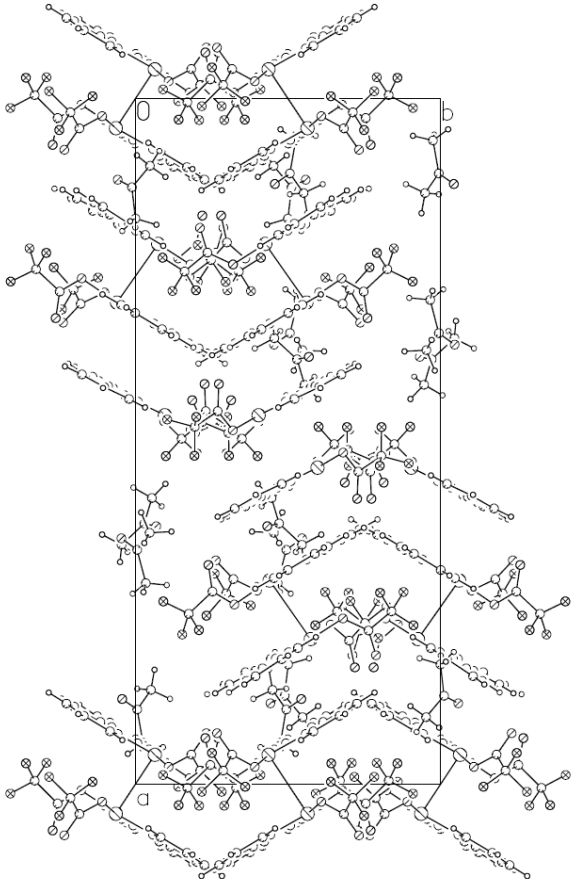

Figure 2. A unit cell diagram of **1** viewed along the c-axis.

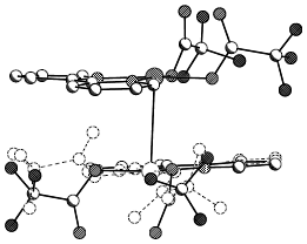

Figure 3. A comparison of the molecular conformation in the two polymorphs of $(bpy)Pd(tfa)_2$ with **1** as the solid bonds and **1'** as the dashed bonds.

The yellow crystals of (bpy)Pd(OAc)$_2$ (**2**) obtained through HTE exhibit a structure very similar to that of **1'** (Figure 4), with the two acetate groups oriented above and below the coordination plane (crystal and refinement data are shown in Table 1). There is a slightly offset face to face π-stacking interaction between the bpy rings of adjacent molecules (shortest contact 3.4 Å) and no evidence for any Pd-Pd interaction.[7] One notable feature of **2** is a hydrogen-bonded network of waters (not shown), which are also hydrogen bonded to the acetate ligands. This water presumably originates from wet solvents which were used in the reaction.

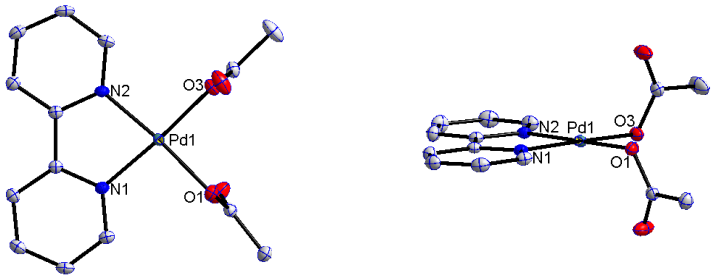

Figure 4. The solid state structure of **2**. Hydrogens have been omitted for clarity. Selected bond distances of **2** (Å): Pd1-N1 1.998(1), Pd1-N2 1.992(1), Pd1-O1 2.013(1), Pd1-O3 2.007(1).

Tetramethylethylenediamine and Palladium(II) Trifluoroacetate. The reaction of tmeda and Pd(tfa)$_2$ in acetone also followed Eq 2 (confirmed by ^{1}H NMR spectroscopy), giving colorless crystals of (tmeda)Pd(tfa)$_2$ (**3**). The structure (Figure 5) is similar to those of **1** and **2** but exhibits disorder in both the tfa groups and the ethylene backbone (crystal and refinement data are shown in Table 1). In the two (uncoupled) conformations in this crystal, the carbonyl oxygens of the tfa ligands are either on the

same or opposite sides of the coordination plane, and the two carbons of the ethylene backbone of tmeda alternate between being up or down with respect to the coordination plane (Figure 6).

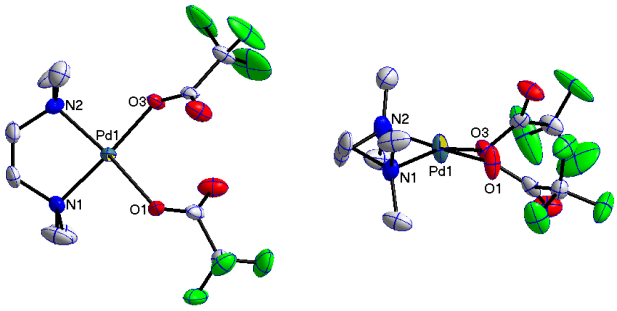

Figure 5. The solid state structure of **3**. Hydrogens have been omitted for clarity. Selected bond distances of **3** (Å): Pd1-N1 2.017(1), Pd1-N2 2.034(1), Pd1-O1 2.025(1), Pd1-O3 2.079(1) or 2.095(1). (If only one value is given the distances are the same in both conformations.)

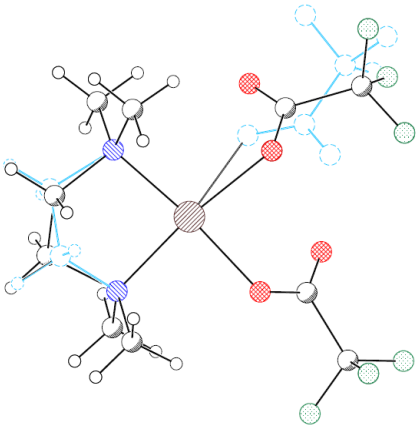

Figure 6. An overlay of the two conformations of **3**.

Phenylpyridine Reactions. The reaction of phenylpyridine with both $Pd(OAc)_2$ and $Pd(tfa)_2$ gave C-H activation products as expected (Eq 3). The yellow crystals of both products exhibit a "clamshell" dimer structure, as reported previously for the acetate complex,[10-11] in which the two phenylpyridines are stacked on top of each other and the bridging acetates are perpendicular to the palladium-ligand coordination planes. The structure of the tfa complex, which features a relatively short palladium-palladium interaction, will be fully discussed in a subsequent paper describing the electronic structure of d^8-d^8 bonding in Pd complexes.[12]

(-)-Sparteine and Palladium (II) Acetate. While there are many examples of sparteine acting as an L_2-type ligand to palladium (Eq 2),[13-16] the grey crystals obtained from mixing (-)-sparteine and $Pd(OAc)_2$ in acetone instead consist of (sparteinyl)Pd(μ-$OC(CH_3)O)_2$Pd(μ-$OC(CH_3)O)_2$Pd(sparteinyl) (**4**), the result of C-H activation at a bridgehead position of sparteine (crystal and refinement data are shown in Table 2). The resulting trimetallic complex contains three palladium atoms (Figures 7 and 8), in an approximately linear arrangement ($\angle$ Pd1-Pd2-Pd3 = 176.03°; Pd-Pd ~ 2.9 Å), each exhibiting square-planar geometry. The central Pd is coordinated to four acetate groups (Pd-O ~ 2.0 Å); these bridge in pairs to the two outer Pds, each of which is additionally coordinated by a (κ^2-N,C)-sparteinyl group. The sparteinyl ligand has undergone an inversion at one of the nitrogen atoms (relative to free sparteine), presumably to assist with coordination. Overall, the structure of the molecule is S-shaped and seems to involve two d^8-d^8 interactions.[12]

When this reaction was performed on a large scale, the presence of **4** as the major product was confirmed by HRMS and ^{1}H NMR spectroscopy. We are unable to propose

a detailed mechanism for formation of **4** at this time, although presumably the hydrogen generated by C-H activation is released as acetic acid. It is probable that the solvent (acetone) is partially responsible for promoting C-H bond activation, as it has been previously reported that reaction of sparteine with $Pd(OAc)_2$ in dichloroethane results in the formation of (sparteine)$Pd(OAc)_2$.[16] To the best of our knowledge, this is the first example of a metal complex containing a metallated sparteine ligand.

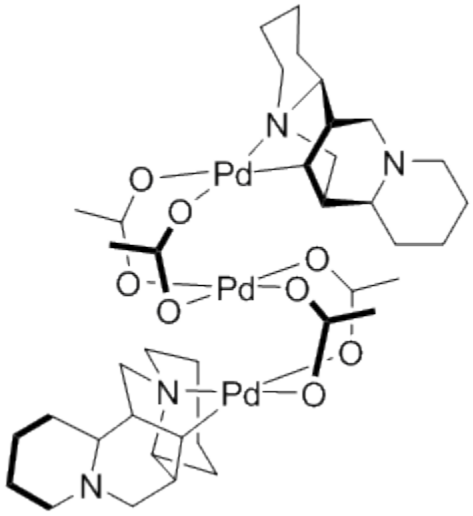

Figure 7. A schematic representation of **4**.

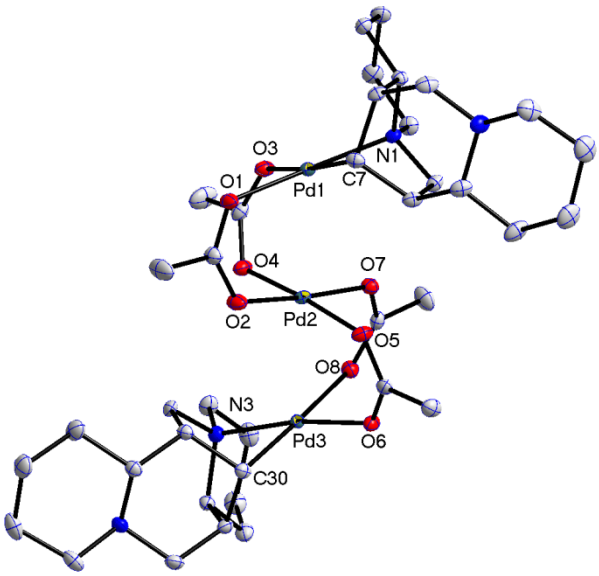

Figure 8. The solid state structure of **4**. Hydrogens have been omitted for clarity. Selected bond distances of **4** (Å): Pd1-N1 2.061(1), Pd1-C7 2.010(1), Pd3-N3 2.069(1), Pd3-C30 1.997(1).

1,2-Bis(diphenylphosphino)ethane and Palladium(II) Acetate. The colorless crystals obtained from the mixture of dp and $Pd(OAc)_2$ in acetone exhibit a tetrametallic structure, $[(Pd(\mu\text{-}PPhCH_2CH_2PPh_2)(\mu\text{-}OC(CH_3)O)PdPh)(\mu\text{-}OC(CH_3)O)]_2$ (**5**), resulting from C-P cleavage of the dp ligand (Figure 9). Two representations of **5** are shown in Figure 10 (crystal and refinement data are shown in Table 2). The four Pd(II) centers are each square planar and are arranged in pairs. One member of each pair (Pd2, Pd4) is bonded to a phenyl group, and the other (Pd1, Pd3) to the intact Ph_2P end of a dp. The other (phosphide) end of the dp, along with one acetate, bridge the two members of each pair; and then the pairs are joined together by two additional bridging acetates (Pd1 to Pd4, Pd2 to Pd3). The overall arrangement is an approximately planar macrocycle

containing the four Pd atoms (torsion angle = 0.43°), the two bridging phosphide P atoms, and the two inter-pair bridging acetates, with the other (intra-pair) bridging acetates and the phosphine P atoms above and below the plane.

Repeated large scale reactions of dp and $Pd(OAc)_2$ in acetone gave only (dp)$Pd(OAc)_2$ (**5m**), the expected monomeric product according to Eq 2. This complex has been previously reported, along with the crystal structure (which includes a coordinated CH_2Cl_2 molecule).[17] The structural parameters of **5m** were identical to those in the literature, with the replacement of CH_2Cl_2 by half a molecule of acetone in the unit cell (Figure 11, crystal and refinement data are shown in Table 2). We were unable to synthesize **5** on a large scale, and thus designate it as a minor product in the reaction of dp and $Pd(OAc)_2$.

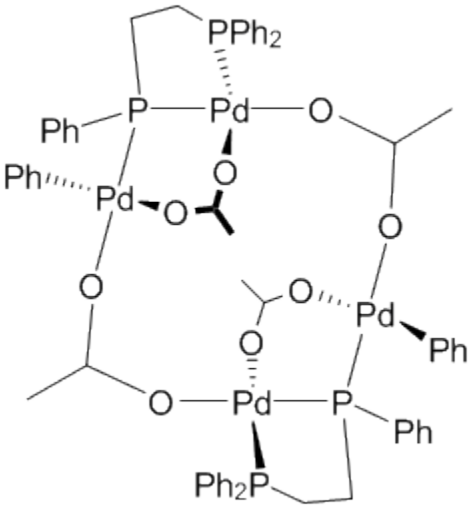

Figure 9. A schematic representation of **5**.

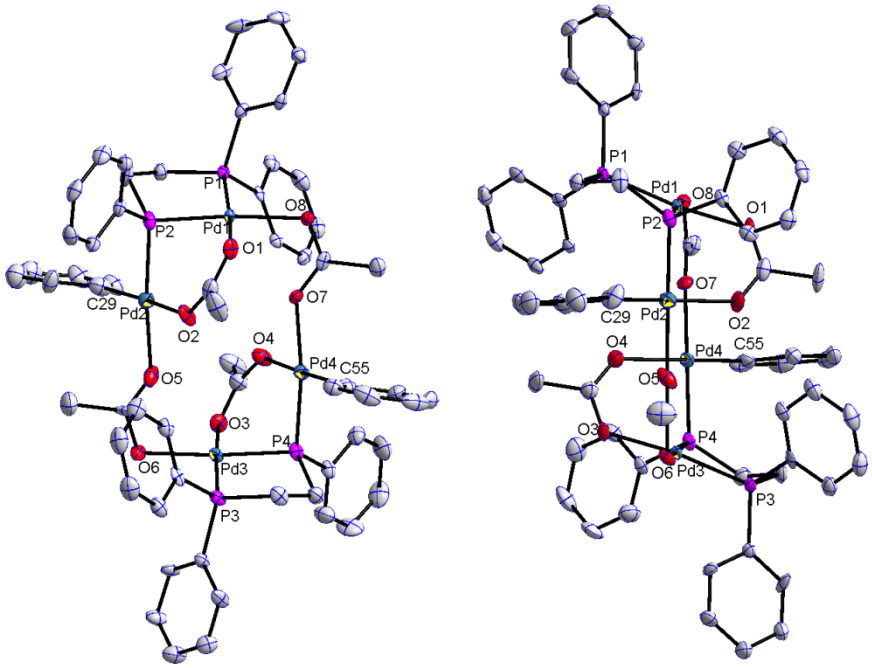

Figure 10. The solid state structure of **5**. Hydrogens have been omitted for clarity. Selected bond distances of **5** (Å): Pd1-P1 2.215(1), Pd1-P2 2.214(1), Pd1-O1 2.080(1), Pd1-O8 2.145(1), Pd2-P2 2.240(1), Pd2-C29 1.973(1), Pd2-O2 2.150(1), Pd2-O5 2.153(1), Pd3-P3 2.214(1), Pd3-P4 2.216(1), Pd3-O3 2.084(1), Pd3-O6 2.149(1), Pd4-P4 2.227(1) Pd4-C55 2.004(1), Pd4-O4 2.169(1), Pd4-O7 2.128(1).

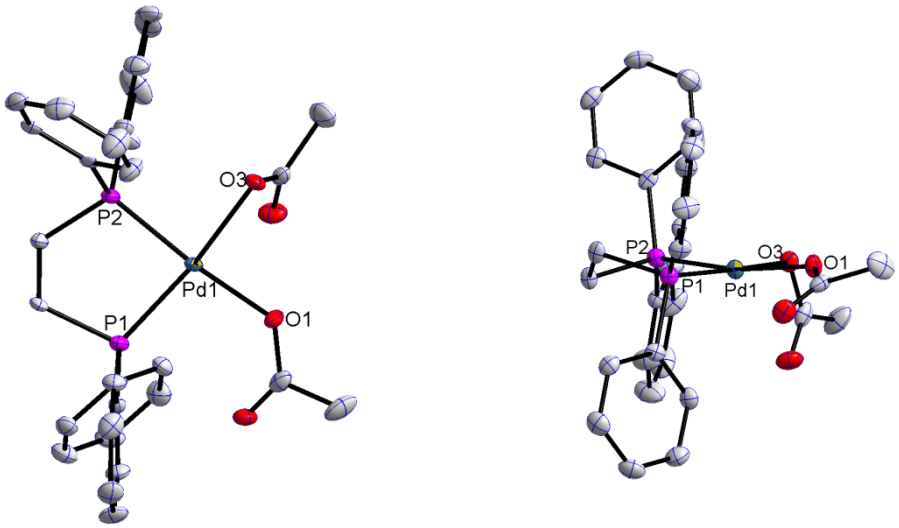

Figure 11. The solid state structure of **5m**. Hydrogens have been omitted for clarity. Selected bond distances of **5m** (Å): Pd1-O1 2.060(2), Pd1-O3 2.107(2), Pd1-P1 2.229(9), Pd1-P2 2.217(9).

1,4-Bis(2,6-diisopropylphenyl)-1,4-diaza-1,3-butadiene and Palladium (II) Acetate. The reaction of diimine with $Pd(OAc)_2$ in acetone yielded small red crystals; X-ray crystallographic studies revealed a remarkable cyclic decameric structure, shown in Figure 12 (crystal and refinement data in Table 3). The connections involve $-OC(CH_3)X-$ groups which are O-bound to one Pd and X-attached to a backbone carbon of a diimine ligand on the neighboring Pd. At first it was thought that X was either O or CH_2, resulting from the acetate or the enolate of acetone, respectively, which would give overall charge neutrality. However, closer inspection of the crystallographic data shows clearly that X is in fact a $=CH-$ group. The structure refines much more poorly with X = O than X = C; electron density peaks corresponding to a single H can be located at the expected positions adjacent to each C; and the relative bond lengths are only consistent

with this formulation, as is the ^{1}H NMR spectrum which includes signals (all of intensity corresponding to one proton) at δ 4.05 (s), 3.15 (d) and 4.83 (d) for the =C**H** and the two non-equivalent backbone CH_2 protons, respectively. (A parent ion for the intact decamer could not be detected by mass spectrometry, perhaps not surprisingly.) The molecular structure is shown schematically in Figure 13, along with the key bond distances.

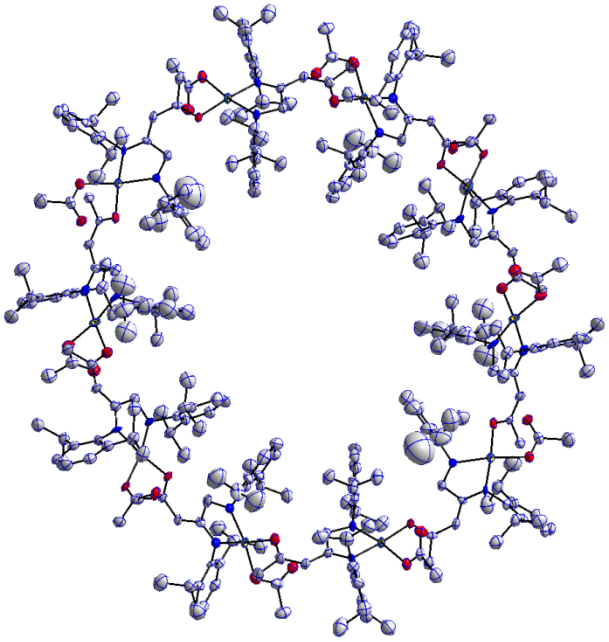

Figure 12. The solid state structure of **6**. Hydrogens have been omitted for clarity.

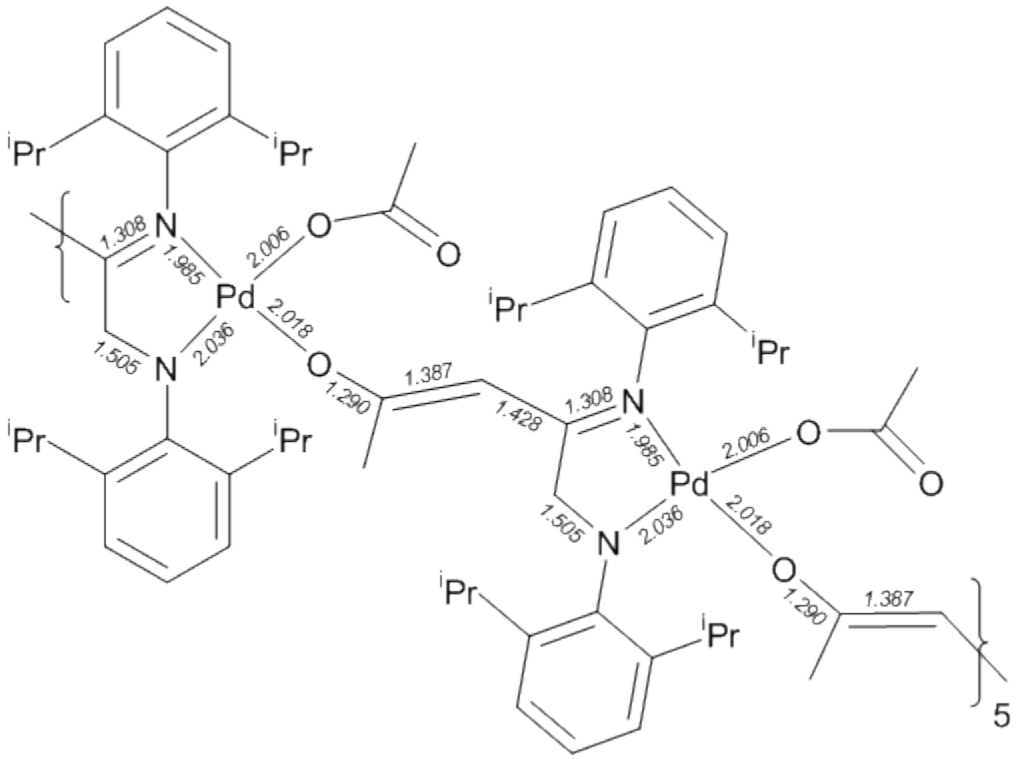

Figure 13. A schematic representation of **6**.

Formation of **6** corresponds to the net double deprotonation of acetone, with the addition of the carbon end to one of the backbone imine carbons, and migration of the hydrogen originally on that carbon to the adjacent carbon; this has taken place ten times, giving the cyclic structure in which each Pd is square-planar, coordinated by one imine N, one amidic N, one normal (monodentate) anionic acetate, and an O from what has become a substituted acetonyl. Since three of those are anionic ligands, each Pd is anionic; hence there must be one additional proton per Pd that was not crystallographically detected. Most probably these are hydrogen-bonded to the dangling oxygens on the periphery of the macrocycles; alternatively, they may be bonded to solvent and/or water molecules inside the channels that are formed by the stacking of

decamers in the crystal packing (Figure 14). There is no covalent bonding between the channels. We were unable to obtain the high-angle diffraction data that would be needed to determine whether any solvent or other molecules are present in the channels, and thermogravimetric analysis was inconclusive, but it seems highly unlikely that they are empty considering the intimate involvement of the solvent.

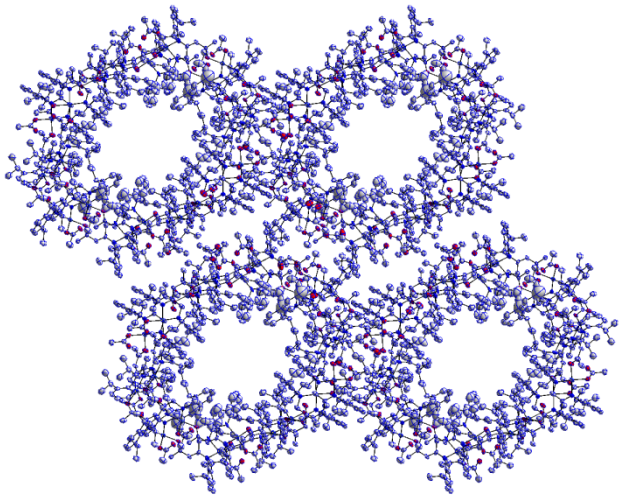

Figure 14. A diagram of the crystal packing of **6**.

It appears that **6** is not merely a minor component of the reaction mixture, as it could be synthesized in reasonable yield (36%) on a large scale. We would expect that a compound of the form (diimine)$Pd(OAc)_2$ might be an intermediate, and ^1H NMR changes during early stages of the reaction between diimine and $Pd(OAc)_2$ in acetone-d_6 suggest that is the case. We were subsequently able to isolate (impure) samples of (diimine)$Pd(OAc)_2$ from the reaction of the diimine ligand and $Pd(OAc)_2$ in $CHCl_3$, and dissolution of isolated (diimine)$Pd(OAc)_2$ in acetone-d_6 led to the formation of **6-*d*$_n$** as confirmed by X-ray crystallography and ^1H NMR spectroscopy. Detailed comparison of

the ^{1}H NMR spectrum with that for the all-protio analog shows that the acetone-derived methyl group is entirely deuterated, but remaining deuterons on the deprotonated end have completely exchanged with the backbone protons of the ligand (Figures 15 and 16), as revealed by signals corresponding to both CH_2 and CHD in the methylene position, and reduction of intensity for all three of the signals cited above. At present we do not have a mechanistic proposal to account for the formation of **6** and the H/D scrambling process.

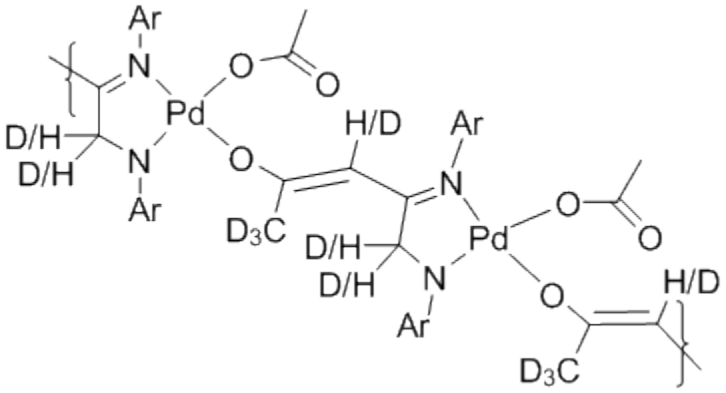

Figure 15. A schematic representation of **6-*d*$_6$**.

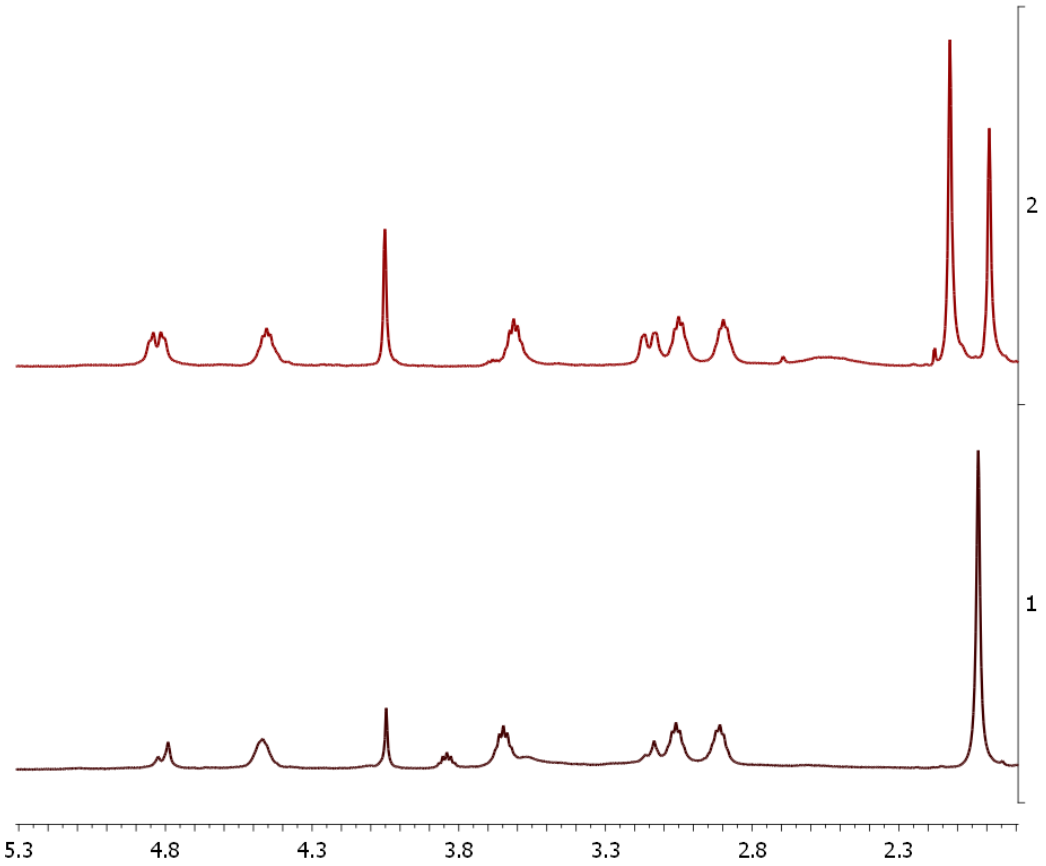

Figure 16. ^{1}H NMR spectra of [(diimine)(Pd)(OAc)$_2$]$_{10}$ (**6**) and [(diimine)(Pd)(OAc)$_2$]$_{10}$-d_n (**6-*d*$_n$**). The top trace is the protio complex and the bottom trace is the deutero complex. The patterns for the signals around δ 4.8 and 3.15 in the bottom trace both arise from an overlay of peaks from the CH_2 (doublet) and CHD (singlet, shifted slightly upfield from the midpoint of the doublet) isotopologs.

Table 1. Crystal and Refinement Data for Complexes **1**, **2**, and **3**.

	1	**2**	**3**
Empirical formula	$C_{14}H_8F_6N_2O_4Pd$ • C_3H_6O	$C_{14}H_{14}N_2O_4Pd$ • $5(H_2O)$	$C_{10}H_{16}F_6N_2O_4Pd$

Formula weight	546.70	470.75	448.65
Temperature (K)	100	100	100
a (Å)	30.402(13)	6.879(3)	8.941(5)
b (Å)	13.601(6)	12.376(5)	9.454(5)
c (Å)	18.821(8)	12.755(6)	10.224(5)
α (°)	90	115.18(2)	75.95(2)
β (°)	90	96.79(2)	74.20(2)
γ (°)	90	97.92(2)	72.61(2)
Volume (Å^3)	7782.1(6)	954.2(7)	781.2(7)
Z	16	2	2
Crystal system	Orthorhombic	Triclinic	Triclinic
Space group	P*nc*2 (#30)	P-1 (#2)	P-1 (#2)
d_{calc} (Mg/m^3)	1.866	1.639	1.907
θ range (deg)	1.97 to 32.23	1.80 to 39.31	2.10 to 30.78
μ (mm^{-1})	1.043	1.020	1.271
Abs. correction	None	Semi-empirical from equivalents	None
GOF	1.57	1.62	2.19
R_1,[a] wR_2[b] $[I>2\sigma(I)]$	0.042, 0.072	0.028, 0.042	0.036, 0.075

[a] $R_1 = \Sigma||F_o| - |F_c||/\Sigma|F_o|$. [b] $wR_2 = [\Sigma[w(F_o^2 - F_c^2)^2]/\Sigma[w(F_o^2)^2]]^{1/2}$.

Table 2. Crystal and Refinement Data for Complexes **4**, **5**, and **5m**.

	4	**5**	**5m**
Empirical formula	$C_{38}H_{62}N_4O_8Pd_3$	$C_{60}H_{60}O_8P_4Pd_4$	$C_{30}H_{30}O_4P_2Pd \cdot 0.5(C_3H_6O)$
Formula weight	1022.12	1458.56	651.92
Temperature (K)	100	100	100
a (Å)	10.837(6)	12.830(6)	11.761 (10)
b (Å)	16.360(9)	20.967(9)	19.196(18)
c (Å)	23.714(12)	21.614(10)	14.328(13)
α (°)	90	90	90
β (°)	90	100.02(3)	113.60(4)
γ (°)	90	90	90
Volume (Å^3)	4204.1(4)	5725.6(4)	2964.3(5)
Z	4	4	4
Crystal system	Orthorhombic	Monoclinic	Monoclinic
Space group	$P2_12_12_1$ (#19)	$P2_1/c$ (#14)	$P2_1/c$ (#14)
d_{calc} (Mg/m^3)	1.615	1.692	1.461
θ range (deg)	1.72 to 37.20	1.91 to 30.44	1.88 to 30.07
μ (mm^{-1})	1.322	1.402	0.770
Abs. correction	none	Semi-empirical from equivalents	Semi-empirical from equivalents
GOF	1.39	2.96	1.46
R_1,[a] wR_2[b] $[I>2\sigma(I)]$	0.020, 0.033	0.072, 0.126	0.065, 0.064

$^{a}R_1 = \Sigma||F_o| - |F_c||/\Sigma|F_o|$. $^{b}wR_2 = [\Sigma[w(F_o^2 - F_c^2)^2]/\Sigma[w(F_o^2)^2]]^{1/2}$.

Table 3. Crystal and Refinement Data for Complex **6**.

	6
Empirical formula	$C_{310}H_{428}N_{20}O_{30}Pd_{10} \bullet 8(C_2H_4O_2) \bullet 2(H_2O)$
Formula weight	6495.17
Temperature (K)	100
a (Å)	12.611(5)
b (Å)	28.787(11)
c (Å)	29.243(12)
α (°)	113.48(2)
β (°)	100.17(3)
γ (°)	93.23(3)
Volume (Å^3)	9489.3(7)
Z	1
Crystal system	Triclinic
Space group	P-1 (#2)
d_{calc} (Mg/m^3)	1.137
θ range (deg)	1.66 to 22.50
μ (mm^{-1})	0.523
Abs. correction	Semi-empirical from equivalents
GOF	2.32

R_1,[a] wR_2[b] $[I>2\sigma(I)]$	0.079, 0.137

[a] $R_1 = \Sigma||F_o| - |F_c||/\Sigma|F_o|$. [b] $wR_2 = [\Sigma[w(F_o^2 - F_c^2)^2]/\Sigma[w(F_o^2)^2]]^{1/2}$.

Conclusion

While the above findings remind us of the potential pitfalls of screening protocols that rely on catalyst self-assembly, they also illustrate their capability for generating intriguing structures. More than half of the ligand-metal combinations tested afforded products resulting from unexpected chemistry—C-H bond activation, C-P bond cleavage, addition of solvent to ligand—that led to further assembly into oligomeric structures with intricate and unusual interconnections, which (while gladdening the collector's heart) are less likely to function as effective catalysts. Because the efficiency of HTE screening for homogeneous catalysts relies on some assumed uniformity of catalyst self-assembly, it is important to carry out some structural verifications of (pre)catalysts so generated, for at least representative ligand/metal complex/solvent combinations. Researchers making use of these powerful methodologies should stay alert to both the risks and the opportunities.

Experimental

General Considerations. All manipulations were performed in air. Acetone, palladium (II) acetate, palladium (II) trifluoroacetate, (-)-sparteine, 2-phenylpyridine and tmeda were purchased from Aldrich and used as received. 2,2'-Bipyridine was purchased from Acros Organics and used as received. 1,2-Bis(diphenylphosphino)ethane was purchased from Pressure Chemical Company and used as received.

1,4-Bis(2,6-diisopropylphenyl)-1,4-diaza-1,3-butadiene was prepared by literature methods.[18] Acetone-d_6 and chloroform-d_3 were purchased from Cambridge Isotopes and used as received. ^{1}H NMR spectra were recorded on a Varian INOVA 500 MHz instrument using the VNMRJ software program, version 2.2d, at room temperature. Proton chemical shifts were reported using the residual solvent signal as the internal standard. High resolution mass spectra (HRMS) were obtained from the California Institute of Technology Mass Spectrometry Facility.

High-Throughput Equipment. Experiments were conducted using a Symyx™ Technologies Core Module robotic system (Santa Clara, CA). The core module was operated with library designs and operating protocols developed using Library Studio software version 7.1.9.50 and Automation Studio version 1.1.1.8. Stock solutions of metal complexes and ligands were prepared at 0.1 M in acetone. The metal solutions were added to the wells followed by an equimolar amount of the ligand solutions. Acetone was ultimately added to each of the wells to keep a constant total volume of 500 μL. Each combination of metal and ligand was performed in quadruplicate, with a concentration gradient for each set of four wells such that the least concentrated contained 5 mmol each of metal and ligand and the most concentrated contained 15 mmol each of metal and ligand. The wells were then left open to the air on the bench-top until crystals formed. Crystal formation was complete in less than 24 hours for some complexes.

X-Ray Crystallography. The crystals were mounted on a glass fiber with Paratone-N oil. Data were collected on a Bruker KAPPA APEX II instrument.

Structures were determined using direct methods or, in some cases, Patterson maps with standard Fourier techniques using the Bruker AXS software package.

General Procedure for Large Scale Reactions. In order to confirm whether the crystals formed in the HTE screening were the major products, reactions between metal precursors and ligands were performed on a larger scale in the laboratory. The conditions utilized in the HTE screening were replicated. In the case of reactions between bpy and $Pd(tfa)_2$, bpy and $Pd(OAc)_2$, tmeda and $Pd(tfa)_2$, and dp and $Pd(OAc)_2$, ^1H NMR spectroscopy was used to monitor the reactions and indicated the clean formation of compounds **1**, **2**, **3** and **5m**, respectively. The chemical shifts for **1**,[19] **2**,[19] **3**,[14] and **5m**[17] were consistent with those previously reported in the literature.

(sparteinyl)Pd(μ-OC(CH_3)O)$_2$Pd(μ-OC(CH_3)O)$_2$Pd(sparteinyl) (4). A solution of (-)-sparteine (104 mg, 0.44 mmol) in acetone (4.4 mL) was added to a solution of $Pd(OAc)_2$ (100 mg, 0.44 mmol) in acetone (4.4 mL). The solution was allowed to evaporate in air to give grey crystals (37 mg, 24% yield) which were filtered from the supernatant before analysis. See Figure 17 for ^1H NMR spectrum. HRMS (FAB+) obsd M+ 1021.160, calcd for $C_{38}H_{62}N_4O_8Pd_3$, 1021.160.

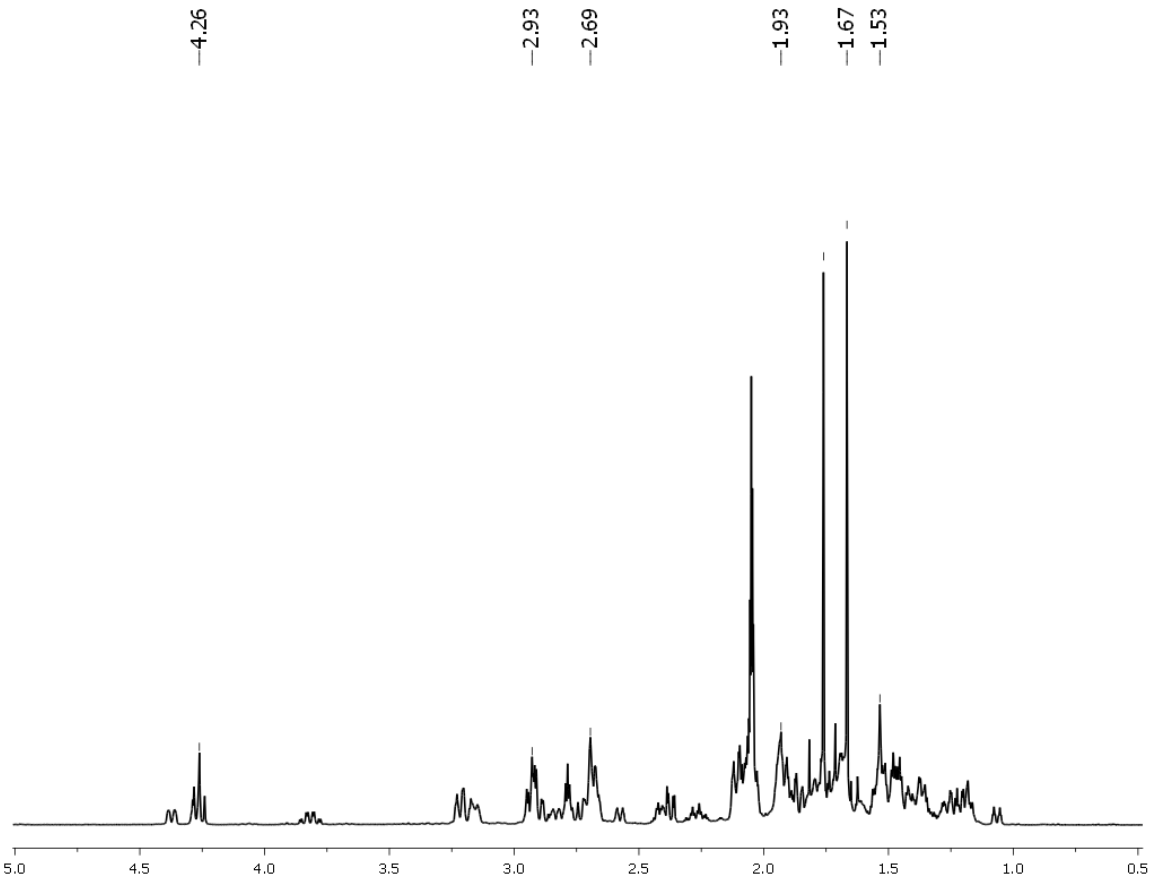

Figure 17. ^{1}H NMR spectrum of (sparteinyl)Pd(μ-OC(CH_3)O)$_2$Pd(μ-OC(CH_3)O)$_2$Pd(sparteinyl) (**4**).

[(diimine)(Pd)(OAc)$_2$]$_{10}$ (6). A solution of diimine (167 mg, 0.44 mmol) in acetone (4.4 mL) was added to a solution of Pd(OAc)$_2$ (100 mg, 0.44 mmol) in acetone (4.4 mL). The solution was allowed to evaporate in air to give red-orange crystals (94.5 mg, 36% yield) which were filtered from the supernatant before analysis. ^{1}H NMR (500 MHz, $CDCl_3$) δ 0.62 (d, *J* = 6, 3H, ^{i}Pr), 0.82 (m, 6H, ^{i}Pr), 0.90 (d, *J* = 6, 3H, ^{i}Pr), 1.00 (s, 3H, ^{i}Pr*), 1.13 (d, *J* = 6, 3H, ^{i}Pr), 1.19 (d, *J* = 6, 3H, ^{i}Pr), 1.22 (d, *J* = 6, 3H, ^{i}Pr), 1.99 (s, 3H, CH_3), 2.13 (s, 3H, CH_3), 2.90 (m, 1H, CH), 3.05 (m, 1H, CH), 3.15 (d, *J* = 13, 1H,

CH_2), 3.61 (m, 1H, CH), 4.05 (s, 1H, CH), 4.45 (m, 1H, CH), 4.83 (d, J = 13, 1H, CH_2), 6.60 (d, J = 7, 1H, Ar), 6.88 (m, 2H, Ar), 7.03 (t, J = 7, 1H, Ar), 7.11 (t, J = 7, 2H, Ar). The resonance with an asterisk corresponds to an unknown peak which has appeared in all spectra of all samples of **6**. This unknown is coincident with an *iso*-propyl resonance.

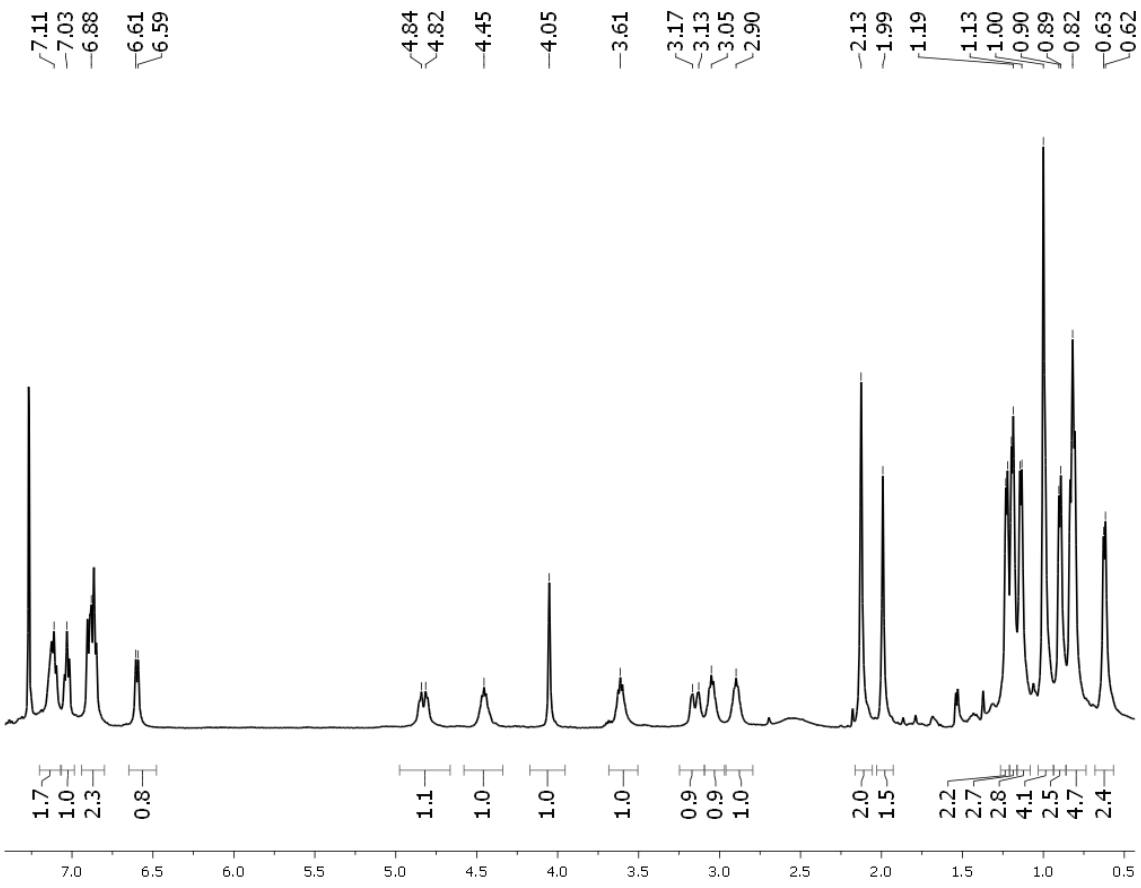

Figure 18. ^{1}H NMR spectrum of $[(\text{diimine})(\text{Pd})(\text{OAc})_2]_{10}$ (**6**).

References

1. Jäkel, C.; Paciello, R. *Chem. Rev.* **2006,** *106*, 2912-2942.

2. Tomasi, S.; Weiss, H.; Ziegler, T. *Organometallics* **2006,** *25*, 3619-3630.

3. Cotton, F. A. *Quart. Rev.* **1966,** *20*, 389-401.

4. Bercaw, J. E.; Hazari, N.; Labinger, J. A. *J. Org. Chem.* **2008,** *73*, 8654-8657.

5. Williams, T. J.; Caffyn, A. J. M.; Hazari, N.; Oblad, P. F.; Labinger, J. A.; Bercaw, J. E. *J. Am. Chem. Soc.* **2008,** *130*, 2418-2419.

6. Canty, A. J.; Denney, M. C.; Skelton, B. W.; White, A. H. *Organometallics* **2004,** *23*, 1122-1131.

7. Janiak, C. *Journal of the Chemical Society-Dalton Transactions* **2000**, 3885-3896.

8. Roundhill, D. M.; Gray, H. B.; Che, C. M. *Acc. Chem. Res.* **1989,** *22*, 55-61.

9. Connick, W. B.; Marsh, R. E.; Schaefer, W. P.; Gray, H. B. *Inorg. Chem.* **1997,** *36*, 913-922.

10. Thu, H.-Y.; Yu, W.-Y.; Che, C.-M. *J. Am. Chem. Soc.* **2006,** *128*, 9048-9049.

11. Dinçer, M.; Özdemir, N.; Günay, M. E.; Çetinkaya, B. *Acta Crystallogr., Sect. E: Struct. Rep. Online* **2008,** *E64*, m381.

12. Bercaw, J. E.; Durrell, A. C.; Gray, H. B.; Green, J. C.; Hazari, N.; Labinger, J. A.; Winkler, J. R. *Inorg. Chem.* **2010,** *49*, 1801-1810.

13. Togni, A.; Rihs, G.; Pregosin, P. S.; Ammann, C. *Helv. Chim. Acta* **1990,** *73*, 723-732.

14. Trend, R. M.; Stoltz, B. M. *J. Am. Chem. Soc.* **2004,** *126*, 4482-4483.

15. Intini, F. P.; Pacifico, C.; Pellicani, R. Z.; Roca, V.; Natile, G. *Inorg. Chim. Acta* **2008,** *361*, 1606-1615.

16. Mueller, J. A.; Sigman, M. S. *J. Am. Chem. Soc.* **2003,** *125*, 7005-7013.

17. Bianchini, C.; Lee, H. M.; Meli, A.; Oberhauser, W.; Peruzzini, M.; Vizza, F. *Organometallics* **2002,** *21*, 16-33.

18. Kliegman, J. M.; Barnes, R. K. *J. Org. Chem.* **1970,** *35*, 3140-3143.

19. Milani, B.; Alessio, E.; Mestroni, G.; Sommazzi, A.; Garbassi, F.; Zangrando, E.; Bresciani-Pahor, N.; Randaccio, L. *J. Chem. Soc., Dalton Trans.* **1994**, 1903-1911.

Appendix B

Activation of the C-N Bond in Nitromethane by Palladium α-Diimine Complexes

Reproduced from Golisz, S.R.; Hazari, N.; Labinger, J.A.; Bercaw, J.E. *J. Org. Chem.*, **2009**, *74*, 8441–8443.

We recently found that a high-throughput screening study, intended to generate a library of complexes of the form $(L_2)PdX_2$, led in several cases to much more complicated palladium products, including one resulting from activation of the solvent, acetone.[1] We report here the unexpected activation of the C-N bond in nitromethane, observed during a similar study using glyoxal-derived α-diimines as bidentate ligands and nitromethane as solvent.

The reaction of palladium acetate ($Pd(OAc)_2$) with either 1,4-bis(2,6-diisopropylphenyl)-1,4-diaza-1,3-butadiene (^{H}diimine-Ar) or 1,4-bis(cyclohexyl)-1,4-diaza-1,3-butadiene (^{H}diimine-Cy) in nitromethane gave (^{Me}diimine)$Pd(NO_2)_2$ (**1a**, **1b**) as orange or gold crystalline solids, respectively (Eq 1); the identity of both species was confirmed by ^{1}H NMR and ^{13}C NMR spectroscopy, high resolution mass spectrometry (HRMS), and X-Ray crystallography (Figures 1 and 2). These reactions correspond to two C-N bond cleavages of nitromethane, with the methyl groups replacing protons on the backbone of the diimine and the nitro groups displacing acetates on palladium, generating two equivalents of acetic acid.

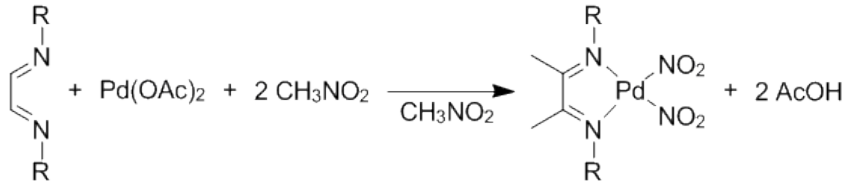

(1)

1a R = 2,6-diisopropylphenyl
1b R = cyclohexyl

The very similar transformation shown in Eq 2 was recently reported;[2] the proposed mechanism is related to well-known organic reactions (Henry reaction or Michael addition followed by denitration)[3] as well as a couple of earlier examples

involving coordination complexes in which nucleophilic addition of the CH_2NO_2 anion to an imine carbon center is followed by loss of nitrite and proton transfer.[4, 5]

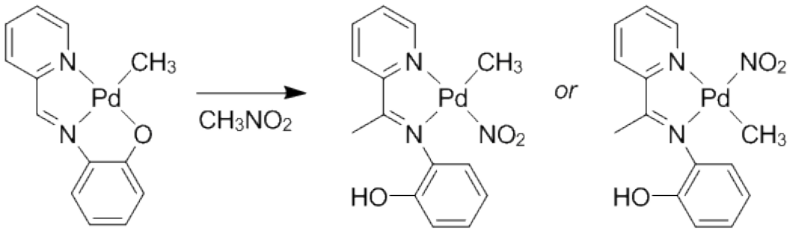

(2)

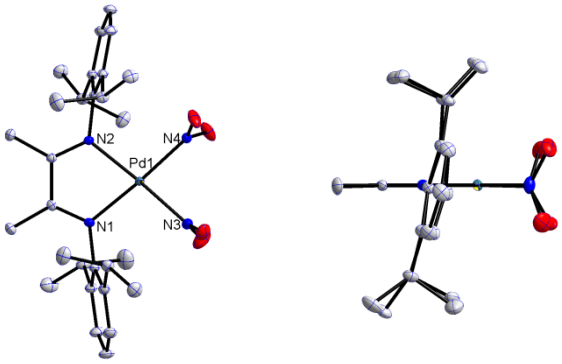

Figure 1. The solid state structure of (^{Me}diimine-Ar)Pd(NO_2)$_2$ (**1a**). Selected bond lengths (Å): Pd1-N1 2.044(7), Pd1-N2 2.050(7), Pd1-N3 2.011(8), Pd1-N4 2.011(7).

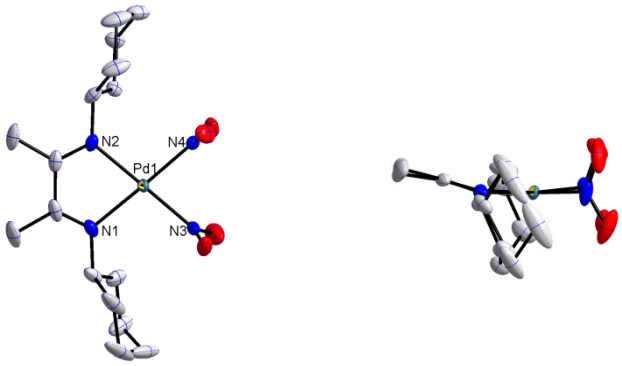

Figure 2. The solid state structure of (^{Me}diimine-Cy)Pd(NO_2)$_2$ (**1b**). Selected bond lengths (Å): Pd1-N1 2.058(12), Pd1-N2 2.046(11), Pd1-N3 2.013(14), Pd1-N4 2.014(12).

A plausible mechanism for the present case, following similar lines, is shown in Scheme 1, which begins with reaction between diimine and Pd(OAc)$_2$ to give **2**. Deprotonation of nitromethane by acetate leads to [(diimine)Pd(η^2-OAc)]$^+$ (**A**) and the carbanion, which adds to the carbon of one imine to give an imine-amide complex (**B**). Elimination of HNO_2 cleaves the C-N bond to give an imine-enamide complex (**C**); readdition of HNO_2 to protonate the amide and attach NO_2 to Pd (**D**) followed by tautomerization generates the singly-methylated diimine complex (**E**). (Protonation of **C** at the methylene to give **E** directly is also possible.) Repeating the entire cycle leads to the observed bis-methylated diimine complex (**1**).

Scheme 1

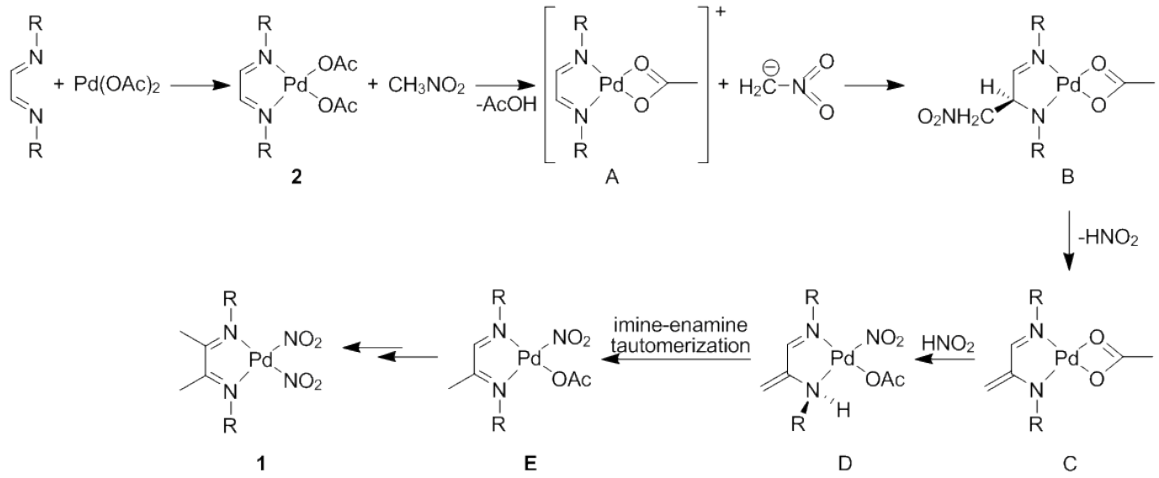

As an initial test of this mechanism, (^{H}diimine-Ar)Pd(OAc)$_2$ (**2a**) was prepared by reacting Pd(OAc)$_2$ with ^{H}diimine-Ar in methylene chloride, as confirmed by ^{1}H NMR and ^{13}C NMR spectroscopy, HRMS, and X-ray crystallography (Figure 3). A dilute (1.5 mM) solution of **2a** in nitromethane, initially dull orange, changes over a few hours to a bright orange solution containing **1a** (by ^{1}H NMR spectroscopy), strongly suggesting that **2a** is a viable reaction intermediate. (A transient yellow color was observed during the course of this reaction, possibly attributable to one or more of the suggested intermediates, but we were unable to isolate or identify this species.)

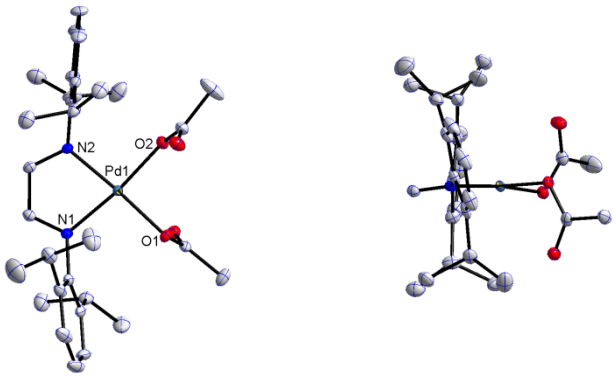

Figure 3. The solid state structure of (^{H}diimine-Ar)Pd(OAc)$_2$ (**2a**). Selected bond lengths (Å): Pd1-N1 2.017(11), Pd1-N2 1.995(12), Pd1-O1 2.009(9), Pd1-O2 2.017(11).

Attempts to follow kinetics of the transformation of **2a** to **1a** by ^{1}H NMR spectroscopy in nitromethane-d_3 (neat or mixed with other deuterated solvents) were unsuccessful, as the reaction did not proceed cleanly to product. It was noted that the backbone methyl signals exhibited the presence of significant amounts of CH_3 and CH_2D isotopologues. These presumably result from exchange with residual water (solvents were used as received with no further drying); such exchange has been observed previously.[6] When the reaction was performed in the presence of small amounts of D_2O, the ^{1}H NMR signals for the backbone methyls were greatly reduced, demonstrating that the latter do originate from the methyl group of nitromethane.

The direct reaction of Eq 1 appears to be quite concentration-dependent: with [diimine] and [Pd(OAc)$_2$] greater than about 9 mM intense colors (dark blue and green) appear. With both reagents at 4.4 mM, formation of **1a** takes place over the course of a few hours, with no such coloration. The reaction also proceeds if excess diimine (but not excess Pd(OAc)$_2$) is used, but clean kinetics could not be obtained. Semiquantitative

reaction rates in the presence of added bases or acids were estimated by following the appearance of product by ^{1}H NMR spectroscopy, since the proposed mechanism suggests there should be an effect. Addition of nitrogen bases (3,5-lutidine, 2,6-lutidine or 2,6-*cis*-dimethylpiperidine) to the dilute mixture of $Pd(OAc)_2$ in nitromethane-d_3 and ^{H}diimine-Ar in acetone-d_6 gave only base-ligated palladium species (supported by ^{1}H NMR chemical shifts), and no productive chemistry involving the ^{H}diimine-Ar. In contrast, addition of either NaOAc or AcOH had little effect on the rate of formation of **1a**.

Addition of the stronger trifluoroacetic acid (tfa) inhibited nitromethane activation and led instead to (^{H}diimine-Ar)$Pd(tfa)_2$ (**3a**), which was prepared separately by the reaction of $Pd(tfa)_2$ and ^{H}diimine-Ar in acetone and characterized by ^{1}H NMR and ^{13}C NMR spectroscopy, HRMS, and X-ray crystallography (Figure 4). Dissolution of **3a** in nitromethane did not yield **1a** cleanly under a variety of conditions, including heating; after prolonged stirring (45 days) of **3a** in nitromethane-d_3, approximately 20% of **1a-*d*$_6$** was observed.

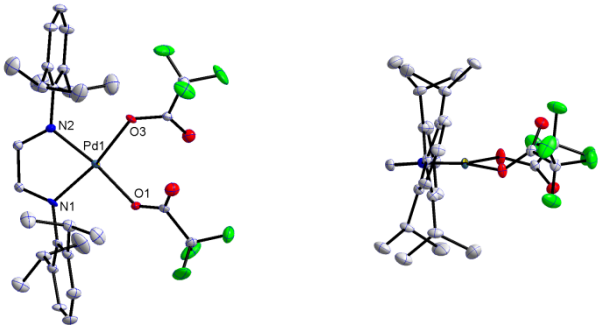

Figure 4. The solid state structure of (^{H}diimine-Ar)$Pd(tfa)_2$ (**3a**). Selected bond lengths (Å): Pd1-N1 1.994(11), Pd1-N2 1.996(10), Pd1-O1 2.002(9), Pd1-O2 2.005(10).

It seems reasonable that the reaction should be much slower for trifluoroacetate than for acetate, if deprotonation of nitromethane is a required early step; it is less clear why addition of excess acetate or acetic acid has little or no effect on the overall rate. In the absence of any characterizable intermediates, the proposed mechanism, while plausible and consistent with related chemistry, remains speculative; alternative mechanisms (for example, oxidative addition of the C-N bond to give a Pd(IV) intermediate) cannot be ruled out. Indeed, small amounts of a C-N activation product were obtained with a different system (Eq 3 and Figure 5)[7] for which a mechanism related to that of Scheme 1 appears highly unlikely. The scope of this type of C-N bond cleavage by coordination complexes,[8] as well as the mechanistic relationship to purely organic activations, remain to be explored.

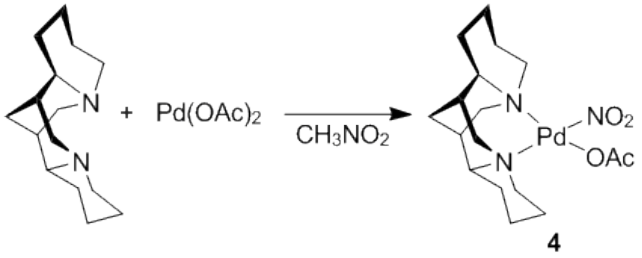

4 (3)

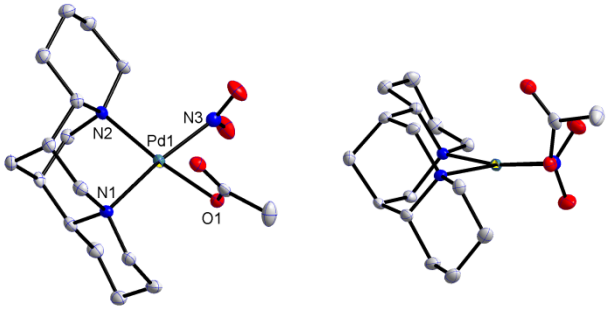

Figure 5. The solid state structure of [(-)-sparteine]Pd(OAc)(NO_2) (**4**). Selected bond lengths (Å) and angles (°): Pd1-N1 2.087(12), Pd1-N2 2.101(12), Pd1-N3 2.019(13), Pd1-O1 2.053(10), N1-Pd1-N2 87.83(5), O1-Pd1-N3 81.00(5).

Experimental

General Considerations. All manipulations were performed in air. Palladium(II) acetate and palladium(II) trifluoroacetate (Aldrich) and nitromethane (Acros Organics) were used as received. 1,4-Bis(2,6-diisopropylphenyl)-1,4-diaza-1,3-butadiene[9] (^{H}diimine-Ar) and 1,4-bis(cyclohexyl)-1,4-diaza-1,3-butadiene[10] (^{H}diimine-Cy) were prepared by literature methods. Nitromethane-d_3, acetone-d_6, methylene chloride-d_2, and chloroform-d_1 were purchased from Cambridge Isotopes and used as received. ^{1}H NMR and ^{13}C NMR spectra were recorded on a Varian INOVA 500 MHz instrument using the VNMRJ software program, version 2.2d, at room temperature. Proton and carbon chemical shifts are reported relative to the residual solvent signal. HRMS were obtained from the California Institute of Technology Mass Spectrometry Facility.

X-Ray Crystallography. The crystals were mounted on a glass fiber with Paratone-N oil. Data were collected on a Bruker KAPPA APEX II instrument.

Structures were determined using direct methods or, in some cases, Patterson maps with standard Fourier techniques using the Bruker AXS software package. Data are shown in Tables 1 and 2.

(^{Me}diimine-Ar)Pd(NO$_2$)$_2$ (1a). A solution of ^{H}diimine-Ar (168 mg, 0.45 mmol) in nitromethane was added to a solution of Pd(OAc)$_2$ (100 mg, 0.45 mmol) in nitromethane. Evaporation of the solvent overnight gave an orange solid (158 mg, 59% yield). ^{1}H NMR (500 MHz, acetone-d_6) δ 1.18 (d, J = 7 Hz, 12H, CH(CH_3)$_2$), 1.54 (d, J = 7 Hz, 12H, CH(CH_3)$_2$), 2.49 (s, 6H, NCCH_3), 3.35 (sept, J = 7 Hz, 4H, CH(CH$_3$)$_2$), 7.24 (d, J = 8 Hz, 4H, m-C$_6H_3$), 7.32 (t, J = 7 Hz, 2H, p-C$_6H_3$). ^{13}C NMR (126 MHz, acetone-d_6) δ 21.57, 23.66, 24.62, 125.03, 129.72, 140.24, 141.44, 181.68. HRMS (FAB+) obsd M-NO$_2$ 556.2172, calcd for C$_{28}$H$_{40}$N$_4$O$_4$Pd-NO$_2$, 556.2166.

(^{Me}diimine-Cy)Pd(NO$_2$)$_2$ (1b). A solution of ^{H}diimine-Cy (49 mg, 0.22 mmol) in nitromethane was added to a solution of Pd(OAc)$_2$ (50 mg, 0.22 mmol) in nitromethane. Evaporation of the solvent overnight gave gold crystals (13 mg, 13% yield). ^{1}H NMR (500 MHz, CDCl$_3$) δ 0.84 (tt, J = 12.5 Hz, 3.5 Hz, 2H, CH), 1.00 (m, 10H, CH_2), 1.47 (dd, J = 13.2 Hz, 1.3 Hz, 5H, CH_2), 1.95 (d, J = 9.5 Hz, 5H, CH_2), 3.58 (s, 6H, NCCH_3). ^{13}C NMR (126 MHz, CDCl$_3$) δ 24.50, 24.64, 34.59, 53.85, 99.48. HRMS (FAB+) obsd M-NO$_2$ 400.1225, calcd for C$_{16}$H$_{28}$N$_4$O$_4$Pd-NO$_2$, 400.1216.

(^{H}diimine-Ar)Pd(OAc)$_2$ (2a). A solution of ^{H}diimine-Ar (335 mg, 0.89 mmol) in CH$_2$Cl$_2$ was added to a solution of Pd(OAc)$_2$ (200 mg, 0.89 mmol) in CH$_2$Cl$_2$. Evaporation of the solvent overnight gave orange needle-like crystals (456 mg, 85% yield). ^{1}H NMR (500 MHz, acetone-d_6) δ 1.16 (s, 6H, OCOCH_3), 1.16 (d, J = 7 Hz, 12H, CH(CH_3)$_2$), 1.48 (d, J = 7 Hz, 12H, CH(CH_3)$_2$), 3.70 (sept, J = 7 Hz, 4H, CH(CH$_3$)$_2$),

7.27 (d, J = 8 Hz, 4H, *m*-C_6H_3), 7.37 (t, J = 7 Hz, 2H, *p*-C_6H_3), 8.45 (s, 2H, NC*H*). ^{13}C NMR (126 MHz, acetone-d_6) δ 21.98, 23.24, 25.53, 55.05, 124.21, 129.59, 142.18, 143.42, 169.29, 175.50. HRMS (FAB+) obsd M-$C_2O_2H_3$ 541.2054, calcd for $C_{30}H_{42}N_2O_4Pd$-$C_2O_2H_3$, 541.2047.

(^{H}diimine-Ar)Pd(tfa)$_2$ (3a). A solution of ^{H}diimine-Ar (340 mg, 0.90 mmol) in acetone was added to a solution of Pd(tfa)$_2$ (300 mg, 0.90 mmol) in acetone. Removal of the solvent *in vacuo* after 30 m gave a bright orange semi-crystalline solid (560 mg, 88% yield). ^{1}H NMR (500 MHz, acetone-d_6) δ 1.21 (d, J = 7 Hz, 12H, CH(CH_3)$_2$), 1.48 (d, J = 7 Hz, 12H, CH(CH_3)$_2$), 3.67 (sept, J = 7 Hz, 4H, C*H*(CH$_3$)$_2$), 7.28 (d, J = 8 Hz, 4H, *m*-C_6H_3), 7.41 (t, J = 7 Hz, 2H, *p*-C_6H_3), 8.61 (s, 2H, NC*H*). ^{13}C NMR (126 MHz, acetone-d_6) δ 22.98, 25.26, 29.83, 124.69, 130.50, 141.89, 142.22, 172.76. HRMS (FAB+) obsd M-$C_2O_2F_3$ 595.1764, calcd for $C_{30}H_{36}N_2O_4F_6Pd$-$C_2O_2F_3$, 595.1764.

Synthesis of [(-)-sparteine]Pd(OAc)(NO$_2$) (4). A solution of (-)-sparteine (10 mg, 0.045 mmol) in acetone-d_6 (0.3 mL) was added to a solution of Pd(OAc)$_2$ (10 mg, 0.045 mmol) in acetone-d_6 (0.3 mL) in an NMR tube. Nitromethane (60 μL) was added to give an orange homogeneous solution. The reaction was monitored by ^{1}H NMR spectroscopy and appeared to contain a mixture of different products. Over two days orange crystals of **4** precipitated out of solution, although the ^{1}H NMR spectrum remained complicated. Although, the yield of **4** is unknown and the fate of the methyl group of nitromethane unclear, crystals of **4** in small quantities were reproducibly generated.

Table 1. Crystal and Refinement Data for Complexes **1a**, **1b**, and **2a**.

	1a	**1b**	**2a**
Empirical formula	$C_{28}H_{40}N_4O_4Pd$	$C_{16}H_{28}N_4O_4Pd$ • ½ (C_3H_6O)	$C_{30}H_{42}N_2O_4Pd$ • (CH_2Cl_2)
Formula weight	603.04	475.86	770.91
Temperature (K)	100	100	100
a (Å)	8.924(3)	12.191(5)	23.852(8)
b (Å)	9.023(3)	13.435(6)	12.797(4)
c (Å)	19.822(8)	25.019(11)	24.021(8)
α (°)	91.74(2)	90	90
β (°)	92.41(2)	90	90
γ (°)	117.76(2)	90	90
Volume ($Å^3$)	1408.9(9)	4098.2(3)	7331.8(4)
Z	2	8	8
Crystal system	Triclinic	Orthorhombic	Orthorhombic
Space group	P-1 (#2)	P*bcn* (#60)	P*bca* (#61)
d_{calc} (Mg/m^3)	1.422	1.542	1.397
θ range (deg)	2.06 to 43.54	1.63 to 35.27	1.71 to 34.34
μ (mm^{-1})	0.698	0.938	0.833
Abs. correction	None	None	None
GOF	1.54	2.11	1.44
R_1,[a] wR_2[b] $[I>2\sigma(I)]$	0.027, 0.063	0.032, 0.069	0.032, 0.053

$^{a}R_1 = \Sigma||F_o| - |F_c||/\Sigma|F_o|$. $^{b}wR_2 = [\Sigma[w(F_o^2 - F_c^2)^2]/\Sigma[w(F_o^2)^2]]^{1/2}$.

Table 2. Crystal and Refinement Data for Complexes **3a** and **4**.

	3a	**4**
Empirical formula	$C_{30}H_{36}F_6N_2O_4Pd$	$C_{17}H_{29}N_3O_4Pd$
Formula weight	709.01	445.8
Temperature (K)	100	100
a (Å)	13.980(6)	8.701(4)
b (Å)	13.117(6)	10.949(4)
c (Å)	17.134(7)	18.505(7)
α (°)	90	90
β (°)	91.48(2)	90
γ (°)	90	90
Volume (Å^3)	3140.9(2)	1763 (12)
Z	4	4
Crystal system	Monoclinic	Orthorhombic
Space group	$P2_1/c$ (#14)	$P2_12_12_1$ (#19)
d_{calc} (Mg/m^3)	1.499	1.680
θ range (deg)	1.96 to 42.61	2.16 to 35.69
μ (mm^{-1})	0.663	1.081
Abs. correction	Semi-empirical from equivalents	Semi-empirical from equivalents

GOF	1.64	1.62
R_1,[a] wR_2[b] $[I>2\sigma(I)]$	0.048, 0.085	0.028, 0.037

[a] $R_1 = \Sigma||F_o| - |F_c||/\Sigma|F_o|$. [b] $wR_2 = [\Sigma[w(F_o^2 - F_c^2)^2]/\Sigma[w(F_o^2)^2]]^{1/2}$.

References

1. Bercaw, J. E.; Day, M. W.; Golisz, S. R.; Hazari, N.; Henling, L. M.; Labinger, J. A.; Schofer, S. J.; Virgil, S. *Organometallics* **2009,** *28*, 5017-5024.

2. Arnaiz, A. M.; Carbayo, A.; Cuevas, J. V.; Diez, V.; García-Herbosa, G.; González, R.; Martínez, A.; Muñoz, A. *Eur. J. Inorg. Chem.* **2007**, 4637-4644.

3. Ono, N., The Nitro Function as a Leaving Group in Organic Synthesis. In *Nitro Compounds: Recent Advances in Synthesis and Chemistry*, Feuer, H.; Nielsen, A. T., Eds. VCH Publishers: New York, 1990; pp 1-135.

4. Butler, P. A.; Crane, C. G.; Golding, B. T.; Hammershøi, A.; Hockless, D. C.; Petersen, T. B.; Sargeson, A. M.; Ware, D. C. *Inorg. Chim. Acta* **2002,** *331*, 318-321.

5. Harrowfield, J. M.; Sargeson, A. M. *J. Am. Chem. Soc.* **1979,** *101*, 1514-1520.

6. Zhong, H. A.; Labinger, J. A.; Bercaw, J. E. *J. Am. Chem. Soc.* **2002,** *124*, 1378-1399.

7. We have as yet been unable to determine what becomes of the methyl group from the nitromethane in this reaction.

8. Solutions of either ^{H}diimine-Ar plus $Pd(OAc)_2$ or **2a** in nitroethane turn orange and exhibit ^{1}H NMR signals consistent with what would be expected for the ethyl analogue of **1a**, but the reaction is considerably less clean than the nitromethane

reactions, as indicated by additional NMR signals and further color changes; no pure product could be isolated.

9. Kliegman, J. M.; Barnes, R. K. *J. Org. Chem.* **1970,** *35*, 3140-3143.

10. Dieck, H. T.; Svoboda, M.; Greiser, T. *Z. Naturforsch., B: Chem. Sci.* **1981,** *36*, 823-832.

Appendix C

Data for Intramolecular C-H Activation of a Bisphenolate(benzene) Ligated Titanium Dibenzyl Complex

Table 1. The thermal decomposition of **1** at 368 K.

Run A1 (3220)					Run A2 (3238)				
seconds	Fp	tBu	[**1**]	ln[**1**]	seconds	Fp	tBu	[**1**]	ln[**1**]
0	1.00	15.95	100.00	4.61	0	1.00	12.95	100.00	4.61
2400	1.00	14.95	93.75	4.54					
4800	1.00	13.48	84.52	4.44					
7200	1.00	12.61	79.10	4.37					
9600	1.00	11.52	72.25	4.28					
12000	1.00	10.83	67.92	4.22					
14400	1.00	10.55	66.16	4.19					
16800	1.00	9.60	60.20	4.10					
19200	1.00	9.54	59.82	4.09	19200	1.00	8.03	62.01	4.13
					21600	1.00	7.74	59.80	4.09
					24000	1.00	7.30	56.41	4.03
					26400	1.00	6.95	53.72	3.98
					28800	1.00	6.70	51.78	3.95
					31200	1.00	6.36	49.17	3.90
					33600	1.00	6.00	46.37	3.84
					36000	1.00	5.74	44.37	3.79
76840	1.00	2.75	17.22	2.85					
79240	1.00	2.51	15.71	2.75					
	k_{obs}	2.22E-05							

Table 2. The thermal decomposition of **1** at 368 K.

Run B1 (3221)					Run B2 (3239)				
seconds	Fp	tBu	[**1**]	ln[**1**]	seconds	Fp	tBu	[**1**]	ln[**1**]
0	1.00	15.20	100.00	4.61	0	1.00	13.19	100.00	4.61
2400	1.00	13.82	90.93	4.51					
4800	1.00	13.24	87.12	4.47					
7200	1.00	12.73	83.79	4.43					
9600	1.00	11.63	76.51	4.34					
12000	1.00	10.97	72.22	4.28					
14400	1.00	10.10	66.49	4.20					
16800	1.00	10.02	65.93	4.19					
19200	1.00	9.508	62.55	4.14	19200	1.00	7.81	59.20	4.08
					21600	1.00	7.41	56.20	4.03
					24000	1.00	7.05	53.46	3.98
					26400	1.00	6.73	50.99	3.93
					28800	1.00	6.43	48.73	3.89
					31200	1.00	6.16	46.74	3.84
					33600	1.00	5.84	44.31	3.79
					36000	1.00	5.57	42.20	3.74
76840	1.00	2.45	16.14	2.78					
79240	1.00	2.38	15.68	2.75					
	k_{obs}	2.32E-05							

Table 3. The thermal decomposition of **1** at 378 K.

Run A (2183)

seconds	Fp	tBu	[**1**]	ln[**1**]
0	1.00	6.17	100.00	4.61
1200	1.00	5.54	89.74	4.50
2400	1.00	5.05	81.75	4.40
3600	1.00	4.59	74.44	4.31
4800	1.00	4.25	68.83	4.23
6000	1.00	4.00	64.88	4.17
7200	1.00	3.66	59.23	4.08
8400	1.00	3.37	54.58	4.00
9600	1.00	3.13	50.71	3.93
10800	1.00	2.98	48.34	3.88
12000	1.00	2.70	43.80	3.78
13200	1.00	2.51	40.61	3.70
14400	1.00	2.31	37.37	3.62
15600	1.00	2.15	34.76	3.55
	k_{obs}	6.59E-05		

Table 4. The thermal decomposition of **1** at 378 K.

Run B (2184)

seconds	Fp	tBu	[**1**]	ln[**1**]
0	1.00	9.39	100.00	4.61
1200	1.00	8.50	90.53	4.51
2400	1.00	7.73	82.40	4.41
3600	1.00	7.10	75.67	4.33
4800	1.00	6.59	70.24	4.25
6000	1.00	6.10	64.99	4.17
7200	1.00	5.60	59.71	4.09
8400	1.00	5.25	55.92	4.02
9600	1.00	4.82	51.32	3.94
10800	1.00	4.51	48.01	3.87
12000	1.00	4.14	44.11	3.79
13200	1.00	3.83	40.80	3.71
14400	1.00	3.53	37.58	3.63
15600	1.00	3.24	34.51	3.54
	k_{obs}	6.65E-05		

Table 5. The thermal decomposition of **1** at 388 K.

Run A (2146)

seconds	Fp	tBu	normalized	[**1**]	ln[**1**]
0	0.54	3.16	5.84	100.00	4.61
600	0.54	2.98	5.49	94.09	4.54
1200	0.53	2.52	4.72	80.92	4.39
1800	0.54	2.19	4.08	69.84	4.25
2400	0.53	1.93	3.63	62.10	4.13
3000	0.54	1.72	3.21	54.91	4.01
3600	0.54	1.54	2.87	49.14	3.89
4200	0.54	1.41	2.63	45.03	3.81
4800	0.53	1.27	2.38	40.74	3.71
5400	0.54	1.13	2.12	36.24	3.59
6000	0.54	0.99	1.85	31.76	3.46
6600	0.53	0.88	1.65	28.18	3.34
7200	0.53	0.82	1.53	26.26	3.27
7800	0.53	0.73	1.36	23.36	3.15
8400	0.53	0.64	1.20	20.55	3.02
9000	0.53	0.56	1.06	18.11	2.90
9600	0.53	0.50	0.94	16.03	2.77
10200	0.53	0.45	0.85	14.54	2.68
10800	0.53	0.41	0.77	13.12	2.57
11400	0.53	0.36	0.68	11.72	2.46
		k_{obs}	1.89E-04		

Table 6. The thermal decomposition of **1** at 388 K.

Run B (2150)

seconds	Fp	tBu	normalized	[**1**]	ln[**1**]
0	1.00	7.48		100.00	4.61
600	1.00	6.36		85.08	4.44
1200	1.00	5.58		74.54	4.31
1800	1.00	4.90		65.54	4.18
2400	1.00	4.39		58.69	4.07
3000	1.00	3.95		52.87	3.97
3600	1.00	3.62		48.37	3.88
4200	1.00	3.30		44.06	3.79
4800	1.00	2.99		40.04	3.69
5400	1.00	2.70		36.08	3.59
6000	1.00	2.44		32.68	3.49
6600	1.00	2.24		29.92	3.40
7200	1.00	2.01		26.88	3.29
7800	1.00	1.94		25.92	3.26
8400	1.00	1.79		23.95	3.18
9000	1.00	1.61		21.55	3.07
9600	1.00	1.46		19.46	2.97
10200	1.00	1.33		17.83	2.88
10800	1.00	1.20		16.09	2.78
11400	1.00	1.09		14.52	2.68
12000	1.00	0.99		13.23	2.58
		k_{obs}	1.60E-04		

Table 7. The thermal decomposition of **1** at 398 K.

Run A (2168)

seconds	Fp	tBu	[**1**]	ln[**1**]
0	1.00	7.72	100.00	4.61
300	1.00	5.63	72.93	4.29
600	1.00	4.52	58.63	4.07
900	1.00	4.01	51.90	3.95
1200	1.00	3.68	47.70	3.86
1500	1.00	3.34	43.22	3.77
1800	1.00	3.04	39.40	3.67
2100	1.00	2.71	35.16	3.56
2400	1.00	2.47	31.98	3.46
2700	1.00	2.13	27.61	3.32
3000	1.00	2.14	27.69	3.32
3300	1.00	1.93	24.99	3.22
3600	1.00	1.73	22.44	3.11
3900	1.00	1.53	19.89	2.99
4200	1.00	1.38	17.85	2.88
4500	1.00	1.16	15.09	2.71
4800	1.00	1.04	13.45	2.60
5100	1.00	0.93	11.99	2.48
5400	1.00	0.83	10.82	2.38
	k_{obs}	3.67E-04		

Table 8. The thermal decomposition of **1** at 398 K.

Run B (2181)

seconds	Fp	tBu	[**1**]	ln[**1**]
0	1.00	4.27	100.00	4.61
300	1.00	3.26	76.54	4.34
600	1.00	2.49	58.32	4.07
900	1.00	2.01	47.07	3.85
1200	1.00	1.77	41.49	3.73
1500	1.00	1.57	36.78	3.60
1800	1.00	1.41	33.07	3.50
2100	1.00	1.27	29.80	3.39
2400	1.00	1.15	26.85	3.29
2700	1.00	1.03	24.10	3.18
3000	1.00	0.93	21.69	3.08
3300	1.00	0.82	19.29	2.96
3600	1.00	0.74	17.39	2.86
3900	1.00	0.67	15.75	2.76
4200	1.00	0.61	14.37	2.66
4500	1.00	0.56	13.03	2.57
4800	1.00	0.51	12.04	2.49
	k_{obs}	4.06E-04		

Table 9. The thermal decomposition of **1** at 398 K.

Run C (2182)

seconds	Fp	tBu	[**1**]	ln[**1**]
0	1.00	5.39	100.00	4.61
300	1.00	4.24	78.56	4.36
600	1.00	3.60	66.71	4.20
900	1.00	3.15	58.47	4.07
1200	1.00	2.77	51.47	3.94
1500	1.00	2.46	45.63	3.82
1800	1.00	2.16	40.19	3.69
2100	1.00	1.89	35.14	3.56
2400	1.00	1.65	30.65	3.42
2700	1.00	1.45	26.85	3.29
3000	1.00	1.24	23.00	3.14
3300	1.00	1.08	20.04	3.00
3600	1.00	0.94	17.47	2.86
3900	1.00	0.81	15.18	2.72
4200	1.00	0.73	13.60	2.61
4500	1.00	0.64	12.00	2.49
4800	1.00	0.58	10.74	2.37
	k_{obs}	4.53E-04		

Table 10. The thermal decomposition of **1-*d*$_3$** at 388 K.

Run A (2190)

seconds	Fp	tBu	normalized	[**1-*d*$_3$**]	ln[**1-*d*$_3$**]
0	0.56	4.73	8.43	100.00	4.61
600	0.55	3.56	6.44	76.37	4.34
1200	0.55	3.08	5.63	66.74	4.20
1800	0.54	2.67	4.90	58.12	4.06
2400	0.55	2.51	4.59	54.40	4.00
3000	0.56	2.32	4.18	49.56	3.90
3600	0.55	2.13	3.84	45.56	3.82
4200	0.55	1.97	3.56	42.21	3.74
4800	0.55	1.81	3.31	39.19	3.67
5400	0.55	1.67	3.01	35.73	3.58
6000	0.54	1.48	2.76	32.74	3.49
6600	0.54	1.38	2.54	30.08	3.40
7200	0.55	1.28	2.32	27.47	3.31
7800	0.55	1.17	2.12	25.18	3.23
8400	0.55	1.07	1.93	22.85	3.13
9000	0.55	0.96	1.76	20.85	3.04
9600	0.55	0.90	1.62	19.23	2.96
10200	0.55	0.81	1.48	17.54	2.86
10800	0.55	0.75	1.36	16.13	2.78
		k_{obs}	1.53E-04		

Table 11. The thermal decomposition of **1-*d*$_3$** at 388 K.

Run B (2191)

seconds	Fp	tBu	normalized	[**1-*d*$_3$**]	ln[**1-*d*$_3$**]
0	0.56	4.15	7.42	100.00	4.61
600	0.55	3.11	5.64	76.05	4.33
1200	0.55	2.66	4.84	65.25	4.18
1800	0.55	2.39	4.36	58.79	4.07
2400	0.54	2.19	4.02	54.13	3.99
3000	0.55	2.01	3.67	49.42	3.90
3600	0.55	1.86	3.39	45.68	3.82
4200	0.55	1.71	3.12	42.09	3.74
4800	0.55	1.57	2.87	38.61	3.65
5400	0.55	1.44	2.64	35.54	3.57
6000	0.53	1.29	2.43	32.77	3.49
6600	0.54	1.20	2.21	29.75	3.39
7200	0.54	1.09	2.01	27.07	3.30
7800	0.53	0.97	1.85	24.88	3.21
8400	0.55	0.92	1.68	22.61	3.12
9000	0.54	0.83	1.55	20.92	3.04
9600	0.55	0.75	1.37	18.44	2.91
10200	0.55	0.68	1.25	16.89	2.83
10800	0.55	0.63	1.15	15.51	2.74
		k_{obs}	1.56E-04		

Table 12. The thermal decomposition of **1-*d*$_4$** at 388 K.

Run A (3120)

seconds	Fp	tBu	normalized	[**1-*d*$_4$**]	ln[**1-*d*$_4$**]
0	1.00	6.38		100.00	4.61
600	1.00	5.94		93.16	4.53
1200	1.00	5.54		86.80	4.46
1800	1.00	5.32		83.40	4.42
2400	1.00	5.04		79.06	4.37
3000	1.00	4.85		76.05	4.33
3600	1.00	4.78		74.93	4.32
4200	1.00	4.55		71.32	4.27
4800	1.00	4.40		69.01	4.23
5400	1.00	4.14		64.96	4.17
6000	1.00	3.94		61.69	4.12
6600	1.00	3.77		59.14	4.08
7200	1.00	3.48		54.62	4.00
7800	1.00	3.32		52.10	3.95
8400	1.00	3.12		48.91	3.89
9000	1.00	2.95		46.27	3.83
9600	1.00	2.77		43.35	3.77
10200	1.00	2.57		40.35	3.70
10800	1.00	2.39		37.51	3.62
11400	1.00	2.24		35.09	3.56
12000	1.00	2.05		32.17	3.47
12600	1.00	1.95		30.57	3.42
13200	1.00	1.76		27.54	3.32
13800	1.00	1.60		25.08	3.22
14400	1.00	1.50		23.52	3.16
15000	1.00	1.38		21.58	3.07
15600	1.00	1.27		19.92	2.99
16200	1.00	1.17		18.40	2.91
		k_{obs}	1.02E-04		

Table 13. The thermal decomposition of **1-*d*$_4$** at 388 K.

Run B (3296)

seconds	Fp	tBu	normalized	[**1-*d*$_4$**]	ln[**1-*d*$_4$**]
0	1.00	25.96		100.00	4.61
600	1.00	20.97		80.78	4.39
1200	1.00	19.33		74.45	4.31
1800	1.00	22.99		88.57	4.48
2400	1.00	22.44		86.43	4.46
3000	1.00	21.97		84.64	4.44
3600	1.00	20.67		79.65	4.38
4200	1.00	20.89		80.48	4.39
4800	1.00	15.15		58.36	4.07
5400	1.00	15.25		58.74	4.07
6000	1.00	14.63		56.38	4.03
6600	1.00	13.73		52.88	3.97
7200	1.00	12.87		49.59	3.90
7800	1.00	12.76		49.16	3.90
8400	1.00	12.24		47.15	3.85
9000	1.00	11.22		43.21	3.77
9600	1.00	10.65		41.03	3.71
10200	1.00	9.97		38.39	3.65
10800	1.00	8.91		34.34	3.54
11400	1.00	8.74		33.66	3.52
12000	1.00	8.10		31.21	3.44
12600	1.00	7.58		29.20	3.37
13200	1.00	7.24		27.89	3.33
13800	1.00	6.69		25.78	3.25
		k_{obs}	9.61E-05		

Table 14. The thermal decomposition of **1-*d*$_4$** at 388 K.

Run C (3297)

seconds	Fp	tBu	normalized	[**1-*d*$_4$**]	ln[**1-*d*$_4$**]
0	1.00	12.13		100.00	4.61
600	1.00	10.78		88.89	4.49
1200	1.00	12.29		101.37	4.62
1800	1.00	12.61		103.98	4.64
2400	1.00	12.12		99.89	4.60
3000	1.00	11.43		94.24	4.55
3600	1.00	10.96		90.40	4.50
4200	1.00	10.77		88.77	4.49
4800	1.00	8.41		69.34	4.24
5400	1.00	8.10		66.79	4.20
6000	1.00	8.02		66.13	4.19
6600	1.00	7.49		61.78	4.12
7200	1.00	7.19		59.31	4.08
7800	1.00	6.76		55.72	4.02
8400	1.00	6.51		53.65	3.98
9000	1.00	6.29		51.86	3.95
9600	1.00	5.89		48.59	3.88
10200	1.00	5.58		45.97	3.83
10800	1.00	5.34		44.06	3.79
11400	1.00	5.01		41.31	3.72
12000	1.00	4.66		38.46	3.65
12600	1.00	4.48		36.94	3.61
13200	1.00	4.18		34.47	3.54
13800	1.00	3.92		32.32	3.48
		k_{obs}	8.81E-05		

Table 15. The thermal decomposition of **1-*d*$_{10}$** at 388 K.

Run A (3171)

seconds	Fp	tBu	normalized	[**1-*d*$_{10}$**]	ln[**1-*d*$_{10}$**]
0	0.31	1.50	4.88	100.00	4.61
600	0.31	1.64	5.24	107.40	4.68
1200	0.30	1.19	3.94	80.74	4.39
1800	0.31	1.14	3.62	74.18	4.31
2400	0.31	1.03	3.30	67.66	4.21
3000	0.31	0.95	3.04	62.34	4.13
3600	0.31	0.86	2.75	56.48	4.03
4200	0.31	0.78	2.51	51.57	3.94
4800	0.31	0.91	2.94	60.25	4.10
5400	0.31	0.65	2.09	42.85	3.76
6000	0.31	0.59	1.90	39.06	3.67
6600	0.31	0.55	1.78	36.41	3.59
7200	0.31	0.49	1.57	32.10	3.47
7800	0.31	0.45	1.46	29.90	3.40
8400	0.31	0.40	1.29	26.49	3.28
9000	0.31	0.36	1.17	23.90	3.17
9600	0.31	0.32	1.03	21.09	3.05
10200	0.30	0.31	1.00	20.61	3.03
10800	0.31	0.27	0.90	18.38	2.91
11400	0.31	0.25	0.82	16.72	2.82
12000	0.31	0.24	0.75	15.45	2.74
12600	0.31	0.21	0.67	13.78	2.62
		k_{obs}	1.60E-04		

Table 16. The thermal decomposition of **1-*d*$_{10}$** at 388 K.

Run B (3172)

seconds	Fp	tBu	normalized	[**1-*d*$_{10}$**]	ln[**1-*d*$_{10}$**]
0	0.30	1.90	6.24	100.00	4.61
600	0.30	1.75	5.75	92.14	4.52
1200	0.31	1.54	4.94	79.10	4.37
1800	0.31	1.45	4.64	74.36	4.31
2400	0.31	1.35	4.36	69.89	4.25
3000	0.31	1.22	3.92	62.82	4.14
3600	0.31	1.09	3.53	56.52	4.03
4200	0.31	1.03	3.30	52.82	3.97
4800	0.31	0.93	3.00	48.12	3.87
5400	0.31	0.84	2.70	43.25	3.77
6000	0.31	0.78	2.51	40.16	3.69
6600	0.31	0.71	2.28	36.48	3.60
7200	0.31	0.65	2.10	33.66	3.52
7800	0.31	0.58	1.84	29.49	3.38
8400	0.31	0.51	1.65	26.39	3.27
9000	0.31	0.47	1.51	24.13	3.18
9600	0.31	0.43	1.38	22.14	3.10
10200	0.31	0.39	1.27	20.29	3.01
10800	0.31	0.36	1.14	18.30	2.91
11400	0.31	0.33	1.04	16.73	2.82
12000	0.31	0.30	0.96	15.40	2.73
12600	0.31	0.28	0.89	14.22	2.65
		k_{obs}	1.56E-04		

Table 17. The thermal decomposition of **1-*d*$_{14}$** at 388 K.

Run A (3086)

seconds	Fp	tBu	normalized	[**1-*d*$_{14}$**]	ln[**1-*d*$_{14}$**]
0	1.00	18.88		100.00	4.61
600	1.00	18.04		95.52	4.56
1200	1.00	16.23		85.97	4.45
1800	1.00	16.80		88.95	4.49
2400	1.00	16.40		86.85	4.46
3000	1.00	15.57		82.47	4.41
3600	1.00	15.71		83.20	4.42
4200	1.00	14.19		75.17	4.32
4800	1.00	13.98		74.05	4.30
5400	1.00	13.50		71.51	4.27
6000	1.00	12.14		64.31	4.16
6600	1.00	11.94		63.24	4.15
7200	1.00	11.63		61.57	4.12
7800	1.00	10.63		56.27	4.03
8400	1.00	10.12		53.62	3.98
9000	1.00	9.70		51.36	3.94
9600	1.00	9.00		47.66	3.86
10200	1.00	8.46		44.79	3.80
10800	1.00	7.94		42.06	3.74
11400	1.00	7.17		37.99	3.64
		k_{obs}	8.04E-05		

Table 18. The thermal decomposition of **1-*d*$_{14}$** at 388 K.

Run B (3087)

seconds	Fp	tBu	normalized	[**1-*d*$_{14}$**]	ln[**1-*d*$_{14}$**]
0	1.00	15.27		100.00	4.61
600	1.00	14.95		97.86	4.58
1200	1.00	13.91		91.05	4.51
1800	1.00	13.52		88.48	4.48
2400	1.00	13.21		86.49	4.46
3000	1.00	12.56		82.21	4.41
3600	1.00	12.14		79.45	4.38
4200	1.00	11.81		77.34	4.35
4800	1.00	11.41		74.72	4.31
5400	1.00	10.74		70.31	4.25
6000	1.00	10.25		67.09	4.21
6600	1.00	9.71		63.57	4.15
7200	1.00	9.41		61.60	4.12
7800	1.00	8.76		57.33	4.05
8400	1.00	8.37		54.78	4.00
9000	1.00	8.43		55.22	4.01
9600	1.00	7.44		48.72	3.89
10200	1.00	7.12		46.65	3.84
10800	1.00	6.68		43.71	3.78
11400	1.00	6.18		40.45	3.70
		k_{obs}	7.67E-05		

Rate Equations

$1.64(2) \times 10^{-4} = k_{obs}(\mathbf{1}, \mathbf{1\text{-}d_{10}}) = k_{\alpha H} + k_{\sigma H}$

$1.55(2) \times 10^{-4} = k_{obs}(\mathbf{1\text{-}d_3}) = k_{\alpha H} + k_{\sigma D}$

$8.65(5) \times 10^{-5} = k_{obs}(\mathbf{1\text{-}d_4}, \mathbf{1\text{-}d_{14}}) = k_{\alpha D} + k_{\sigma H}$

$k_{\alpha H} = 1.3\ k_{\sigma D}$

$k_{\sigma H} = 4.4\ k_{\alpha D}$

$1.55(2) \times 10^{-4} = 1.3\ k_{\sigma D} + k_{\sigma D}$

$k_{\sigma D} = 6.74(2) \times 10^{-5}$

$8.65(5) \times 10^{-5} = k_{\alpha D} + 4.4\ k_{\alpha D}$

$k_{\alpha D} = 1.60(5) \times 10^{-5}$

$1.64(2) \times 10^{-4} = 1.3\ k_{\sigma D} + 4.4\ k_{\alpha D}$

$1.64(2) \times 10^{-4} = 1.58(5) \times 10^{-4}$ *(check)*

$k_{\alpha H} = 8.75(2) \times 10^{-5}$

$k_{\alpha D} = 1.60(5) \times 10^{-5}$

KIE (α-abstraction) = 5.5(3)

$k_{\sigma H} = 7.04(5) \times 10^{-5}$

$k_{\sigma D} = 6.74(2) \times 10^{-5}$

KIE (σ-bond metathesis) = 1.0(1)

Appendix D

Full Crystallographic Data

1.1-TiOiPr$_2$ (CCDC 639874)

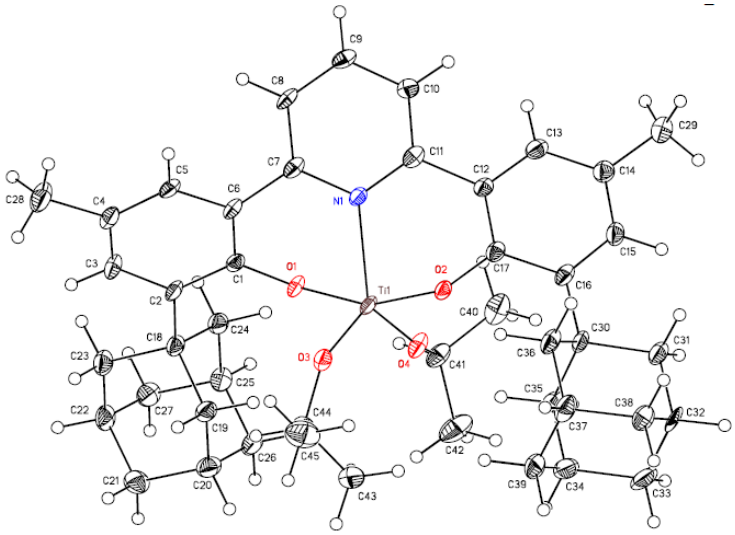

Special Refinement Details

Refinement of F^2 against ALL reflections. The weighted R-factor (wR) and goodness of fit (S) are based on F^2, conventional R-factors (R) are based on F, with F set to zero for negative F^2. The threshold expression of $F^2 > 2\sigma(F^2)$ is used only for calculating R-factors(gt) etc. and is not relevant to the choice of reflections for refinement. R-factors based on F^2 are statistically about twice as large as those based on F, and R-factors based on ALL data will be even larger.

All esds (except the esd in the dihedral angle between two l.s. planes) are estimated using the full covariance matrix. The cell esds are taken into account individually in the estimation of esds in distances, angles and torsion angles; correlations between esds in cell parameters are only used when they are defined by crystal symmetry. An approximate (isotropic) treatment of cell esds is used for estimating esds involving l.s. planes.

Table 1. Atomic coordinates (x 10^4) and equivalent isotropic displacement parameters (Å^2 x 10^3). U(eq) is defined as the trace of the orthogonalized Uij tensor.

	x	y	z	Ueq	Occ
Ti(1)	5536(1)	7750(1)	6712(1)	15(1)	1
O(1)	4112(1)	7369(1)	7109(1)	15(1)	1
O(2)	6860(1)	8225(1)	5918(1)	15(1)	1
O(3)	5233(2)	8550(1)	7600(1)	20(1)	1
O(4)	6242(2)	6441(1)	6862(1)	19(1)	1
N(1)	5004(2)	8419(2)	5558(2)	14(1)	1
C(1)	3150(2)	8093(2)	7273(2)	14(1)	1
C(2)	2214(2)	7987(2)	8071(2)	17(1)	1
C(3)	1268(2)	8803(2)	8227(2)	20(1)	1
C(4)	1204(2)	9723(2)	7648(2)	19(1)	1
C(5)	2102(2)	9781(2)	6851(2)	17(1)	1
C(6)	3067(2)	8965(2)	6639(2)	14(1)	1
C(7)	3905(2)	8949(2)	5710(2)	16(1)	1
C(8)	3576(2)	9424(2)	4978(2)	18(1)	1
C(9)	4342(2)	9380(2)	4096(2)	17(1)	1
C(10)	5434(2)	8828(2)	3958(2)	17(1)	1
C(11)	5738(2)	8342(2)	4694(2)	15(1)	1
C(12)	6929(2)	7756(2)	4518(2)	14(1)	1

C(13)	7518(2)	7245(2)	3725(2)	19(1)	1
C(14)	8655(2)	6791(2)	3476(2)	19(1)	1
C(15)	9185(2)	6910(2)	4054(2)	19(1)	1
C(16)	8645(2)	7396(2)	4860(2)	16(1)	1
C(17)	7460(2)	7804(2)	5119(2)	15(1)	1
C(18)	2255(2)	7004(2)	8735(2)	17(1)	1
C(19)	3088(2)	6974(2)	9211(2)	19(1)	1
C(20)	3152(2)	5986(2)	9872(2)	23(1)	1
C(21)	2000(2)	6007(2)	10607(2)	24(1)	1
C(22)	1158(2)	6023(2)	10152(2)	22(1)	1
C(23)	1105(2)	7007(2)	9493(2)	22(1)	1
C(24)	2615(2)	5998(2)	8239(2)	18(1)	1
C(25)	2688(2)	5014(2)	8902(2)	20(1)	1
C(26)	3528(2)	5006(2)	9347(2)	24(1)	1
C(27)	1529(2)	5040(2)	9639(2)	22(1)	1
C(28)	164(2)	10610(2)	7894(2)	30(1)	1
C(29)	9301(2)	6242(2)	2609(2)	26(1)	1
C(30)	9276(2)	7534(2)	5447(2)	17(1)	1
C(31)	10555(2)	7117(2)	4991(2)	20(1)	1
C(32)	11184(2)	7287(2)	5573(2)	24(1)	1
C(33)	10805(2)	6681(3)	6503(2)	30(1)	1
C(34)	9535(2)	7091(3)	6976(2)	29(1)	1
C(35)	8916(2)	6916(2)	6387(2)	21(1)	1
C(36)	9068(2)	8706(2)	5586(2)	22(1)	1
C(37)	9688(2)	8865(2)	6183(2)	25(1)	1
C(38)	10951(2)	8443(2)	5703(2)	27(1)	1
C(39)	9290(2)	8256(3)	7105(2)	30(1)	1
C(40)	7041(2)	4976(2)	5959(2)	31(1)	1
C(41)	6354(2)	5338(2)	6900(2)	20(1)	1
C(42)	6875(3)	4814(2)	7597(2)	35(1)	1
C(43)	6073(2)	7692(2)	8721(2)	28(1)	1
C(44)	5252(2)	8637(2)	8483(2)	21(1)	1
C(45)	5532(3)	9659(2)	8479(2)	36(1)	1
C(51)	6635(3)	2062(3)	6966(2)	35(1)	1
C(52)	7445(3)	1776(2)	7362(2)	32(1)	1
C(53)	7165(3)	1853(2)	8282(2)	30(1)	1
C(54)	6060(3)	2209(2)	8823(2)	28(1)	1
C(55)	5244(3)	2492(2)	8422(2)	30(1)	1
C(56)	5536(3)	2425(2)	7506(2)	33(1)	1
C(61)	1932(3)	2224(2)	9268(2)	30(1)	1
C(62)	2170(2)	1477(2)	8683(2)	26(1)	1
C(63)	2453(3)	425(2)	8958(2)	29(1)	1
C(64)	2449(3)	147(2)	9835(2)	32(1)	1
C(65)	2198(2)	895(2)	10421(2)	29(1)	1
C(66)	1938(2)	1940(2)	10146(2)	31(1)	1
C(71)	4858(3)	6045(2)	4691(2)	30(1)	1
C(72)	4249(3)	5763(3)	5583(2)	30(1)	1
C(73)	4396(3)	4710(3)	5885(2)	31(1)	1

Table 2. Bond lengths [Å] and angles [°].

Ti(1)-O(4)	1.7529(18)	O(4)-Ti(1)-O(3)	115.30(9)
Ti(1)-O(3)	1.758(2)	O(4)-Ti(1)-O(2)	95.55(8)
Ti(1)-O(2)	1.9216(18)	O(3)-Ti(1)-O(2)	95.25(9)
Ti(1)-O(1)	1.9235(19)	O(4)-Ti(1)-O(1)	91.96(8)

Ti(1)-N(1)	2.169(2)	O(3)-Ti(1)-O(1)	98.44(8)
O(1)-C(1)	1.329(3)	O(2)-Ti(1)-O(1)	159.79(8)
O(2)-C(17)	1.328(3)	O(4)-Ti(1)-N(1)	125.57(9)
O(3)-C(44)	1.431(3)	O(3)-Ti(1)-N(1)	119.12(9)
O(4)-C(41)	1.419(3)	O(2)-Ti(1)-N(1)	80.84(8)
N(1)-C(11)	1.342(3)	O(1)-Ti(1)-N(1)	79.53(8)
N(1)-C(7)	1.374(3)	C(1)-O(1)-Ti(1)	121.64(17)
C(1)-C(6)	1.406(3)	C(17)-O(2)-Ti(1)	119.41(17)
C(1)-C(2)	1.409(4)	C(44)-O(3)-Ti(1)	148.41(17)
C(2)-C(3)	1.380(3)	C(41)-O(4)-Ti(1)	152.02(17)
C(2)-C(18)	1.531(4)	C(11)-N(1)-C(7)	119.2(2)
C(3)-C(4)	1.399(4)	C(11)-N(1)-Ti(1)	120.95(17)
C(4)-C(5)	1.370(4)	C(7)-N(1)-Ti(1)	119.84(18)
C(4)-C(28)	1.510(4)	O(1)-C(1)-C(6)	119.4(2)
C(5)-C(6)	1.395(3)	O(1)-C(1)-C(2)	120.5(2)
C(6)-C(7)	1.464(4)	C(6)-C(1)-C(2)	120.0(2)
C(7)-C(8)	1.383(4)	C(3)-C(2)-C(1)	117.3(2)
C(8)-C(9)	1.375(4)	C(3)-C(2)-C(18)	121.7(2)
C(9)-C(10)	1.377(4)	C(1)-C(2)-C(18)	121.0(2)
C(10)-C(11)	1.377(4)	C(2)-C(3)-C(4)	123.5(3)
C(11)-C(12)	1.491(4)	C(5)-C(4)-C(3)	118.0(2)
C(12)-C(13)	1.373(4)	C(5)-C(4)-C(28)	121.6(3)
C(12)-C(17)	1.397(4)	C(3)-C(4)-C(28)	120.5(3)
C(13)-C(14)	1.380(4)	C(4)-C(5)-C(6)	121.1(3)
C(14)-C(15)	1.394(4)	C(5)-C(6)-C(1)	119.6(3)
C(14)-C(29)	1.497(4)	C(5)-C(6)-C(7)	119.5(2)
C(15)-C(16)	1.369(4)	C(1)-C(6)-C(7)	120.2(2)
C(16)-C(17)	1.426(4)	N(1)-C(7)-C(8)	120.0(3)
C(16)-C(30)	1.523(4)	N(1)-C(7)-C(6)	120.2(2)
C(18)-C(24)	1.528(4)	C(8)-C(7)-C(6)	119.7(2)
C(18)-C(23)	1.534(4)	C(9)-C(8)-C(7)	120.6(2)
C(18)-C(19)	1.542(4)	C(8)-C(9)-C(10)	118.5(3)
C(19)-C(20)	1.537(4)	C(11)-C(10)-C(9)	119.9(3)
C(20)-C(21)	1.519(4)	N(1)-C(11)-C(10)	121.7(2)
C(20)-C(26)	1.521(4)	N(1)-C(11)-C(12)	119.8(2)
C(21)-C(22)	1.531(4)	C(10)-C(11)-C(12)	118.4(2)
C(22)-C(27)	1.514(4)	C(13)-C(12)-C(17)	120.7(2)
C(22)-C(23)	1.529(4)	C(13)-C(12)-C(11)	119.3(3)
C(24)-C(25)	1.534(4)	C(17)-C(12)-C(11)	119.8(2)
C(25)-C(26)	1.521(4)	C(12)-C(13)-C(14)	121.8(3)
C(25)-C(27)	1.525(4)	C(13)-C(14)-C(15)	116.6(3)
C(30)-C(36)	1.538(4)	C(13)-C(14)-C(29)	121.9(3)
C(30)-C(31)	1.541(4)	C(15)-C(14)-C(29)	121.5(2)
C(30)-C(35)	1.541(4)	C(16)-C(15)-C(14)	124.5(3)
C(31)-C(32)	1.530(4)	C(15)-C(16)-C(17)	117.2(3)
C(32)-C(38)	1.508(4)	C(15)-C(16)-C(30)	122.1(2)
C(32)-C(33)	1.524(4)	C(17)-C(16)-C(30)	120.6(2)
C(33)-C(34)	1.532(4)	O(2)-C(17)-C(12)	120.0(2)
C(34)-C(39)	1.519(4)	O(2)-C(17)-C(16)	121.1(3)
C(34)-C(35)	1.532(4)	C(12)-C(17)-C(16)	118.9(3)
C(36)-C(37)	1.535(4)	C(24)-C(18)-C(2)	111.5(2)
C(37)-C(39)	1.518(4)	C(24)-C(18)-C(23)	107.6(2)
C(37)-C(38)	1.528(4)	C(2)-C(18)-C(23)	111.7(2)
C(40)-C(41)	1.496(4)	C(24)-C(18)-C(19)	109.2(2)
C(41)-C(42)	1.493(4)	C(2)-C(18)-C(19)	109.6(2)

C(43)-C(44)	1.515(4)	C(23)-C(18)-C(19)	107.0(2)
C(44)-C(45)	1.495(4)	C(20)-C(19)-C(18)	110.5(2)
C(51)-C(56)	1.371(4)	C(21)-C(20)-C(26)	109.4(2)
C(51)-C(52)	1.375(4)	C(21)-C(20)-C(19)	109.5(2)
C(52)-C(53)	1.372(4)	C(26)-C(20)-C(19)	109.7(2)
C(53)-C(54)	1.375(4)	C(20)-C(21)-C(22)	109.2(2)
C(54)-C(55)	1.385(4)	C(27)-C(22)-C(23)	110.4(2)
C(55)-C(56)	1.362(4)	C(27)-C(22)-C(21)	109.4(2)
C(61)-C(62)	1.359(4)	C(23)-C(22)-C(21)	108.9(2)
C(61)-C(66)	1.379(4)	C(22)-C(23)-C(18)	111.2(2)
C(62)-C(63)	1.379(4)	C(18)-C(24)-C(25)	111.3(2)
C(63)-C(64)	1.373(4)	C(26)-C(25)-C(27)	109.6(2)
C(64)-C(65)	1.356(4)	C(26)-C(25)-C(24)	108.9(2)
C(65)-C(66)	1.369(4)	C(27)-C(25)-C(24)	109.4(2)
C(71)-C(73)#1	1.372(4)	C(20)-C(26)-C(25)	109.8(2)
C(71)-C(72)	1.378(4)	C(22)-C(27)-C(25)	109.2(2)
C(72)-C(73)	1.381(4)	C(16)-C(30)-C(36)	110.5(2)
C(73)-C(71)#1	1.372(4)	C(16)-C(30)-C(31)	111.4(2)
		C(36)-C(30)-C(31)	107.4(2)
		C(16)-C(30)-C(35)	111.2(2)
		C(36)-C(30)-C(35)	109.5(2)
		C(31)-C(30)-C(35)	106.7(2)
		C(32)-C(31)-C(30)	111.0(2)
		C(38)-C(32)-C(33)	109.7(3)
		C(38)-C(32)-C(31)	110.5(2)
		C(33)-C(32)-C(31)	109.2(2)
		C(32)-C(33)-C(34)	108.7(2)
		C(39)-C(34)-C(35)	110.2(2)
		C(39)-C(34)-C(33)	109.2(3)
		C(35)-C(34)-C(33)	109.5(3)
		C(34)-C(35)-C(30)	110.3(2)
		C(37)-C(36)-C(30)	111.4(2)
		C(39)-C(37)-C(38)	109.6(2)
		C(39)-C(37)-C(36)	108.9(2)
		C(38)-C(37)-C(36)	108.7(2)
		C(32)-C(38)-C(37)	109.6(2)
		C(37)-C(39)-C(34)	110.2(3)
		O(4)-C(41)-C(42)	108.7(2)
		O(4)-C(41)-C(40)	108.1(2)
		C(42)-C(41)-C(40)	112.9(3)
		O(3)-C(44)-C(45)	108.8(2)
		O(3)-C(44)-C(43)	109.7(2)
		C(45)-C(44)-C(43)	112.9(3)
		C(56)-C(51)-C(52)	118.9(3)
		C(53)-C(52)-C(51)	120.9(3)
		C(52)-C(53)-C(54)	120.0(3)
		C(53)-C(54)-C(55)	119.0(3)
		C(56)-C(55)-C(54)	120.4(3)
		C(55)-C(56)-C(51)	120.8(3)
		C(62)-C(61)-C(66)	120.6(3)
		C(61)-C(62)-C(63)	119.9(3)
		C(64)-C(63)-C(62)	119.2(3)
		C(65)-C(64)-C(63)	120.7(3)
		C(64)-C(65)-C(66)	120.3(3)
		C(65)-C(66)-C(61)	119.3(3)

		C(73)#1-C(71)-C(72)	120.3(3)
		C(71)-C(72)-C(73)	119.1(3)
		C(71)#1-C(73)-C(72)	120.6(3)

Symmetry transformations used to generate equivalent atoms: #1 -x+1,-y+1,-z+1

Table 3. Anisotropic displacement parameters ($Å^2$ x 10^4). The anisotropic displacement factor exponent takes the form: $-2\pi^2[h^2a^*2U^{11} + ... + 2 h k a^* b^* U^{12}]$.

	U^{11}	U^{22}	U^{33}	U^{23}	U^{13}	U^{12}
Ti(1)	85(3)	161(3)	179(3)	24(2)	-65(2)	-4(2)
O(1)	87(10)	131(10)	225(11)	24(8)	-65(8)	-10(8)
O(2)	84(10)	190(11)	163(11)	19(8)	-47(8)	-40(8)
O(3)	113(10)	263(12)	189(11)	10(9)	-42(9)	-26(9)
O(4)	114(10)	153(11)	289(12)	37(8)	-75(9)	-14(8)
N(1)	105(12)	149(12)	157(13)	14(10)	-58(10)	-25(10)
C(1)	114(15)	160(15)	169(16)	-30(12)	-74(12)	-27(12)
C(2)	99(15)	174(15)	216(17)	4(12)	-77(12)	2(12)
C(3)	94(15)	204(16)	265(18)	-17(13)	-49(13)	-12(12)
C(4)	135(15)	185(16)	252(18)	-38(13)	-92(13)	12(12)
C(5)	142(15)	157(15)	220(17)	27(12)	-108(13)	-8(12)
C(6)	102(14)	122(14)	227(17)	2(12)	-90(12)	-21(11)
C(7)	136(15)	127(15)	235(17)	34(12)	-97(13)	-31(12)
C(8)	116(15)	173(15)	270(18)	18(13)	-127(13)	-23(12)
C(9)	188(16)	145(15)	223(17)	48(12)	-127(13)	-60(12)
C(10)	177(16)	166(15)	177(16)	-8(12)	-79(13)	-38(12)
C(11)	136(15)	134(15)	236(17)	7(12)	-94(13)	-79(12)
C(12)	133(15)	132(14)	156(16)	52(12)	-55(12)	-43(12)
C(13)	165(16)	214(16)	203(17)	39(13)	-93(13)	-71(13)
C(14)	172(17)	177(16)	191(17)	8(12)	-58(13)	-40(13)
C(15)	116(15)	215(16)	187(17)	20(13)	-19(13)	-27(12)
C(16)	124(15)	141(15)	222(17)	41(12)	-79(13)	-25(12)
C(17)	128(15)	134(15)	178(16)	29(12)	-54(12)	-28(12)
C(18)	109(15)	199(16)	183(16)	30(12)	-44(12)	-46(12)
C(19)	150(15)	227(16)	200(17)	6(13)	-83(13)	-56(13)
C(20)	209(17)	272(18)	225(17)	9(13)	-108(14)	-81(14)
C(21)	241(17)	292(18)	197(17)	40(13)	-67(14)	-106(14)
C(22)	130(16)	271(18)	233(17)	31(13)	-23(13)	-82(13)
C(23)	136(15)	235(17)	237(18)	2(13)	-35(13)	-32(13)
C(24)	149(15)	208(16)	183(16)	17(12)	-58(12)	-51(12)
C(25)	181(16)	181(16)	226(17)	14(13)	-57(13)	-42(13)
C(26)	145(16)	260(18)	270(18)	88(14)	-85(14)	-37(13)
C(27)	201(17)	229(17)	239(17)	51(13)	-80(14)	-83(13)
C(28)	164(17)	261(18)	390(20)	42(15)	-80(15)	15(14)
C(29)	174(17)	312(18)	280(19)	-40(14)	-73(14)	-16(14)
C(30)	83(15)	190(16)	201(16)	17(12)	-47(12)	-11(12)
C(31)	119(15)	227(16)	244(17)	-8(13)	-78(13)	-23(13)
C(32)	49(15)	332(19)	332(19)	-9(14)	-96(13)	-16(13)
C(33)	196(18)	400(20)	340(20)	45(15)	-190(15)	-43(15)
C(34)	194(17)	450(20)	216(18)	87(15)	-104(14)	-102(15)
C(35)	121(16)	260(17)	254(18)	76(13)	-95(13)	-48(13)
C(36)	112(15)	239(17)	288(18)	16(13)	-79(13)	-43(13)
C(37)	152(17)	278(18)	350(20)	-77(14)	-112(14)	-32(14)
C(38)	129(16)	420(20)	285(19)	-37(15)	-83(14)	-88(14)
C(39)	118(16)	520(20)	270(19)	-100(16)	-70(14)	-54(15)
C(40)	222(18)	272(18)	440(20)	-70(15)	-131(16)	-17(15)

C(41)	169(16)	166(16)	307(19)	50(13)	-127(14)	-71(13)
C(42)	350(20)	254(19)	500(20)	113(16)	-267(18)	-81(16)
C(43)	243(18)	390(20)	216(18)	-1(14)	-106(14)	-65(15)
C(44)	201(17)	253(17)	189(17)	-19(13)	-59(13)	-68(13)
C(45)	460(20)	390(20)	320(20)	-2(16)	-175(18)	-197(18)
C(51)	450(20)	370(20)	241(19)	9(15)	-89(17)	-181(18)
C(52)	212(18)	283(19)	350(20)	30(15)	-32(15)	-23(15)
C(53)	205(18)	270(18)	370(20)	66(15)	-110(15)	-19(14)
C(54)	292(19)	254(18)	266(19)	13(14)	-92(15)	-32(15)
C(55)	221(18)	238(18)	410(20)	-21(15)	-135(16)	22(14)
C(56)	310(20)	298(19)	410(20)	11(16)	-204(17)	-47(16)
C(61)	269(19)	214(18)	410(20)	-3(15)	-150(16)	-30(14)
C(62)	196(17)	330(19)	243(18)	38(15)	-88(14)	-49(14)
C(63)	307(19)	259(18)	310(20)	-69(15)	-114(16)	-38(15)
C(64)	360(20)	234(18)	330(20)	38(15)	-130(16)	-40(15)
C(65)	199(17)	360(20)	282(19)	-9(15)	-116(15)	25(15)
C(66)	231(19)	294(19)	440(20)	-136(16)	-159(16)	3(15)
C(71)	410(20)	217(18)	360(20)	37(15)	-247(17)	-108(16)
C(72)	300(19)	330(20)	340(20)	-76(15)	-179(16)	-46(16)
C(73)	330(20)	390(20)	272(19)	36(16)	-142(16)	-186(17)

1.1-$ZrBn_2$ (CCDC 639875)

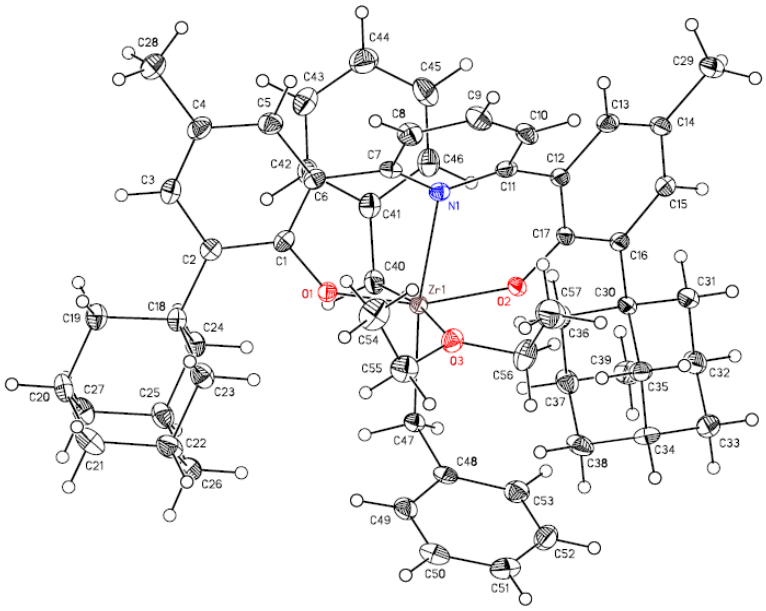

Special Refinement Details

Refinement of F^2 against ALL reflections. The weighted R-factor (wR) and goodness of fit (S) are based on F^2, conventional R-factors (R) are based on F, with F set to zero for negative F^2. The threshold expression of $F^2 > 2\sigma(F^2)$ is used only for calculating R-factors(gt) etc. and is not relevant to the choice of reflections for refinement. R-factors based on F^2 are statistically about twice as large as those based on F, and R-factors based on ALL data will be even larger.

All esds (except the esd in the dihedral angle between two l.s. planes) are estimated using the full covariance matrix. The cell esds are taken into account individually in the estimation of esds in distances, angles and torsion angles; correlations between esds in cell parameters are only used when they are defined by crystal symmetry. An approximate (isotropic) treatment of cell esds is used for estimating esds involving l.s. planes.

Table 4. Atomic coordinates (x 10^4) and equivalent isotropic displacement parameters (Å^2 x 10^3). U(eq) is defined as the trace of the orthogonalized Uij tensor.

	x	y	z	Ueq
Zr(1)	6495(1)	7500(1)	7467(1)	14(1)
O(1)	6318(1)	8035(1)	8287(1)	15(1)
O(2)	6399(1)	6391(1)	6722(1)	15(1)
O(3)	4032(1)	7363(1)	7279(1)	20(1)
O(4)	786(1)	1861(1)	7473(1)	24(1)
N(1)	5893(1)	5522(1)	7752(1)	14(1)
C(1)	6464(2)	7651(2)	8817(1)	16(1)
C(2)	6947(2)	8466(2)	9352(1)	16(1)
C(3)	7199(2)	7961(2)	9872(1)	20(1)
C(4)	6958(2)	6728(2)	9880(1)	22(1)
C(5)	6404(2)	5978(2)	9355(1)	21(1)
C(6)	6133(2)	6408(2)	8814(1)	16(1)
C(7)	5478(2)	5525(2)	8274(1)	16(1)
C(8)	4440(2)	4663(2)	8333(1)	21(1)
C(9)	3850(2)	3755(2)	7867(1)	23(1)

C(10)	4378(2)	3675(2)	7368(1)	20(1)
C(11)	5420(2)	4545(2)	7317(1)	16(1)
C(12)	6030(2)	4325(2)	6787(1)	15(1)
C(13)	6154(2)	3124(2)	6572(1)	18(1)
C(14)	6674(2)	2819(2)	6075(1)	18(1)
C(15)	7078(2)	3751(2)	5785(1)	18(1)
C(16)	7002(2)	7002(2)	5975(1)	15(1)
C(17)	6471(2)	5237(2)	6492(1)	15(1)
C(18)	7136(2)	9836(2)	9368(1)	17(1)
C(19)	7589(2)	10539(2)	10008(1)	21(1)
C(20)	7714(2)	11905(2)	10015(1)	23(1)
C(21)	6326(2)	12265(2)	9729(1)	28(1)
C(22)	5884(2)	11618(2)	9088(1)	25(1)
C(23)	5743(2)	10249(2)	9081(1)	22(1)
C(24)	8238(2)	10235(2)	9029(1)	19(1)
C(25)	8367(2)	11604(2)	9033(1)	22(1)
C(26)	6972(2)	11963(2)	8741(1)	27(1)
C(27)	8802(2)	12268(2)	9671(1)	23(1)
C(28)	7297(2)	6238(2)	10456(1)	34(1)
C(29)	6810(2)	1527(2)	5848(1)	24(1)
C(30)	7483(2)	5938(2)	5640(1)	14(1)
C(31)	8054(2)	5410(2)	5108(1)	20(1)
C(32)	8531(2)	6406(2)	4781(1)	24(1)
C(33)	7299(2)	7056(2)	4552(1)	26(1)
C(34)	6742(2)	7625(2)	5077(1)	22(1)
C(35)	6268(2)	6626(2)	5401(1)	19(1)
C(36)	8648(2)	6854(2)	6047(1)	18(1)
C(37)	9119(2)	7853(2)	5722(1)	21(1)
C(38)	7892(2)	8507(2)	5496(1)	24(1)
C(39)	9675(2)	7298(2)	5196(1)	25(1)
C(40)	8849(2)	7907(2)	7706(1)	20(1)
C(41)	9162(2)	6840(2)	7989(1)	19(1)
C(42)	9366(2)	6884(2)	8605(1)	21(1)
C(43)	9533(2)	5863(2)	8864(1)	27(1)
C(44)	9515(2)	4758(2)	8524(1)	30(1)
C(45)	9334(2)	4687(2)	7915(1)	28(1)
C(46)	9172(2)	5703(2)	7653(1)	23(1)
C(47)	6415(2)	9298(2)	7089(1)	16(1)
C(48)	5081(2)	9619(2)	6762(1)	18(1)
C(49)	4269(2)	10329(2)	7048(1)	21(1)
C(50)	2983(2)	10565(2)	6760(1)	24(1)
C(51)	2474(2)	10114(2)	6165(1)	25(1)
C(52)	3284(2)	9440(2)	5865(1)	26(1)
C(53)	4553(2)	9195(2)	6157(1)	22(1)
C(54)	2864(2)	7428(2)	8127(1)	33(1)
C(55)	3263(2)	8063(2)	7646(1)	27(1)
C(56)	3197(2)	6842(2)	6695(1)	29(1)
C(57)	2138(2)	5837(2)	6726(1)	38(1)
C(61)	1527(2)	857(2)	8292(1)	34(1)
C(62)	456(2)	839(2)	7733(1)	27(1)
C(63)	-148(2)	1863(2)	6924(1)	27(1)
C(64)	376(2)	2873(2)	6636(1)	34(1)

Table 5. Bond lengths [Å] and angles [°].

Zr(1)-O(1)	1.9756(11)	O(1)-Zr(1)-O(2)	158.53(4)
Zr(1)-O(2)	1.9771(12)	O(1)-Zr(1)-C(40)	93.21(6)
Zr(1)-C(40)	2.2871(16)	O(2)-Zr(1)-C(40)	95.72(6)
Zr(1)-C(47)	2.3229(16)	O(1)-Zr(1)-C(47)	101.00(6)
Zr(1)-O(3)	2.3919(11)	O(2)-Zr(1)-C(47)	98.74(5)
Zr(1)-N(1)	2.4714(13)	C(40)-Zr(1)-C(47)	88.31(6)
O(1)-C(1)	1.3519(18)	O(1)-Zr(1)-O(3)	82.07(4)
O(2)-C(17)	1.353(2)	O(2)-Zr(1)-O(3)	90.97(4)
O(3)-C(56)	1.457(2)	C(40)-Zr(1)-O(3)	171.89(6)
O(3)-C(55)	1.463(2)	C(47)-Zr(1)-O(3)	86.14(5)
N(1)-C(7)	1.365(2)	O(1)-Zr(1)-N(1)	80.32(5)
N(1)-C(11)	1.367(2)	O(2)-Zr(1)-N(1)	78.39(5)
C(1)-C(6)	1.409(2)	C(40)-Zr(1)-N(1)	107.36(5)
C(1)-C(2)	1.414(2)	C(47)-Zr(1)-N(1)	164.24(5)
C(2)-C(3)	1.397(2)	O(3)-Zr(1)-N(1)	78.46(4)
C(2)-C(18)	1.535(2)	C(1)-O(1)-Zr(1)	140.71(11)
C(3)-C(4)	1.394(3)	C(17)-O(2)-Zr(1)	144.05(10)
C(4)-C(5)	1.369(3)	C(56)-O(3)-C(55)	112.85(13)
C(4)-C(28)	1.513(2)	C(56)-O(3)-Zr(1)	120.49(11)
C(5)-C(6)	1.401(2)	C(55)-O(3)-Zr(1)	124.38(10)
C(6)-C(7)	1.487(2)	C(7)-N(1)-C(11)	117.79(14)
C(7)-C(8)	1.397(2)	C(7)-N(1)-Zr(1)	117.34(11)
C(8)-C(9)	1.378(2)	C(11)-N(1)-Zr(1)	119.04(10)
C(9)-C(10)	1.370(2)	O(1)-C(1)-C(6)	117.50(15)
C(10)-C(11)	1.398(2)	O(1)-C(1)-C(2)	121.05(15)
C(11)-C(12)	1.488(2)	C(6)-C(1)-C(2)	121.45(15)
C(12)-C(17)	1.402(2)	C(3)-C(2)-C(1)	116.51(16)
C(12)-C(13)	1.403(2)	C(3)-C(2)-C(18)	121.39(16)
C(13)-C(14)	1.381(2)	C(1)-C(2)-C(18)	122.06(14)
C(14)-C(15)	1.399(2)	C(4)-C(3)-C(2)	123.18(17)
C(14)-C(29)	1.508(2)	C(5)-C(4)-C(3)	118.41(16)
C(15)-C(16)	1.389(2)	C(5)-C(4)-C(28)	121.14(17)
C(16)-C(17)	1.422(2)	C(3)-C(4)-C(28)	120.44(17)
C(16)-C(30)	1.535(2)	C(4)-C(5)-C(6)	122.02(17)
C(18)-C(24)	1.550(2)	C(5)-C(6)-C(1)	118.14(16)
C(18)-C(19)	1.548(2)	C(5)-C(6)-C(7)	117.65(15)
C(18)-C(23)	1.555(2)	C(1)-C(6)-C(7)	124.19(14)
C(19)-C(20)	1.532(3)	N(1)-C(7)-C(8)	121.26(16)
C(20)-C(21)	1.525(2)	N(1)-C(7)-C(6)	122.33(14)
C(20)-C(27)	1.536(2)	C(8)-C(7)-C(6)	116.38(15)
C(21)-C(22)	1.529(3)	C(9)-C(8)-C(7)	120.23(17)
C(22)-C(23)	1.535(2)	C(10)-C(9)-C(8)	118.23(16)
C(22)-C(26)	1.536(3)	C(9)-C(10)-C(11)	120.60(17)
C(24)-C(25)	1.536(2)	N(1)-C(11)-C(10)	120.95(16)
C(25)-C(27)	1.528(2)	N(1)-C(11)-C(12)	121.98(14)
C(25)-C(26)	1.535(2)	C(10)-C(11)-C(12)	117.00(16)
C(30)-C(36)	1.543(2)	C(17)-C(12)-C(13)	118.72(16)
C(30)-C(31)	1.539(2)	C(17)-C(12)-C(11)	124.04(16)
C(30)-C(35)	1.547(2)	C(13)-C(12)-C(11)	117.24(15)
C(31)-C(32)	1.537(2)	C(14)-C(13)-C(12)	121.88(16)
C(32)-C(39)	1.525(3)	C(13)-C(14)-C(15)	117.76(17)
C(32)-C(33)	1.528(3)	C(13)-C(14)-C(29)	121.56(15)
C(33)-C(34)	1.534(3)	C(15)-C(14)-C(29)	120.68(16)
C(34)-C(38)	1.526(3)	C(16)-C(15)-C(14)	123.66(17)
C(34)-C(35)	1.533(2)	C(15)-C(16)-C(17)	116.77(15)

C(36)-C(37)	1.534(2)	C(15)-C(16)-C(30)	120.86(16)
C(37)-C(39)	1.529(3)	C(17)-C(16)-C(30)	122.36(15)
C(37)-C(38)	1.525(2)	O(2)-C(17)-C(12)	117.66(15)
C(40)-C(41)	1.479(2)	O(2)-C(17)-C(16)	121.13(14)
C(41)-C(42)	1.404(2)	C(12)-C(17)-C(16)	121.19(16)
C(41)-C(46)	1.411(3)	C(2)-C(18)-C(24)	112.25(14)
C(42)-C(43)	1.381(3)	C(2)-C(18)-C(19)	112.42(14)
C(43)-C(44)	1.379(3)	C(24)-C(18)-C(19)	106.88(13)
C(44)-C(45)	1.387(3)	C(2)-C(18)-C(23)	109.51(13)
C(45)-C(46)	1.379(3)	C(24)-C(18)-C(23)	108.24(13)
C(47)-C(48)	1.493(2)	C(19)-C(18)-C(23)	107.34(14)
C(48)-C(49)	1.391(2)	C(20)-C(19)-C(18)	111.58(14)
C(48)-C(53)	1.403(2)	C(21)-C(20)-C(19)	109.83(14)
C(49)-C(50)	1.387(2)	C(21)-C(20)-C(27)	109.53(15)
C(50)-C(51)	1.384(3)	C(19)-C(20)-C(27)	109.44(15)
C(51)-C(52)	1.384(3)	C(20)-C(21)-C(22)	109.35(15)
C(52)-C(53)	1.381(2)	C(21)-C(22)-C(23)	109.39(15)
C(54)-C(55)	1.510(3)	C(21)-C(22)-C(26)	109.84(15)
C(56)-C(57)	1.498(3)	C(23)-C(22)-C(26)	109.16(16)
O(4)-C(62)	1.419(2)	C(22)-C(23)-C(18)	111.31(14)
O(4)-C(63)	1.423(2)	C(25)-C(24)-C(18)	111.05(15)
C(61)-C(62)	1.506(3)	C(27)-C(25)-C(26)	109.15(15)
C(63)-C(64)	1.507(3)	C(27)-C(25)-C(24)	109.97(15)
		C(26)-C(25)-C(24)	109.67(14)
		C(25)-C(26)-C(22)	109.41(14)
		C(25)-C(27)-C(20)	109.14(14)
		C(16)-C(30)-C(36)	111.04(13)
		C(16)-C(30)-C(31)	112.27(14)
		C(36)-C(30)-C(31)	106.81(13)
		C(16)-C(30)-C(35)	110.44(13)
		C(36)-C(30)-C(35)	108.57(14)
		C(31)-C(30)-C(35)	107.54(13)
		C(32)-C(31)-C(30)	111.29(15)
		C(39)-C(32)-C(33)	110.14(16)
		C(39)-C(32)-C(31)	110.25(14)
		C(33)-C(32)-C(31)	108.96(15)
		C(32)-C(33)-C(34)	109.25(14)
		C(38)-C(34)-C(33)	108.84(15)
		C(38)-C(34)-C(35)	109.98(14)
		C(33)-C(34)-C(35)	109.01(15)
		C(34)-C(35)-C(30)	110.96(13)
		C(37)-C(36)-C(30)	111.68(14)
		C(39)-C(37)-C(38)	109.14(14)
		C(39)-C(37)-C(36)	109.61(15)
		C(38)-C(37)-C(36)	109.24(14)
		C(34)-C(38)-C(37)	110.38(15)
		C(32)-C(39)-C(37)	108.64(14)
		C(41)-C(40)-Zr(1)	98.32(10)
		C(42)-C(41)-C(46)	116.38(17)
		C(42)-C(41)-C(40)	121.69(17)
		C(46)-C(41)-C(40)	121.78(16)
		C(43)-C(42)-C(41)	121.66(18)
		C(44)-C(43)-C(42)	120.83(18)
		C(43)-C(44)-C(45)	118.91(19)
		C(46)-C(45)-C(44)	120.70(19)

C(45)-C(46)-C(41)	121.50(17)
C(48)-C(47)-Zr(1)	120.58(11)
C(49)-C(48)-C(53)	116.11(16)
C(49)-C(48)-C(47)	121.53(16)
C(53)-C(48)-C(47)	122.34(17)
C(50)-C(49)-C(48)	122.17(18)
C(51)-C(50)-C(49)	120.48(18)
C(50)-C(51)-C(52)	118.52(17)
C(53)-C(52)-C(51)	120.60(18)
C(52)-C(53)-C(48)	122.05(18)
O(3)-C(55)-C(54)	113.71(16)
O(3)-C(56)-C(57)	111.99(15)
C(62)-O(4)-C(63)	111.73(13)
O(4)-C(62)-C(61)	108.93(15)
O(4)-C(63)-C(64)	108.62(15)

Table 6. Anisotropic displacement parameters ($Å^2$ x 10^4). The anisotropic displacement factor exponent takes the form: $-2\pi^2[h^2a^*2U^{11} + ... + 2 h k a^* b^* U^{12}]$.

	U^{11}	U^{22}	U^{33}	U^{23}	U^{13}	U^{12}
Zr(1)	166(1)	117(1)	127(1)	23(1)	19(1)	-13(1)
O(1)	190(6)	136(7)	130(6)	28(5)	28(5)	-12(5)
O(2)	211(6)	113(6)	138(6)	18(5)	44(5)	8(5)
O(3)	171(6)	212(7)	192(7)	31(6)	5(5)	-9(5)
O(4)	246(7)	193(7)	271(7)	21(6)	52(6)	-35(5)
N(1)	127(6)	139(8)	164(8)	39(6)	22(6)	19(6)
C(1)	127(8)	208(10)	137(9)	50(8)	32(6)	8(7)
C(2)	123(8)	194(10)	170(9)	35(8)	48(7)	26(7)
C(3)	197(9)	249(11)	147(9)	14(8)	34(7)	20(8)
C(4)	266(9)	264(11)	165(10)	80(8)	68(8)	57(8)
C(5)	232(9)	194(10)	213(10)	70(8)	77(7)	23(8)
C(6)	152(8)	186(10)	147(9)	56(7)	61(7)	23(7)
C(7)	174(8)	121(9)	193(9)	56(7)	41(7)	28(7)
C(8)	241(9)	189(10)	233(10)	70(8)	98(8)	-16(8)
C(9)	218(9)	165(10)	297(11)	48(9)	77(8)	-45(8)
C(10)	207(9)	117(10)	237(10)	14(8)	22(7)	-22(7)
C(11)	143(8)	134(9)	180(9)	60(7)	-4(7)	17(7)
C(12)	154(8)	119(9)	154(9)	23(7)	-3(7)	0(7)
C(13)	190(8)	140(10)	195(9)	65(8)	4(7)	-21(7)
C(14)	203(9)	120(10)	210(10)	22(8)	0(7)	21(7)
C(15)	199(8)	174(10)	157(9)	23(8)	25(7)	44(7)
C(16)	154(8)	135(10)	151(9)	27(7)	-5(7)	14(7)
C(17)	140(8)	105(9)	163(9)	3(7)	-32(7)	-2(7)
C(18)	163(8)	185(10)	145(9)	2(8)	36(7)	5(7)
C(19)	208(9)	243(11)	177(10)	7(8)	55(7)	6(8)
C(20)	254(9)	213(11)	182(10)	-50(8)	54(8)	-18(8)
C(21)	256(10)	177(11)	403(12)	-6(9)	128(9)	17(8)
C(22)	200(9)	175(11)	336(11)	11(9)	-12(8)	35(8)
C(23)	179(9)	207(11)	260(10)	-4(8)	28(8)	8(8)
C(24)	174(8)	191(10)	176(9)	-9(8)	48(7)	-15(7)
C(25)	246(9)	179(10)	225(10)	-6(8)	82(8)	-33(8)

C(26)	357(11)	161(11)	236(11)	23(8)	-8(8)	-14(8)
C(27)	220(9)	193(11)	256(10)	-28(8)	41(8)	-21(8)
C(28)	543(13)	294(13)	182(10)	81(9)	68(9)	48(10)
C(29)	316(10)	158(10)	245(10)	48(8)	65(8)	41(8)
C(30)	179(8)	112(9)	147(9)	14(7)	43(7)	32(7)
C(31)	279(9)	150(10)	190(10)	29(8)	59(8)	47(8)
C(32)	355(10)	198(11)	192(10)	34(8)	121(8)	58(8)
C(33)	395(11)	213(11)	181(10)	60(8)	55(8)	16(9)
C(34)	267(9)	192(11)	231(10)	103(8)	27(8)	73(8)
C(35)	200(9)	162(10)	198(10)	56(8)	20(7)	18(7)
C(36)	188(8)	197(10)	154(9)	13(8)	26(7)	0(7)
C(37)	242(9)	173(10)	220(10)	14(8)	73(8)	-24(8)
C(38)	347(10)	142(10)	271(11)	64(8)	164(8)	38(8)
C(39)	273(10)	232(11)	280(11)	90(9)	127(8)	49(8)
C(40)	199(9)	189(10)	175(9)	-1(8)	22(7)	-4(7)
C(41)	104(7)	233(11)	199(10)	10(8)	10(7)	-1(7)
C(42)	170(8)	223(11)	204(10)	-25(8)	9(7)	0(7)
C(43)	265(10)	333(13)	198(10)	61(9)	35(8)	1(9)
C(44)	321(11)	275(12)	303(12)	98(10)	17(9)	1(9)
C(45)	261(10)	210(11)	340(12)	-40(9)	38(9)	0(8)
C(46)	184(9)	270(12)	207(10)	-10(9)	36(7)	5(8)
C(47)	185(8)	132(9)	169(9)	31(7)	41(7)	19(7)
C(48)	212(9)	101(9)	232(10)	59(8)	66(7)	1(7)
C(49)	257(9)	155(10)	219(10)	33(8)	64(8)	-8(8)
C(50)	241(9)	161(10)	358(12)	73(9)	131(9)	51(8)
C(51)	192(9)	233(11)	337(12)	130(9)	23(8)	16(8)
C(52)	297(10)	262(12)	196(10)	61(9)	13(8)	-3(9)
C(53)	274(10)	201(11)	216(10)	58(8)	99(8)	54(8)
C(54)	235(10)	437(14)	326(12)	77(10)	74(9)	43(9)
C(55)	201(9)	293(12)	303(11)	52(9)	49(8)	37(8)
C(56)	220(9)	389(13)	211(10)	13(9)	-22(8)	-3(9)
C(57)	300(11)	279(13)	443(14)	22(10)	-103(9)	-25(9)
C(61)	361(11)	341(13)	286(12)	53(10)	11(9)	-58(10)
C(62)	281(10)	250(12)	266(11)	27(9)	75(8)	-47(8)
C(63)	245(9)	244(12)	302(11)	32(9)	49(8)	21(8)
C(64)	293(11)	371(13)	390(13)	138(11)	105(9)	49(9)

1.4-TiBn$_2$ (CCDC 690431)

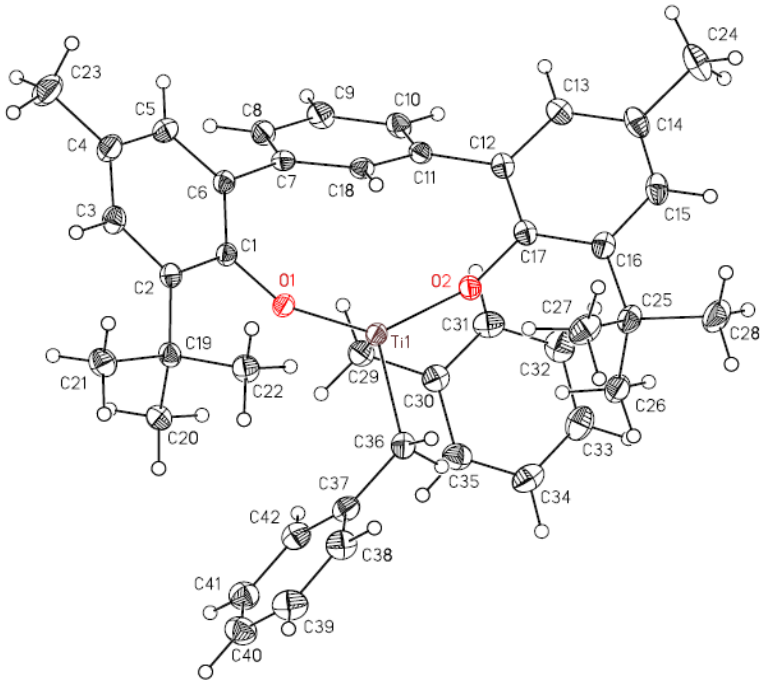

Special Refinement Details

Crystals were mounted on a glass fiber using Paratone oil then placed on the diffractometer under a nitrogen stream at 100K.

The solvent area of the crystal (~15% of cell volume) is disordered to the degree that molecules were not discernable. Consequently, SQUEEZE[1] was used to adjust observations and flatten the solvent area. A total of 40 electrons were accounted for, well within expectations for any formulation of petroleum ether.

Refinement of F^2 against ALL reflections. The weighted R-factor (wR) and goodness of fit (S) are based on F^2, conventional R-factors (R) are based on F, with F set to zero for negative F^2. The threshold expression of $F^2 > 2\sigma(F^2)$ is used only for calculating R-factors(gt) etc. and is not relevant to the choice of reflections for refinement. R-factors based on F^2 are statistically about twice as large as those based on F, and R-factors based on ALL data will be even larger.

All esds (except the esd in the dihedral angle between two l.s. planes) are estimated using the full covariance matrix. The cell esds are taken into account individually in the estimation of esds in distances, angles and torsion angles; correlations between esds in cell parameters are only used when they are defined by crystal symmetry. An approximate (isotropic) treatment of cell esds is used for estimating esds involving l.s. planes.

Table 7. Atomic coordinates (x 10^4) and equivalent isotropic displacement parameters (Å^2 x 10^3). U(eq) is defined as the trace of the orthogonalized Uij tensor.

	x	y	z	Ueq
Ti(1)	8616(1)	6703(1)	2629(1)	16(1)
O(1)	7804(1)	5493(1)	2989(1)	17(1)
O(2)	9367(1)	6747(1)	1596(1)	17(1)

[1] SQUEEZE - Sluis, P. v.d.; Spek, A. L. Acta Crystallogr., Sect A 1990, 46, 194-201.

C(1)	7577(1)	4419(1)	3142(1)	15(1)
C(2)	6419(1)	3855(1)	3168(1)	16(1)
C(3)	6288(1)	2775(1)	3353(1)	20(1)
C(4)	7210(1)	2251(1)	3518(1)	23(1)
C(5)	8336(1)	2843(1)	3497(1)	22(1)
C(6)	8534(1)	3917(1)	3305(1)	16(1)
C(7)	9746(1)	4514(1)	3272(1)	16(1)
C(8)	10739(1)	4648(1)	4054(1)	20(1)
C(9)	11852(1)	5240(1)	3999(1)	22(1)
C(10)	11981(1)	5706(1)	3166(1)	19(1)
C(11)	10998(1)	5575(1)	2366(1)	16(1)
C(12)	11093(1)	6075(1)	1472(1)	17(1)
C(13)	12045(1)	6019(1)	1008(1)	20(1)
C(14)	12152(1)	6479(1)	175(1)	22(1)
C(15)	11291(1)	7008(1)	-195(1)	22(1)
C(16)	10324(1)	7101(1)	234(1)	18(1)
C(17)	10248(1)	6629(1)	1090(1)	17(1)
C(18)	9899(1)	4959(1)	2426(1)	16(1)
C(19)	5361(1)	4394(1)	3033(1)	18(1)
C(20)	5624(1)	5463(1)	3886(1)	21(1)
C(21)	4208(1)	3602(1)	3101(1)	24(1)
C(22)	5118(1)	4680(1)	1974(1)	22(1)
C(23)	7006(1)	1072(1)	3702(1)	33(1)
C(24)	13179(1)	6394(1)	-331(1)	33(1)
C(25)	9420(1)	7728(1)	-181(1)	22(1)
C(26)	9532(1)	8801(1)	630(1)	25(1)
C(27)	8149(1)	6968(1)	-475(1)	28(1)
C(28)	9654(1)	8088(1)	-1162(1)	33(1)
C(29)	9882(1)	7719(1)	3938(1)	21(1)
C(30)	10572(1)	8739(1)	3691(1)	20(1)
C(31)	11605(1)	8726(1)	3340(1)	23(1)
C(32)	12226(1)	9648(1)	3065(1)	27(1)
C(33)	11835(1)	10619(1)	3139(1)	28(1)
C(34)	10809(1)	10658(1)	3486(1)	27(1)
C(35)	10186(1)	9739(1)	3761(1)	24(1)
C(36)	7485(1)	7756(1)	2339(1)	21(1)
C(37)	6548(1)	7958(1)	2893(1)	22(1)
C(38)	5366(1)	7759(1)	2360(1)	26(1)
C(39)	4482(1)	7963(1)	2854(1)	29(1)
C(40)	4754(1)	8366(1)	3909(1)	28(1)
C(41)	5909(1)	8561(1)	4452(1)	26(1)
C(42)	6801(1)	8368(1)	3956(1)	23(1)

Table 8. Bond lengths [Å] and angles [°].

Ti(1)-O(2)	1.8052(7)	O(2)-Ti(1)-O(1)	129.27(3)
Ti(1)-O(1)	1.8117(7)	O(2)-Ti(1)-C(36)	101.07(4)
Ti(1)-C(36)	2.0949(11)	O(1)-Ti(1)-C(36)	108.89(4)
Ti(1)-C(29)	2.1015(11)	O(2)-Ti(1)-C(29)	104.77(4)
O(1)-C(1)	1.3731(11)	O(1)-Ti(1)-C(29)	108.04(4)

O(2)-C(17)	1.3704(11)
C(1)-C(6)	1.4045(14)
C(1)-C(2)	1.4111(14)
C(2)-C(3)	1.3984(14)
C(2)-C(19)	1.5352(15)
C(3)-C(4)	1.3865(15)
C(4)-C(5)	1.3884(15)
C(4)-C(23)	1.5152(15)
C(5)-C(6)	1.3921(14)
C(6)-C(7)	1.4818(14)
C(7)-C(8)	1.3888(15)
C(7)-C(18)	1.3960(13)
C(8)-C(9)	1.3892(14)
C(9)-C(10)	1.3875(14)
C(10)-C(11)	1.3954(15)
C(11)-C(18)	1.3890(14)
C(11)-C(12)	1.4817(13)
C(12)-C(13)	1.3987(14)
C(12)-C(17)	1.4034(15)
C(13)-C(14)	1.3793(14)
C(14)-C(15)	1.3913(16)
C(14)-C(24)	1.5165(15)
C(15)-C(16)	1.3943(15)
C(16)-C(17)	1.4110(14)
C(16)-C(25)	1.5351(15)
C(19)-C(20)	1.5340(14)
C(19)-C(21)	1.5364(14)
C(19)-C(22)	1.5412(14)
C(25)-C(27)	1.5346(15)
C(25)-C(26)	1.5376(15)
C(25)-C(28)	1.5424(14)
C(29)-C(30)	1.4911(14)
C(30)-C(31)	1.3946(15)
C(30)-C(35)	1.4078(15)
C(31)-C(32)	1.3819(15)
C(32)-C(33)	1.3773(17)
C(33)-C(34)	1.3881(16)
C(34)-C(35)	1.3803(15)
C(36)-C(37)	1.4908(14)
C(37)-C(42)	1.3994(15)
C(37)-C(38)	1.3955(15)
C(38)-C(39)	1.3865(16)
C(39)-C(40)	1.3879(17)
C(40)-C(41)	1.3739(17)
C(41)-C(42)	1.3926(15)

C(36)-Ti(1)-C(29)	101.46(4)
C(1)-O(1)-Ti(1)	155.84(6)
C(17)-O(2)-Ti(1)	156.28(7)
O(1)-C(1)-C(6)	118.10(9)
O(1)-C(1)-C(2)	120.60(9)
C(6)-C(1)-C(2)	121.25(9)
C(3)-C(2)-C(1)	116.14(9)
C(3)-C(2)-C(19)	121.16(9)
C(1)-C(2)-C(19)	122.68(9)
C(4)-C(3)-C(2)	124.33(10)
C(5)-C(4)-C(3)	117.50(10)
C(5)-C(4)-C(23)	120.76(10)
C(3)-C(4)-C(23)	121.74(10)
C(4)-C(5)-C(6)	121.50(10)
C(5)-C(6)-C(1)	119.27(9)
C(5)-C(6)-C(7)	119.84(9)
C(1)-C(6)-C(7)	120.88(9)
C(8)-C(7)-C(18)	118.59(10)
C(8)-C(7)-C(6)	122.35(9)
C(18)-C(7)-C(6)	119.06(9)
C(7)-C(8)-C(9)	120.15(10)
C(10)-C(9)-C(8)	120.44(10)
C(9)-C(10)-C(11)	120.52(10)
C(18)-C(11)-C(10)	118.12(9)
C(18)-C(11)-C(12)	119.62(9)
C(10)-C(11)-C(12)	122.26(9)
C(13)-C(12)-C(17)	119.00(9)
C(13)-C(12)-C(11)	120.09(10)
C(17)-C(12)-C(11)	120.90(9)
C(14)-C(13)-C(12)	121.15(10)
C(13)-C(14)-C(15)	118.47(10)
C(13)-C(14)-C(24)	120.55(11)
C(15)-C(14)-C(24)	120.97(10)
C(14)-C(15)-C(16)	123.39(10)
C(15)-C(16)-C(17)	116.58(10)
C(15)-C(16)-C(25)	121.35(9)
C(17)-C(16)-C(25)	122.02(9)
O(2)-C(17)-C(12)	118.36(9)
O(2)-C(17)-C(16)	120.20(9)
C(12)-C(17)-C(16)	121.38(9)
C(11)-C(18)-C(7)	122.11(10)
C(2)-C(19)-C(20)	109.42(9)
C(2)-C(19)-C(21)	112.03(9)
C(20)-C(19)-C(21)	107.47(8)
C(2)-C(19)-C(22)	110.80(8)
C(20)-C(19)-C(22)	110.21(9)
C(21)-C(19)-C(22)	106.83(9)
C(27)-C(25)-C(16)	110.96(9)
C(27)-C(25)-C(26)	111.22(10)

C(16)-C(25)-C(26)	109.02(9)
C(27)-C(25)-C(28)	106.31(9)
C(16)-C(25)-C(28)	111.56(9)
C(26)-C(25)-C(28)	107.72(9)
C(30)-C(29)-Ti(1)	110.53(7)
C(31)-C(30)-C(35)	117.09(10)
C(31)-C(30)-C(29)	121.13(10)
C(35)-C(30)-C(29)	121.73(10)
C(32)-C(31)-C(30)	121.89(11)
C(31)-C(32)-C(33)	120.20(11)
C(34)-C(33)-C(32)	119.25(11)
C(33)-C(34)-C(35)	120.75(11)
C(34)-C(35)-C(30)	120.82(11)
C(37)-C(36)-Ti(1)	125.80(7)
C(42)-C(37)-C(38)	116.82(10)
C(42)-C(37)-C(36)	122.47(10)
C(38)-C(37)-C(36)	120.71(10)
C(39)-C(38)-C(37)	121.90(11)
C(40)-C(39)-C(38)	120.21(12)
C(41)-C(40)-C(39)	119.02(11)
C(40)-C(41)-C(42)	120.79(11)
C(41)-C(42)-C(37)	121.26(11)

Table 9. Anisotropic displacement parameters (Å2 x 104). The anisotropic displacement factor exponent takes the form: $-2\pi^2[h^2a^*2U^{11} + ... + 2 h k a^* b^* U^{12}]$.

	U^{11}	U^{22}	U^{33}	U^{23}	U^{13}	U^{12}
Ti(1)	146(1)	167(1)	173(1)	68(1)	46(1)	48(1)
O(1)	152(4)	169(4)	202(4)	78(3)	53(3)	48(3)
O(2)	165(4)	204(4)	167(3)	68(3)	52(3)	59(3)
C(1)	174(5)	158(5)	137(5)	47(4)	42(4)	42(4)
C(2)	166(5)	175(5)	140(5)	40(4)	35(4)	32(4)
C(3)	183(6)	197(5)	228(5)	71(4)	54(5)	12(4)
C(4)	243(6)	202(5)	257(6)	98(5)	61(5)	56(5)
C(5)	227(6)	226(6)	235(6)	100(4)	62(5)	103(5)
C(6)	168(5)	185(5)	154(5)	59(4)	44(4)	54(4)
C(7)	163(5)	165(5)	175(5)	46(4)	48(4)	70(4)
C(8)	198(6)	269(6)	173(5)	90(4)	51(4)	104(5)
C(9)	156(5)	305(6)	195(5)	77(5)	15(4)	90(5)
C(10)	126(5)	244(6)	208(5)	59(4)	48(4)	53(4)
C(11)	174(5)	175(5)	152(5)	33(4)	48(4)	63(4)
C(12)	161(5)	172(5)	144(5)	22(4)	28(4)	15(4)
C(13)	176(5)	217(5)	179(5)	13(4)	37(4)	36(4)
C(14)	220(6)	256(6)	159(5)	-3(4)	69(5)	3(5)
C(15)	267(6)	216(6)	143(5)	32(4)	52(5)	-10(5)
C(16)	231(6)	154(5)	137(5)	16(4)	25(4)	8(4)
C(17)	166(5)	168(5)	142(5)	16(4)	31(4)	16(4)
C(18)	150(5)	174(5)	158(5)	38(4)	22(4)	66(4)
C(19)	144(5)	203(5)	188(5)	63(4)	54(4)	40(4)
C(20)	193(6)	227(6)	234(5)	64(4)	78(5)	67(5)

C(21)	172(6)	273(6)	275(6)	63(5)	64(5)	39(5)
C(22)	167(6)	297(6)	225(5)	91(5)	36(5)	79(5)
C(23)	340(8)	225(6)	483(8)	177(6)	118(6)	66(6)
C(24)	282(7)	488(8)	229(6)	74(6)	126(5)	75(6)
C(25)	297(6)	188(5)	165(5)	61(4)	41(5)	51(5)
C(26)	334(7)	199(6)	237(6)	80(5)	89(5)	68(5)
C(27)	293(7)	268(6)	251(6)	82(5)	-37(5)	84(5)
C(28)	534(9)	284(7)	200(6)	113(5)	79(6)	144(6)
C(29)	201(6)	226(6)	190(5)	50(4)	38(5)	65(5)
C(30)	199(6)	205(5)	148(5)	19(4)	-9(4)	41(4)
C(31)	179(6)	229(6)	255(6)	29(5)	5(5)	54(5)
C(32)	183(6)	294(6)	302(6)	72(5)	36(5)	20(5)
C(33)	264(7)	254(6)	275(6)	95(5)	5(5)	-3(5)
C(34)	330(7)	200(6)	269(6)	53(5)	9(5)	76(5)
C(35)	250(6)	244(6)	223(6)	35(5)	50(5)	81(5)
C(36)	223(6)	223(6)	216(5)	78(4)	74(5)	57(5)
C(37)	207(6)	179(5)	265(6)	67(4)	44(5)	51(4)
C(38)	237(6)	268(6)	239(6)	42(5)	15(5)	63(5)
C(39)	192(6)	289(7)	343(7)	30(5)	-3(5)	46(5)
C(40)	225(6)	279(6)	341(7)	48(5)	90(5)	66(5)
C(41)	275(7)	232(6)	248(6)	30(5)	53(5)	61(5)
C(42)	203(6)	196(5)	259(6)	48(4)	22(5)	30(5)

2.2 (CCDC 726163)

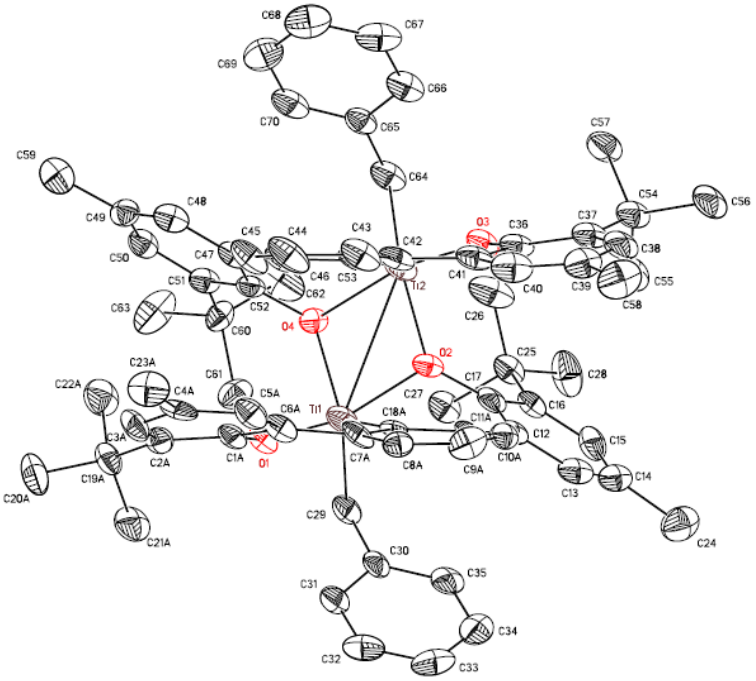

Special Refinement Details

Crystals were mounted on a glass fiber using Paratone oil then placed on the diffractometer under a nitrogen stream at 100K.

One of the phenolate ligands (and its bridging phenyl), composed of atoms C(1)-C(11) and C(18)-C(23), is disordered over two orientations. The major orientation (78%) was refined without restraint, the minor component was assigned one isotropic temperature factor applied to all atoms and the six member rings were restrained to ideal hexagons.

Refinement of F^2 against ALL reflections. The weighted R-factor (wR) and goodness of fit (S) are based on F^2, conventional R-factors (R) are based on F, with F set to zero for negative F^2. The threshold expression of $F^2 > 2\sigma(F^2)$ is used only for calculating R-factors(gt) etc. and is not relevant to the choice of reflections for refinement. R-factors based on F^2 are statistically about twice as large as those based on F, and R-factors based on ALL data will be even larger.

All esds (except the esd in the dihedral angle between two l.s. planes) are estimated using the full covariance matrix. The cell esds are taken into account individually in the estimation of esds in distances, angles and torsion angles; correlations between esds in cell parameters are only used when they are defined by crystal symmetry. An approximate (isotropic) treatment of cell esds is used for estimating esds involving l.s. planes.

Table 10. Atomic coordinates (x 10^4) and equivalent isotropic displacement parameters ($Å^2$ x 10^3). U(eq) is defined as the trace of the orthogonalized Uij tensor.

	x	y	z	Ueq	Occ
Ti(1)	7067(1)	1566(1)	1891(1)	31(1)	1
Ti(2)	7023(1)	3740(1)	2285(1)	32(1)	1
O(1)	7385(2)	928(1)	2860(2)	27(1)	1
O(2)	6889(2)	2656(2)	1163(2)	26(1)	1
O(3)	7869(2)	4532(1)	1982(2)	32(1)	1

O(4)	6362(2)	2570(2)	2539(2)	26(1)	1
C(1A)	8131(4)	880(3)	3683(4)	28(2)	0.781(3)
C(2A)	7962(4)	440(3)	4417(4)	28(2)	0.781(3)
C(3A)	8731(4)	566(3)	5264(4)	37(2)	0.781(3)
C(4A)	9620(5)	1065(4)	5376(5)	33(2)	0.781(3)
C(5A)	9798(4)	1407(3)	4602(5)	35(2)	0.781(3)
C(6A)	9080(3)	1316(3)	3723(4)	28(2)	0.781(3)
C(7A)	9307(4)	1658(4)	2896(5)	28(2)	0.781(3)
C(8A)	10317(5)	1836(6)	2940(5)	28(2)	0.781(3)
C(9A)	10594(5)	2235(8)	2285(8)	37(3)	0.781(3)
C(10A)	9911(7)	2449(6)	1509(8)	30(2)	0.781(3)
C(11A)	8890(6)	2230(6)	1376(6)	22(2)	0.781(3)
C(1B)	8136(7)	541(8)	3217(10)	28(2)	0.219(3)
C(2B)	7971(6)	-160(8)	3716(9)	28(2)	0.219(3)
C(3B)	8723(8)	-718(7)	4033(8)	28(2)	0.219(3)
C(4B)	9639(7)	-573(7)	3852(9)	28(2)	0.219(3)
C(5B)	9803(6)	128(8)	3353(8)	28(2)	0.219(3)
C(6B)	9052(9)	685(7)	3036(9)	28(2)	0.219(3)
C(7B)	9263(19)	1447(16)	2489(15)	28(2)	0.219(3)
C(8B)	10263(17)	1730(20)	2649(19)	28(2)	0.219(3)
C(9B)	10561(19)	2310(30)	2090(30)	28(2)	0.219(3)
C(10B)	9860(30)	2610(30)	1370(30)	28(2)	0.219(3)
C(11B)	8860(30)	2320(30)	1210(20)	28(2)	0.219(3)
C(12)	8200(3)	2389(2)	428(4)	28(1)	1
C(13)	8518(3)	2263(2)	-403(4)	34(1)	1
C(14)	7906(3)	2327(3)	-1278(4)	34(1)	1
C(15)	6946(3)	2549(3)	-1316(4)	35(1)	1
C(16)	6566(3)	2686(2)	-536(4)	29(1)	1
C(17)	7212(3)	2586(2)	347(4)	31(1)	1
C(18A)	8585(4)	1851(5)	2097(4)	18(2)	0.781(3)
C(19A)	6994(8)	-138(6)	4321(5)	33(3)	0.781(3)
C(20A)	7082(6)	-702(5)	5131(5)	51(2)	0.781(3)
C(21A)	6681(4)	-847(4)	3384(5)	46(2)	0.781(3)
C(22A)	6164(3)	506(5)	4372(6)	48(2)	0.781(3)
C(23A)	10407(4)	1238(4)	6346(4)	47(2)	0.781(3)
C(18B)	8561(17)	1740(20)	1768(19)	28(2)	0.219(3)
C(19B)	6890(40)	-300(30)	3970(30)	28(2)	0.219(3)
C(20B)	6960(20)	-995(17)	4683(17)	28(2)	0.219(3)
C(21B)	6141(13)	-726(14)	3044(16)	28(2)	0.219(3)
C(22B)	6604(16)	604(18)	4460(20)	28(2)	0.219(3)
C(23B)	10310(20)	-1283(16)	4115(18)	28(2)	0.219(3)
C(24)	8242(3)	2127(3)	-2183(3)	50(2)	1
C(25)	5471(3)	2900(3)	-650(3)	31(1)	1
C(26)	5368(2)	3752(2)	64(3)	52(2)	1
C(27)	4865(2)	2048(2)	-514(3)	34(1)	1
C(28)	4997(3)	3103(3)	-1643(3)	53(2)	1
C(29)	6429(3)	416(2)	804(3)	32(1)	1
C(30)	7276(3)	-28(3)	550(4)	29(1)	1
C(31)	7815(3)	-635(3)	1095(3)	35(1)	1

C(32)	8632(3)	-999(3)	880(4)	48(2)	1
C(33)	8943(3)	-794(3)	132(4)	48(2)	1
C(34)	8432(3)	-208(3)	-437(3)	41(1)	1
C(35)	7601(3)	165(3)	-221(4)	35(1)	1
C(36)	8863(3)	4771(2)	2142(3)	31(1)	1
C(37)	9194(3)	5303(3)	1546(3)	35(1)	1
C(38)	10218(3)	5434(2)	1705(3)	41(1)	1
C(39)	10887(3)	5078(3)	2412(4)	41(1)	1
C(40)	10524(3)	4624(3)	3008(4)	42(2)	1
C(41)	9496(3)	4458(2)	2917(4)	33(1)	1
C(42)	9142(3)	4016(2)	3630(4)	34(1)	1
C(43)	9832(3)	3939(3)	4484(4)	41(2)	1
C(44)	9586(3)	3543(3)	5190(4)	46(2)	1
C(45)	8610(3)	3224(2)	5074(3)	41(2)	1
C(46)	7882(3)	3301(2)	4248(3)	31(1)	1
C(47)	6837(3)	3013(3)	4238(4)	29(1)	1
C(48)	6566(3)	3116(3)	5088(4)	33(1)	1
C(49)	5627(3)	2858(3)	5129(3)	30(1)	1
C(50)	4910(3)	2509(2)	4268(4)	32(1)	1
C(51)	5115(3)	2387(2)	3394(4)	29(1)	1
C(52)	6093(3)	2643(2)	3376(4)	27(1)	1
C(53)	8124(2)	3692(2)	3508(3)	30(1)	1
C(54)	8488(3)	5720(3)	775(3)	36(1)	1
C(55)	7862(2)	4924(2)	-1(3)	44(2)	1
C(56)	9040(2)	6324(2)	283(3)	46(2)	1
C(57)	7812(3)	6347(2)	1214(3)	46(2)	1
C(58)	11991(2)	5163(3)	2502(3)	55(2)	1
C(59)	5365(3)	2941(3)	6048(3)	43(1)	1
C(60)	4291(2)	1955(3)	2472(3)	30(1)	1
C(61)	4618(2)	1104(2)	1912(3)	39(1)	1
C(62)	3991(3)	2682(3)	1835(3)	57(2)	1
C(63)	3360(2)	1587(3)	2730(3)	58(2)	1
C(64)	5984(2)	4707(2)	2494(3)	36(1)	1
C(65)	6406(3)	5279(3)	3463(4)	31(1)	1
C(66)	7176(2)	6005(2)	3639(4)	39(1)	1
C(67)	7571(3)	6508(3)	4546(4)	47(2)	1
C(68)	7254(3)	6309(3)	5309(4)	53(2)	1
C(69)	6506(3)	5606(3)	5160(4)	49(2)	1
C(70)	6099(3)	5101(3)	4244(4)	41(2)	1

Table 11. Bond lengths [Å] and angles [°].

Ti(1)-O(1)	1.799(3)	O(1)-Ti(1)-O(2)	160.70(11)
Ti(1)-O(2)	2.038(3)	O(1)-Ti(1)-O(4)	96.85(12)
Ti(1)-O(4)	2.042(3)	O(2)-Ti(1)-O(4)	70.20(11)
Ti(1)-C(18A)	2.082(6)	O(1)-Ti(1)-C(18A)	86.60(19)
Ti(1)-C(29)	2.095(3)	O(2)-Ti(1)-C(18A)	86.8(2)
Ti(1)-C(18B)	2.15(3)	O(4)-Ti(1)-C(18A)	116.87(19)
Ti(1)-Ti(2)	3.1134(9)	O(1)-Ti(1)-C(29)	97.51(13)
Ti(2)-O(3)	1.796(2)	O(2)-Ti(1)-C(29)	101.76(13)

Ti(2)-O(4)	2.025(2)	O(4)-Ti(1)-C(29)	127.97(12)
Ti(2)-O(2)	2.049(3)	C(18A)-Ti(1)-C(29)	113.7(2)
Ti(2)-C(53)	2.062(4)	O(1)-Ti(1)-C(18B)	94.5(8)
Ti(2)-C(64)	2.112(4)	O(2)-Ti(1)-C(18B)	82.5(8)
O(1)-C(1B)	1.251(8)	O(4)-Ti(1)-C(18B)	125.6(8)
O(1)-C(1A)	1.398(5)	C(18A)-Ti(1)-C(18B)	12.8(8)
O(2)-C(17)	1.380(5)	C(29)-Ti(1)-C(18B)	102.7(8)
O(3)-C(36)	1.370(4)	O(1)-Ti(1)-Ti(2)	120.78(9)
O(4)-C(52)	1.370(5)	O(2)-Ti(1)-Ti(2)	40.50(9)
C(1A)-C(2A)	1.404(7)	O(4)-Ti(1)-Ti(2)	39.83(7)
C(1A)-C(6A)	1.428(6)	C(18A)-Ti(1)-Ti(2)	85.44(19)
C(2A)-C(3A)	1.403(6)	C(29)-Ti(1)-Ti(2)	138.71(11)
C(2A)-C(19A)	1.522(11)	C(18B)-Ti(1)-Ti(2)	89.9(8)
C(3A)-C(4A)	1.368(8)	O(3)-Ti(2)-O(4)	162.67(11)
C(4A)-C(5A)	1.388(9)	O(3)-Ti(2)-O(2)	97.94(12)
C(4A)-C(23A)	1.539(7)	O(4)-Ti(2)-O(2)	70.34(11)
C(5A)-C(6A)	1.404(6)	O(3)-Ti(2)-C(53)	87.66(13)
C(6A)-C(7A)	1.486(8)	O(4)-Ti(2)-C(53)	86.37(13)
C(7A)-C(8A)	1.410(6)	O(2)-Ti(2)-C(53)	116.10(13)
C(7A)-C(18A)	1.418(6)	O(3)-Ti(2)-C(64)	97.18(12)
C(8A)-C(9A)	1.330(7)	O(4)-Ti(2)-C(64)	100.12(13)
C(9A)-C(10A)	1.379(6)	O(2)-Ti(2)-C(64)	128.19(13)
C(10A)-C(11A)	1.406(6)	C(53)-Ti(2)-C(64)	113.77(17)
C(11A)-C(18A)	1.419(7)	O(3)-Ti(2)-Ti(1)	122.90(9)
C(11A)-C(12)	1.540(8)	O(4)-Ti(2)-Ti(1)	40.25(8)
C(1B)-C(2B)	1.39	O(2)-Ti(2)-Ti(1)	40.25(8)
C(1B)-C(6B)	1.39	C(53)-Ti(2)-Ti(1)	84.47(10)
C(2B)-C(3B)	1.39	C(64)-Ti(2)-Ti(1)	137.28(9)
C(2B)-C(19B)	1.66(5)	C(1B)-O(1)-C(1A)	33.6(7)
C(3B)-C(4B)	1.39	C(1B)-O(1)-Ti(1)	133.8(6)
C(4B)-C(5B)	1.39	C(1A)-O(1)-Ti(1)	142.2(2)
C(4B)-C(23B)	1.46(2)	C(17)-O(2)-Ti(1)	117.9(2)
C(5B)-C(6B)	1.39	C(17)-O(2)-Ti(2)	132.1(2)
C(6B)-C(7B)	1.53(2)	Ti(1)-O(2)-Ti(2)	99.25(14)
C(7B)-C(8B)	1.39	C(36)-O(3)-Ti(2)	141.1(2)
C(7B)-C(18B)	1.39	C(52)-O(4)-Ti(2)	117.2(2)
C(8B)-C(9B)	1.39	C(52)-O(4)-Ti(1)	130.9(2)
C(9B)-C(10B)	1.39	Ti(2)-O(4)-Ti(1)	99.92(13)
C(10B)-C(11B)	1.39	O(1)-C(1A)-C(2A)	122.7(4)
C(11B)-C(12)	1.30(2)	O(1)-C(1A)-C(6A)	114.8(5)
C(11B)-C(18B)	1.39	C(2A)-C(1A)-C(6A)	122.5(5)
C(19B)-C(22B)	1.51(5)	C(3A)-C(2A)-C(1A)	116.8(4)
C(19B)-C(21B)	1.51(4)	C(3A)-C(2A)-C(19A)	120.7(6)
C(19B)-C(20B)	1.56(6)	C(1A)-C(2A)-C(19A)	122.6(5)
C(12)-C(13)	1.395(6)	C(4A)-C(3A)-C(2A)	122.7(5)
C(12)-C(17)	1.406(5)	C(3A)-C(4A)-C(5A)	118.9(5)
C(13)-C(14)	1.374(5)	C(3A)-C(4A)-C(23A)	120.2(6)
C(14)-C(15)	1.388(5)	C(5A)-C(4A)-C(23A)	120.9(5)
C(14)-C(24)	1.514(6)	C(4A)-C(5A)-C(6A)	122.8(5)

C(15)-C(16)	1.376(6)	C(5A)-C(6A)-C(1A)	115.6(5)
C(16)-C(17)	1.416(5)	C(5A)-C(6A)-C(7A)	121.4(5)
C(16)-C(25)	1.552(5)	C(1A)-C(6A)-C(7A)	122.9(5)
C(19A)-C(21A)	1.529(8)	C(8A)-C(7A)-C(18A)	118.4(5)
C(19A)-C(20A)	1.536(12)	C(8A)-C(7A)-C(6A)	116.8(5)
C(19A)-C(22A)	1.535(13)	C(18A)-C(7A)-C(6A)	124.7(5)
C(25)-C(26)	1.524(5)	C(9A)-C(8A)-C(7A)	121.2(5)
C(25)-C(28)	1.526(5)	C(8A)-C(9A)-C(10A)	121.7(5)
C(25)-C(27)	1.533(4)	C(9A)-C(10A)-C(11A)	120.6(5)
C(29)-C(30)	1.478(5)	C(10A)-C(11A)-C(18A)	118.1(5)
C(30)-C(35)	1.391(6)	C(10A)-C(11A)-C(12)	116.4(6)
C(30)-C(31)	1.404(5)	C(18A)-C(11A)-C(12)	125.5(6)
C(31)-C(32)	1.372(6)	O(1)-C(1B)-C(2B)	115.3(9)
C(32)-C(33)	1.353(6)	O(1)-C(1B)-C(6B)	124.1(9)
C(33)-C(34)	1.385(5)	C(2B)-C(1B)-C(6B)	120
C(34)-C(35)	1.394(5)	C(1B)-C(2B)-C(3B)	120
C(36)-C(37)	1.405(5)	C(1B)-C(2B)-C(19B)	119.7(18)
C(36)-C(41)	1.408(5)	C(3B)-C(2B)-C(19B)	120.3(18)
C(37)-C(38)	1.393(5)	C(2B)-C(3B)-C(4B)	120
C(37)-C(54)	1.529(5)	C(3B)-C(4B)-C(5B)	120
C(38)-C(39)	1.397(5)	C(3B)-C(4B)-C(23B)	114.1(13)
C(39)-C(40)	1.358(6)	C(5B)-C(4B)-C(23B)	125.4(13)
C(39)-C(58)	1.515(5)	C(4B)-C(5B)-C(6B)	120
C(40)-C(41)	1.418(5)	C(5B)-C(6B)-C(1B)	120
C(41)-C(42)	1.488(6)	C(5B)-C(6B)-C(7B)	118.3(13)
C(42)-C(43)	1.401(5)	C(1B)-C(6B)-C(7B)	121.7(13)
C(42)-C(53)	1.437(5)	C(8B)-C(7B)-C(18B)	120
C(43)-C(44)	1.374(6)	C(8B)-C(7B)-C(6B)	114.6(18)
C(44)-C(45)	1.381(5)	C(18B)-C(7B)-C(6B)	124.6(17)
C(45)-C(46)	1.397(5)	C(7B)-C(8B)-C(9B)	120
C(46)-C(53)	1.414(6)	C(10B)-C(9B)-C(8B)	120
C(46)-C(47)	1.500(5)	C(11B)-C(10B)-C(9B)	120
C(47)-C(48)	1.387(6)	C(12)-C(11B)-C(10B)	123(2)
C(47)-C(52)	1.425(5)	C(12)-C(11B)-C(18B)	115(2)
C(48)-C(49)	1.370(5)	C(10B)-C(11B)-C(18B)	120
C(49)-C(50)	1.401(5)	C(11B)-C(18B)-C(7B)	120
C(49)-C(59)	1.479(6)	C(11B)-C(18B)-Ti(1)	123.9(16)
C(50)-C(51)	1.375(6)	C(7B)-C(18B)-Ti(1)	113.8(16)
C(51)-C(52)	1.411(5)	C(22B)-C(19B)-C(21B)	113(3)
C(51)-C(60)	1.556(5)	C(22B)-C(19B)-C(20B)	106(3)
C(54)-C(56)	1.522(5)	C(21B)-C(19B)-C(20B)	109(3)
C(54)-C(57)	1.531(5)	C(22B)-C(19B)-C(2B)	113(3)
C(54)-C(55)	1.537(5)	C(21B)-C(19B)-C(2B)	107(3)
C(60)-C(62)	1.526(5)	C(20B)-C(19B)-C(2B)	109(3)
C(60)-C(61)	1.525(5)	C(11B)-C(12)-C(13)	115.9(17)
C(60)-C(63)	1.543(5)	C(11B)-C(12)-C(17)	126.4(18)
C(64)-C(65)	1.486(5)	C(13)-C(12)-C(17)	117.7(4)
C(65)-C(70)	1.384(6)	C(11B)-C(12)-C(11A)	6.8(19)
C(65)-C(66)	1.413(4)	C(13)-C(12)-C(11A)	120.2(5)

C(66)-C(67)	1.374(6)
C(67)-C(68)	1.376(6)
C(68)-C(69)	1.375(5)
C(69)-C(70)	1.388(6)

C(17)-C(12)-C(11A)	121.9(6)
C(14)-C(13)-C(12)	122.4(4)
C(13)-C(14)-C(15)	117.7(5)
C(13)-C(14)-C(24)	121.7(4)
C(15)-C(14)-C(24)	120.5(5)
C(16)-C(15)-C(14)	124.1(4)
C(15)-C(16)-C(17)	116.4(4)
C(15)-C(16)-C(25)	120.6(4)
C(17)-C(16)-C(25)	123.0(5)
O(2)-C(17)-C(12)	117.2(4)
O(2)-C(17)-C(16)	121.1(4)
C(12)-C(17)-C(16)	121.7(5)
C(11A)-C(18A)-C(7A)	119.8(4)
C(11A)-C(18A)-Ti(1)	117.0(4)
C(7A)-C(18A)-Ti(1)	123.2(4)
C(2A)-C(19A)-C(21A)	111.6(7)
C(2A)-C(19A)-C(20A)	111.6(6)
C(21A)-C(19A)-C(20A)	106.8(6)
C(2A)-C(19A)-C(22A)	110.5(6)
C(21A)-C(19A)-C(22A)	109.2(6)
C(20A)-C(19A)-C(22A)	106.9(8)
C(26)-C(25)-C(28)	106.7(3)
C(26)-C(25)-C(27)	108.4(4)
C(28)-C(25)-C(27)	107.6(3)
C(26)-C(25)-C(16)	112.6(3)
C(28)-C(25)-C(16)	111.4(4)
C(27)-C(25)-C(16)	109.8(3)
C(30)-C(29)-Ti(1)	105.1(2)
C(35)-C(30)-C(31)	116.7(4)
C(35)-C(30)-C(29)	121.4(4)
C(31)-C(30)-C(29)	121.8(5)
C(32)-C(31)-C(30)	121.0(5)
C(33)-C(32)-C(31)	121.3(5)
C(32)-C(33)-C(34)	120.1(5)
C(33)-C(34)-C(35)	118.8(5)
C(30)-C(35)-C(34)	122.0(5)
O(3)-C(36)-C(37)	119.6(4)
O(3)-C(36)-C(41)	116.3(4)
C(37)-C(36)-C(41)	124.1(4)
C(38)-C(37)-C(36)	115.4(4)
C(38)-C(37)-C(54)	121.6(4)
C(36)-C(37)-C(54)	122.9(3)
C(37)-C(38)-C(39)	123.3(4)
C(40)-C(39)-C(38)	118.4(4)
C(40)-C(39)-C(58)	120.2(4)
C(38)-C(39)-C(58)	121.4(4)
C(39)-C(40)-C(41)	123.1(4)
C(36)-C(41)-C(40)	115.3(4)
C(36)-C(41)-C(42)	123.9(4)

C(40)-C(41)-C(42)	120.7(4)
C(43)-C(42)-C(53)	117.9(4)
C(43)-C(42)-C(41)	118.4(4)
C(53)-C(42)-C(41)	123.7(4)
C(44)-C(43)-C(42)	123.2(4)
C(43)-C(44)-C(45)	119.1(4)
C(44)-C(45)-C(46)	120.5(4)
C(45)-C(46)-C(53)	121.2(3)
C(45)-C(46)-C(47)	115.8(4)
C(53)-C(46)-C(47)	122.9(4)
C(48)-C(47)-C(52)	117.9(4)
C(48)-C(47)-C(46)	119.8(4)
C(52)-C(47)-C(46)	122.3(5)
C(49)-C(48)-C(47)	122.7(4)
C(48)-C(49)-C(50)	117.9(5)
C(48)-C(49)-C(59)	121.7(4)
C(50)-C(49)-C(59)	120.4(4)
C(51)-C(50)-C(49)	123.1(4)
C(50)-C(51)-C(52)	117.7(4)
C(50)-C(51)-C(60)	120.1(4)
C(52)-C(51)-C(60)	122.2(4)
O(4)-C(52)-C(51)	122.0(4)
O(4)-C(52)-C(47)	117.4(4)
C(51)-C(52)-C(47)	120.6(5)
C(46)-C(53)-C(42)	118.1(4)
C(46)-C(53)-Ti(2)	119.3(3)
C(42)-C(53)-Ti(2)	122.6(4)
C(56)-C(54)-C(37)	112.2(3)
C(56)-C(54)-C(57)	107.3(3)
C(37)-C(54)-C(57)	110.4(4)
C(56)-C(54)-C(55)	107.1(4)
C(37)-C(54)-C(55)	109.7(3)
C(57)-C(54)-C(55)	110.2(3)
C(62)-C(60)-C(61)	109.8(4)
C(62)-C(60)-C(63)	108.1(3)
C(61)-C(60)-C(63)	105.7(3)
C(62)-C(60)-C(51)	111.2(3)
C(61)-C(60)-C(51)	111.4(3)
C(63)-C(60)-C(51)	110.4(4)
C(65)-C(64)-Ti(2)	106.2(2)
C(70)-C(65)-C(66)	116.7(4)
C(70)-C(65)-C(64)	121.8(4)
C(66)-C(65)-C(64)	121.4(5)
C(67)-C(66)-C(65)	120.3(5)
C(68)-C(67)-C(66)	121.6(4)
C(69)-C(68)-C(67)	119.4(5)
C(68)-C(69)-C(70)	119.2(5)
C(69)-C(70)-C(65)	122.8(4)

Table 12. Anisotropic displacement parameters ($Å^2$ x 10^4). The anisotropic displacement factor exponent takes the form: $-2\pi^2[h^2a^*2U^{11} + ... + 2 h k a^* b^* U^{12}]$.

	U^{11}	U^{22}	U^{33}	U^{23}	U^{13}	U^{12}
Ti(1)	221(4)	215(4)	483(7)	47(4)	96(4)	-27(3)
Ti(2)	223(4)	212(4)	523(7)	38(5)	98(4)	-36(3)
O(1)	239(15)	199(14)	360(20)	82(15)	21(15)	-8(11)
O(2)	166(15)	184(15)	410(20)	7(16)	77(16)	3(11)
O(3)	196(15)	227(15)	550(20)	61(15)	124(15)	-25(11)
O(4)	165(15)	232(15)	390(20)	-19(16)	124(16)	-46(11)
C(1A)	290(30)	200(30)	370(50)	110(30)	70(30)	100(30)
C(2A)	330(30)	270(30)	250(40)	80(30)	50(30)	90(30)
C(3A)	470(40)	270(30)	370(50)	190(30)	50(30)	50(30)
C(4A)	380(40)	130(40)	340(50)	-50(30)	-70(40)	20(30)
C(5A)	290(30)	290(30)	460(50)	150(30)	30(40)	60(20)
C(6A)	190(30)	240(30)	380(50)	90(30)	-40(30)	50(20)
C(7A)	180(30)	150(30)	450(60)	80(40)	-20(40)	-50(30)
C(8A)	260(30)	250(40)	280(60)	-20(40)	30(40)	-10(30)
C(9A)	120(30)	490(50)	410(70)	-50(50)	0(40)	0(30)
C(10A)	260(30)	230(50)	420(60)	40(30)	150(40)	-10(30)
C(11A)	220(30)	110(40)	290(50)	30(30)	30(40)	-20(20)
C(12)	240(30)	160(20)	420(40)	10(20)	90(30)	-56(19)
C(13)	180(30)	220(20)	570(40)	-50(30)	120(30)	-79(19)
C(14)	220(30)	270(30)	500(40)	-60(30)	140(30)	-70(20)
C(15)	340(30)	330(30)	380(40)	110(30)	60(30)	-90(20)
C(16)	290(30)	180(20)	380(40)	80(30)	60(30)	-23(19)
C(17)	310(30)	160(20)	470(40)	30(30)	140(30)	-80(20)
C(18A)	180(30)	110(30)	210(50)	0(40)	-10(30)	60(20)
C(19A)	350(50)	280(50)	320(70)	100(50)	30(50)	-90(30)
C(20A)	620(40)	470(50)	470(60)	240(40)	140(50)	-90(40)
C(21A)	400(40)	350(40)	580(60)	30(40)	120(40)	-120(30)
C(22A)	390(40)	450(40)	640(60)	120(40)	190(50)	-20(40)
C(23A)	390(40)	500(40)	380(50)	10(40)	-100(40)	60(30)
C(24)	400(30)	520(30)	580(40)	-40(30)	210(30)	-40(20)
C(25)	200(20)	260(20)	460(40)	110(30)	60(20)	17(19)
C(26)	310(30)	310(30)	900(50)	50(30)	110(30)	30(20)
C(27)	210(20)	320(20)	490(40)	80(20)	70(20)	-25(18)
C(28)	340(30)	680(30)	700(50)	440(30)	160(30)	140(20)
C(29)	300(20)	230(20)	420(40)	70(20)	80(20)	-50(19)
C(30)	320(30)	190(20)	330(40)	30(30)	70(30)	-90(20)
C(31)	440(30)	230(20)	380(40)	50(30)	110(30)	-20(20)
C(32)	520(40)	320(30)	570(50)	10(30)	120(30)	170(20)
C(33)	400(30)	420(30)	550(50)	-120(30)	130(30)	110(20)
C(34)	390(30)	370(30)	400(40)	-110(30)	120(30)	-170(20)
C(35)	330(30)	220(30)	420(40)	-50(30)	70(30)	-100(20)
C(36)	180(30)	180(20)	560(40)	-30(30)	140(30)	-22(19)
C(37)	220(30)	220(20)	580(40)	-50(30)	130(30)	-80(20)
C(38)	390(30)	230(20)	610(40)	0(30)	180(30)	-90(20)
C(39)	260(30)	380(30)	540(40)	-90(30)	120(30)	-100(20)
C(40)	220(30)	360(30)	580(40)	-70(30)	20(30)	-30(20)

C(41)	200(30)	200(20)	520(40)	-40(30)	40(30)	-21(19)
C(42)	250(30)	160(20)	550(40)	0(30)	80(30)	3(19)
C(43)	210(30)	280(30)	670(50)	90(30)	10(30)	-10(20)
C(44)	270(30)	290(30)	750(50)	180(30)	-60(30)	-30(20)
C(45)	270(30)	260(20)	630(40)	160(30)	-30(30)	-40(20)
C(46)	210(20)	170(20)	500(40)	40(20)	30(30)	-26(19)
C(47)	230(30)	200(20)	400(40)	70(30)	20(30)	16(19)
C(48)	220(30)	270(30)	430(40)	20(30)	10(30)	6(19)
C(49)	320(30)	300(30)	260(40)	40(30)	60(30)	50(20)
C(50)	230(30)	270(20)	460(40)	80(30)	110(30)	6(19)
C(51)	200(20)	220(20)	430(40)	10(30)	100(30)	-9(18)
C(52)	260(30)	180(20)	400(40)	20(30)	140(30)	39(19)
C(53)	150(20)	130(20)	580(40)	40(20)	60(20)	31(17)
C(54)	260(20)	240(20)	570(40)	-10(30)	160(30)	-60(20)
C(55)	330(30)	370(30)	610(40)	100(30)	110(30)	-50(20)
C(56)	390(30)	280(20)	730(40)	90(30)	220(30)	-100(20)
C(57)	390(30)	310(30)	820(50)	140(30)	340(30)	90(20)
C(58)	220(20)	660(30)	690(40)	-60(30)	120(30)	-70(20)
C(59)	360(30)	420(30)	440(40)	100(30)	10(30)	-20(20)
C(60)	180(20)	390(30)	290(30)	-10(30)	90(20)	-50(20)
C(61)	360(30)	390(30)	340(40)	-80(30)	90(30)	-70(20)
C(62)	410(30)	450(30)	640(40)	150(30)	-240(30)	-10(20)
C(63)	280(30)	890(40)	430(40)	-200(30)	90(30)	-250(20)
C(64)	220(20)	260(20)	590(40)	80(30)	80(20)	9(18)
C(65)	250(20)	230(30)	460(40)	80(30)	90(30)	60(20)
C(66)	200(20)	300(30)	650(40)	60(30)	100(30)	10(20)
C(67)	210(30)	350(30)	720(50)	-120(30)	60(30)	-10(20)
C(68)	350(30)	540(30)	600(50)	-60(30)	40(30)	100(20)
C(69)	430(30)	520(30)	520(40)	30(30)	160(30)	140(20)
C(70)	310(30)	250(30)	660(50)	100(30)	110(30)	60(20)

3.1 (CCDC 743415)

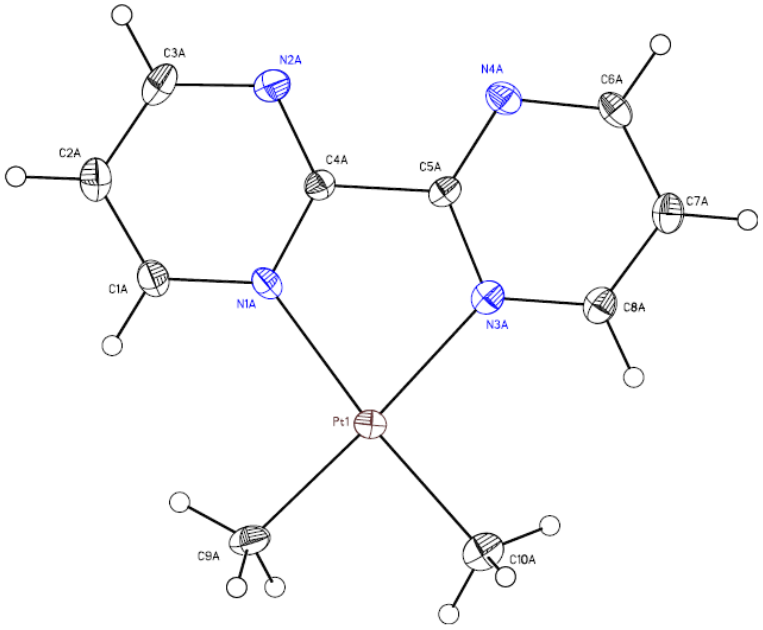

Special Refinement Details

Crystals were mounted on a glass fiber using Paratone oil then placed on the diffractometer under a nitrogen stream at 100K.

Refinement of F^2 against ALL reflections. All esds are estimated using the full covariance matrix. The cell esds are taken into account individually in the estimation of esds in distances, angles and torsion angles; correlations between esds in cell parameters are only used when they are defined by crystal symmetry.

Table 13. Atomic coordinates (x 10^4) and equivalent isotropic displacement parameters ($Å^2$ x 10^3). U(eq) is defined as the trace of the orthogonalized Uij tensor.

	x	y	z	Ueq
Pt(1)	1196(1)	4253(1)	3017(1)	15(1)
N(1A)	1345(2)	5599(2)	3096(3)	15(1)
N(2A)	1452(2)	6838(2)	1736(3)	19(1)
N(3A)	1254(2)	4557(2)	1031(3)	14(1)
N(4A)	1274(2)	5758(2)	-450(3)	17(1)
C(1A)	1410(3)	6120(2)	4173(4)	18(1)
C(2A)	1493(3)	6999(3)	4082(4)	22(1)
C(3A)	1515(3)	7329(3)	2828(4)	22(1)
C(4A)	1380(3)	5998(2)	1927(3)	13(1)
C(5A)	1310(3)	5416(2)	749(3)	13(1)
C(6A)	1194(3)	5204(2)	-1464(4)	17(1)
C(7A)	1166(3)	4317(3)	-1293(3)	18(1)
C(8A)	1194(3)	4022(2)	-13(3)	17(1)
C(9A)	1077(3)	4033(2)	4956(4)	20(1)
C(10A)	1048(3)	2954(2)	2754(4)	23(1)
Pt(2)	3896(1)	5652(1)	1118(1)	16(1)
N(1B)	3750(2)	5453(2)	-940(3)	13(1)

N(2B)	3444(2)	4351(2)	-2606(3)	18(1)
N(3B)	3745(2)	4315(2)	978(3)	16(1)
N(4B)	3464(3)	3157(2)	-603(3)	21(1)
C(1B)	3758(3)	6045(2)	-1907(4)	20(1)
C(2B)	3614(3)	5813(3)	-3237(4)	24(1)
C(3B)	3442(3)	4952(3)	-3541(4)	20(1)
C(4B)	3620(3)	4628(2)	-1352(3)	14(1)
C(5B)	3615(3)	3982(2)	-272(3)	15(1)
C(6B)	3436(3)	2610(3)	416(4)	26(1)
C(7B)	3563(3)	2872(3)	1712(4)	26(1)
C(8B)	3704(3)	3738(3)	1963(4)	22(1)
C(9B)	3999(3)	6960(2)	1096(4)	22(1)
C(10B)	4033(3)	5744(3)	3139(4)	30(1)

Table 14. Bond lengths [Å] and angles [°].

Pt(1)-C(10A)	2.037(4)	C(10A)-Pt(1)-C(9A)	86.48(15)
Pt(1)-C(9A)	2.038(4)	C(10A)-Pt(1)-N(3A)	96.60(14)
Pt(1)-N(3A)	2.092(3)	C(9A)-Pt(1)-N(3A)	175.97(14)
Pt(1)-N(1A)	2.095(3)	C(10A)-Pt(1)-N(1A)	174.65(13)
N(1A)-C(4A)	1.350(4)	C(9A)-Pt(1)-N(1A)	98.85(13)
N(1A)-C(1A)	1.351(4)	N(3A)-Pt(1)-N(1A)	78.05(11)
N(2A)-C(4A)	1.321(4)	C(4A)-N(1A)-C(1A)	115.8(3)
N(2A)-C(3A)	1.337(5)	C(4A)-N(1A)-Pt(1)	116.2(2)
N(3A)-C(8A)	1.338(4)	C(1A)-N(1A)-Pt(1)	128.1(2)
N(3A)-C(5A)	1.368(4)	C(4A)-N(2A)-C(3A)	115.7(3)
N(4A)-C(5A)	1.324(4)	C(8A)-N(3A)-C(5A)	115.7(3)
N(4A)-C(6A)	1.332(4)	C(8A)-N(3A)-Pt(1)	128.4(3)
C(1A)-C(2A)	1.372(5)	C(5A)-N(3A)-Pt(1)	115.8(2)
C(2A)-C(3A)	1.381(5)	C(5A)-N(4A)-C(6A)	116.1(3)
C(4A)-C(5A)	1.490(5)	N(1A)-C(1A)-C(2A)	122.1(4)
C(6A)-C(7A)	1.387(5)	C(1A)-C(2A)-C(3A)	116.5(4)
C(7A)-C(8A)	1.375(5)	N(2A)-C(3A)-C(2A)	123.3(4)
Pt(2)-C(9B)	2.032(4)	N(2A)-C(4A)-N(1A)	126.6(3)
Pt(2)-C(10B)	2.038(4)	N(2A)-C(4A)-C(5A)	118.2(3)
Pt(2)-N(3B)	2.085(3)	N(1A)-C(4A)-C(5A)	115.2(3)
Pt(2)-N(1B)	2.091(3)	N(4A)-C(5A)-N(3A)	126.1(3)
N(1B)-C(1B)	1.347(4)	N(4A)-C(5A)-C(4A)	119.1(3)
N(1B)-C(4B)	1.347(4)	N(3A)-C(5A)-C(4A)	114.7(3)
N(2B)-C(4B)	1.327(4)	N(4A)-C(6A)-C(7A)	122.8(3)
N(2B)-C(3B)	1.332(5)	C(8A)-C(7A)-C(6A)	116.9(3)
N(3B)-C(5B)	1.354(4)	N(3A)-C(8A)-C(7A)	122.3(4)
N(3B)-C(8B)	1.353(4)	C(9B)-Pt(2)-C(10B)	86.96(17)
N(4B)-C(5B)	1.329(5)	C(9B)-Pt(2)-N(3B)	175.46(13)
N(4B)-C(6B)	1.345(5)	C(10B)-Pt(2)-N(3B)	97.38(15)
C(1B)-C(2B)	1.380(5)	C(9B)-Pt(2)-N(1B)	97.48(13)
C(2B)-C(3B)	1.380(6)	C(10B)-Pt(2)-N(1B)	175.56(16)
C(4B)-C(5B)	1.488(5)	N(3B)-Pt(2)-N(1B)	78.18(11)
C(6B)-C(7B)	1.361(5)	C(1B)-N(1B)-C(4B)	115.9(3)

C(7B)-C(8B)	1.373(6)	C(1B)-N(1B)-Pt(2)	128.4(3)
		C(4B)-N(1B)-Pt(2)	115.8(2)
		C(4B)-N(2B)-C(3B)	116.0(3)
		C(5B)-N(3B)-C(8B)	115.5(3)
		C(5B)-N(3B)-Pt(2)	115.9(2)
		C(8B)-N(3B)-Pt(2)	128.5(3)
		C(5B)-N(4B)-C(6B)	115.8(3)
		N(1B)-C(1B)-C(2B)	121.4(4)
		C(3B)-C(2B)-C(1B)	117.4(4)
		N(2B)-C(3B)-C(2B)	122.5(4)
		N(2B)-C(4B)-N(1B)	126.7(3)
		N(2B)-C(4B)-C(5B)	118.0(3)
		N(1B)-C(4B)-C(5B)	115.2(3)
		N(4B)-C(5B)-N(3B)	126.3(3)
		N(4B)-C(5B)-C(4B)	118.8(3)
		N(3B)-C(5B)-C(4B)	114.9(3)
		N(4B)-C(6B)-C(7B)	123.0(4)
		C(6B)-C(7B)-C(8B)	117.4(4)
		N(3B)-C(8B)-C(7B)	122.1(4)

Table 15. Anisotropic displacement parameters ($Å^2$ x 10^4). The anisotropic displacement factor exponent takes the form: $-2\pi^2[h^2a^*2U^{11} + ... + 2 h k a^* b^* U^{12}]$.

	U^{11}	U^{22}	U^{33}	U^{23}	U^{13}	U^{12}
Pt(1)	165(1)	134(1)	139(1)	17(1)	27(1)	0(1)
N(1A)	156(18)	177(18)	105(13)	9(12)	27(12)	13(14)
N(2A)	230(20)	149(17)	200(16)	13(13)	51(14)	11(15)
N(3A)	103(17)	149(17)	175(15)	-9(12)	6(12)	-6(13)
N(4A)	149(18)	191(17)	153(13)	24(13)	15(11)	24(15)
C(1A)	190(20)	210(20)	140(18)	-12(14)	24(15)	28(18)
C(2A)	220(30)	240(20)	185(18)	-62(16)	16(16)	1(19)
C(3A)	220(20)	150(20)	280(20)	-67(16)	24(17)	-12(18)
C(4A)	120(20)	126(18)	149(17)	-2(13)	38(14)	10(15)
C(5A)	90(20)	113(18)	173(17)	-2(13)	8(14)	6(15)
C(6A)	160(20)	230(20)	125(16)	12(14)	49(14)	-1(17)
C(7A)	140(20)	200(20)	181(17)	-46(16)	19(14)	-9(18)
C(8A)	130(20)	170(20)	194(19)	-23(14)	8(15)	-13(16)
C(9A)	220(20)	130(20)	240(20)	40(15)	16(17)	-22(17)
C(10A)	230(30)	190(20)	270(20)	2(16)	42(17)	-6(19)
Pt(2)	161(1)	155(1)	177(1)	-38(1)	37(1)	8(1)
N(1B)	87(17)	124(16)	189(15)	-4(12)	30(12)	55(13)
N(2B)	171(18)	168(17)	190(14)	12(13)	42(12)	-8(15)
N(3B)	129(17)	178(16)	176(13)	37(14)	31(11)	23(15)
N(4B)	260(20)	119(17)	256(18)	15(13)	99(15)	-28(15)
C(1B)	180(20)	130(20)	280(20)	23(15)	36(17)	-24(17)
C(2B)	250(20)	230(20)	220(19)	82(16)	41(16)	-7(19)
C(3B)	190(20)	250(20)	170(18)	12(15)	54(16)	16(18)
C(4B)	120(20)	145(19)	173(18)	16(14)	47(14)	16(16)
C(5B)	140(20)	155(19)	171(18)	-3(14)	53(15)	2(16)

C(6B)	350(30)	130(20)	340(20)	53(17)	140(20)	-8(19)
C(7B)	290(30)	260(20)	260(20)	130(18)	119(19)	40(20)
C(8B)	260(30)	220(20)	178(19)	31(16)	38(17)	44(19)
C(9B)	240(30)	190(20)	240(20)	-74(16)	33(17)	-4(18)
C(10B)	290(30)	400(30)	199(19)	-100(20)	28(17)	10(20)

3.2 (CCDC 757798)

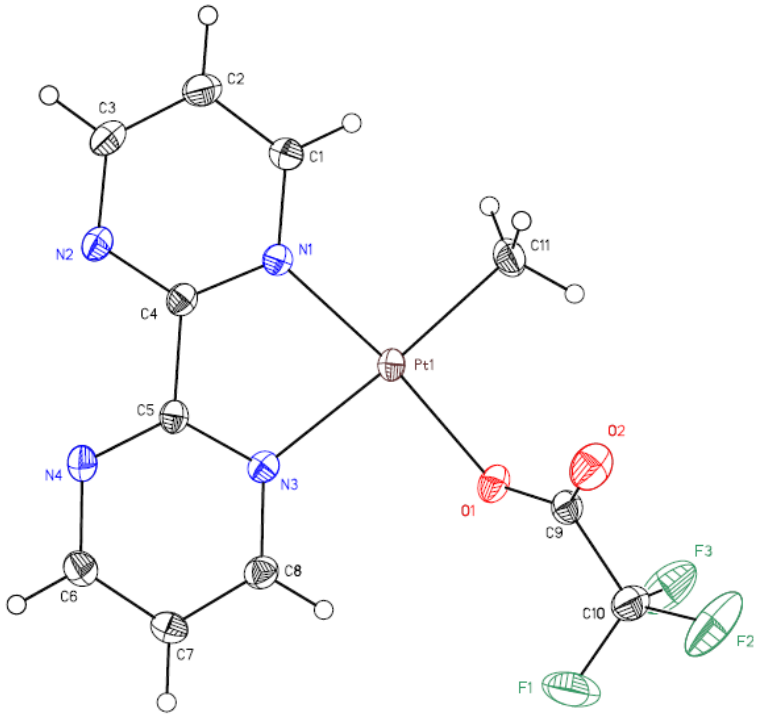

Special Refinement Details

Crystals were mounted on a glass fiber using Paratone oil then placed on the diffractometer under a nitrogen stream at 100K.

Refinement of F^2 against ALL reflections. The weighted R-factor (wR) and goodness of fit (S) are based on F^2, conventional R-factors (R) are based on F, with F set to zero for negative F^2. The threshold expression of $F^2 > 2\sigma (F^2)$ is used only for calculating R-factors(gt) etc. and is not relevant to the choice of reflections for refinement. R-factors based on F^2 are statistically about twice as large as those based on F, and R-factors based on ALL data will be even larger.

All esds (except the esd in the dihedral angle between two l.s. planes) are estimated using the full covariance matrix. The cell esds are taken into account individually in the estimation of esds in distances, angles and torsion angles; correlations between esds in cell parameters are only used when they are defined by crystal symmetry. An approximate (isotropic) treatment of cell esds is used for estimating esds involving l.s. planes.

Table 16. Atomic coordinates (x 10^4) and equivalent isotropic displacement parameters (Å^2 x 10^3). U(eq) is defined as the trace of the orthogonalized Uij tensor.

	x	y	z	Ueq
Pt(1)	1062(1)	2114(1)	3210(1)	14(1)
F(1)	1076(3)	105(1)	3793(4)	87(1)
F(2)	3469(3)	51(1)	4243(2)	58(1)
F(3)	2427(2)	259(1)	1744(2)	44(1)
O(1)	1374(2)	1262(1)	2931(2)	20(1)
O(2)	3341(2)	1158(1)	5025(2)	31(1)
N(1)	512(2)	2931(1)	3517(2)	15(1)
N(2)	-1262(2)	3533(1)	4703(2)	19(1)

N(3)	-983(2)	2006(1)	4235(2)	15(1)
N(4)	-2864(2)	2549(1)	5415(2)	18(1)
C(1)	1272(2)	3398(1)	3074(2)	19(1)
C(2)	805(3)	3941(1)	3444(3)	23(1)
C(3)	-475(2)	3994(1)	4282(3)	22(1)
C(4)	-739(2)	3026(1)	4307(2)	16(1)
C(5)	-1590(2)	2501(1)	4696(2)	15(1)
C(6)	-3587(2)	2061(1)	5665(2)	20(1)
C(7)	-3054(2)	1526(1)	5215(2)	20(1)
C(8)	-1715(2)	1517(1)	4490(2)	19(1)
C(9)	2397(2)	988(1)	3883(2)	18(1)
C(10)	2339(3)	344(1)	3419(3)	26(1)
C(11)	3057(2)	2278(1)	2300(3)	24(1)
C(21)	5629(3)	1075(1)	945(3)	25(1)
Cl(1)	6602(1)	449(1)	1709(1)	31(1)
Cl(2)	4937(1)	1022(1)	-1284(1)	29(1)

Table 17. Bond lengths [Å] and angles [°].

Pt(1)-N(1)	1.9864(16)	N(1)-Pt(1)-O(1)	173.47(6)
Pt(1)-O(1)	2.0162(15)	N(1)-Pt(1)-C(11)	95.85(8)
Pt(1)-C(11)	2.033(2)	O(1)-Pt(1)-C(11)	90.50(8)
Pt(1)-N(3)	2.0948(16)	N(1)-Pt(1)-N(3)	80.18(6)
F(1)-C(10)	1.322(3)	O(1)-Pt(1)-N(3)	93.51(6)
F(2)-C(10)	1.319(3)	C(11)-Pt(1)-N(3)	175.70(8)
F(3)-C(10)	1.325(3)	C(9)-O(1)-Pt(1)	121.94(13)
O(1)-C(9)	1.277(2)	C(1)-N(1)-C(4)	116.96(17)
O(2)-C(9)	1.215(3)	C(1)-N(1)-Pt(1)	126.96(13)
N(1)-C(1)	1.347(3)	C(4)-N(1)-Pt(1)	116.05(13)
N(1)-C(4)	1.356(2)	C(4)-N(2)-C(3)	116.52(17)
N(2)-C(4)	1.318(3)	C(8)-N(3)-C(5)	118.01(16)
N(2)-C(3)	1.345(3)	C(8)-N(3)-Pt(1)	128.54(13)
N(3)-C(8)	1.340(3)	C(5)-N(3)-Pt(1)	113.45(12)
N(3)-C(5)	1.342(2)	C(6)-N(4)-C(5)	116.30(18)
N(4)-C(6)	1.334(3)	N(1)-C(1)-C(2)	120.88(17)
N(4)-C(5)	1.332(2)	C(1)-C(2)-C(3)	117.88(19)
C(1)-C(2)	1.373(3)	N(2)-C(3)-C(2)	121.92(19)
C(2)-C(3)	1.388(3)	N(2)-C(4)-N(1)	125.81(18)
C(4)-C(5)	1.489(3)	N(2)-C(4)-C(5)	118.80(16)
C(6)-C(7)	1.392(3)	N(1)-C(4)-C(5)	115.36(17)
C(7)-C(8)	1.382(3)	N(4)-C(5)-N(3)	125.32(18)
C(9)-C(10)	1.541(3)	N(4)-C(5)-C(4)	120.00(17)
C(21)-Cl(1)	1.763(2)	N(3)-C(5)-C(4)	114.66(16)
C(21)-Cl(2)	1.769(2)	N(4)-C(6)-C(7)	122.60(18)
		C(8)-C(7)-C(6)	117.11(19)
		N(3)-C(8)-C(7)	120.66(19)
		O(2)-C(9)-O(1)	130.3(2)
		O(2)-C(9)-C(10)	119.24(19)
		O(1)-C(9)-C(10)	110.47(17)
		F(2)-C(10)-F(1)	107.7(2)

F(2)-C(10)-F(3)	105.41(19)
F(1)-C(10)-F(3)	107.7(2)
F(2)-C(10)-C(9)	112.7(2)
F(1)-C(10)-C(9)	111.30(19)
F(3)-C(10)-C(9)	111.68(17)
Cl(1)-C(21)-Cl(2)	111.85(12)

Table 18. Anisotropic displacement parameters ($Å^2$ x 10^4). The anisotropic displacement factor exponent takes the form: $-2\pi^2[h^2a^*2U^{11} + ... + 2 h k a^* b^* U^{12}]$.

	U^{11}	U^{22}	U^{33}	U^{23}	U^{13}	U^{12}
Pt(1)	137(1)	156(1)	123(1)	-16(1)	8(1)	19(1)
F(1)	788(16)	310(10)	1670(20)	-173(13)	838(18)	-230(11)
F(2)	809(15)	304(9)	554(10)	-11(8)	-161(10)	254(10)
F(3)	765(13)	249(8)	305(7)	-86(6)	48(7)	82(8)
O(1)	212(6)	172(7)	206(6)	-43(5)	4(5)	36(5)
O(2)	291(8)	278(9)	332(8)	-32(6)	-99(6)	38(7)
N(1)	146(6)	156(7)	135(6)	7(5)	1(5)	7(5)
N(2)	190(7)	159(7)	208(7)	9(5)	13(5)	35(6)
N(3)	169(7)	150(7)	134(6)	-19(5)	0(5)	1(5)
N(4)	162(7)	203(8)	175(6)	6(6)	23(5)	36(6)
C(1)	183(8)	186(9)	192(8)	1(6)	29(6)	-18(7)
C(2)	247(10)	176(9)	259(9)	24(7)	19(7)	-21(7)
C(3)	255(10)	149(8)	248(9)	6(7)	8(7)	27(7)
C(4)	161(7)	163(8)	149(7)	13(6)	-10(6)	19(6)
C(5)	143(7)	167(8)	141(6)	-5(6)	-1(5)	20(6)
C(6)	176(8)	231(10)	193(7)	18(7)	22(6)	1(7)
C(7)	190(8)	203(9)	207(8)	-6(7)	21(6)	-45(7)
C(8)	200(8)	163(8)	206(8)	-21(6)	16(6)	-5(7)
C(9)	190(8)	186(8)	173(7)	-6(6)	55(6)	13(7)
C(10)	298(11)	191(9)	287(10)	24(7)	84(8)	12(8)
C(11)	189(8)	270(10)	262(9)	33(8)	85(7)	28(8)
C(21)	287(10)	197(9)	273(9)	-4(7)	111(8)	-27(8)
Cl(1)	458(3)	210(2)	267(2)	26(2)	18(2)	-13(2)
Cl(2)	233(2)	302(3)	335(2)	46(2)	-22(2)	-34(2)

3.4 (CCDC 779474)

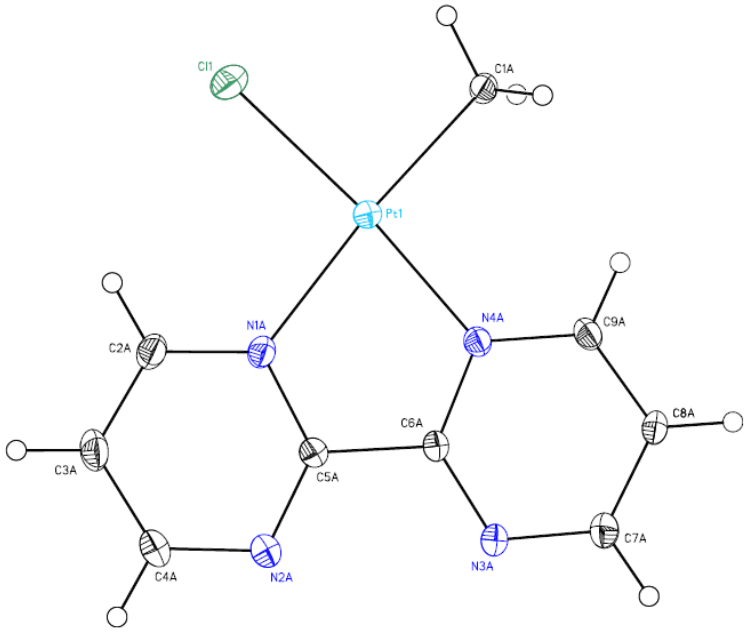

Special Refinement Details

Crystals were mounted on a glass fiber using Paratone oil then placed on the diffractometer under a nitrogen stream at 100K.

Two of the four molecules in the asymmetric unit are disordered with chlorine partially occupying the methyl site 24% of the time. There is no evidence for this disorder in the other two molecules. Is was not possible to tell if there is a corresponding percentage of methyl group in the chlorine site. Therefore the empirical formula reflects the presence of the dichloro moiety.

Refinement of F^2 against ALL reflections. The weighted R-factor (*w*R) and goodness of fit (S) are based on F^2, conventional R-factors (R) are based on F, with F set to zero for negative F^2. The threshold expression of $F^2 > 2\sigma(F^2)$ is used only for calculating R-factors(gt) etc. and is not relevant to the choice of reflections for refinement. R-factors based on F^2 are statistically about twice as large as those based on F, and R-factors based on ALL data will be even larger.

All esds (except the esd in the dihedral angle between two l.s. planes) are estimated using the full covariance matrix. The cell esds are taken into account individually in the estimation of esds in distances, angles and torsion angles; correlations between esds in cell parameters are only used when they are defined by crystal symmetry. An approximate (isotropic) treatment of cell esds is used for estimating esds involving l.s. planes.

Table 19. Atomic coordinates (x 10^4) and equivalent isotropic displacement parameters (Å^2 x 10^3). U(eq) is defined as the trace of the orthogonalized Uij tensor.

	x	y	z	Ueq	Occ
Pt(1)	9338(1)	3141(1)	1156(1)	13(1)	1
Cl(1)	7969(1)	2853(1)	2134(1)	26(1)	1
N(1A)	9322(3)	3728(1)	1764(2)	14(1)	1
N(2A)	10198(3)	4396(1)	1615(2)	18(1)	1
N(3A)	11531(3)	4091(1)	164(2)	16(1)	1
N(4A)	10540(2)	3443(1)	372(2)	13(1)	1
C(1A)	9385(3)	2591(1)	434(2)	16(1)	1
C(2A)	8654(3)	3856(1)	2465(2)	17(1)	1

C(3A)	8719(3)	4258(1)	2765(2)	21(1)	1
C(4A)	9515(4)	4518(1)	2322(2)	21(1)	1
C(5A)	10057(3)	4008(1)	1366(2)	14(1)	1
C(6A)	10758(3)	3843(1)	585(2)	12(1)	1
C(7A)	12134(3)	3931(1)	-542(2)	17(1)	1
C(8A)	11984(3)	3525(1)	-809(2)	16(1)	1
C(9A)	11183(3)	3287(1)	-322(2)	16(1)	1
Pt(2)	2939(1)	2889(1)	2467(1)	12(1)	1
Cl(2)	3773(1)	2579(1)	1209(1)	21(1)	1
N(1B)	3726(2)	3467(1)	2270(2)	12(1)	1
N(2B)	3770(3)	4142(1)	2909(2)	16(1)	1
N(3B)	1997(3)	3875(1)	4129(2)	16(1)	1
N(4B)	2179(3)	3209(1)	3494(2)	13(1)	1
C(1B)	2194(3)	2334(1)	2830(2)	14(1)	1
C(2B)	4569(3)	3574(1)	1661(2)	15(1)	1
C(3B)	5022(3)	3973(1)	1637(2)	18(1)	1
C(4B)	4598(3)	4245(1)	2283(2)	18(1)	1
C(5B)	3361(3)	3756(1)	2868(2)	13(1)	1
C(6B)	2456(3)	3612(1)	3539(2)	13(1)	1
C(7B)	1191(4)	3730(1)	4722(2)	20(1)	1
C(8B)	844(4)	3322(1)	4731(2)	23(1)	1
C(9B)	1355(3)	3068(1)	4090(2)	19(1)	1
Pt(3)	4820(1)	4167(1)	6592(1)	12(1)	1
Cl(3)	4229(1)	4656(1)	7627(1)	23(1)	1
N(1C)	6090(3)	4541(1)	5927(2)	13(1)	1
N(2C)	7302(3)	4543(1)	4595(2)	18(1)	1
N(3C)	6778(3)	3712(1)	4379(2)	16(1)	1
N(4C)	5459(3)	3768(1)	5660(2)	13(1)	1
C(1C)	3535(6)	3757(2)	7173(5)	8(1)	0.762(4)
Cl(1C)	3530(13)	3755(4)	7156(9)	66(3)	0.238(4)
C(2C)	6423(3)	4933(1)	6115(2)	15(1)	1
C(3C)	7194(3)	5145(1)	5556(2)	18(1)	1
C(4C)	7602(3)	4937(1)	4782(2)	18(1)	1
C(5C)	6578(3)	4361(1)	5181(2)	14(1)	1
C(6C)	6261(3)	3922(1)	5053(2)	14(1)	1
C(7C)	6526(3)	3311(1)	4335(2)	18(1)	1
C(8C)	5761(3)	3125(1)	4958(2)	19(1)	1
C(9C)	5229(3)	3364(1)	5612(2)	18(1)	1
Pt(4)	8601(1)	3913(1)	7747(1)	14(1)	1
Cl(4)	9884(1)	4368(1)	7075(1)	30(1)	1
N(1D)	7952(3)	4316(1)	8725(2)	14(1)	1
N(2D)	6658(3)	4342(1)	10013(2)	17(1)	1

N(3D)	5997(3)	3523(1)	9622(2)	16(1)	1
N(4D)	7388(3)	3541(1)	8386(2)	13(1)	1
C(1D)	9265(10)	3442(2)	6893(7)	20(1)	0.762(4)
Cl(4B)	9247(9)	3487(2)	6739(6)	19(1)	0.238(4)
C(2D)	8264(3)	4712(1)	8866(2)	18(1)	1
C(3D)	7771(3)	4937(1)	9564(2)	20(1)	1
C(4D)	6966(3)	4739(1)	10129(2)	19(1)	1
C(5D)	7156(3)	4150(1)	9315(2)	12(1)	1
C(6D)	6818(3)	3711(1)	9111(2)	13(1)	1
C(7D)	5677(3)	3135(1)	9375(2)	18(1)	1
C(8D)	6153(3)	2939(1)	8608(2)	19(1)	1
C(9D)	7032(3)	3152(1)	8131(2)	17(1)	1

Table 20. Bond lengths [Å] and angles [°].

Pt(1)-N(4A)	2.015(2)	N(4A)-Pt(1)-C(1A)	96.03(10)
Pt(1)-C(1A)	2.068(3)	N(4A)-Pt(1)-N(1A)	79.11(9)
Pt(1)-N(1A)	2.104(2)	C(1A)-Pt(1)-N(1A)	174.62(10)
Pt(1)-Cl(1)	2.2930(7)	N(4A)-Pt(1)-Cl(1)	174.58(7)
N(1A)-C(2A)	1.338(4)	C(1A)-Pt(1)-Cl(1)	89.38(8)
N(1A)-C(5A)	1.354(3)	N(1A)-Pt(1)-Cl(1)	95.49(6)
N(2A)-C(5A)	1.322(4)	C(2A)-N(1A)-C(5A)	117.0(2)
N(2A)-C(4A)	1.349(4)	C(2A)-N(1A)-Pt(1)	128.24(19)
N(3A)-C(6A)	1.326(3)	C(5A)-N(1A)-Pt(1)	114.71(17)
N(3A)-C(7A)	1.340(4)	C(5A)-N(2A)-C(4A)	115.6(2)
N(4A)-C(6A)	1.356(3)	C(6A)-N(3A)-C(7A)	116.9(2)
N(4A)-C(9A)	1.348(3)	C(6A)-N(4A)-C(9A)	116.5(2)
C(2A)-C(3A)	1.385(4)	C(6A)-N(4A)-Pt(1)	116.66(17)
C(3A)-C(4A)	1.381(4)	C(9A)-N(4A)-Pt(1)	126.77(18)
C(5A)-C(6A)	1.489(4)	N(1A)-C(2A)-C(3A)	121.1(3)
C(7A)-C(8A)	1.386(4)	C(2A)-C(3A)-C(4A)	117.2(3)
C(8A)-C(9A)	1.378(4)	N(2A)-C(4A)-C(3A)	122.8(3)
Pt(2)-N(4B)	2.019(2)	N(2A)-C(5A)-N(1A)	126.3(2)
Pt(2)-C(1B)	2.070(2)	N(2A)-C(5A)-C(6A)	119.9(2)
Pt(2)-N(1B)	2.095(2)	N(1A)-C(5A)-C(6A)	113.9(2)
Pt(2)-Cl(2)	2.2920(7)	N(3A)-C(6A)-N(4A)	125.6(2)
N(1B)-C(2B)	1.339(3)	N(3A)-C(6A)-C(5A)	118.8(2)
N(1B)-C(5B)	1.351(3)	N(4A)-C(6A)-C(5A)	115.6(2)
N(2B)-C(5B)	1.331(4)	N(3A)-C(7A)-C(8A)	122.0(3)
N(2B)-C(4B)	1.343(4)	C(9A)-C(8A)-C(7A)	117.5(2)
N(3B)-C(6B)	1.326(3)	N(4A)-C(9A)-C(8A)	121.4(2)
N(3B)-C(7B)	1.334(4)	N(4B)-Pt(2)-C(1B)	95.40(10)

N(4B)-C(6B)	1.356(3)	N(4B)-Pt(2)-N(1B)	79.38(9)
N(4B)-C(9B)	1.347(4)	C(1B)-Pt(2)-N(1B)	173.76(10)
C(2B)-C(3B)	1.391(4)	N(4B)-Pt(2)-Cl(2)	174.67(7)
C(3B)-C(4B)	1.383(4)	C(1B)-Pt(2)-Cl(2)	89.25(8)
C(5B)-C(6B)	1.482(4)	N(1B)-Pt(2)-Cl(2)	96.13(6)
C(7B)-C(8B)	1.390(4)	C(2B)-N(1B)-C(5B)	118.0(2)
C(8B)-C(9B)	1.382(4)	C(2B)-N(1B)-Pt(2)	127.76(18)
Pt(3)-N(4C)	2.019(2)	C(5B)-N(1B)-Pt(2)	114.21(17)
Pt(3)-Cl(1C)	2.107(12)	C(5B)-N(2B)-C(4B)	115.7(2)
Pt(3)-N(1C)	2.092(2)	C(6B)-N(3B)-C(7B)	117.2(2)
Pt(3)-C(1C)	2.111(5)	C(6B)-N(4B)-C(9B)	116.9(2)
Pt(3)-Cl(3)	2.2984(7)	C(6B)-N(4B)-Pt(2)	116.30(18)
N(1C)-C(2C)	1.340(3)	C(9B)-N(4B)-Pt(2)	126.68(18)
N(1C)-C(5C)	1.349(3)	N(1B)-C(2B)-C(3B)	120.4(2)
N(2C)-C(5C)	1.323(4)	C(2B)-C(3B)-C(4B)	117.2(3)
N(2C)-C(4C)	1.340(4)	N(2B)-C(4B)-C(3B)	123.1(3)
N(3C)-C(6C)	1.335(3)	N(2B)-C(5B)-N(1B)	125.6(2)
N(3C)-C(7C)	1.344(4)	N(2B)-C(5B)-C(6B)	119.6(2)
N(4C)-C(9C)	1.350(4)	N(1B)-C(5B)-C(6B)	114.8(2)
N(4C)-C(6C)	1.357(4)	N(3B)-C(6B)-N(4B)	125.3(2)
C(2C)-C(3C)	1.375(4)	N(3B)-C(6B)-C(5B)	119.5(2)
C(3C)-C(4C)	1.386(4)	N(4B)-C(6B)-C(5B)	115.2(2)
C(5C)-C(6C)	1.483(4)	N(3B)-C(7B)-C(8B)	122.0(3)
C(7C)-C(8C)	1.392(4)	C(9B)-C(8B)-C(7B)	117.4(3)
C(8C)-C(9C)	1.375(4)	N(4B)-C(9B)-C(8B)	121.2(3)
Pt(4)-N(4D)	2.030(2)	N(4C)-Pt(3)-Cl(1C)	96.0(3)
Pt(4)-N(1D)	2.076(2)	N(4C)-Pt(3)-N(1C)	79.40(9)
Pt(4)-C(1D)	2.128(8)	Cl(1C)-Pt(3)-N(1C)	175.1(3)
Pt(4)-Cl(4B)	2.153(8)	N(4C)-Pt(3)-C(1C)	96.46(16)
Pt(4)-Cl(4)	2.2729(8)	Cl(1C)-Pt(3)-C(1C)	0.6(5)
N(1D)-C(2D)	1.346(4)	N(1C)-Pt(3)-C(1C)	175.70(16)
N(1D)-C(5D)	1.352(3)	N(4C)-Pt(3)-Cl(3)	175.35(7)
N(2D)-C(5D)	1.322(3)	Cl(1C)-Pt(3)-Cl(3)	88.6(3)
N(2D)-C(4D)	1.342(4)	N(1C)-Pt(3)-Cl(3)	96.03(6)
N(3D)-C(6D)	1.325(4)	C(1C)-Pt(3)-Cl(3)	88.12(15)
N(3D)-C(7D)	1.341(4)	C(2C)-N(1C)-C(5C)	117.0(2)
N(4D)-C(9D)	1.350(4)	C(2C)-N(1C)-Pt(3)	128.76(18)
N(4D)-C(6D)	1.356(3)	C(5C)-N(1C)-Pt(3)	114.19(18)
C(2D)-C(3D)	1.373(4)	C(5C)-N(2C)-C(4C)	116.7(2)
C(3D)-C(4D)	1.381(4)	C(6C)-N(3C)-C(7C)	116.6(2)
C(5D)-C(6D)	1.495(4)	C(9C)-N(4C)-C(6C)	116.9(2)
C(7D)-C(8D)	1.390(4)	C(9C)-N(4C)-Pt(3)	126.98(19)

C(8D)-C(9D)	1.375(4)	C(6C)-N(4C)-Pt(3)	116.08(18)
		N(1C)-C(2C)-C(3C)	121.7(3)
		C(2C)-C(3C)-C(4C)	116.9(3)
		N(2C)-C(4C)-C(3C)	122.3(3)
		N(2C)-C(5C)-N(1C)	125.4(2)
		N(2C)-C(5C)-C(6C)	119.9(2)
		N(1C)-C(5C)-C(6C)	114.7(2)
		N(3C)-C(6C)-N(4C)	125.6(2)
		N(3C)-C(6C)-C(5C)	119.1(2)
		N(4C)-C(6C)-C(5C)	115.3(2)
		N(3C)-C(7C)-C(8C)	121.7(3)
		C(7C)-C(8C)-C(9C)	118.1(3)
		N(4C)-C(9C)-C(8C)	121.0(3)
		N(4D)-Pt(4)-N(1D)	79.68(9)
		N(4D)-Pt(4)-C(1D)	94.0(2)
		N(1D)-Pt(4)-C(1D)	172.5(2)
		N(4D)-Pt(4)-Cl(4B)	99.3(2)
		N(1D)-Pt(4)-Cl(4B)	178.9(2)
		C(1D)-Pt(4)-Cl(4B)	6.7(3)
		N(4D)-Pt(4)-Cl(4)	175.89(7)
		N(1D)-Pt(4)-Cl(4)	96.36(7)
		C(1D)-Pt(4)-Cl(4)	90.0(2)
		Cl(4B)-Pt(4)-Cl(4)	84.68(19)
		C(2D)-N(1D)-C(5D)	116.8(2)
		C(2D)-N(1D)-Pt(4)	128.38(19)
		C(5D)-N(1D)-Pt(4)	114.81(17)
		C(5D)-N(2D)-C(4D)	116.3(2)
		C(6D)-N(3D)-C(7D)	116.5(2)
		C(9D)-N(4D)-C(6D)	117.0(2)
		C(9D)-N(4D)-Pt(4)	127.12(19)
		C(6D)-N(4D)-Pt(4)	115.84(17)
		N(1D)-C(2D)-C(3D)	121.4(3)
		C(2D)-C(3D)-C(4D)	117.3(3)
		N(2D)-C(4D)-C(3D)	122.5(3)
		N(2D)-C(5D)-N(1D)	125.8(2)
		N(2D)-C(5D)-C(6D)	119.8(2)
		N(1D)-C(5D)-C(6D)	114.5(2)
		N(3D)-C(6D)-N(4D)	125.8(2)
		N(3D)-C(6D)-C(5D)	119.1(2)
		N(4D)-C(6D)-C(5D)	115.1(2)
		N(3D)-C(7D)-C(8D)	122.0(3)
		C(9D)-C(8D)-C(7D)	117.9(3)

N(4D)-C(9D)-C(8D)	120.8(3)

Symmetry transformations used to generate equivalent atoms.

Table 21. Anisotropic displacement parameters ($Å^2$ x 10^4). The anisotropic displacement factor exponent takes the form: $-2\pi^2[h^2a^*2U^{11} + ... + 2 h k a^* b^* U^{12}]$

	U^{11}	U^{22}	U^{33}	U^{23}	U^{13}	U^{12}
Pt(1)	138(1)	116(1)	137(1)	-2(1)	51(1)	-6(1)
Cl(1)	302(4)	210(3)	328(4)	-5(3)	199(3)	-49(3)
N(1A)	148(10)	154(10)	145(10)	1(8)	68(8)	4(8)
N(2A)	215(12)	152(11)	182(11)	-27(9)	86(10)	-5(9)
N(3A)	196(11)	158(11)	172(11)	-27(8)	104(9)	-16(9)
N(4A)	139(10)	121(10)	122(10)	-6(8)	41(8)	8(8)
C(1A)	215(13)	103(11)	180(13)	19(9)	113(11)	34(9)
C(2A)	181(13)	195(13)	172(13)	12(10)	91(11)	4(10)
C(3A)	209(14)	245(14)	195(14)	-53(11)	102(11)	18(11)
C(4A)	253(15)	182(13)	200(14)	-59(11)	96(12)	-1(11)
C(5A)	151(12)	128(11)	147(12)	-16(9)	56(10)	-6(9)
C(6A)	129(11)	131(11)	121(11)	-11(9)	47(9)	9(9)
C(7A)	217(13)	185(13)	131(12)	-12(10)	67(10)	-4(10)
C(8A)	207(13)	167(12)	146(12)	-9(10)	100(10)	2(10)
C(9A)	228(14)	120(11)	150(12)	-20(9)	76(11)	14(10)
Pt(2)	152(1)	92(1)	125(1)	0(1)	49(1)	-5(1)
Cl(2)	268(4)	163(3)	231(3)	-19(3)	130(3)	6(3)
N(1B)	152(10)	114(9)	118(10)	-10(8)	58(8)	-13(8)
N(2B)	203(11)	118(10)	180(11)	-8(8)	91(9)	-29(8)
N(3B)	196(11)	147(10)	169(11)	-6(8)	91(9)	-9(9)
N(4B)	165(10)	104(9)	145(10)	-7(8)	63(8)	-9(8)
C(1B)	187(12)	115(11)	137(11)	19(9)	84(10)	-26(9)
C(2B)	192(13)	132(11)	158(12)	-17(9)	82(10)	-5(9)
C(3B)	211(14)	180(13)	171(13)	-8(10)	95(11)	-46(10)
C(4B)	235(14)	123(11)	200(13)	0(10)	91(11)	-34(10)
C(5B)	132(11)	135(11)	121(11)	-18(9)	38(9)	-3(9)
C(6B)	174(12)	117(11)	105(11)	-9(9)	41(9)	-20(9)
C(7B)	313(16)	128(12)	195(14)	-6(10)	151(12)	15(11)
C(8B)	320(17)	169(13)	264(16)	-13(11)	197(14)	-42(12)
C(9B)	281(15)	129(12)	190(13)	-4(10)	127(12)	-27(10)
Pt(3)	146(1)	117(1)	111(1)	5(1)	49(1)	9(1)
Cl(3)	287(4)	208(3)	224(3)	-28(3)	122(3)	10(3)
N(1C)	156(10)	120(9)	139(10)	-1(8)	63(8)	14(8)
N(2C)	247(12)	143(10)	166(11)	-1(8)	100(10)	-13(9)
N(3C)	219(12)	122(10)	144(11)	-12(8)	65(9)	7(8)
N(4C)	146(10)	126(10)	128(10)	11(8)	34(8)	-7(8)
C(1C)	65(14)	95(15)	122(16)	-41(11)	85(11)	-46(10)
C(2C)	185(12)	93(10)	179(13)	-16(9)	71(10)	-3(9)
C(3C)	219(14)	141(12)	196(13)	-17(10)	74(11)	-26(10)
C(4C)	240(14)	142(12)	183(13)	22(10)	101(11)	-1(10)
C(5C)	191(12)	124(11)	109(11)	-5(9)	48(10)	10(9)
C(6C)	167(12)	134(11)	117(11)	-19(9)	38(9)	9(9)

C(7C)	226(14)	147(12)	170(13)	-41(10)	44(11)	3(10)
C(8C)	259(15)	125(11)	185(13)	-16(10)	54(11)	-4(10)
C(9C)	204(13)	141(12)	176(13)	11(10)	30(11)	-22(10)
Pt(4)	136(1)	173(1)	130(1)	21(1)	53(1)	29(1)
Cl(4)	285(4)	290(4)	363(5)	45(3)	148(4)	6(3)
N(1D)	154(10)	132(10)	152(11)	11(8)	68(9)	10(8)
N(2D)	212(12)	145(10)	181(11)	-19(9)	90(10)	-6(9)
N(3D)	180(11)	148(10)	150(11)	6(8)	60(9)	-4(8)
N(4D)	151(10)	125(10)	116(10)	-6(8)	34(8)	18(8)
C(1D)	250(30)	150(30)	230(30)	50(20)	120(20)	93(19)
C(2D)	213(13)	121(11)	225(14)	11(10)	96(11)	-22(10)
C(3D)	257(15)	126(12)	239(15)	-23(10)	93(12)	-26(11)
C(4D)	258(15)	138(12)	195(14)	-33(10)	93(12)	5(10)
C(5D)	148(11)	101(10)	134(11)	9(9)	58(9)	15(9)
C(6D)	145(11)	118(11)	133(11)	3(9)	33(9)	4(9)
C(7D)	220(14)	141(12)	193(13)	2(10)	76(11)	-28(10)
C(8D)	228(14)	126(12)	200(14)	18(10)	50(11)	4(10)
C(9D)	204(13)	136(11)	165(13)	3(10)	51(10)	31(10)

3.5 (CCDC 775835)

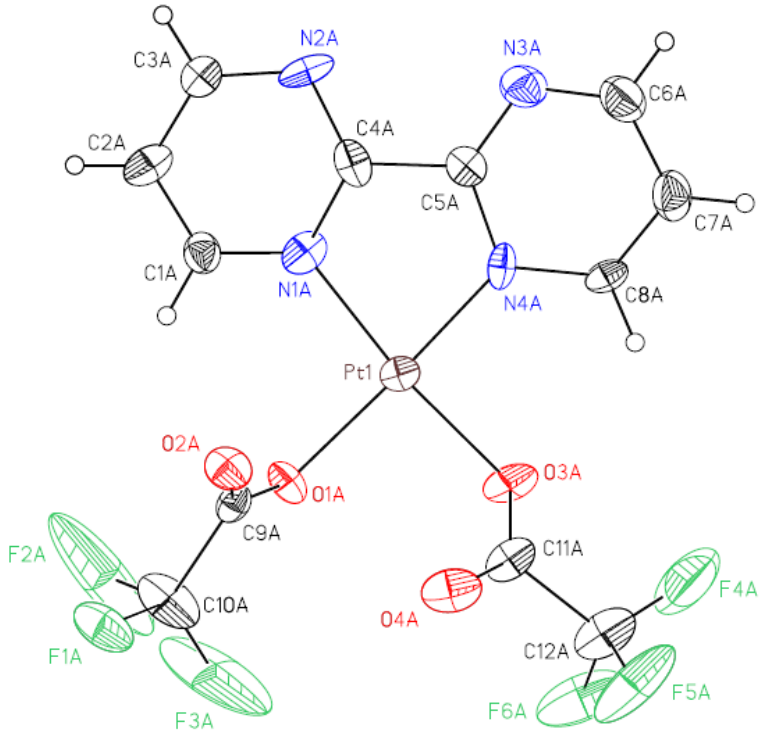

Special Refinement Details

Crystals were mounted on a glass fiber using Paratone oil then placed on the diffractometer under a nitrogen stream at 100K.

This crystal exhibits racemic twining and was refined as such. Additionally, the crystal appears to be undergoing a temperature induce phase transition and although the atomic positions suggest a higher symmetry space group, i.e., P 21/c, the required glide plane is only 90% present.

Refinement of F^2 against ALL reflections. The weighted R-factor (wR) and goodness of fit (S) are based on F^2, conventional R-factors (R) are based on F, with F set to zero for negative F^2. The threshold expression of $F^2 > 2\sigma (F^2)$ is used only for calculating R-factors(gt) etc. and is not relevant to the choice of reflections for refinement. R-factors based on F^2 are statistically about twice as large as those based on F, and R-factors based on ALL data will be even larger.

All esds (except the esd in the dihedral angle between two l.s. planes) are estimated using the full covariance matrix. The cell esds are taken into account individually in the estimation of esds in distances, angles and torsion angles; correlations between esds in cell parameters are only used when they are defined by crystal symmetry. An approximate (isotropic) treatment of cell esds is used for estimating esds involving l.s. planes.

Table 22. Atomic coordinates (x 10^4) and equivalent isotropic displacement parameters (Å^2 x 10^3). U(eq) is defined as the trace of the orthogonalized Uij tensor.

	x	y	z	Ueq
Pt(1)	6945(1)	4916(1)	2372(1)	21(1)
F(1A)	7652(11)	5746(5)	-2602(7)	48(2)
F(2A)	5326(12)	5747(10)	-2162(13)	195(10)
F(3A)	7020(30)	6423(6)	-1161(12)	193(9)
F(4A)	9338(17)	6571(7)	5277(11)	100(4)

F(5A)	10978(11)	6864(6)	4015(12)	85(4)
F(6A)	8477(12)	7206(5)	3545(12)	77(3)
O(1A)	6408(9)	5433(4)	541(7)	26(2)
O(2A)	8298(8)	4919(5)	-453(6)	32(2)
O(3A)	7848(10)	5746(5)	3395(9)	34(2)
O(4A)	9630(11)	6033(5)	2005(10)	40(2)
N(1A)	6045(11)	4044(5)	1595(10)	27(2)
N(2A)	5690(12)	2927(6)	2280(10)	33(2)
N(3A)	7220(13)	3311(6)	4992(10)	36(3)
N(4A)	7414(10)	4391(5)	4063(8)	21(2)
C(1A)	5347(14)	3909(6)	293(10)	28(2)
C(2A)	4814(15)	3295(7)	-82(14)	34(3)
C(3A)	5019(13)	2819(7)	916(11)	25(2)
C(4A)	6232(13)	3552(7)	2534(10)	25(2)
C(5A)	6993(13)	3726(6)	3971(10)	23(2)
C(6A)	7935(17)	3519(8)	6207(12)	40(3)
C(7A)	8335(16)	4199(7)	6501(12)	38(3)
C(8A)	8065(11)	4604(6)	5373(10)	23(2)
C(9A)	7269(12)	5313(6)	-366(10)	22(2)
C(10A)	6873(17)	5848(7)	-1531(13)	46(4)
C(11A)	8966(13)	6072(6)	2995(12)	28(2)
C(12A)	9526(17)	6689(8)	3961(16)	45(4)
Pt(2)	2947(1)	5084(1)	2443(1)	20(1)
F(1B)	-1163(12)	3160(6)	854(14)	106(5)
F(2B)	657(14)	3430(6)	-469(10)	78(3)
F(3B)	1254(14)	2809(6)	1221(12)	84(4)
F(4B)	2365(15)	3543(4)	5861(10)	89(4)
F(5B)	4562(11)	4016(6)	6739(11)	83(3)
F(6B)	2272(12)	4240(6)	7393(8)	61(3)
O(1B)	2070(10)	4241(4)	1416(9)	32(2)
O(2B)	229(11)	3986(5)	2874(9)	38(2)
O(3B)	3503(9)	4561(4)	4199(7)	22(2)
O(4B)	1583(8)	5088(5)	5298(6)	26(2)
N(1B)	2509(10)	5623(4)	686(8)	17(2)
N(2B)	2706(12)	6708(5)	-135(9)	30(2)
N(3B)	4242(13)	7045(6)	2613(10)	35(3)
N(4B)	3768(10)	5950(5)	3235(8)	17(2)
C(1B)	1797(13)	5406(7)	-529(10)	30(3)
C(2B)	1500(15)	5854(7)	-1705(14)	38(3)
C(3B)	2014(15)	6494(7)	-1422(11)	32(3)
C(4B)	2948(13)	6251(6)	858(10)	26(2)
C(5B)	3707(12)	6452(5)	2272(11)	22(2)
C(6B)	4841(15)	7190(7)	3867(12)	33(3)
C(7B)	4998(15)	6716(7)	4988(12)	31(3)
C(8B)	4459(12)	6079(6)	4544(10)	23(2)
C(9B)	914(15)	3884(6)	1839(13)	31(3)
C(10B)	439(16)	3314(7)	819(16)	43(3)
C(11B)	2563(12)	4637(6)	5181(10)	22(2)
C(12B)	3012(15)	4156(9)	6375(13)	51(4)

Table 23. Bond lengths [Å] and angles [°].

Pt(1)-N(4A)	1.941(8)	N(4A)-Pt(1)-N(1A)	81.0(4)
Pt(1)-N(1A)	2.011(11)	N(4A)-Pt(1)-O(3A)	92.0(4)
Pt(1)-O(3A)	2.027(9)	N(1A)-Pt(1)-O(3A)	172.8(4)
Pt(1)-O(1A)	2.049(6)	N(4A)-Pt(1)-O(1A)	177.5(4)
F(1A)-C(10A)	1.329(13)	N(1A)-Pt(1)-O(1A)	96.4(4)
F(2A)-C(10A)	1.326(18)	O(3A)-Pt(1)-O(1A)	90.5(3)
F(3A)-C(10A)	1.22(2)	C(9A)-O(1A)-Pt(1)	117.0(7)
F(4A)-C(12A)	1.337(16)	C(11A)-O(3A)-Pt(1)	120.9(7)
F(5A)-C(12A)	1.234(15)	C(1A)-N(1A)-C(4A)	118.5(11)
F(6A)-C(12A)	1.371(18)	C(1A)-N(1A)-Pt(1)	127.6(8)
O(1A)-C(9A)	1.245(11)	C(4A)-N(1A)-Pt(1)	113.8(8)
O(2A)-C(9A)	1.174(12)	C(4A)-N(2A)-C(3A)	113.2(10)
O(3A)-C(11A)	1.246(14)	C(5A)-N(3A)-C(6A)	118.3(13)
O(4A)-C(11A)	1.188(13)	C(8A)-N(4A)-C(5A)	114.8(9)
N(1A)-C(1A)	1.326(13)	C(8A)-N(4A)-Pt(1)	127.4(8)
N(1A)-C(4A)	1.343(15)	C(5A)-N(4A)-Pt(1)	117.8(6)
N(2A)-C(4A)	1.349(16)	N(1A)-C(1A)-C(2A)	121.0(11)
N(2A)-C(3A)	1.365(13)	C(1A)-C(2A)-C(3A)	117.9(12)
N(3A)-C(5A)	1.291(14)	N(2A)-C(3A)-C(2A)	124.1(13)
N(3A)-C(6A)	1.296(15)	N(2A)-C(4A)-N(1A)	125.1(10)
N(4A)-C(8A)	1.365(12)	N(2A)-C(4A)-C(5A)	118.1(10)
N(4A)-C(5A)	1.389(15)	N(1A)-C(4A)-C(5A)	116.7(11)
C(1A)-C(2A)	1.348(18)	N(3A)-C(5A)-N(4A)	125.5(10)
C(2A)-C(3A)	1.358(17)	N(3A)-C(5A)-C(4A)	123.8(12)
C(4A)-C(5A)	1.472(13)	N(4A)-C(5A)-C(4A)	110.7(9)
C(6A)-C(7A)	1.43(2)	N(3A)-C(6A)-C(7A)	123.1(12)
C(7A)-C(8A)	1.357(16)	C(8A)-C(7A)-C(6A)	114.8(11)
C(9A)-C(10A)	1.562(16)	N(4A)-C(8A)-C(7A)	123.2(12)
C(11A)-C(12A)	1.583(17)	O(2A)-C(9A)-O(1A)	133.3(11)
Pt(2)-N(4B)	1.987(10)	O(2A)-C(9A)-C(10A)	118.8(9)
Pt(2)-N(1B)	2.008(8)	O(1A)-C(9A)-C(10A)	107.8(9)
Pt(2)-O(3B)	1.996(7)	F(3A)-C(10A)-F(2A)	108.9(14)
Pt(2)-O(1B)	2.046(8)	F(3A)-C(10A)-F(1A)	110.1(14)
F(1B)-C(10B)	1.355(15)	F(2A)-C(10A)-F(1A)	99.3(12)
F(2B)-C(10B)	1.318(15)	F(3A)-C(10A)-C(9A)	116.8(12)
F(3B)-C(10B)	1.246(17)	F(2A)-C(10A)-C(9A)	107.0(13)
F(4B)-C(12B)	1.41(2)	F(1A)-C(10A)-C(9A)	113.2(10)
F(5B)-C(12B)	1.290(14)	O(4A)-C(11A)-O(3A)	133.0(12)
F(6B)-C(12B)	1.259(14)	O(4A)-C(11A)-C(12A)	114.1(11)
O(1B)-C(9B)	1.313(14)	O(3A)-C(11A)-C(12A)	112.7(10)
O(2B)-C(9B)	1.251(13)	F(5A)-C(12A)-F(6A)	110.1(15)
O(3B)-C(11B)	1.336(12)	F(5A)-C(12A)-F(4A)	106.2(13)
O(4B)-C(11B)	1.235(13)	F(6A)-C(12A)-F(4A)	104.5(12)
N(1B)-C(1B)	1.301(12)	F(5A)-C(12A)-C(11A)	115.5(11)
N(1B)-C(4B)	1.325(15)	F(6A)-C(12A)-C(11A)	108.9(12)
N(2B)-C(3B)	1.354(14)	F(4A)-C(12A)-C(11A)	111.0(13)

N(2B)-C(4B)	1.328(14)	N(4B)-Pt(2)-N(1B)	81.3(3)
N(3B)-C(6B)	1.269(14)	N(4B)-Pt(2)-O(3B)	97.2(3)
N(3B)-C(5B)	1.303(16)	N(1B)-Pt(2)-O(3B)	177.1(3)
N(4B)-C(8B)	1.328(12)	N(4B)-Pt(2)-O(1B)	173.7(4)
N(4B)-C(5B)	1.377(13)	N(1B)-Pt(2)-O(1B)	92.4(3)
C(1B)-C(2B)	1.448(18)	O(3B)-Pt(2)-O(1B)	89.1(3)
C(2B)-C(3B)	1.377(19)	C(9B)-O(1B)-Pt(2)	121.2(7)
C(4B)-C(5B)	1.467(13)	C(11B)-O(3B)-Pt(2)	118.5(6)
C(6B)-C(7B)	1.443(17)	C(1B)-N(1B)-C(4B)	120.5(9)
C(7B)-C(8B)	1.407(18)	C(1B)-N(1B)-Pt(2)	125.3(8)
C(9B)-C(10B)	1.529(18)	C(4B)-N(1B)-Pt(2)	114.2(6)
C(11B)-C(12B)	1.511(15)	C(3B)-N(2B)-C(4B)	115.8(11)
		C(6B)-N(3B)-C(5B)	121.0(11)
		C(8B)-N(4B)-C(5B)	117.9(10)
		C(8B)-N(4B)-Pt(2)	127.2(7)
		C(5B)-N(4B)-Pt(2)	114.7(7)
		N(1B)-C(1B)-C(2B)	119.7(13)
		C(3B)-C(2B)-C(1B)	115.3(12)
		N(2B)-C(3B)-C(2B)	123.5(11)
		N(2B)-C(4B)-N(1B)	125.1(10)
		N(2B)-C(4B)-C(5B)	118.4(11)
		N(1B)-C(4B)-C(5B)	116.5(9)
		N(3B)-C(5B)-N(4B)	122.4(10)
		N(3B)-C(5B)-C(4B)	124.3(10)
		N(4B)-C(5B)-C(4B)	113.2(10)
		N(3B)-C(6B)-C(7B)	122.9(13)
		C(8B)-C(7B)-C(6B)	113.3(10)
		N(4B)-C(8B)-C(7B)	122.3(10)
		O(2B)-C(9B)-O(1B)	127.5(12)
		O(2B)-C(9B)-C(10B)	123.2(11)
		O(1B)-C(9B)-C(10B)	109.2(10)
		F(3B)-C(10B)-F(2B)	107.1(13)
		F(3B)-C(10B)-F(1B)	105.8(13)
		F(2B)-C(10B)-F(1B)	110.8(14)
		F(3B)-C(10B)-C(9B)	110.7(13)
		F(2B)-C(10B)-C(9B)	114.9(12)
		F(1B)-C(10B)-C(9B)	107.2(11)
		O(4B)-C(11B)-O(3B)	128.0(10)
		O(4B)-C(11B)-C(12B)	118.8(10)
		O(3B)-C(11B)-C(12B)	112.5(10)
		F(6B)-C(12B)-F(5B)	113.5(11)
		F(6B)-C(12B)-F(4B)	101.3(12)
		F(5B)-C(12B)-F(4B)	101.3(14)
		F(6B)-C(12B)-C(11B)	115.6(13)
		F(5B)-C(12B)-C(11B)	116.8(10)
		F(4B)-C(12B)-C(11B)	105.5(11)

Table 24. Anisotropic displacement parameters ($Å^2$ x 10^4). The anisotropic displacement factor exponent takes the form: $-2\pi^2[h^2a^*2U^{11} + ... + 2 h k a^* b^* U^{12}]$.

	U^{11}	U^{22}	U^{33}	U^{23}	U^{13}	U^{12}
Pt(1)	159(2)	207(2)	274(2)	-17(1)	97(1)	13(1)
F(1A)	560(50)	510(70)	440(40)	180(30)	280(40)	150(50)
F(2A)	370(50)	4300(300)	1160(100)	1770(140)	100(60)	30(90)
F(3A)	4400(300)	600(80)	1190(100)	560(70)	1550(140)	1360(120)
F(4A)	1420(110)	820(90)	860(80)	-490(60)	450(70)	-610(80)
F(5A)	330(50)	840(100)	1510(100)	-750(80)	470(60)	-350(50)
F(6A)	580(50)	270(60)	1530(90)	-250(50)	400(60)	90(40)
O(1A)	220(40)	350(50)	200(30)	70(30)	70(30)	60(30)
O(2A)	350(40)	270(50)	360(30)	30(30)	90(30)	130(40)
O(3A)	240(40)	320(50)	530(50)	-80(40)	260(40)	-150(40)
O(4A)	270(40)	360(70)	620(60)	-10(40)	250(40)	-20(40)
N(1A)	130(40)	240(50)	420(50)	-40(40)	-20(40)	70(30)
N(2A)	260(50)	150(60)	580(60)	-40(40)	110(50)	-60(40)
N(3A)	360(60)	300(70)	400(50)	70(40)	-10(40)	40(50)
N(4A)	100(30)	350(60)	180(40)	-90(30)	10(30)	20(40)
C(1A)	320(60)	270(70)	240(50)	-10(40)	20(40)	50(50)
C(2A)	290(60)	240(70)	490(70)	-70(50)	50(50)	-10(50)
C(3A)	200(50)	260(70)	310(50)	-40(40)	70(40)	30(50)
C(4A)	120(40)	430(80)	210(40)	20(40)	80(30)	60(50)
C(5A)	170(50)	270(60)	270(50)	10(40)	80(40)	70(40)
C(6A)	410(70)	460(90)	330(60)	80(50)	60(50)	-50(60)
C(7A)	310(60)	520(90)	280(60)	0(50)	-10(50)	-80(60)
C(8A)	150(40)	210(60)	350(50)	-30(40)	80(40)	-70(40)
C(9A)	180(40)	250(50)	250(50)	-60(30)	50(40)	-50(40)
C(10A)	480(80)	460(90)	500(70)	190(60)	220(60)	410(70)
C(11A)	160(50)	260(70)	470(60)	-120(50)	150(40)	30(40)
C(12A)	310(70)	380(100)	710(90)	-200(60)	280(60)	-40(60)
Pt(2)	163(2)	183(2)	289(2)	0(1)	100(1)	10(1)
F(1B)	410(50)	580(90)	2320(140)	-580(80)	610(70)	-260(50)
F(2B)	980(80)	690(80)	730(60)	-280(50)	330(60)	-410(70)
F(3B)	640(60)	350(60)	1460(90)	-140(60)	-60(60)	160(50)
F(4B)	1510(100)	220(40)	920(70)	140(40)	110(60)	-350(60)
F(5B)	370(40)	1120(80)	1070(70)	620(60)	300(50)	470(50)
F(6B)	680(60)	780(90)	440(50)	200(40)	320(40)	270(60)
O(1B)	260(40)	100(40)	640(50)	-130(30)	220(40)	-50(30)
O(2B)	320(50)	420(70)	450(50)	-60(40)	180(40)	-40(40)
O(3B)	230(30)	180(40)	250(30)	-20(30)	100(30)	20(30)
O(4B)	230(30)	230(40)	330(30)	20(30)	70(30)	50(40)
N(1B)	180(40)	160(40)	190(40)	30(30)	120(30)	30(30)
N(2B)	310(50)	260(60)	370(50)	40(40)	170(40)	-30(40)
N(3B)	370(60)	230(70)	500(60)	20(40)	210(50)	40(50)
N(4B)	140(30)	190(40)	230(30)	20(30)	150(30)	-30(30)
C(1B)	220(50)	480(90)	180(50)	-110(40)	10(40)	60(50)
C(2B)	230(50)	300(70)	640(80)	-70(60)	190(60)	0(50)
C(3B)	390(60)	270(70)	290(50)	70(40)	70(40)	30(50)
C(4B)	230(50)	330(70)	210(50)	20(40)	70(40)	-30(50)
C(5B)	170(50)	120(50)	420(50)	40(40)	120(40)	0(40)
C(6B)	330(60)	210(70)	470(70)	-40(50)	110(50)	10(50)

C(7B)	320(60)	350(80)	310(50)	-10(50)	160(40)	-40(50)
C(8B)	180(40)	220(60)	320(50)	80(40)	90(40)	20(40)
C(9B)	240(50)	200(60)	520(70)	10(50)	160(50)	-20(50)
C(10B)	330(70)	240(80)	830(100)	-60(60)	400(70)	-110(60)
C(11B)	140(40)	210(50)	280(50)	0(40)	-20(40)	-30(40)
C(12B)	240(60)	910(130)	420(70)	310(70)	180(50)	90(70)

A.1 (CCDC 708866)

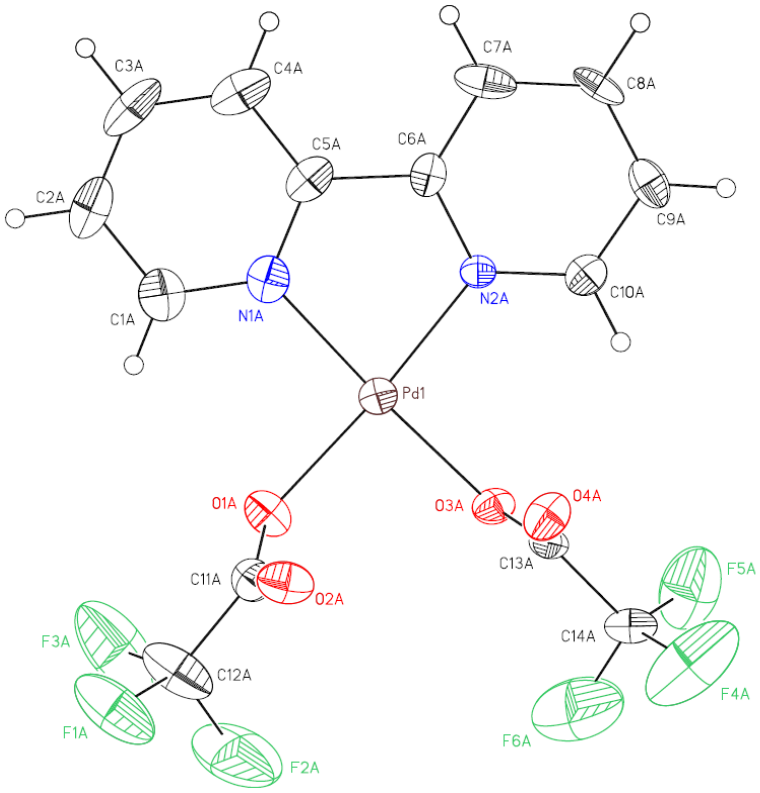

Special Refinement Details

Crystals were mounted on a glass fiber using Paratone oil then placed on the diffractometer under a nitrogen stream at 100K.

This crystal was refined as a racemic twin using TWIN and BASF in SHELXL.

Refinement of F^2 against ALL reflections. The weighted R-factor (wR) and goodness of fit (S) are based on F^2, conventional R-factors (R) are based on F, with F set to zero for negative F^2. The threshold expression of $F^2 > 2\sigma (F^2)$ is used only for calculating R-factors(gt) etc. and is not relevant to the choice of reflections for refinement. R-factors based on F^2 are statistically about twice as large as those based on F, and R-factors based on ALL data will be even larger.

All esds (except the esd in the dihedral angle between two l.s. planes) are estimated using the full covariance matrix. The cell esds are taken into account individually in the estimation of esds in distances, angles and torsion angles; correlations between esds in cell parameters are only used when they are defined by crystal symmetry. An approximate (isotropic) treatment of cell esds is used for estimating esds involving l.s. planes.

Table 25. Atomic coordinates (x 10^4) and equivalent isotropic displacement parameters ($Å^2$ x 10^3). U(eq) is defined as the trace of the orthogonalized Uij tensor.

	x	y	z	Ueq
Pd(1)	429(1)	9363(1)	4850(1)	21(1)
F(1A)	457(1)	7507(4)	7288(2)	75(1)
F(2A)	-109(1)	7176(4)	6668(2)	101(2)
F(3A)	-36(1)	8595(3)	7106(2)	103(2)
F(4A)	135(1)	5905(3)	3684(3)	112(2)

F(5A)	-312(1)	7090(3)	3484(3)	82(1)
F(6A)	-305(1)	6417(3)	4489(3)	109(2)
O(1A)	254(1)	8910(2)	5830(2)	30(1)
O(2A)	746(1)	7675(2)	5922(2)	36(1)
O(3A)	88(1)	8228(2)	4450(2)	24(1)
O(4A)	674(1)	7291(2)	4167(2)	32(1)
N(1A)	734(1)	10578(3)	5198(2)	26(1)
N(2A)	599(1)	9930(2)	3913(2)	18(1)
C(1A)	771(2)	10830(4)	5881(3)	35(1)
C(2A)	998(2)	11689(4)	6073(3)	40(1)
C(3A)	1178(2)	12259(3)	5553(4)	44(2)
C(4A)	1132(1)	12008(3)	4861(4)	38(1)
C(5A)	909(1)	11150(3)	4680(3)	27(1)
C(6A)	834(2)	10782(3)	3953(3)	21(1)
C(7A)	993(1)	11249(3)	3357(3)	34(1)
C(8A)	898(1)	10839(3)	2688(3)	29(1)
C(9A)	654(1)	9987(3)	2643(3)	29(1)
C(10A)	507(1)	9552(3)	3271(3)	25(1)
C(11A)	433(1)	8167(3)	6108(3)	28(1)
C(12A)	199(2)	7876(4)	6800(3)	51(2)
C(13A)	281(1)	7454(3)	4223(3)	23(1)
C(14A)	-52(2)	6701(3)	3948(3)	29(1)
Pd(2)	2972(1)	5606(1)	8467(1)	20(1)
F(1B)	3073(1)	7403(3)	5989(2)	61(1)
F(2B)	2459(1)	7672(2)	6521(2)	55(1)
F(3B)	2608(1)	6223(2)	6139(2)	54(1)
F(4B)	2666(1)	9084(2)	9541(2)	70(1)
F(5B)	2249(1)	7916(3)	9929(3)	82(1)
F(6B)	2184(1)	8468(3)	8841(2)	89(1)
O(1B)	2826(1)	6013(2)	7463(2)	27(1)
O(2B)	3265(1)	7367(3)	7422(2)	36(1)
O(3B)	2621(1)	6758(2)	8827(2)	24(1)
O(4B)	3199(1)	7608(2)	9248(2)	31(1)
N(1B)	3279(1)	4396(2)	8153(2)	23(1)
N(2B)	3106(1)	5047(3)	9421(2)	22(1)
C(1B)	3347(1)	4133(4)	7473(3)	30(1)
C(2B)	3566(1)	3268(3)	7303(3)	35(1)
C(3B)	3713(1)	2661(3)	7846(3)	36(1)
C(4B)	3642(1)	2923(3)	8540(3)	30(1)
C(5B)	3419(1)	3812(3)	8690(2)	23(1)
C(6B)	3333(1)	4157(3)	9394(3)	23(1)
C(7B)	3467(1)	3697(3)	10029(3)	26(1)
C(8B)	3362(1)	4126(4)	10671(3)	34(1)
C(9B)	3125(1)	5005(4)	10681(3)	31(1)
C(10B)	3006(1)	5466(3)	10050(2)	25(1)
C(11B)	2992(1)	6791(3)	7178(3)	28(1)
C(12B)	2785(2)	7024(4)	6461(3)	41(1)
C(13B)	2812(1)	7479(3)	9124(2)	24(1)
C(14B)	2486(2)	8254(3)	9342(3)	32(1)

Pd(3)	2117(1)	4256(1)	8431(1)	21(1)
F(1C)	2134(1)	2044(4)	6133(3)	134(3)
F(2C)	2598(2)	1770(4)	6932(3)	167(3)
F(3C)	2671(1)	2957(4)	6341(2)	117(2)
F(4C)	2319(1)	891(4)	9642(4)	169(3)
F(5C)	2793(1)	1984(3)	9898(3)	107(2)
F(6C)	2805(2)	1214(4)	8917(3)	144(2)
O(1C)	2328(1)	3600(2)	7535(2)	33(1)
O(2C)	1704(1)	2807(2)	7241(2)	41(1)
O(3C)	2418(1)	3197(2)	8995(2)	27(1)
O(4C)	1882(1)	2115(2)	8849(2)	50(1)
N(1C)	1835(1)	5403(3)	7956(2)	20(1)
N(2C)	1924(1)	4981(3)	9290(2)	22(1)
C(1C)	1828(1)	5568(3)	7259(3)	28(1)
C(2C)	1635(1)	6394(3)	6970(3)	32(1)
C(3C)	1448(1)	7075(3)	7422(3)	36(1)
C(4C)	1456(1)	6921(3)	8148(3)	27(1)
C(5C)	1655(1)	6074(3)	8413(3)	25(1)
C(6C)	1691(1)	5835(3)	9147(3)	21(1)
C(7C)	1510(1)	6361(3)	9728(3)	27(1)
C(8C)	1576(1)	6064(4)	10397(3)	31(1)
C(9C)	1823(1)	5210(3)	10533(3)	31(1)
C(10C)	1987(1)	4678(3)	9968(2)	22(1)
C(11C)	2096(1)	2998(3)	7186(3)	28(1)
C(12C)	2352(2)	2475(4)	6598(4)	59(2)
C(13C)	2244(1)	2360(3)	9035(3)	27(1)
C(14C)	2521(2)	1611(3)	9394(3)	40(1)
Pd(4)	4618(1)	4036(1)	9807(1)	23(1)
F(1D)	4707(1)	940(3)	8171(3)	101(1)
F(2D)	5214(3)	997(8)	8876(6)	342(8)
F(3D)	5172(3)	2012(6)	8008(9)	402(11)
F(4D)	4644(2)	1993(5)	12121(3)	156(3)
F(5D)	5210(1)	1935(3)	11472(2)	72(1)
F(6D)	4680(2)	1043(4)	11270(5)	204(4)
O(1D)	4877(1)	3045(2)	9133(2)	31(1)
O(2D)	4399(1)	1864(2)	9430(2)	51(1)
O(3D)	4837(1)	3191(2)	10612(2)	34(1)
O(4D)	4163(1)	2735(2)	10993(2)	41(1)
N(1D)	4421(1)	4913(3)	9024(2)	18(1)
N(2D)	4378(1)	5143(3)	10385(2)	28(1)
C(1D)	4479(1)	4729(3)	8322(3)	25(1)
C(2D)	4324(1)	5362(3)	7811(3)	24(1)
C(3D)	4112(1)	6207(3)	8004(3)	26(1)
C(4D)	4054(1)	6405(3)	8726(2)	24(1)
C(5D)	4218(1)	5737(3)	9228(3)	21(1)
C(6D)	4192(1)	5892(3)	10002(2)	22(1)
C(7D)	4003(1)	6694(3)	10336(3)	33(1)
C(8D)	4022(2)	6749(4)	11062(3)	41(1)
C(9D)	4208(1)	6018(4)	11452(3)	42(1)

C(10D)	4381(1)	5207(4)	11096(3)	34(1)
C(11D)	4716(2)	2192(3)	9120(3)	37(1)
C(12D)	4960(2)	1514(4)	8614(5)	67(2)
C(13D)	4560(1)	2695(3)	10970(3)	34(1)
C(14D)	4788(2)	1944(5)	11464(3)	56(2)
O(1)	1244(1)	10431(2)	1035(2)	50(1)
C(1)	1091(2)	9940(3)	567(3)	44(1)
C(2)	1375(2)	9491(5)	4(4)	88(2)
C(3)	609(2)	9751(4)	501(3)	65(2)
O(2)	1181(1)	5578(3)	2041(2)	48(1)
C(4)	1291(2)	5112(4)	2563(3)	41(1)
C(5)	979(2)	4524(6)	2988(4)	97(3)
C(6)	1748(2)	4997(5)	2756(3)	74(2)
O(3)	3764(1)	9319(3)	1296(2)	42(1)
C(7)	3803(2)	9707(3)	717(3)	35(1)
C(8)	3493(2)	10451(4)	447(3)	53(1)
C(9)	4174(2)	9459(4)	214(3)	59(2)
O(4)	3586(1)	4543(3)	2317(2)	46(1)
C(10)	3419(2)	5060(3)	2752(3)	37(1)
C(11)	2934(2)	5341(4)	2722(3)	56(2)
C(12)	3667(2)	5465(5)	3360(3)	65(2)

Table 26. Bond lengths [Å] and angles [°].

Pd(1)-N(1A)	2.004(4)	N(1A)-Pd(1)-N(2A)	81.41(16)
Pd(1)-N(2A)	1.993(4)	N(1A)-Pd(1)-O(3A)	174.63(13)
Pd(1)-O(3A)	2.007(3)	N(2A)-Pd(1)-O(3A)	95.63(14)
Pd(1)-O(1A)	2.016(3)	N(1A)-Pd(1)-O(1A)	94.30(16)
Pd(1)-Pd(1)#1	3.1340(5)	N(2A)-Pd(1)-O(1A)	175.00(13)
F(1A)-C(12A)	1.308(6)	O(3A)-Pd(1)-O(1A)	88.43(13)
F(2A)-C(12A)	1.359(7)	N(1A)-Pd(1)-Pd(1)#1	85.87(9)
F(3A)-C(12A)	1.342(6)	N(2A)-Pd(1)-Pd(1)#1	90.06(9)
F(4A)-C(14A)	1.321(6)	O(3A)-Pd(1)-Pd(1)#1	89.65(8)
F(5A)-C(14A)	1.292(6)	O(1A)-Pd(1)-Pd(1)#1	87.06(8)
F(6A)-C(14A)	1.332(6)	C(11A)-O(1A)-Pd(1)	120.7(3)
O(1A)-C(11A)	1.261(5)	C(13A)-O(3A)-Pd(1)	121.3(3)
O(2A)-C(11A)	1.215(5)	C(1A)-N(1A)-C(5A)	120.7(4)
O(3A)-C(13A)	1.280(5)	C(1A)-N(1A)-Pd(1)	124.4(4)
O(4A)-C(13A)	1.217(5)	C(5A)-N(1A)-Pd(1)	114.9(3)
N(1A)-C(1A)	1.335(7)	C(10A)-N(2A)-C(6A)	118.9(4)
N(1A)-C(5A)	1.356(6)	C(10A)-N(2A)-Pd(1)	126.5(3)
N(2A)-C(10A)	1.343(6)	C(6A)-N(2A)-Pd(1)	114.5(3)
N(2A)-C(6A)	1.365(6)	N(1A)-C(1A)-C(2A)	120.2(5)
C(1A)-C(2A)	1.404(7)	C(3A)-C(2A)-C(1A)	119.1(5)
C(2A)-C(3A)	1.363(8)	C(2A)-C(3A)-C(4A)	120.3(5)
C(3A)-C(4A)	1.354(8)	C(3A)-C(4A)-C(5A)	119.8(5)
C(4A)-C(5A)	1.392(6)	N(1A)-C(5A)-C(4A)	119.8(5)
C(5A)-C(6A)	1.475(7)	N(1A)-C(5A)-C(6A)	114.3(4)
C(6A)-C(7A)	1.376(7)	C(4A)-C(5A)-C(6A)	125.9(5)
C(7A)-C(8A)	1.406(7)	N(2A)-C(6A)-C(7A)	122.0(5)

C(8A)-C(9A)	1.379(6)	N(2A)-C(6A)-C(5A)	114.8(4)
C(9A)-C(10A)	1.395(6)	C(7A)-C(6A)-C(5A)	123.1(4)
C(11A)-C(12A)	1.535(7)	C(6A)-C(7A)-C(8A)	118.4(4)
C(13A)-C(14A)	1.531(6)	C(9A)-C(8A)-C(7A)	119.8(5)
Pd(2)-N(1B)	1.981(4)	C(8A)-C(9A)-C(10A)	118.6(5)
Pd(2)-N(2B)	1.992(4)	N(2A)-C(10A)-C(9A)	122.2(4)
Pd(2)-O(3B)	2.013(3)	O(2A)-C(11A)-O(1A)	131.2(5)
Pd(2)-O(1B)	2.018(3)	O(2A)-C(11A)-C(12A)	117.7(4)
Pd(2)-Pd(3)	3.1814(4)	O(1A)-C(11A)-C(12A)	111.1(4)
F(1B)-C(12B)	1.349(5)	F(1A)-C(12A)-F(3A)	107.3(5)
F(2B)-C(12B)	1.332(5)	F(1A)-C(12A)-F(2A)	105.9(5)
F(3B)-C(12B)	1.359(6)	F(3A)-C(12A)-F(2A)	102.9(4)
F(4B)-C(14B)	1.309(5)	F(1A)-C(12A)-C(11A)	114.7(4)
F(5B)-C(14B)	1.398(6)	F(3A)-C(12A)-C(11A)	115.0(4)
F(6B)-C(14B)	1.349(6)	F(2A)-C(12A)-C(11A)	110.1(5)
O(1B)-C(11B)	1.289(5)	O(4A)-C(13A)-O(3A)	129.0(4)
O(2B)-C(11B)	1.229(5)	O(4A)-C(13A)-C(14A)	119.9(4)
O(3B)-C(13B)	1.267(5)	O(3A)-C(13A)-C(14A)	111.0(4)
O(4B)-C(13B)	1.215(5)	F(5A)-C(14A)-F(4A)	110.2(5)
N(1B)-C(1B)	1.346(6)	F(5A)-C(14A)-F(6A)	106.4(4)
N(1B)-C(5B)	1.354(6)	F(4A)-C(14A)-F(6A)	107.4(4)
N(2B)-C(10B)	1.350(6)	F(5A)-C(14A)-C(13A)	111.1(4)
N(2B)-C(6B)	1.395(5)	F(4A)-C(14A)-C(13A)	112.9(4)
C(1B)-C(2B)	1.390(6)	F(6A)-C(14A)-C(13A)	108.6(5)
C(2B)-C(3B)	1.388(7)	N(1B)-Pd(2)-N(2B)	81.66(16)
C(3B)-C(4B)	1.371(7)	N(1B)-Pd(2)-O(3B)	175.02(13)
C(4B)-C(5B)	1.414(5)	N(2B)-Pd(2)-O(3B)	95.84(14)
C(5B)-C(6B)	1.430(6)	N(1B)-Pd(2)-O(1B)	93.07(15)
C(6B)-C(7B)	1.407(6)	N(2B)-Pd(2)-O(1B)	173.51(14)
C(7B)-C(8B)	1.379(7)	O(3B)-Pd(2)-O(1B)	89.13(12)
C(8B)-C(9B)	1.397(7)	N(1B)-Pd(2)-Pd(3)	84.25(9)
C(9B)-C(10B)	1.389(6)	N(2B)-Pd(2)-Pd(3)	88.05(9)
C(11B)-C(12B)	1.523(7)	O(3B)-Pd(2)-Pd(3)	91.38(7)
C(13B)-C(14B)	1.503(6)	O(1B)-Pd(2)-Pd(3)	87.65(8)
Pd(3)-N(2C)	1.981(4)	C(11B)-O(1B)-Pd(2)	121.8(3)
Pd(3)-N(1C)	1.992(4)	C(13B)-O(3B)-Pd(2)	120.6(2)
Pd(3)-O(3C)	2.009(3)	C(1B)-N(1B)-C(5B)	120.4(4)
Pd(3)-O(1C)	2.013(3)	C(1B)-N(1B)-Pd(2)	125.1(3)
F(1C)-C(12C)	1.245(6)	C(5B)-N(1B)-Pd(2)	114.4(3)
F(2C)-C(12C)	1.369(8)	C(10B)-N(2B)-C(6B)	120.7(4)
F(3C)-C(12C)	1.267(6)	C(10B)-N(2B)-Pd(2)	125.7(3)
F(4C)-C(14C)	1.248(6)	C(6B)-N(2B)-Pd(2)	113.6(3)
F(5C)-C(14C)	1.357(7)	N(1B)-C(1B)-C(2B)	121.1(5)
F(6C)-C(14C)	1.357(7)	C(3B)-C(2B)-C(1B)	119.2(5)
O(1C)-C(11C)	1.265(5)	C(4B)-C(3B)-C(2B)	119.8(4)
O(2C)-C(11C)	1.223(5)	C(3B)-C(4B)-C(5B)	119.2(5)
O(3C)-C(13C)	1.258(5)	N(1B)-C(5B)-C(4B)	120.3(4)
O(4C)-C(13C)	1.200(5)	N(1B)-C(5B)-C(6B)	116.2(4)
N(1C)-C(1C)	1.331(6)	C(4B)-C(5B)-C(6B)	123.6(4)

N(1C)-C(5C)	1.367(5)	N(2B)-C(6B)-C(7B)	119.9(4)
N(2C)-C(10C)	1.354(6)	N(2B)-C(6B)-C(5B)	114.1(4)
N(2C)-C(6C)	1.387(5)	C(7B)-C(6B)-C(5B)	126.0(4)
C(1C)-C(2C)	1.379(6)	C(8B)-C(7B)-C(6B)	119.3(4)
C(2C)-C(3C)	1.381(7)	C(7B)-C(8B)-C(9B)	119.5(5)
C(3C)-C(4C)	1.382(7)	C(10B)-C(9B)-C(8B)	120.6(5)
C(4C)-C(5C)	1.394(6)	N(2B)-C(10B)-C(9B)	120.0(4)
C(5C)-C(6C)	1.424(7)	O(2B)-C(11B)-O(1B)	129.3(5)
C(6C)-C(7C)	1.419(7)	O(2B)-C(11B)-C(12B)	118.4(4)
C(7C)-C(8C)	1.338(7)	O(1B)-C(11B)-C(12B)	112.1(4)
C(8C)-C(9C)	1.408(7)	F(2B)-C(12B)-F(1B)	106.7(4)
C(9C)-C(10C)	1.379(7)	F(2B)-C(12B)-F(3B)	105.9(4)
C(11C)-C(12C)	1.529(7)	F(1B)-C(12B)-F(3B)	105.7(4)
C(13C)-C(14C)	1.485(7)	F(2B)-C(12B)-C(11B)	111.7(4)
Pd(4)-N(1D)	1.988(4)	F(1B)-C(12B)-C(11B)	113.3(4)
Pd(4)-N(2D)	1.996(4)	F(3B)-C(12B)-C(11B)	113.0(4)
Pd(4)-O(3D)	2.014(3)	O(4B)-C(13B)-O(3B)	129.8(4)
Pd(4)-O(1D)	2.011(3)	O(4B)-C(13B)-C(14B)	118.9(4)
F(1D)-C(12D)	1.377(7)	O(3B)-C(13B)-C(14B)	111.3(4)
F(2D)-C(12D)	1.154(9)	F(4B)-C(14B)-F(6B)	107.4(4)
F(3D)-C(12D)	1.475(14)	F(4B)-C(14B)-F(5B)	105.8(4)
F(4D)-C(14D)	1.313(7)	F(6B)-C(14B)-F(5B)	105.7(4)
F(5D)-C(14D)	1.282(5)	F(4B)-C(14B)-C(13B)	114.1(4)
F(6D)-C(14D)	1.321(8)	F(6B)-C(14B)-C(13B)	114.1(4)
O(1D)-C(11D)	1.260(5)	F(5B)-C(14B)-C(13B)	109.0(4)
O(2D)-C(11D)	1.211(6)	N(2C)-Pd(3)-N(1C)	81.32(16)
O(3D)-C(13D)	1.272(5)	N(2C)-Pd(3)-O(3C)	93.50(14)
O(4D)-C(13D)	1.207(5)	N(1C)-Pd(3)-O(3C)	173.96(14)
N(1D)-C(5D)	1.337(5)	N(2C)-Pd(3)-O(1C)	176.44(14)
N(1D)-C(1D)	1.357(6)	N(1C)-Pd(3)-O(1C)	96.21(14)
N(2D)-C(10D)	1.341(6)	O(3C)-Pd(3)-O(1C)	88.82(14)
N(2D)-C(6D)	1.369(5)	N(2C)-Pd(3)-Pd(2)	86.47(10)
C(1D)-C(2D)	1.373(6)	N(1C)-Pd(3)-Pd(2)	84.82(9)
C(2D)-C(3D)	1.367(6)	O(3C)-Pd(3)-Pd(2)	91.79(8)
C(3D)-C(4D)	1.397(6)	O(1C)-Pd(3)-Pd(2)	90.76(8)
C(4D)-C(5D)	1.402(6)	C(11C)-O(1C)-Pd(3)	123.0(3)
C(5D)-C(6D)	1.474(6)	C(13C)-O(3C)-Pd(3)	119.3(3)
C(6D)-C(7D)	1.385(6)	C(1C)-N(1C)-C(5C)	120.0(4)
C(7D)-C(8D)	1.369(7)	C(1C)-N(1C)-Pd(3)	125.6(3)
C(8D)-C(9D)	1.359(7)	C(5C)-N(1C)-Pd(3)	114.3(3)
C(9D)-C(10D)	1.394(7)	C(10C)-N(2C)-C(6C)	120.6(4)
C(11D)-C(12D)	1.521(8)	C(10C)-N(2C)-Pd(3)	125.1(3)
C(13D)-C(14D)	1.547(7)	C(6C)-N(2C)-Pd(3)	114.2(4)
O(1)-C(1)	1.200(6)	N(1C)-C(1C)-C(2C)	122.2(5)
C(1)-C(2)	1.498(8)	C(1C)-C(2C)-C(3C)	118.6(5)
C(1)-C(3)	1.493(7)	C(4C)-C(3C)-C(2C)	120.0(4)
O(2)-C(4)	1.216(6)	C(3C)-C(4C)-C(5C)	119.1(4)
C(4)-C(6)	1.445(7)	N(1C)-C(5C)-C(4C)	120.1(5)
C(4)-C(5)	1.476(7)	N(1C)-C(5C)-C(6C)	115.3(4)

O(3)-C(7)	1.216(5)
C(7)-C(8)	1.473(7)
C(7)-C(9)	1.512(7)
O(4)-C(10)	1.194(5)
C(10)-C(12)	1.477(7)
C(10)-C(11)	1.525(7)

C(4C)-C(5C)-C(6C)	124.6(4)
N(2C)-C(6C)-C(7C)	118.1(5)
N(2C)-C(6C)-C(5C)	114.7(4)
C(7C)-C(6C)-C(5C)	127.2(4)
C(8C)-C(7C)-C(6C)	121.1(4)
C(7C)-C(8C)-C(9C)	120.0(5)
C(10C)-C(9C)-C(8C)	119.1(5)
N(2C)-C(10C)-C(9C)	121.1(4)
O(2C)-C(11C)-O(1C)	129.6(4)
O(2C)-C(11C)-C(12C)	117.3(4)
O(1C)-C(11C)-C(12C)	113.1(4)
F(1C)-C(12C)-F(3C)	112.5(6)
F(1C)-C(12C)-F(2C)	106.5(6)
F(3C)-C(12C)-F(2C)	96.9(5)
F(1C)-C(12C)-C(11C)	117.3(4)
F(3C)-C(12C)-C(11C)	115.1(5)
F(2C)-C(12C)-C(11C)	105.8(6)
O(4C)-C(13C)-O(3C)	128.3(4)
O(4C)-C(13C)-C(14C)	117.6(4)
O(3C)-C(13C)-C(14C)	114.1(4)
F(4C)-C(14C)-F(6C)	104.4(5)
F(4C)-C(14C)-F(5C)	109.4(6)
F(6C)-C(14C)-F(5C)	102.9(5)
F(4C)-C(14C)-C(13C)	115.4(5)
F(6C)-C(14C)-C(13C)	109.4(5)
F(5C)-C(14C)-C(13C)	114.1(4)
N(1D)-Pd(4)-N(2D)	80.85(15)
N(1D)-Pd(4)-O(3D)	177.52(14)
N(2D)-Pd(4)-O(3D)	98.15(15)
N(1D)-Pd(4)-O(1D)	92.97(14)
N(2D)-Pd(4)-O(1D)	172.93(14)
O(3D)-Pd(4)-O(1D)	87.88(12)
C(11D)-O(1D)-Pd(4)	118.5(3)
C(13D)-O(3D)-Pd(4)	118.7(3)
C(5D)-N(1D)-C(1D)	119.6(4)
C(5D)-N(1D)-Pd(4)	115.4(3)
C(1D)-N(1D)-Pd(4)	125.0(3)
C(10D)-N(2D)-C(6D)	118.7(4)
C(10D)-N(2D)-Pd(4)	126.1(3)
C(6D)-N(2D)-Pd(4)	115.2(3)
N(1D)-C(1D)-C(2D)	121.5(4)
C(1D)-C(2D)-C(3D)	120.2(5)
C(2D)-C(3D)-C(4D)	118.7(5)
C(3D)-C(4D)-C(5D)	119.0(4)
N(1D)-C(5D)-C(4D)	121.0(5)
N(1D)-C(5D)-C(6D)	115.3(4)
C(4D)-C(5D)-C(6D)	123.7(4)
N(2D)-C(6D)-C(7D)	121.2(4)
N(2D)-C(6D)-C(5D)	113.1(4)

C(7D)-C(6D)-C(5D)	125.7(4)
C(8D)-C(7D)-C(6D)	118.6(5)
C(9D)-C(8D)-C(7D)	121.1(5)
C(8D)-C(9D)-C(10D)	118.4(5)
N(2D)-C(10D)-C(9D)	121.9(5)
O(2D)-C(11D)-O(1D)	129.8(5)
O(2D)-C(11D)-C(12D)	117.9(4)
O(1D)-C(11D)-C(12D)	112.3(5)
F(2D)-C(12D)-F(1D)	106.7(6)
F(2D)-C(12D)-F(3D)	108.7(8)
F(1D)-C(12D)-F(3D)	92.1(8)
F(2D)-C(12D)-C(11D)	115.3(9)
F(1D)-C(12D)-C(11D)	116.6(4)
F(3D)-C(12D)-C(11D)	114.8(5)
O(4D)-C(13D)-O(3D)	131.1(4)
O(4D)-C(13D)-C(14D)	117.2(4)
O(3D)-C(13D)-C(14D)	111.7(3)
F(5D)-C(14D)-F(4D)	108.8(6)
F(5D)-C(14D)-F(6D)	104.0(6)
F(4D)-C(14D)-F(6D)	103.0(6)
F(5D)-C(14D)-C(13D)	117.5(4)
F(4D)-C(14D)-C(13D)	112.6(5)
F(6D)-C(14D)-C(13D)	109.6(5)
O(1)-C(1)-C(2)	121.5(5)
O(1)-C(1)-C(3)	122.6(6)
C(2)-C(1)-C(3)	115.9(5)
O(2)-C(4)-C(6)	121.6(5)
O(2)-C(4)-C(5)	122.9(5)
C(6)-C(4)-C(5)	115.0(6)
O(3)-C(7)-C(8)	123.0(5)
O(3)-C(7)-C(9)	122.5(5)
C(8)-C(7)-C(9)	114.5(4)
O(4)-C(10)-C(12)	122.2(5)
O(4)-C(10)-C(11)	122.4(5)
C(12)-C(10)-C(11)	115.5(5)

Symmetry transformations used to generate equivalent atoms: #1 -x,-y+2,z

Table 27. Anisotropic displacement parameters ($Å^2$ x 10^4). The anisotropic displacement factor exponent takes the form: $-2\pi^2[h^2a^*2U^{11} + ... + 2 h k a^* b^* U^{12}]$.

	U^{11}	U^{22}	U^{33}	U^{23}	U^{13}	U^{12}
Pd(1)	175(1)	218(1)	239(2)	4(2)	-4(2)	12(1)
F(1A)	452(17)	1200(30)	590(20)	490(20)	10(20)	250(20)
F(2A)	600(20)	1480(40)	940(40)	470(30)	120(20)	-350(20)
F(3A)	1100(30)	1370(40)	610(30)	200(30)	370(20)	760(30)
F(4A)	800(20)	640(20)	1920(60)	-290(30)	-370(30)	0(20)
F(5A)	850(20)	770(20)	850(30)	-210(30)	-280(30)	151(19)
F(6A)	980(30)	870(30)	1410(50)	110(30)	20(30)	-350(20)
O(1A)	254(14)	353(16)	280(20)	48(16)	47(14)	97(13)
O(2A)	311(16)	300(20)	450(20)	90(18)	79(18)	72(14)
O(3A)	183(14)	233(15)	300(20)	-7(13)	55(13)	-21(12)

O(4A)	188(14)	349(17)	420(20)	-99(16)	45(14)	-16(13)
N(1A)	208(17)	278(19)	310(30)	4(18)	-81(17)	101(15)
N(2A)	133(16)	195(17)	200(20)	5(15)	16(15)	-8(14)
C(1A)	300(20)	400(30)	360(30)	-40(20)	20(20)	80(20)
C(2A)	350(30)	380(30)	480(40)	-180(30)	-150(30)	90(20)
C(3A)	320(20)	220(20)	790(50)	-150(30)	-250(30)	51(19)
C(4A)	223(19)	240(20)	670(40)	10(30)	-100(30)	21(15)
C(5A)	151(17)	230(20)	430(40)	-30(20)	-90(20)	64(15)
C(6A)	139(18)	230(20)	240(30)	-50(20)	-14(19)	73(16)
C(7A)	204(19)	340(20)	490(40)	200(30)	80(20)	25(17)
C(8A)	220(20)	390(30)	240(30)	160(20)	129(19)	56(19)
C(9A)	230(20)	430(30)	210(30)	40(20)	-16(19)	90(19)
C(10A)	180(20)	260(20)	310(30)	-15(19)	-11(18)	1(16)
C(11A)	220(20)	350(20)	270(30)	10(20)	-40(20)	-30(20)
C(12A)	290(20)	760(40)	490(40)	320(30)	90(30)	200(30)
C(13A)	250(20)	220(20)	220(30)	59(19)	0(20)	-47(17)
C(14A)	230(20)	240(20)	410(30)	90(20)	20(20)	-6(18)
Pd(2)	157(1)	234(1)	204(2)	13(2)	-3(2)	-23(1)
F(1B)	454(15)	920(20)	470(20)	316(18)	8(17)	-212(18)
F(2B)	359(15)	740(20)	540(20)	188(18)	-91(15)	71(15)
F(3B)	703(18)	680(20)	225(16)	79(15)	-58(14)	-209(16)
F(4B)	740(20)	630(20)	720(30)	-134(19)	90(20)	-50(18)
F(5B)	610(19)	780(20)	1060(40)	-100(30)	140(20)	-60(18)
F(6B)	840(20)	940(30)	890(30)	-190(20)	-230(20)	300(20)
O(1B)	274(14)	311(15)	219(17)	29(14)	-1(13)	-19(13)
O(2B)	323(16)	370(20)	390(20)	10(18)	11(18)	-83(16)
O(3B)	200(13)	236(14)	276(19)	-30(13)	42(13)	0(12)
O(4B)	269(15)	338(17)	311(19)	-13(15)	-28(14)	-43(13)
N(1B)	173(16)	240(17)	280(20)	-11(17)	-15(16)	-51(14)
N(2B)	171(17)	239(18)	250(20)	52(16)	-5(16)	-53(14)
C(1B)	240(20)	390(30)	260(30)	-70(20)	75(19)	-70(20)
C(2B)	260(20)	320(30)	480(40)	-180(20)	60(20)	-42(19)
C(3B)	250(20)	270(20)	570(40)	-160(20)	40(20)	-45(18)
C(4B)	247(18)	230(18)	420(30)	30(20)	0(20)	-10(15)
C(5B)	115(17)	270(20)	310(30)	-39(19)	-7(17)	-52(15)
C(6B)	155(19)	180(20)	360(30)	30(20)	30(20)	-50(17)
C(7B)	181(19)	240(20)	340(30)	5(19)	-32(19)	-8(16)
C(8B)	290(20)	410(30)	320(30)	190(20)	-30(20)	-120(20)
C(9B)	230(20)	500(30)	190(30)	-40(20)	-15(19)	-70(20)
C(10B)	230(20)	340(20)	190(30)	0(20)	19(18)	-95(18)
C(11B)	260(20)	340(20)	240(30)	50(20)	90(20)	30(19)
C(12B)	400(30)	510(30)	320(30)	170(30)	80(20)	-80(20)
C(13B)	270(20)	250(20)	190(30)	60(18)	28(19)	19(19)
C(14B)	330(20)	290(20)	350(30)	-20(20)	10(20)	-50(20)
Pd(3)	159(1)	206(1)	253(2)	-22(2)	-16(2)	-9(1)
F(1C)	421(19)	2180(60)	1420(50)	-1550(50)	190(20)	-250(20)
F(2C)	1860(50)	1690(50)	1470(50)	-30(40)	510(40)	1350(50)
F(3C)	910(30)	1970(50)	630(30)	-700(30)	400(20)	-700(30)
F(4C)	950(30)	1230(40)	2900(90)	1370(50)	-130(50)	-120(30)
F(5C)	1140(30)	890(30)	1180(40)	160(30)	-630(30)	270(20)
F(6C)	1340(40)	1530(40)	1460(50)	-270(40)	60(40)	880(40)
O(1C)	254(15)	403(19)	330(20)	-166(16)	-28(14)	-48(13)
O(2C)	234(15)	550(20)	440(30)	-190(20)	1(17)	-7(14)
O(3C)	244(15)	207(15)	350(20)	35(13)	-84(14)	38(12)
O(4C)	375(18)	430(20)	710(30)	145(19)	-98(19)	-76(16)

N(1C)	123(15)	248(18)	240(20)	-6(15)	-60(14)	-21(13)
N(2C)	168(18)	194(17)	310(20)	7(17)	-3(17)	3(14)
C(1C)	220(19)	400(30)	240(30)	0(20)	7(18)	-48(18)
C(2C)	280(20)	400(30)	290(30)	130(20)	-50(20)	-77(19)
C(3C)	220(20)	360(30)	490(40)	210(20)	-110(20)	-21(19)
C(4C)	192(19)	260(20)	370(30)	70(20)	-28(19)	-20(16)
C(5C)	144(16)	238(17)	370(30)	-40(30)	30(20)	-25(14)
C(6C)	150(20)	150(20)	330(30)	-40(20)	8(18)	-45(16)
C(7C)	204(18)	199(19)	410(30)	-40(20)	-10(20)	9(15)
C(8C)	160(20)	410(30)	360(30)	-100(20)	10(20)	-48(19)
C(9C)	190(20)	410(30)	310(30)	120(20)	-16(19)	-37(19)
C(10C)	166(17)	229(19)	250(30)	-2(18)	-15(19)	-46(15)
C(11C)	300(20)	280(20)	270(30)	-60(20)	20(20)	56(18)
C(12C)	380(30)	640(40)	750(50)	-400(40)	140(30)	-10(30)
C(13C)	230(20)	330(20)	270(30)	-40(20)	20(20)	31(19)
C(14C)	460(30)	220(20)	540(40)	50(20)	-80(30)	-30(20)
Pd(4)	147(1)	300(1)	251(2)	61(2)	12(2)	-32(1)
F(1D)	960(30)	1080(30)	990(40)	-60(30)	-90(30)	-120(20)
F(2D)	2250(80)	3720(110)	4290(140)	-3000(110)	-2340(90)	2230(90)
F(3D)	2590(100)	1460(70)	8000(300)	-1440(100)	3220(150)	-850(70)
F(4D)	990(30)	2850(80)	840(40)	1010(50)	410(30)	980(40)
F(5D)	275(14)	910(20)	980(30)	690(20)	174(17)	166(15)
F(6D)	1660(50)	810(30)	3640(100)	1170(50)	-1810(60)	-500(30)
O(1D)	312(16)	241(16)	370(20)	50(15)	98(15)	26(13)
O(2D)	350(17)	450(20)	740(30)	223(19)	-71(19)	-140(15)
O(3D)	248(15)	460(20)	295(19)	202(16)	15(14)	-9(14)
O(4D)	189(14)	520(20)	530(30)	290(20)	69(17)	25(14)
N(1D)	152(16)	253(18)	140(20)	-37(15)	51(14)	-53(14)
N(2D)	239(17)	400(20)	200(20)	-2(17)	-12(15)	-89(16)
C(1D)	145(18)	236(19)	380(40)	-60(20)	-10(20)	-26(14)
C(2D)	230(20)	340(20)	160(20)	30(20)	-1(18)	-49(19)
C(3D)	200(20)	300(30)	280(30)	80(20)	-67(19)	-54(18)
C(4D)	192(19)	240(20)	290(30)	48(19)	-20(18)	-9(16)
C(5D)	123(18)	250(20)	240(30)	20(20)	38(18)	-97(16)
C(6D)	151(17)	340(20)	170(20)	-93(18)	55(15)	-64(16)
C(7D)	210(20)	410(30)	360(30)	-120(20)	10(20)	-30(18)
C(8D)	240(20)	590(30)	400(40)	-230(30)	60(20)	-90(20)
C(9D)	310(20)	590(30)	360(30)	-230(30)	90(20)	-150(20)
C(10D)	210(19)	560(30)	240(30)	60(20)	-7(19)	-140(20)
C(11D)	250(20)	250(20)	610(40)	80(20)	-50(20)	6(18)
C(12D)	320(20)	330(30)	1360(70)	-320(40)	20(40)	10(20)
C(13D)	250(19)	420(30)	340(30)	140(20)	-40(20)	-7(19)
C(14D)	310(30)	790(40)	560(40)	370(40)	120(30)	0(30)
O(1)	800(30)	336(19)	370(20)	-4(17)	-170(20)	30(18)
C(1)	620(30)	290(20)	400(30)	110(20)	10(30)	80(20)
C(2)	840(40)	1070(50)	740(60)	-370(50)	40(40)	50(40)
C(3)	850(40)	500(30)	610(50)	30(30)	-260(40)	120(30)
O(2)	570(20)	440(20)	420(30)	-12(19)	-50(20)	-41(17)
C(4)	340(30)	410(30)	480(40)	-50(30)	0(30)	-80(20)
C(5)	640(40)	1500(70)	770(60)	400(50)	-20(40)	-630(40)
C(6)	660(40)	1100(60)	450(40)	200(40)	-140(30)	-170(40)
O(3)	530(20)	490(20)	230(20)	33(17)	21(16)	24(17)
C(7)	440(30)	410(30)	180(30)	50(20)	-30(20)	-30(20)
C(8)	650(30)	570(30)	370(30)	60(30)	-90(30)	120(30)
C(9)	630(30)	740(40)	410(40)	150(30)	80(30)	160(30)

O(4)	740(20)	420(20)	220(20)	-9(17)	68(19)	-14(18)
C(10)	560(30)	280(20)	260(30)	60(20)	80(20)	-80(20)
C(11)	560(30)	540(30)	590(40)	110(30)	-10(30)	-70(30)
C(12)	550(30)	970(40)	430(40)	-210(40)	-140(30)	130(30)

A.2 (CCDC 713343)

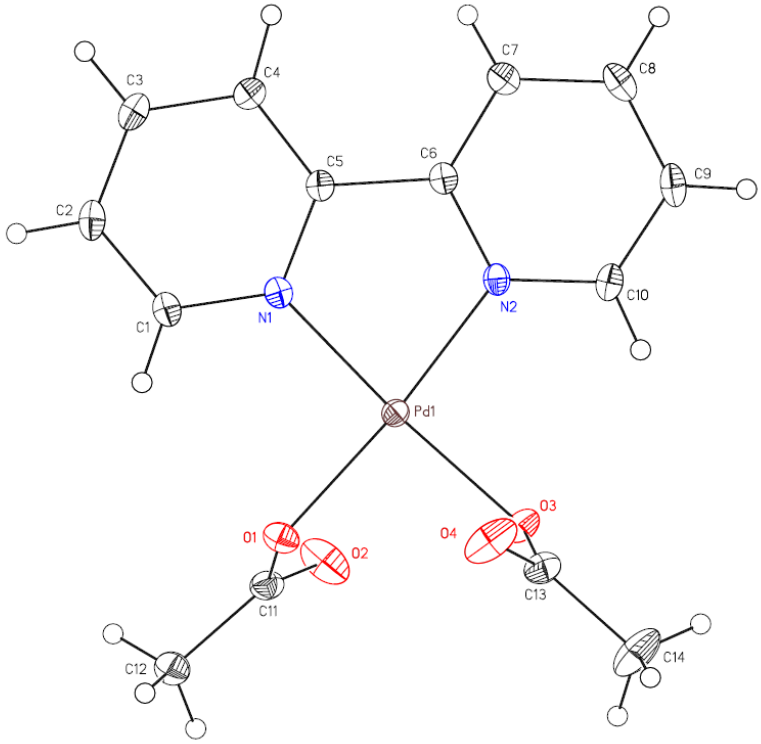

Special Refinement Details

Crystals were mounted on a glass fiber using Paratone oil then placed on the diffractometer under a nitrogen stream at 100K.

One hydrogen atom H(4) refined with a negative temperature factor, within two sigma.

Refinement of F^2 against ALL reflections. The weighted R-factor (wR) and goodness of fit (S) are based on F^2, conventional R-factors (R) are based on F, with F set to zero for negative F^2. The threshold expression of $F^2 > 2\sigma (F^2)$ is used only for calculating R-factors(gt) etc. and is not relevant to the choice of reflections for refinement. R-factors based on F^2 are statistically about twice as large as those based on F, and R-factors based on ALL data will be even larger.

All esds (except the esd in the dihedral angle between two l.s. planes) are estimated using the full covariance matrix. The cell esds are taken into account individually in the estimation of esds in distances, angles and torsion angles; correlations between esds in cell parameters are only used when they are defined by crystal symmetry. An approximate (isotropic) treatment of cell esds is used for estimating esds involving l.s. planes.

Table 28. Atomic coordinates (x 10^4) and equivalent isotropic displacement parameters (Å^2 x 10^3). U(eq) is defined as the trace of the orthogonalized Uij tensor.

	x	y	z	Ueq
Pd(1)	8324(1)	7352(1)	6253(1)	11(1)
O(1)	8856(1)	8043(1)	8021(1)	16(1)
O(2)	12093(1)	8370(1)	8001(1)	27(1)
O(3)	8851(1)	9046(1)	6372(1)	16(1)
O(4)	5736(1)	9158(1)	6632(1)	28(1)
N(1)	7875(1)	5625(1)	6010(1)	12(1)

N(2)	7691(1)	6517(1)	4493(1)	12(1)
C(1)	7977(2)	5269(1)	6870(1)	14(1)
C(2)	7658(2)	4046(1)	6615(1)	16(1)
C(3)	7214(2)	3177(1)	5448(1)	16(1)
C(4)	7089(2)	3539(1)	4552(1)	15(1)
C(5)	7425(1)	4772(1)	4857(1)	11(1)
C(6)	7326(1)	5277(1)	4001(1)	12(1)
C(7)	6895(2)	4580(1)	2789(1)	16(1)
C(8)	6842(2)	5158(1)	2068(1)	20(1)
C(9)	7218(2)	6417(1)	2574(1)	19(1)
C(10)	7633(2)	7073(1)	3788(1)	16(1)
C(11)	10727(2)	8384(1)	8541(1)	15(1)
C(12)	11120(2)	8757(1)	9841(1)	18(1)
C(13)	7377(2)	9610(1)	6555(1)	17(1)
C(14)	7837(2)	10875(1)	6646(2)	30(1)
O(21)	5911(1)	7702(1)	850(1)	22(1)
O(22)	5668(2)	8389(1)	9147(1)	28(1)
O(23)	7607(2)	3692(1)	9101(1)	29(1)
O(24)	2751(1)	482(1)	6874(1)	23(1)
O(25)	1438(2)	3838(1)	226(1)	29(1)

Table 29. Bond lengths [Å] and angles [°].

Pd(1)-N(2)	1.9926(9)	N(2)-Pd(1)-N(1)	81.45(4)
Pd(1)-N(1)	1.9976(9)	N(2)-Pd(1)-O(1)	174.65(3)
Pd(1)-O(1)	2.0067(8)	N(1)-Pd(1)-O(1)	93.38(3)
Pd(1)-O(3)	2.0134(8)	N(2)-Pd(1)-O(3)	94.47(3)
O(1)-C(11)	1.2984(12)	N(1)-Pd(1)-O(3)	175.31(4)
O(2)-C(11)	1.2270(13)	O(1)-Pd(1)-O(3)	90.75(3)
O(3)-C(13)	1.2976(13)	C(11)-O(1)-Pd(1)	115.86(7)
O(4)-C(13)	1.2227(13)	C(13)-O(3)-Pd(1)	115.98(7)
N(1)-C(1)	1.3428(14)	C(1)-N(1)-C(5)	119.75(9)
N(1)-C(5)	1.3613(13)	C(1)-N(1)-Pd(1)	125.63(8)
N(2)-C(10)	1.3437(14)	C(5)-N(1)-Pd(1)	114.61(7)
N(2)-C(6)	1.3604(13)	C(10)-N(2)-C(6)	119.46(9)
C(1)-C(2)	1.3858(16)	C(10)-N(2)-Pd(1)	125.77(8)
C(1)-H(1)	0.918(13)	C(6)-N(2)-Pd(1)	114.77(7)
C(2)-C(3)	1.3796(17)	N(1)-C(1)-C(2)	121.55(11)
C(2)-H(2)	0.913(14)	N(1)-C(1)-H(1)	117.3(8)
C(3)-C(4)	1.3920(16)	C(2)-C(1)-H(1)	121.2(8)
C(3)-H(3)	0.925(13)	C(3)-C(2)-C(1)	118.93(11)
C(4)-C(5)	1.3816(15)	C(3)-C(2)-H(2)	120.9(9)
C(4)-H(4)	0.970(10)	C(1)-C(2)-H(2)	120.2(9)
C(5)-C(6)	1.4713(14)	C(2)-C(3)-C(4)	119.83(11)
C(6)-C(7)	1.3811(15)	C(2)-C(3)-H(3)	119.8(8)
C(7)-C(8)	1.3836(16)	C(4)-C(3)-H(3)	120.3(8)
C(7)-H(7)	0.872(13)	C(5)-C(4)-C(3)	118.79(11)
C(8)-C(9)	1.3804(18)	C(5)-C(4)-H(4)	126.9(6)
C(8)-H(8)	0.905(13)	C(3)-C(4)-H(4)	114.3(6)

C(9)-C(10)	1.3785(17)	N(1)-C(5)-C(4)	121.14(10)
C(9)-H(9)	0.875(15)	N(1)-C(5)-C(6)	114.54(9)
C(10)-H(10)	0.885(13)	C(4)-C(5)-C(6)	124.32(10)
C(11)-C(12)	1.4976(16)	N(2)-C(6)-C(7)	120.99(10)
C(12)-H(12A)	0.896(17)	N(2)-C(6)-C(5)	114.62(9)
C(12)-H(12B)	0.942(14)	C(7)-C(6)-C(5)	124.39(10)
C(12)-H(12C)	0.919(14)	C(6)-C(7)-C(8)	119.27(11)
C(13)-C(14)	1.5036(17)	C(6)-C(7)-H(7)	119.3(9)
C(14)-H(14A)	0.93(2)	C(8)-C(7)-H(7)	121.4(9)
C(14)-H(14B)	0.925(17)	C(9)-C(8)-C(7)	119.40(11)
C(14)-H(14C)	0.962(19)	C(9)-C(8)-H(8)	121.7(9)
O(21)-H(21A)	0.773(18)	C(7)-C(8)-H(8)	118.9(9)
O(21)-H(21B)	0.802(16)	C(10)-C(9)-C(8)	119.21(11)
O(22)-H(22A)	0.777(16)	C(10)-C(9)-H(9)	119.9(9)
O(22)-H(22B)	0.768(18)	C(8)-C(9)-H(9)	120.9(9)
O(23)-H(23A)	0.599(16)	N(2)-C(10)-C(9)	121.67(11)
O(23)-H(23B)	0.818(17)	N(2)-C(10)-H(10)	116.2(9)
O(24)-H(24A)	0.724(17)	C(9)-C(10)-H(10)	122.1(9)
O(24)-H(24B)	0.784(17)	O(2)-C(11)-O(1)	122.39(10)
O(25)-H(25A)	0.696(18)	O(2)-C(11)-C(12)	121.89(10)
O(25)-H(25B)	0.759(17)	O(1)-C(11)-C(12)	115.69(10)
		C(11)-C(12)-H(12A)	107.8(10)
		C(11)-C(12)-H(12B)	114.4(8)
		H(12A)-C(12)-H(12B)	104.4(13)
		C(11)-C(12)-H(12C)	108.4(9)
		H(12A)-C(12)-H(12C)	111.3(13)
		H(12B)-C(12)-H(12C)	110.5(12)
		O(4)-C(13)-O(3)	123.53(10)
		O(4)-C(13)-C(14)	122.16(11)
		O(3)-C(13)-C(14)	114.30(10)
		C(13)-C(14)-H(14A)	110.7(12)
		C(13)-C(14)-H(14B)	111.0(10)
		H(14A)-C(14)-H(14B)	114.1(16)
		C(13)-C(14)-H(14C)	109.5(12)
		H(14A)-C(14)-H(14C)	102.5(15)
		H(14B)-C(14)-H(14C)	108.7(15)
		H(21A)-O(21)-H(21B)	108.7(17)
		H(22A)-O(22)-H(22B)	106.5(17)
		H(23A)-O(23)-H(23B)	113(2)
		H(24A)-O(24)-H(24B)	109.2(18)
		H(25A)-O(25)-H(25B)	105.1(18)

Table 30. Anisotropic displacement parameters ($Å^2$ x 10^4). The anisotropic displacement factor exponent takes the form: $-2\pi^2[h^2a^*2U^{11} + ... + 2 h k a^* b^* U^{12}]$.

	U^{11}	U^{22}	U^{33}	U^{23}	U^{13}	U^{12}
Pd(1)	107(1)	104(1)	115(1)	50(1)	22(1)	26(1)
O(1)	135(3)	171(4)	131(4)	43(3)	19(3)	25(3)
O(2)	148(4)	425(6)	185(4)	94(4)	40(3)	58(4)

O(3)	143(3)	124(4)	224(4)	83(3)	48(3)	34(3)
O(4)	167(4)	179(4)	501(6)	139(4)	115(4)	52(3)
N(1)	102(4)	142(4)	122(4)	67(4)	23(3)	30(3)
N(2)	106(4)	142(4)	126(4)	77(3)	23(3)	31(3)
C(1)	132(5)	179(5)	135(5)	88(4)	27(4)	34(4)
C(2)	151(5)	211(6)	191(6)	146(5)	36(4)	43(4)
C(3)	151(5)	150(5)	228(6)	117(5)	39(4)	35(4)
C(4)	145(5)	135(5)	163(5)	67(4)	31(4)	25(4)
C(5)	88(4)	138(5)	128(5)	69(4)	32(3)	30(3)
C(6)	98(4)	144(5)	130(5)	71(4)	28(4)	31(4)
C(7)	175(5)	165(5)	138(5)	62(4)	28(4)	32(4)
C(8)	223(6)	259(6)	120(5)	90(5)	31(4)	60(5)
C(9)	216(5)	266(6)	188(6)	169(5)	56(4)	76(5)
C(10)	168(5)	169(5)	188(6)	120(5)	42(4)	45(4)
C(11)	168(5)	121(5)	152(5)	46(4)	21(4)	42(4)
C(12)	195(6)	177(6)	159(6)	65(5)	8(4)	23(4)
C(13)	166(5)	134(5)	193(6)	59(4)	29(4)	40(4)
C(14)	272(7)	180(6)	523(10)	194(7)	150(7)	98(5)
O(21)	253(4)	211(5)	226(5)	126(4)	49(4)	62(4)
O(22)	176(4)	486(6)	319(6)	280(5)	106(4)	129(4)
O(23)	284(6)	299(6)	255(5)	138(4)	13(4)	-52(5)
O(24)	147(4)	186(4)	363(6)	123(4)	56(4)	40(4)
O(25)	404(6)	261(6)	288(6)	145(5)	124(5)	175(5)

Table 31. Hydrogen coordinates (x 10^4) and isotropic displacement parameters (Å^2 x 10^3).

	x	y	z	Uiso
H(1)	8278(17)	5871(12)	7636(12)	16(3)
H(2)	7737(18)	3823(12)	7212(12)	22(3)
H(3)	6936(17)	2357(12)	5266(11)	16(3)
H(4)	6731(13)	2869(9)	3761(9)	-4(2)
H(7)	6672(18)	3786(13)	2494(12)	19(3)
H(8)	6589(17)	4698(12)	1275(12)	19(3)
H(9)	7190(19)	6800(13)	2135(13)	26(4)
H(10)	7908(17)	7880(12)	4148(11)	16(3)
H(12A)	11440(20)	8126(15)	9944(14)	42(5)
H(12B)	9997(19)	8914(12)	10195(12)	26(4)
H(12C)	12152(19)	9430(13)	10203(12)	28(4)
H(14A)	8400(30)	10868(18)	6015(18)	66(6)
H(14B)	6720(20)	11224(15)	6742(15)	48(5)
H(14C)	8900(30)	11380(18)	7315(18)	67(6)
H(21A)	5780(20)	7925(16)	369(16)	45(5)
H(21B)	6320(20)	8285(15)	1481(15)	32(4)
H(22A)	6500(20)	8338(14)	8778(14)	33(4)
H(22B)	4750(20)	8456(16)	8793(16)	46(5)
H(23A)	8380(20)	3623(17)	9311(16)	36(6)
H(23B)	6620(20)	3251(16)	9116(14)	41(5)
H(24A)	3520(20)	134(16)	6843(15)	45(5)
H(24B)	1710(20)	64(16)	6767(15)	46(5)
H(25A)	1870(20)	4427(17)	333(16)	43(6)

H(25B)	2100(20)	3435(15)	-122(15)	33(5)

Table 32. Hydrogen bonds [Å and °].

D-H...A	d(D-H)	d(H...A)	d(D...A)	<(DHA)
O(21)-H(21A)...O(22)#1	0.773(18)	1.874(19)	2.6442(14)	174.3(18)
O(21)-H(21B)...O(24)#2	0.802(16)	1.958(17)	2.7524(14)	170.7(16)
O(22)-H(22A)...O(1)	0.777(16)	1.979(16)	2.7447(13)	168.4(16)
O(22)-H(22B)...O(2)#3	0.768(18)	1.945(17)	2.7000(13)	167.2(18)
O(23)-H(23A)...O(25)#4	0.599(16)	2.206(16)	2.7910(17)	166(2)
O(23)-H(23B)...O(21)#2	0.818(17)	1.981(17)	2.7963(14)	174.5(16)
O(24)-H(24A)...O(4)#5	0.724(17)	2.042(18)	2.7642(13)	175.3(19)
O(24)-H(24B)...O(3)#6	0.784(17)	2.061(17)	2.8419(12)	173.8(18)
O(25)-H(25A)...O(23)#2	0.696(18)	2.085(19)	2.7546(16)	162(2)
O(25)-H(25B)...O(21)#7	0.759(17)	2.104(17)	2.8576(15)	171.4(17)

Symmetry transformations used to generate equivalent atoms: #1 x,y,z-1, #2 -x+1,-y+1,-z+1, #3 x-1,y,z , #4 x+1,y,z+1, #5 x,y-1,z , #6 x-1,y-1,z, #7 -x+1,-y+1,-z

A.3 (CCDC 717612)

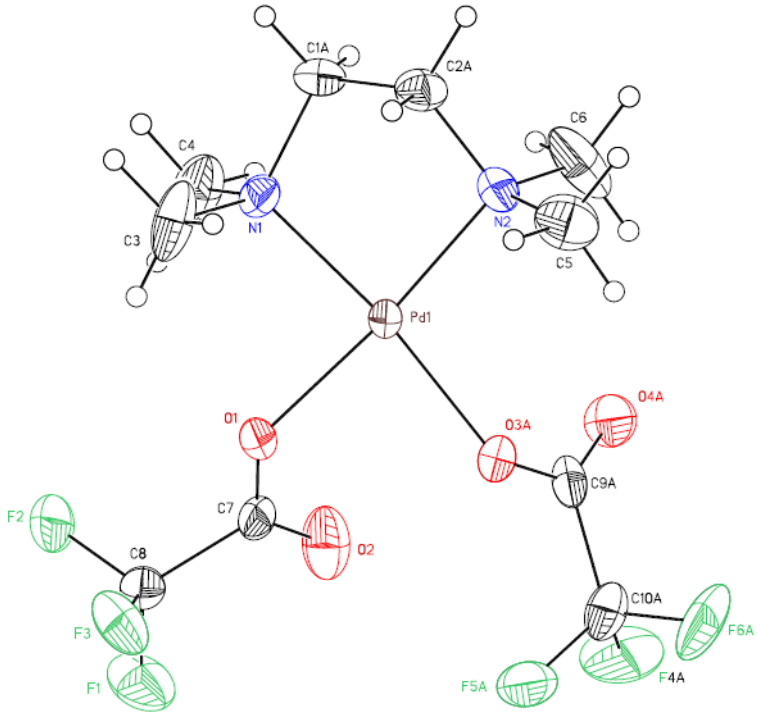

Special Refinement Details

Crystals were mounted on a glass fiber using Paratone oil then placed on the diffractometer under a nitrogen stream at 100K.

This structure is disordered in two ways. First, the ethane bridge of the diamine flips back and for in a commonly observed manner. Secondly, the tri-fluoro acetate ligands occur with the carbonyl oxygens as cis- or trans- to each other. These two disorders no NOT appear to be coupled.

Refinement of F^2 against ALL reflections. The weighted R-factor (wR) and goodness of fit (S) are based on F^2, conventional R-factors (R) are based on F, with F set to zero for negative F^2. The threshold expression of $F^2 > 2\sigma$ (F2) is used only for calculating R-factors(gt) etc. and is not relevant to the choice of reflections for refinement. R-factors based on F^2 are statistically about twice as large as those based on F, and R-factors based on ALL data will be even larger.

All esds (except the esd in the dihedral angle between two l.s. planes) are estimated using the full covariance matrix. The cell esds are taken into account individually in the estimation of esds in distances, angles and torsion angles; correlations between esds in cell parameters are only used when they are defined by crystal symmetry. An approximate (isotropic) treatment of cell esds is used for estimating esds involving l.s. planes.

Table 33. Atomic coordinates (x 10^4) and equivalent isotropic displacement parameters ($Å^2$ x 10^3). U(eq) is defined as the trace of the orthogonalized Uij tensor.

	x	y	z	Ueq	Occ
Pd(1)	-132(1)	4626(1)	7529(1)	35(1)	1
F(1)	-3409(2)	10217(2)	8238(2)	56(1)	1
F(2)	-4580(2)	8450(2)	9083(2)	61(1)	1
F(3)	-3955(2)	9129(2)	6906(2)	46(1)	1
F(4A)	3132(17)	8403(9)	6295(15)	67(3)	0.519(3)

F(5A)	1577(4)	8695(3)	5080(3)	50(1)	0.519(3)
F(6A)	3978(11)	7355(10)	4480(9)	62(2)	0.519(3)
O(3A)	1241(4)	5924(4)	5996(3)	25(1)	0.519(3)
O(4A)	3074(5)	5492(4)	7268(4)	37(1)	0.519(3)
C(9A)	2353(11)	6188(10)	6392(11)	28(2)	0.519(3)
C(10A)	2770(10)	7664(11)	5549(10)	34(2)	0.519(3)
F(4B)	3808(13)	7831(12)	4549(9)	90(4)	0.481(3)
F(5B)	3269(19)	8111(15)	6560(19)	107(5)	0.481(3)
F(6B)	4567(6)	6277(6)	6168(7)	130(3)	0.481(3)
O(3B)	1794(5)	5589(4)	7102(4)	26(1)	0.481(3)
O(4B)	1034(5)	7086(5)	5220(4)	41(1)	0.481(3)
C(9B)	1899(10)	6600(10)	6050(10)	24(2)	0.481(3)
C(10B)	3316(11)	7279(12)	5819(10)	33(2)	0.481(3)
O(1)	-1893(2)	6547(2)	7689(2)	45(1)	1
O(2)	-772(2)	7995(2)	8396(2)	48(1)	1
N(1)	-1784(3)	3474(2)	8598(2)	28(1)	1
N(2)	1411(3)	2587(2)	7287(2)	39(1)	1
C(1A)	-896(6)	1823(5)	8926(8)	28(1)	0.641(14)
C(2A)	331(6)	1470(5)	7606(8)	31(2)	0.641(14)
C(1B)	-1034(12)	1944(10)	8159(18)	38(3)	0.359(14)
C(2B)	614(13)	1515(9)	8321(16)	42(4)	0.359(14)
C(3)	-3124(4)	3821(4)	7915(3)	50(1)	1
C(4)	-2425(4)	3831(4)	10002(3)	46(1)	1
C(5)	2146(4)	2535(3)	5820(3)	47(1)	1
C(6)	2695(4)	2236(4)	8034(3)	58(1)	1
C(7)	-1826(3)	7713(3)	8054(3)	30(1)	1
C(8)	-3444(3)	8893(3)	8060(3)	29(1)	1

Table 34. Bond lengths [Å] and angles [°].

Pd(1)-N(1)	2.017(2)	N(1)-Pd(1)-O(1)	88.01(8)
Pd(1)-O(1)	2.0251(17)	N(1)-Pd(1)-N(2)	86.42(9)
Pd(1)-N(2)	2.034(2)	O(1)-Pd(1)-N(2)	171.82(9)
Pd(1)-O(3B)	2.079(4)	N(1)-Pd(1)-O(3B)	159.63(12)
Pd(1)-O(3A)	2.095(3)	O(1)-Pd(1)-O(3B)	97.04(11)
F(1)-C(8)	1.319(3)	N(2)-Pd(1)-O(3B)	90.24(12)
F(2)-C(8)	1.328(3)	N(1)-Pd(1)-O(3A)	164.37(11)
F(3)-C(8)	1.325(3)	O(1)-Pd(1)-O(3A)	87.12(10)
F(4A)-C(10A)	1.305(15)	N(2)-Pd(1)-O(3A)	96.70(11)
F(5A)-C(10A)	1.322(9)	O(3B)-Pd(1)-O(3A)	35.98(14)
F(6A)-C(10A)	1.331(13)	C(9A)-O(3A)-Pd(1)	113.9(5)
O(3A)-C(9A)	1.277(10)	O(4A)-C(9A)-O(3A)	130.8(10)
O(4A)-C(9A)	1.195(9)	O(4A)-C(9A)-C(10A)	118.3(8)
C(9A)-C(10A)	1.543(15)	O(3A)-C(9A)-C(10A)	111.0(7)
F(4B)-C(10B)	1.284(14)	F(4A)-C(10A)-F(5A)	100.9(8)
F(5B)-C(10B)	1.203(18)	F(4A)-C(10A)-F(6A)	110.3(10)
F(6B)-C(10B)	1.302(10)	F(5A)-C(10A)-F(6A)	108.3(8)
O(3B)-C(9B)	1.257(11)	F(4A)-C(10A)-C(9A)	112.3(9)
O(4B)-C(9B)	1.218(9)	F(5A)-C(10A)-C(9A)	115.4(7)

C(9B)-C(10B)	1.524(14)	F(6A)-C(10A)-C(9A)	109.3(8)
O(1)-C(7)	1.269(3)	C(9B)-O(3B)-Pd(1)	116.5(5)
O(2)-C(7)	1.206(3)	O(4B)-C(9B)-O(3B)	128.8(9)
N(1)-C(3)	1.463(4)	O(4B)-C(9B)-C(10B)	117.6(8)
N(1)-C(4)	1.475(3)	O(3B)-C(9B)-C(10B)	113.6(8)
N(1)-C(1B)	1.521(9)	F(5B)-C(10B)-F(4B)	110.5(12)
N(1)-C(1A)	1.526(5)	F(5B)-C(10B)-F(6B)	94.6(10)
N(2)-C(6)	1.463(4)	F(4B)-C(10B)-F(6B)	104.7(9)
N(2)-C(5)	1.470(4)	F(5B)-C(10B)-C(9B)	119.4(11)
N(2)-C(2B)	1.467(9)	F(4B)-C(10B)-C(9B)	113.3(9)
N(2)-C(2A)	1.557(6)	F(6B)-C(10B)-C(9B)	111.9(8)
C(1A)-C(2A)	1.527(11)	C(7)-O(1)-Pd(1)	126.64(19)
C(1B)-C(2B)	1.45(2)	C(3)-N(1)-C(4)	108.5(2)
C(7)-C(8)	1.539(4)	C(3)-N(1)-C(1B)	94.0(6)
		C(4)-N(1)-C(1B)	128.9(7)
		C(3)-N(1)-C(1A)	117.5(3)
		C(4)-N(1)-C(1A)	100.5(3)
		C(3)-N(1)-Pd(1)	111.67(18)
		C(4)-N(1)-Pd(1)	110.64(17)
		C(1B)-N(1)-Pd(1)	101.8(4)
		C(1A)-N(1)-Pd(1)	107.4(2)
		C(6)-N(2)-C(5)	108.3(2)
		C(6)-N(2)-C(2B)	91.2(7)
		C(5)-N(2)-C(2B)	128.9(6)
		C(6)-N(2)-C(2A)	118.8(3)
		C(5)-N(2)-C(2A)	100.9(3)
		C(6)-N(2)-Pd(1)	111.86(18)
		C(5)-N(2)-Pd(1)	110.98(17)
		C(2B)-N(2)-Pd(1)	103.8(4)
		C(2A)-N(2)-Pd(1)	105.4(2)
		C(2A)-C(1A)-N(1)	106.0(5)
		C(1A)-C(2A)-N(2)	105.3(5)
		C(2B)-C(1B)-N(1)	106.3(11)
		C(1B)-C(2B)-N(2)	105.7(13)
		O(2)-C(7)-O(1)	131.5(3)
		O(2)-C(7)-C(8)	119.2(2)
		O(1)-C(7)-C(8)	109.2(2)
		F(1)-C(8)-F(3)	106.6(2)
		F(1)-C(8)-F(2)	106.3(2)
		F(3)-C(8)-F(2)	106.5(2)
		F(1)-C(8)-C(7)	113.2(2)
		F(3)-C(8)-C(7)	113.1(2)
		F(2)-C(8)-C(7)	110.62(19)

Table 35. Anisotropic displacement parameters ($Å^2$ x 10^4). The anisotropic displacement factor exponent takes the form: $-2\pi^2[h^2a^*2U^{11} + ... + 2 h k a^* b^* U^{12}]$.

	U^{11}	U^{22}	U^{33}	U^{23}	U^{13}	U^{12}
Pd(1)	162(1)	201(1)	590(2)	-10(1)	29(1)	-39(1)

F(1)	582(12)	320(9)	923(14)	-232(9)	-323(11)	-58(8)
F(2)	335(10)	479(10)	683(12)	10(9)	197(9)	8(8)
F(3)	395(10)	443(9)	572(11)	-187(8)	-246(9)	77(8)
F(4A)	980(60)	380(20)	830(50)	-250(30)	-170(40)	-330(30)
F(5A)	470(20)	354(18)	650(20)	118(15)	-216(18)	-175(16)
F(6A)	500(30)	820(40)	580(40)	-340(40)	320(30)	-420(30)
O(3A)	202(18)	302(18)	260(20)	-57(15)	-20(14)	-79(15)
O(4A)	350(20)	400(20)	420(20)	-24(17)	-177(19)	-123(17)
C(9A)	170(40)	330(50)	350(50)	-130(40)	-30(30)	-20(30)
C(10A)	260(50)	470(50)	350(50)	-130(40)	-40(30)	-170(40)
F(4B)	750(60)	1490(90)	510(50)	630(50)	-350(40)	-790(60)
F(5B)	770(60)	1670(120)	1300(100)	-760(90)	-200(60)	-710(80)
F(6B)	440(30)	1010(40)	2240(70)	920(40)	-710(40)	-490(30)
O(3B)	180(20)	300(20)	290(20)	41(17)	-57(17)	-94(17)
O(4B)	330(20)	620(30)	290(20)	80(20)	-136(19)	-190(20)
C(9B)	160(50)	310(50)	240(50)	-120(40)	50(30)	-80(30)
C(10B)	230(50)	490(50)	290(50)	30(40)	-60(30)	-170(40)
O(1)	192(10)	211(9)	822(15)	-29(9)	6(10)	-29(7)
O(2)	300(12)	730(15)	413(12)	-159(11)	-101(10)	-71(11)
N(1)	236(11)	250(10)	366(12)	-65(9)	-17(9)	-106(9)
N(2)	263(13)	266(11)	471(14)	-5(10)	35(11)	16(10)
C(1A)	370(30)	200(20)	280(30)	10(20)	-110(20)	-74(18)
C(2A)	390(30)	220(20)	330(30)	-80(20)	-70(20)	-75(18)
C(1B)	400(50)	250(40)	500(80)	-50(50)	-20(50)	-200(40)
C(2B)	490(60)	220(40)	500(70)	-110(40)	70(50)	-150(40)
C(3)	284(16)	920(30)	427(17)	-265(17)	8(13)	-303(17)
C(4)	377(18)	720(20)	269(15)	6(14)	-53(13)	-200(16)
C(5)	570(20)	403(16)	461(18)	-103(13)	-138(16)	-89(15)
C(6)	560(20)	590(20)	340(16)	-114(15)	-146(15)	284(17)
C(7)	205(13)	317(13)	282(13)	49(11)	13(11)	-66(11)
C(8)	284(14)	245(12)	343(14)	-62(10)	-44(11)	-73(10)

A.4 (CCDC 711734)

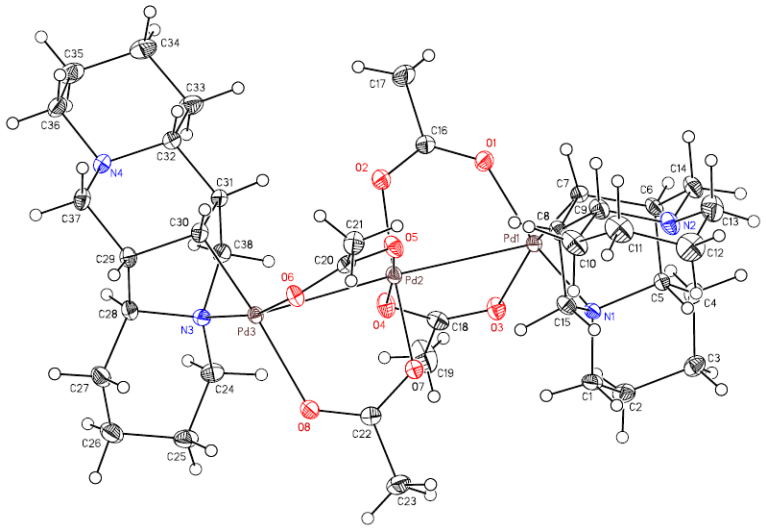

Special Refinement Details

Crystals were mounted on a glass fiber using Paratone oil then placed on the diffractometer under a nitrogen stream at 100K.

Refinement of F^2 against ALL reflections. The weighted R-factor (wR) and goodness of fit (S) are based on F^2, conventional R-factors (R) are based on F, with F set to zero for negative F^2. The threshold expression of $F^2 > 2\sigma (F^2)$ is used only for calculating R-factors(gt) etc. and is not relevant to the choice of reflections for refinement. R-factors based on F^2 are statistically about twice as large as those based on F, and R-factors based on ALL data will be even larger.

All esds (except the esd in the dihedral angle between two l.s. planes) are estimated using the full covariance matrix. The cell esds are taken into account individually in the estimation of esds in distances, angles and torsion angles; correlations between esds in cell parameters are only used when they are defined by crystal symmetry. An approximate (isotropic) treatment of cell esds is used for estimating esds involving l.s. planes.

Table 36. Atomic coordinates (x 10^4) and equivalent isotropic displacement parameters (Å^2 x 10^3). U(eq) is defined as the trace of the orthogonalized Uij tensor.

	x	y	z	Ueq
Pd(1)	2577(1)	578(1)	8249(1)	11(1)
Pd(2)	5262(1)	650(1)	8034(1)	12(1)
Pd(3)	7919(1)	844(1)	7831(1)	11(1)
O(1)	2718(1)	48(1)	7457(1)	18(1)
O(2)	4790(1)	-82(1)	7387(1)	20(1)
O(3)	2990(1)	1811(1)	7921(1)	17(1)
O(4)	4902(1)	1651(1)	7579(1)	18(1)
O(5)	5773(1)	-344(1)	8476(1)	17(1)
O(6)	7807(1)	-44(1)	8459(1)	15(1)
O(7)	5601(1)	1364(1)	8705(1)	15(1)
O(8)	7474(1)	1814(1)	8436(1)	16(1)
N(1)	2313(1)	852(1)	9089(1)	11(1)
N(2)	1504(1)	-1012(1)	9795(1)	17(1)
N(3)	8218(1)	1526(1)	7109(1)	12(1)

N(4)	9063(1)	20(1)	6022(1)	15(1)
C(1)	2552(1)	1695(1)	9293(1)	16(1)
C(2)	1627(1)	2308(1)	9065(1)	18(1)
C(3)	309(1)	2060(1)	9203(1)	19(1)
C(4)	82(1)	1200(1)	8985(1)	16(1)
C(5)	1006(1)	585(1)	9212(1)	12(1)
C(6)	854(1)	-265(1)	8938(1)	15(1)
C(7)	2076(1)	-461(1)	8640(1)	14(1)
C(8)	3043(1)	-575(1)	9101(1)	15(1)
C(9)	2673(1)	-1243(1)	9526(1)	17(1)
C(10)	3689(1)	-1384(1)	9963(1)	24(1)
C(11)	3291(2)	-1969(1)	10431(1)	27(1)
C(12)	2094(2)	-1664(1)	10688(1)	29(1)
C(13)	1122(2)	-1588(1)	10232(1)	25(1)
C(14)	535(1)	-924(1)	9368(1)	19(1)
C(15)	3181(1)	276(1)	9374(1)	14(1)
C(16)	3681(1)	-205(1)	7226(1)	17(1)
C(17)	3546(2)	-726(2)	6706(1)	31(1)
C(18)	3902(1)	2049(1)	7652(1)	16(1)
C(19)	3875(2)	2878(1)	7378(1)	31(1)
C(20)	6902(1)	-466(1)	8602(1)	14(1)
C(21)	7158(1)	-1205(1)	8961(1)	19(1)
C(22)	6558(1)	1819(1)	8751(1)	14(1)
C(23)	6536(2)	2402(1)	9242(1)	24(1)
C(24)	8009(1)	2415(1)	7124(1)	17(1)
C(25)	8967(1)	2862(1)	7479(1)	20(1)
C(26)	10260(1)	2688(1)	7254(1)	22(1)
C(27)	10478(1)	1775(1)	7249(1)	18(1)
C(28)	9507(1)	1299(1)	6920(1)	14(1)
C(29)	9634(1)	370(1)	7003(1)	14(1)
C(30)	8392(1)	61(1)	7223(1)	13(1)
C(31)	7451(1)	206(1)	6756(1)	13(1)
C(32)	7821(1)	-234(1)	6209(1)	15(1)
C(33)	6884(1)	-91(1)	5736(1)	21(1)
C(34)	7256(1)	-508(1)	5188(1)	23(1)
C(35)	8581(2)	-288(1)	5031(1)	24(1)
C(36)	9430(1)	-448(1)	5521(1)	19(1)
C(37)	9988(1)	-86(1)	6466(1)	16(1)
C(38)	7336(1)	1139(1)	6700(1)	14(1)

Table 37. Bond lengths [Å] and angles [°].

Pd(1)-C(7)	2.0100(14)	C(7)-Pd(1)-N(1)	72.58(5)
Pd(1)-N(1)	2.0612(10)	C(7)-Pd(1)-O(1)	94.82(5)
Pd(1)-O(1)	2.0740(9)	N(1)-Pd(1)-O(1)	167.39(4)
Pd(1)-O(3)	2.2083(10)	C(7)-Pd(1)-O(3)	171.70(4)
Pd(1)-Pd(2)	2.9562(2)	N(1)-Pd(1)-O(3)	99.81(4)
Pd(2)-O(4)	1.9998(10)	O(1)-Pd(1)-O(3)	92.73(4)
Pd(2)-O(7)	2.0068(10)	C(7)-Pd(1)-Pd(2)	112.25(4)

Pd(2)-O(2)	2.0118(10)	N(1)-Pd(1)-Pd(2)	107.12(3)
Pd(2)-O(5)	2.0128(10)	O(1)-Pd(1)-Pd(2)	77.75(2)
Pd(2)-Pd(3)	2.9370(2)	O(3)-Pd(1)-Pd(2)	72.73(2)
Pd(3)-C(30)	1.9967(15)	O(4)-Pd(2)-O(7)	89.24(4)
Pd(3)-N(3)	2.0690(11)	O(4)-Pd(2)-O(2)	91.46(5)
Pd(3)-O(6)	2.0833(9)	O(7)-Pd(2)-O(2)	175.54(4)
Pd(3)-O(8)	2.1927(10)	O(4)-Pd(2)-O(5)	175.22(4)
O(1)-C(16)	1.2497(16)	O(7)-Pd(2)-O(5)	90.43(4)
O(2)-C(16)	1.2777(16)	O(2)-Pd(2)-O(5)	89.24(4)
O(3)-C(18)	1.2378(16)	O(4)-Pd(2)-Pd(3)	90.79(3)
O(4)-C(18)	1.2766(17)	O(7)-Pd(2)-Pd(3)	83.52(3)
O(5)-C(20)	1.2747(15)	O(2)-Pd(2)-Pd(3)	100.87(3)
O(6)-C(20)	1.2466(16)	O(5)-Pd(2)-Pd(3)	84.43(3)
O(7)-C(22)	1.2816(16)	O(4)-Pd(2)-Pd(1)	86.20(3)
O(8)-C(22)	1.2423(16)	O(7)-Pd(2)-Pd(1)	93.83(3)
N(1)-C(1)	1.4845(18)	O(2)-Pd(2)-Pd(1)	81.82(3)
N(1)-C(15)	1.4927(17)	O(5)-Pd(2)-Pd(1)	98.58(3)
N(1)-C(5)	1.5110(15)	Pd(3)-Pd(2)-Pd(1)	176.028(5)
N(2)-C(13)	1.462(2)	C(30)-Pd(3)-N(3)	72.98(5)
N(2)-C(14)	1.4656(18)	C(30)-Pd(3)-O(6)	94.82(5)
N(2)-C(9)	1.4673(18)	N(3)-Pd(3)-O(6)	167.48(4)
N(3)-C(24)	1.4723(18)	C(30)-Pd(3)-O(8)	173.51(5)
N(3)-C(38)	1.5026(16)	N(3)-Pd(3)-O(8)	100.71(4)
N(3)-C(28)	1.5128(16)	O(6)-Pd(3)-O(8)	91.40(4)
N(4)-C(37)	1.4640(18)	C(30)-Pd(3)-Pd(2)	107.51(4)
N(4)-C(36)	1.4678(18)	N(3)-Pd(3)-Pd(2)	110.36(3)
N(4)-C(32)	1.4763(17)	O(6)-Pd(3)-Pd(2)	75.52(2)
C(1)-C(2)	1.518(2)	O(8)-Pd(3)-Pd(2)	75.85(2)
C(1)-H(1A)	0.959(15)	C(16)-O(1)-Pd(1)	126.75(8)
C(1)-H(1B)	0.931(16)	C(16)-O(2)-Pd(2)	124.19(9)
C(2)-C(3)	1.521(2)	C(18)-O(3)-Pd(1)	129.09(9)
C(2)-H(2A)	0.932(16)	C(18)-O(4)-Pd(2)	120.65(9)
C(2)-H(2B)	0.910(17)	C(20)-O(5)-Pd(2)	120.81(9)
C(3)-C(4)	1.518(2)	C(20)-O(6)-Pd(3)	128.83(8)
C(3)-H(3A)	0.905(16)	C(22)-O(7)-Pd(2)	123.69(9)
C(3)-H(3B)	0.993(18)	C(22)-O(8)-Pd(3)	125.00(9)
C(4)-C(5)	1.5189(19)	C(1)-N(1)-C(15)	109.18(10)
C(4)-H(4A)	1.016(15)	C(1)-N(1)-C(5)	111.66(11)
C(4)-H(4B)	0.941(14)	C(15)-N(1)-C(5)	108.71(11)
C(5)-C(6)	1.544(2)	C(1)-N(1)-Pd(1)	119.55(8)
C(5)-H(5)	0.992(14)	C(15)-N(1)-Pd(1)	102.27(8)
C(6)-C(14)	1.525(2)	C(5)-N(1)-Pd(1)	104.72(7)
C(6)-C(7)	1.5348(18)	C(13)-N(2)-C(14)	110.49(12)
C(6)-H(6)	0.898(15)	C(13)-N(2)-C(9)	112.78(12)
C(7)-C(8)	1.5260(18)	C(14)-N(2)-C(9)	110.04(11)
C(7)-H(7)	0.937(15)	C(24)-N(3)-C(38)	109.56(10)
C(8)-C(9)	1.539(2)	C(24)-N(3)-C(28)	113.08(10)
C(8)-C(15)	1.542(2)	C(38)-N(3)-C(28)	107.00(10)
C(8)-H(8)	0.915(14)	C(24)-N(3)-Pd(3)	119.19(9)

C(9)-C(10)	1.529(2)	C(38)-N(3)-Pd(3)	101.97(8)
C(9)-H(9)	0.927(18)	C(28)-N(3)-Pd(3)	104.93(8)
C(10)-C(11)	1.529(2)	C(37)-N(4)-C(36)	109.53(11)
C(10)-H(10A)	0.981(19)	C(37)-N(4)-C(32)	111.99(11)
C(10)-H(10B)	0.988(17)	C(36)-N(4)-C(32)	110.12(11)
C(11)-C(12)	1.517(3)	N(1)-C(1)-C(2)	112.50(11)
C(11)-H(11A)	0.992(17)	N(1)-C(1)-H(1A)	106.2(10)
C(11)-H(11B)	0.977(18)	C(2)-C(1)-H(1A)	110.9(9)
C(12)-C(13)	1.515(2)	N(1)-C(1)-H(1B)	106.9(10)
C(12)-H(12A)	0.993(18)	C(2)-C(1)-H(1B)	108.5(9)
C(12)-H(12B)	0.951(17)	H(1A)-C(1)-H(1B)	111.8(13)
C(13)-H(13A)	0.990(16)	C(1)-C(2)-C(3)	111.48(13)
C(13)-H(13B)	0.899(16)	C(1)-C(2)-H(2A)	108.2(9)
C(14)-H(14A)	0.964(15)	C(3)-C(2)-H(2A)	112.5(9)
C(14)-H(14B)	1.032(17)	C(1)-C(2)-H(2B)	110.0(10)
C(15)-H(15A)	0.943(15)	C(3)-C(2)-H(2B)	111.8(10)
C(15)-H(15B)	1.046(13)	H(2A)-C(2)-H(2B)	102.4(14)
C(16)-C(17)	1.504(2)	C(4)-C(3)-C(2)	109.03(12)
C(17)-H(17A)	0.70(3)	C(4)-C(3)-H(3A)	110.6(10)
C(17)-H(17B)	0.952(18)	C(2)-C(3)-H(3A)	110.2(10)
C(17)-H(17C)	0.95(3)	C(4)-C(3)-H(3B)	112.5(10)
C(18)-C(19)	1.505(2)	C(2)-C(3)-H(3B)	107.7(10)
C(19)-H(19A)	0.81(3)	H(3A)-C(3)-H(3B)	106.7(13)
C(19)-H(19B)	0.83(2)	C(3)-C(4)-C(5)	112.72(12)
C(19)-H(19C)	0.83(4)	C(3)-C(4)-H(4A)	109.7(9)
C(20)-C(21)	1.505(2)	C(5)-C(4)-H(4A)	108.1(9)
C(21)-H(21A)	0.89(2)	C(3)-C(4)-H(4B)	106.1(9)
C(21)-H(21B)	0.951(17)	C(5)-C(4)-H(4B)	112.1(9)
C(21)-H(21C)	0.956(18)	H(4A)-C(4)-H(4B)	108.1(12)
C(22)-C(23)	1.506(2)	N(1)-C(5)-C(4)	110.93(11)
C(23)-H(23A)	0.92(3)	N(1)-C(5)-C(6)	106.19(10)
C(23)-H(23B)	1.02(3)	C(4)-C(5)-C(6)	112.16(11)
C(23)-H(23C)	0.81(3)	N(1)-C(5)-H(5)	104.5(7)
C(24)-C(25)	1.523(2)	C(4)-C(5)-H(5)	107.6(8)
C(24)-H(24A)	0.995(13)	C(6)-C(5)-H(5)	115.2(9)
C(24)-H(24B)	0.995(17)	C(14)-C(6)-C(7)	110.83(12)
C(25)-C(26)	1.527(2)	C(14)-C(6)-C(5)	112.27(12)
C(25)-H(25A)	0.979(15)	C(7)-C(6)-C(5)	106.82(10)
C(25)-H(25B)	0.878(19)	C(14)-C(6)-H(6)	109.8(11)
C(26)-C(27)	1.512(2)	C(7)-C(6)-H(6)	107.7(10)
C(26)-H(26A)	0.943(13)	C(5)-C(6)-H(6)	109.3(11)
C(26)-H(26B)	1.058(19)	C(8)-C(7)-C(6)	106.77(11)
C(27)-C(28)	1.5239(19)	C(8)-C(7)-Pd(1)	104.41(9)
C(27)-H(27A)	0.964(14)	C(6)-C(7)-Pd(1)	105.60(9)
C(27)-H(27B)	0.945(16)	C(8)-C(7)-H(7)	113.7(9)
C(28)-C(29)	1.539(2)	C(6)-C(7)-H(7)	116.1(9)
C(28)-H(28)	0.943(15)	Pd(1)-C(7)-H(7)	109.4(9)
C(29)-C(37)	1.5233(19)	C(7)-C(8)-C(9)	112.14(11)
C(29)-C(30)	1.5285(18)	C(7)-C(8)-C(15)	104.86(11)

C(29)-H(29)	0.888(15)
C(30)-C(31)	1.5241(18)
C(30)-H(30)	0.831(16)
C(31)-C(32)	1.5362(18)
C(31)-C(38)	1.5365(19)
C(31)-H(31)	0.944(16)
C(32)-C(33)	1.531(2)
C(32)-H(32)	0.881(15)
C(33)-C(34)	1.523(2)
C(33)-H(33A)	1.012(15)
C(33)-H(33B)	0.866(18)
C(34)-C(35)	1.525(2)
C(34)-H(34A)	1.019(17)
C(34)-H(34B)	1.009(16)
C(35)-C(36)	1.506(2)
C(35)-H(35A)	0.954(19)
C(35)-H(35B)	0.947(19)
C(36)-H(36A)	0.978(18)
C(36)-H(36B)	0.955(16)
C(37)-H(37A)	0.997(14)
C(37)-H(37B)	0.965(18)
C(38)-H(38A)	0.896(14)
C(38)-H(38B)	1.004(14)

C(9)-C(8)-C(15)	113.08(11)
C(7)-C(8)-H(8)	110.1(9)
C(9)-C(8)-H(8)	107.9(10)
C(15)-C(8)-H(8)	108.7(10)
N(2)-C(9)-C(10)	111.48(12)
N(2)-C(9)-C(8)	109.09(11)
C(10)-C(9)-C(8)	111.28(12)
N(2)-C(9)-H(9)	106.6(11)
C(10)-C(9)-H(9)	109.4(11)
C(8)-C(9)-H(9)	108.8(11)
C(11)-C(10)-C(9)	112.61(13)
C(11)-C(10)-H(10A)	109.5(10)
C(9)-C(10)-H(10A)	107.2(10)
C(11)-C(10)-H(10B)	110.3(11)
C(9)-C(10)-H(10B)	107.3(10)
H(10A)-C(10)-H(10B)	109.8(13)
C(12)-C(11)-C(10)	109.09(14)
C(12)-C(11)-H(11A)	108.2(9)
C(10)-C(11)-H(11A)	109.1(9)
C(12)-C(11)-H(11B)	107.1(11)
C(10)-C(11)-H(11B)	113.6(11)
H(11A)-C(11)-H(11B)	109.6(14)
C(13)-C(12)-C(11)	109.60(14)
C(13)-C(12)-H(12A)	110.2(10)
C(11)-C(12)-H(12A)	107.9(10)
C(13)-C(12)-H(12B)	108.4(10)
C(11)-C(12)-H(12B)	112.8(10)
H(12A)-C(12)-H(12B)	107.8(14)
N(2)-C(13)-C(12)	111.21(13)
N(2)-C(13)-H(13A)	111.7(9)
C(12)-C(13)-H(13A)	108.1(9)
N(2)-C(13)-H(13B)	106.7(11)
C(12)-C(13)-H(13B)	108.0(10)
H(13A)-C(13)-H(13B)	111.1(14)
N(2)-C(14)-C(6)	111.69(11)
N(2)-C(14)-H(14A)	109.6(9)
C(6)-C(14)-H(14A)	112.2(10)
N(2)-C(14)-H(14B)	109.3(9)
C(6)-C(14)-H(14B)	110.2(9)
H(14A)-C(14)-H(14B)	103.6(13)
N(1)-C(15)-C(8)	108.60(11)
N(1)-C(15)-H(15A)	109.0(9)
C(8)-C(15)-H(15A)	115.8(9)
N(1)-C(15)-H(15B)	106.2(8)
C(8)-C(15)-H(15B)	111.3(8)
H(15A)-C(15)-H(15B)	105.5(11)
O(1)-C(16)-O(2)	126.94(13)
O(1)-C(16)-C(17)	117.77(12)
O(2)-C(16)-C(17)	115.28(12)

C(16)-C(17)-H(17A)	104(2)
C(16)-C(17)-H(17B)	113.5(11)
H(17A)-C(17)-H(17B)	121(3)
C(16)-C(17)-H(17C)	109(2)
H(17A)-C(17)-H(17C)	109(3)
H(17B)-C(17)-H(17C)	101(2)
O(3)-C(18)-O(4)	125.96(14)
O(3)-C(18)-C(19)	119.39(14)
O(4)-C(18)-C(19)	114.65(14)
C(18)-C(19)-H(19A)	110.4(19)
C(18)-C(19)-H(19B)	114.8(16)
H(19A)-C(19)-H(19B)	106(2)
C(18)-C(19)-H(19C)	112(3)
H(19A)-C(19)-H(19C)	111(3)
H(19B)-C(19)-H(19C)	102(3)
O(6)-C(20)-O(5)	127.20(13)
O(6)-C(20)-C(21)	117.05(12)
O(5)-C(20)-C(21)	115.75(12)
C(20)-C(21)-H(21A)	107.0(13)
C(20)-C(21)-H(21B)	112.1(11)
H(21A)-C(21)-H(21B)	115.4(16)
C(20)-C(21)-H(21C)	110.8(11)
H(21A)-C(21)-H(21C)	108.6(16)
H(21B)-C(21)-H(21C)	102.9(14)
O(8)-C(22)-O(7)	126.25(13)
O(8)-C(22)-C(23)	118.82(13)
O(7)-C(22)-C(23)	114.93(13)
C(22)-C(23)-H(23A)	113.8(16)
C(22)-C(23)-H(23B)	110.3(14)
H(23A)-C(23)-H(23B)	121(2)
C(22)-C(23)-H(23C)	116(2)
H(23A)-C(23)-H(23C)	107(2)
H(23B)-C(23)-H(23C)	86(2)
N(3)-C(24)-C(25)	112.55(12)
N(3)-C(24)-H(24A)	105.9(8)
C(25)-C(24)-H(24A)	111.4(8)
N(3)-C(24)-H(24B)	106.1(10)
C(25)-C(24)-H(24B)	109.1(9)
H(24A)-C(24)-H(24B)	111.7(12)
C(24)-C(25)-C(26)	110.02(12)
C(24)-C(25)-H(25A)	108.2(8)
C(26)-C(25)-H(25A)	110.9(8)
C(24)-C(25)-H(25B)	106.9(11)
C(26)-C(25)-H(25B)	114.4(11)
H(25A)-C(25)-H(25B)	106.1(14)
C(27)-C(26)-C(25)	109.31(12)
C(27)-C(26)-H(26A)	109.7(9)
C(25)-C(26)-H(26A)	109.8(8)
C(27)-C(26)-H(26B)	108.8(11)

C(25)-C(26)-H(26B)	108.6(10)
H(26A)-C(26)-H(26B)	110.6(13)
C(26)-C(27)-C(28)	113.61(12)
C(26)-C(27)-H(27A)	109.4(9)
C(28)-C(27)-H(27A)	106.1(9)
C(26)-C(27)-H(27B)	106.3(10)
C(28)-C(27)-H(27B)	111.3(10)
H(27A)-C(27)-H(27B)	110.0(13)
N(3)-C(28)-C(27)	111.13(11)
N(3)-C(28)-C(29)	106.71(10)
C(27)-C(28)-C(29)	112.20(12)
N(3)-C(28)-H(28)	105.9(9)
C(27)-C(28)-H(28)	110.7(9)
C(29)-C(28)-H(28)	110.0(10)
C(37)-C(29)-C(30)	110.20(12)
C(37)-C(29)-C(28)	113.52(12)
C(30)-C(29)-C(28)	106.88(11)
C(37)-C(29)-H(29)	106.3(10)
C(30)-C(29)-H(29)	109.1(9)
C(28)-C(29)-H(29)	110.8(10)
C(31)-C(30)-C(29)	106.89(11)
C(31)-C(30)-Pd(3)	104.67(9)
C(29)-C(30)-Pd(3)	105.15(9)
C(31)-C(30)-H(30)	114.3(10)
C(29)-C(30)-H(30)	113.0(9)
Pd(3)-C(30)-H(30)	112.0(10)
C(30)-C(31)-C(32)	111.39(11)
C(30)-C(31)-C(38)	105.72(11)
C(32)-C(31)-C(38)	114.43(12)
C(30)-C(31)-H(31)	109.2(10)
C(32)-C(31)-H(31)	107.7(10)
C(38)-C(31)-H(31)	108.2(10)
N(4)-C(32)-C(33)	109.93(12)
N(4)-C(32)-C(31)	111.10(11)
C(33)-C(32)-C(31)	111.92(11)
N(4)-C(32)-H(32)	111.5(9)
C(33)-C(32)-H(32)	107.0(9)
C(31)-C(32)-H(32)	105.3(9)
C(34)-C(33)-C(32)	112.48(12)
C(34)-C(33)-H(33A)	110.5(9)
C(32)-C(33)-H(33A)	109.5(9)
C(34)-C(33)-H(33B)	105.7(11)
C(32)-C(33)-H(33B)	106.6(11)
H(33A)-C(33)-H(33B)	112.0(14)
C(33)-C(34)-C(35)	110.57(13)
C(33)-C(34)-H(34A)	110.5(10)
C(35)-C(34)-H(34A)	110.8(10)
C(33)-C(34)-H(34B)	108.1(9)
C(35)-C(34)-H(34B)	110.1(9)

H(34A)-C(34)-H(34B)	106.5(13)
C(36)-C(35)-C(34)	110.25(12)
C(36)-C(35)-H(35A)	110.1(11)
C(34)-C(35)-H(35A)	110.4(11)
C(36)-C(35)-H(35B)	107.3(10)
C(34)-C(35)-H(35B)	107.0(10)
H(35A)-C(35)-H(35B)	111.8(15)
N(4)-C(36)-C(35)	111.59(13)
N(4)-C(36)-H(36A)	111.3(10)
C(35)-C(36)-H(36A)	110.2(10)
N(4)-C(36)-H(36B)	107.4(10)
C(35)-C(36)-H(36B)	113.2(10)
H(36A)-C(36)-H(36B)	102.8(14)
N(4)-C(37)-C(29)	111.76(11)
N(4)-C(37)-H(37A)	106.0(8)
C(29)-C(37)-H(37A)	110.8(9)
N(4)-C(37)-H(37B)	108.2(9)
C(29)-C(37)-H(37B)	110.1(9)
H(37A)-C(37)-H(37B)	109.9(12)
N(3)-C(38)-C(31)	108.16(10)
N(3)-C(38)-H(38A)	109.0(10)
C(31)-C(38)-H(38A)	112.3(10)
N(3)-C(38)-H(38B)	103.8(8)
C(31)-C(38)-H(38B)	111.0(9)
H(38A)-C(38)-H(38B)	112.2(12)

Table 38. Anisotropic displacement parameters ($Å^2$ x 10^4). The anisotropic displacement factor exponent takes the form: $-2\pi^2[h^2a^*2U^{11} + ... + 2 h k a^* b^* U^{12}]$.

	U^{11}	U^{22}	U^{33}	U^{23}	U^{13}	U^{12}
Pd(1)	96(1)	117(1)	129(1)	-7(1)	-2(1)	4(1)
Pd(2)	88(1)	131(1)	139(1)	0(1)	-9(1)	5(1)
Pd(3)	98(1)	121(1)	105(1)	8(1)	-3(1)	-2(1)
O(1)	119(4)	256(6)	175(5)	-59(4)	-14(3)	9(4)
O(2)	124(4)	252(6)	213(5)	-65(4)	-3(4)	-12(4)
O(3)	140(4)	156(5)	211(5)	39(4)	13(4)	18(4)
O(4)	125(4)	210(6)	208(5)	53(4)	6(4)	19(4)
O(5)	118(4)	137(5)	255(5)	38(4)	-10(4)	4(4)
O(6)	116(4)	173(5)	154(4)	42(4)	-6(3)	-20(4)
O(7)	134(4)	157(6)	156(5)	-4(4)	12(4)	-13(4)
O(8)	149(4)	169(5)	153(4)	-9(4)	3(4)	-26(4)
N(1)	97(5)	100(5)	143(5)	-5(4)	-13(3)	-5(4)
N(2)	153(5)	147(7)	220(6)	62(5)	10(4)	-14(5)
N(3)	127(5)	115(6)	133(5)	-4(4)	-8(4)	-4(4)
N(4)	147(5)	160(6)	134(5)	-18(4)	25(4)	9(5)
C(1)	173(6)	122(7)	182(6)	-30(5)	-11(5)	-24(6)
C(2)	221(7)	108(8)	222(8)	-12(5)	5(5)	17(6)
C(3)	190(7)	168(8)	203(7)	-20(5)	4(6)	53(6)
C(4)	151(6)	164(7)	149(6)	12(5)	0(5)	22(5)

C(5)	110(5)	135(7)	131(6)	-2(5)	8(4)	-12(5)
C(6)	97(6)	148(7)	193(7)	-1(5)	-24(5)	-24(5)
C(7)	135(5)	121(7)	176(6)	-27(5)	14(5)	-2(5)
C(8)	120(5)	122(7)	208(6)	13(5)	4(5)	1(6)
C(9)	148(6)	105(7)	253(7)	23(5)	2(5)	0(5)
C(10)	202(8)	169(9)	340(9)	85(7)	-61(6)	-10(6)
C(11)	302(9)	179(9)	322(9)	106(7)	-46(7)	4(7)
C(12)	388(9)	205(9)	280(8)	101(7)	20(7)	14(8)
C(13)	256(8)	176(9)	313(9)	79(7)	65(7)	-6(7)
C(14)	139(6)	152(8)	274(7)	30(6)	11(5)	-27(6)
C(15)	126(6)	139(7)	170(7)	27(5)	-32(5)	-13(5)
C(16)	158(6)	184(8)	163(7)	-36(5)	2(5)	-10(5)
C(17)	214(7)	449(13)	270(8)	-202(9)	11(6)	-36(8)
C(18)	164(6)	142(7)	179(7)	15(5)	-40(5)	-17(5)
C(19)	243(9)	240(10)	448(12)	187(9)	-4(8)	19(7)
C(20)	150(6)	139(7)	131(6)	-21(5)	5(4)	26(5)
C(21)	197(7)	154(8)	214(7)	44(5)	31(6)	31(6)
C(22)	164(6)	136(7)	121(6)	14(5)	-27(5)	10(5)
C(23)	304(9)	243(10)	187(8)	-77(6)	42(6)	-49(8)
C(24)	220(7)	112(7)	187(7)	10(5)	-14(6)	16(5)
C(25)	283(8)	132(8)	185(7)	-11(6)	3(5)	-38(6)
C(26)	234(7)	208(8)	232(8)	-7(6)	4(6)	-87(6)
C(27)	153(6)	229(8)	170(7)	0(6)	-10(5)	-51(6)
C(28)	116(6)	164(7)	127(6)	19(5)	3(4)	-16(5)
C(29)	106(6)	147(7)	151(6)	23(5)	-7(5)	18(5)
C(30)	135(6)	117(7)	146(6)	30(5)	20(5)	14(5)
C(31)	114(5)	144(7)	142(5)	-21(5)	8(5)	-3(5)
C(32)	149(6)	141(7)	147(6)	-15(5)	10(5)	-5(5)
C(33)	224(8)	225(9)	192(7)	-65(6)	-49(6)	32(6)
C(34)	291(8)	236(9)	174(6)	-53(6)	-44(5)	12(7)
C(35)	373(9)	212(9)	149(7)	-28(6)	53(6)	-40(7)
C(36)	234(7)	167(8)	181(7)	-32(5)	82(5)	-14(6)
C(37)	131(6)	174(8)	191(7)	7(5)	34(5)	36(5)
C(38)	124(6)	168(7)	116(6)	2(5)	-30(5)	16(5)

Table 39. Hydrogen coordinates (x 10^4) and isotropic displacement parameters (Å^2 x 10^3).

	x	y	z	Uiso
H(1A)	3373(14)	1829(10)	9175(6)	9(4)
H(1B)	2484(14)	1682(9)	9684(7)	17(4)
H(2A)	1760(13)	2363(10)	8679(7)	14(4)
H(2B)	1807(14)	2817(11)	9196(7)	16(4)
H(3A)	180(14)	2084(10)	9580(7)	14(4)
H(3B)	-251(15)	2469(11)	9029(7)	27(5)
H(4A)	-777(14)	1013(10)	9097(6)	18(4)
H(4B)	109(12)	1237(9)	8589(6)	8(4)
H(5)	946(11)	593(10)	9629(6)	7(3)
H(6)	262(14)	-240(10)	8673(7)	18(4)
H(7)	2055(13)	-888(9)	8378(6)	13(4)
H(8)	3782(13)	-721(10)	8945(6)	14(4)

H(9)	2525(15)	-1724(11)	9332(7)	27(5)
H(10A)	3895(15)	-851(12)	10126(7)	29(5)
H(10B)	4411(15)	-1607(11)	9760(7)	26(5)
H(11A)	3139(14)	-2518(11)	10267(6)	18(4)
H(11B)	3891(16)	-2014(12)	10738(8)	31(5)
H(12A)	1829(15)	-2066(11)	10978(7)	26(5)
H(12B)	2181(14)	-1148(10)	10868(6)	16(4)
H(13A)	967(14)	-2140(10)	10076(7)	13(4)
H(13B)	435(14)	-1381(10)	10390(7)	17(4)
H(14A)	-245(14)	-823(11)	9551(7)	24(4)
H(14B)	403(15)	-1478(11)	9169(7)	20(4)
H(15A)	3048(13)	299(9)	9767(7)	12(4)
H(15B)	4066(11)	513(10)	9311(6)	8(4)
H(17A)	3110(30)	-1018(18)	6786(13)	93(11)
H(17B)	4313(17)	-883(12)	6545(8)	36(5)
H(17C)	3210(30)	-400(20)	6411(14)	130(13)
H(19A)	3260(20)	2929(17)	7189(12)	87(10)
H(19B)	4460(20)	2973(14)	7164(10)	51(7)
H(19C)	3930(30)	3250(20)	7612(15)	129(15)
H(21A)	7634(18)	-1539(13)	8757(9)	47(6)
H(21B)	6421(15)	-1442(11)	9105(7)	21(5)
H(21C)	7596(15)	-1056(11)	9296(7)	28(5)
H(23A)	7180(20)	2765(15)	9246(11)	78(8)
H(23B)	6270(20)	2106(15)	9600(10)	62(7)
H(23C)	5910(20)	2667(18)	9278(12)	80(9)
H(24A)	7163(12)	2491(9)	7279(6)	6(3)
H(24B)	8070(14)	2606(10)	6727(7)	21(4)
H(25A)	8885(12)	2678(9)	7870(7)	8(3)
H(25B)	8761(15)	3382(12)	7478(7)	28(5)
H(26A)	10338(12)	2897(9)	6884(6)	2(3)
H(26B)	10912(16)	2964(12)	7526(8)	39(5)
H(27A)	10449(12)	1569(9)	7630(6)	8(4)
H(27B)	11274(14)	1696(10)	7095(7)	20(4)
H(28)	9545(13)	1429(10)	6533(7)	13(4)
H(29)	10216(12)	256(9)	7255(6)	11(4)
H(30)	8421(12)	-417(10)	7339(6)	10(4)
H(31)	6678(14)	-3(10)	6870(7)	20(4)
H(32)	7799(12)	-759(9)	6291(6)	9(4)
H(33A)	6042(13)	-286(10)	5862(6)	13(4)
H(33B)	6892(14)	428(11)	5666(7)	21(5)
H(34A)	6664(15)	-353(12)	4872(7)	29(5)
H(34B)	7177(14)	-1117(10)	5242(6)	17(4)
H(35A)	8841(15)	-594(13)	4710(8)	36(5)
H(35B)	8597(14)	282(12)	4960(7)	24(5)
H(36A)	9466(14)	-1033(11)	5602(7)	22(4)
H(36B)	10272(14)	-316(10)	5443(7)	20(4)
H(37A)	10777(13)	130(10)	6309(6)	12(4)
H(37B)	10068(13)	-662(11)	6543(6)	22(4)
H(38A)	7513(13)	1313(9)	6351(6)	11(4)

H(38B)	6505(13)	1332(9)	6831(6)	7(4)

A.5 (CCDC 717605)

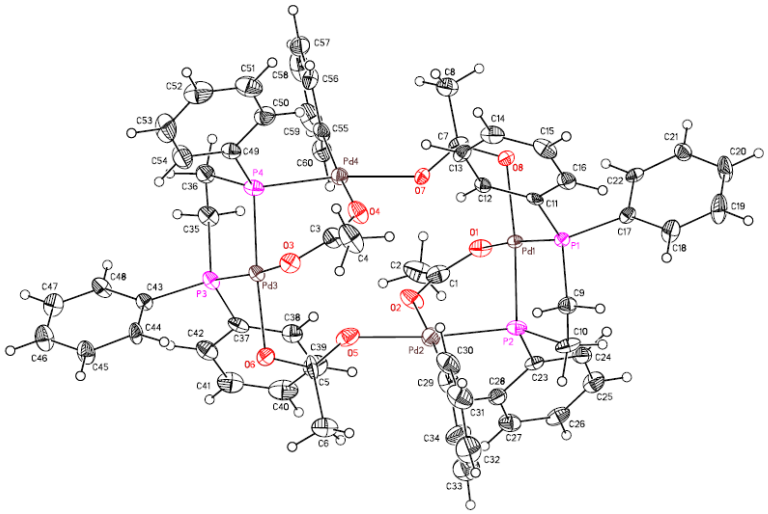

Special Refinement Details

Crystals were mounted on a glass fiber using Paratone oil then placed on the diffractometer under a nitrogen stream at 100K.

This crystal is twinned, or worse (see last figures), and we were unable to obtain a meaningful integration accounting for the multiple crystals. Therefore only the major component was used. The figures clearly show reflections not predicted by the orientation represented by the circles. This undoubtedly accounts for the higher than usual agreement factors.

Refinement of F^2 against ALL reflections. The weighted R-factor (wR) and goodness of fit (S) are based on F^2, conventional R-factors (R) are based on F, with F set to zero for negative F^2. The threshold expression of $F^2 > 2\sigma (F^2)$ is used only for calculating R-factors(gt) etc. and is not relevant to the choice of reflections for refinement. R-factors based on F^2 are statistically about twice as large as those based on F, and R-factors based on ALL data will be even larger.

All esds (except the esd in the dihedral angle between two l.s. planes) are estimated using the full covariance matrix. The cell esds are taken into account individually in the estimation of esds in distances, angles and torsion angles; correlations between esds in cell parameters are only used when they are defined by crystal symmetry. An approximate (isotropic) treatment of cell esds is used for estimating esds involving l.s. planes.

Table 40. Atomic coordinates (x 10^4) and equivalent isotropic displacement parameters ($Å^2$ x 10^3). U(eq) is defined as the trace of the orthogonalized Uij tensor.

	x	y	z	Ueq
Pd(1)	2038(1)	8043(1)	2513(1)	12(1)
Pd(2)	3438(1)	9141(1)	3385(1)	24(1)
Pd(3)	2914(1)	11206(1)	2478(1)	15(1)
Pd(4)	1470(1)	10123(1)	1591(1)	19(1)
P(1)	3277(1)	7470(1)	2174(1)	13(1)
P(2)	3141(1)	8090(1)	3421(1)	19(1)
P(3)	1724(1)	11766(1)	2875(1)	18(1)
P(4)	1727(1)	11174(1)	1601(1)	18(1)
O(1)	853(3)	8468(2)	2916(2)	21(1)
O(2)	1777(3)	9341(2)	3311(2)	27(1)
O(3)	4063(3)	10792(2)	2032(2)	22(1)

O(4)	3141(3)	9925(2)	1639(2)	28(1)
O(5)	3618(3)	10152(2)	3261(2)	29(1)
O(6)	3998(3)	11162(2)	3355(2)	21(1)
O(7)	1341(3)	9120(2)	1704(2)	18(1)
O(8)	1007(3)	8085(2)	1619(2)	17(1)
C(1)	975(5)	9006(4)	3213(3)	27(2)
C(2)	-14(5)	9225(4)	3450(3)	40(2)
C(3)	3957(5)	10252(3)	1744(3)	26(2)
C(4)	4903(5)	10032(4)	1498(4)	40(2)
C(5)	4021(6)	10605(3)	3547(3)	27(2)
C(6)	4784(6)	10502(4)	4186(3)	45(2)
C(7)	883(4)	8653(3)	1419(3)	16(1)
C(8)	163(5)	8745(3)	800(3)	27(2)
C(9)	4483(5)	7456(3)	2765(3)	21(1)
C(10)	4144(5)	7481(3)	3429(3)	26(2)
C(11)	3672(4)	7768(3)	1457(3)	15(1)
C(12)	3451(4)	8390(3)	1278(3)	15(1)
C(13)	3742(5)	8613(3)	726(3)	21(2)
C(14)	4217(5)	8231(3)	355(3)	27(2)
C(15)	4454(5)	7605(3)	531(3)	27(2)
C(16)	4178(5)	7368(3)	1085(3)	22(2)
C(17)	2864(4)	6656(3)	2007(3)	16(1)
C(18)	3576(5)	6142(3)	2068(3)	28(2)
C(19)	3237(6)	5540(3)	1893(4)	36(2)
C(20)	2176(5)	5434(3)	1636(3)	31(2)
C(21)	1463(5)	5932(3)	1563(3)	21(1)
C(22)	1801(5)	6538(3)	1749(3)	15(1)
C(23)	2542(5)	7904(3)	4109(3)	17(1)
C(24)	2086(5)	7319(3)	4173(3)	23(2)
C(25)	1625(5)	7198(3)	4697(3)	29(2)
C(26)	1617(5)	7660(3)	5149(3)	26(2)
C(27)	2048(5)	8251(3)	5075(3)	26(2)
C(28)	2502(5)	8377(3)	4562(3)	22(2)
C(29)	4968(5)	8960(3)	3594(4)	31(2)
C(30)	5614(6)	8949(3)	3151(4)	34(2)
C(31)	6716(6)	8832(4)	3320(4)	39(2)
C(32)	7158(6)	8772(4)	3948(4)	42(2)
C(33)	6516(6)	8812(4)	4399(4)	43(2)
C(34)	5461(6)	8883(4)	4219(3)	35(2)
C(35)	455(5)	11747(3)	2327(3)	23(2)
C(36)	693(5)	11751(3)	1654(3)	24(2)
C(37)	1435(4)	11468(3)	3617(3)	18(1)
C(38)	1568(5)	10822(3)	3748(3)	23(2)
C(39)	1336(5)	10567(4)	4296(3)	32(2)
C(40)	958(5)	10975(4)	4715(3)	36(2)
C(41)	829(5)	11611(4)	4597(3)	32(2)
C(42)	1070(5)	11871(3)	4050(3)	26(2)
C(43)	2124(5)	12593(3)	3004(3)	18(1)
C(44)	3196(5)	12719(3)	3135(3)	22(2)

C(45)	3533(5)	13340(3)	3263(3)	28(2)
C(46)	2817(5)	13833(3)	3226(3)	32(2)
C(47)	1745(5)	13700(3)	3074(3)	26(2)
C(48)	1415(5)	13097(3)	2966(3)	25(2)
C(49)	2231(5)	11421(3)	912(3)	20(1)
C(50)	2283(5)	10983(3)	434(3)	27(2)
C(51)	2663(6)	11154(4)	-107(3)	38(2)
C(52)	3013(6)	11770(4)	-166(4)	40(2)
C(53)	2998(6)	12195(4)	310(4)	41(2)
C(54)	2611(6)	12017(3)	846(3)	35(2)
C(55)	-86(5)	10306(3)	1390(3)	22(2)
C(56)	-552(5)	10401(3)	768(3)	29(2)
C(57)	-1647(6)	10503(3)	605(4)	36(2)
C(58)	-2263(6)	10523(3)	1065(4)	43(2)
C(59)	-1801(6)	10428(4)	1677(4)	38(2)
C(60)	-727(5)	10317(3)	1841(3)	27(2)

Table 41. Bond lengths [Å] and angles [°].

Pd(1)-O(1)	2.080(4)	O(1)-Pd(1)-O(8)	88.77(15)
Pd(1)-O(8)	2.145(4)	O(1)-Pd(1)-P(2)	90.56(12)
Pd(1)-P(2)	2.2136(17)	O(8)-Pd(1)-P(2)	174.80(12)
Pd(1)-P(1)	2.2147(16)	O(1)-Pd(1)-P(1)	171.64(13)
Pd(2)-C(29)	1.973(7)	O(8)-Pd(1)-P(1)	95.18(11)
Pd(2)-O(5)	2.153(5)	P(2)-Pd(1)-P(1)	86.16(6)
Pd(2)-O(2)	2.150(4)	C(29)-Pd(2)-O(5)	95.4(2)
Pd(2)-P(2)	2.2399(18)	C(29)-Pd(2)-O(2)	171.2(2)
Pd(3)-O(3)	2.084(4)	O(5)-Pd(2)-O(2)	85.72(17)
Pd(3)-O(6)	2.149(4)	C(29)-Pd(2)-P(2)	88.4(2)
Pd(3)-P(3)	2.2138(17)	O(5)-Pd(2)-P(2)	174.24(12)
Pd(3)-P(4)	2.2163(17)	O(2)-Pd(2)-P(2)	91.24(13)
Pd(4)-C(55)	2.004(6)	O(3)-Pd(3)-O(6)	89.33(16)
Pd(4)-O(7)	2.127(4)	O(3)-Pd(3)-P(3)	172.01(13)
Pd(4)-O(4)	2.169(4)	O(6)-Pd(3)-P(3)	93.70(12)
Pd(4)-P(4)	2.2268(18)	O(3)-Pd(3)-P(4)	91.63(12)
P(1)-C(17)	1.805(6)	O(6)-Pd(3)-P(4)	174.87(12)
P(1)-C(11)	1.823(6)	P(3)-Pd(3)-P(4)	86.01(6)
P(1)-C(9)	1.827(6)	C(55)-Pd(4)-O(7)	96.9(2)
P(2)-C(23)	1.829(6)	C(55)-Pd(4)-O(4)	170.4(2)
P(2)-C(10)	1.811(7)	O(7)-Pd(4)-O(4)	84.32(16)
P(3)-C(43)	1.816(6)	C(55)-Pd(4)-P(4)	87.30(18)
P(3)-C(37)	1.817(6)	O(7)-Pd(4)-P(4)	172.44(12)
P(3)-C(35)	1.841(6)	O(4)-Pd(4)-P(4)	92.60(13)
P(4)-C(49)	1.800(6)	C(17)-P(1)-C(11)	105.6(3)
P(4)-C(36)	1.815(6)	C(17)-P(1)-C(9)	107.9(3)
O(1)-C(1)	1.294(8)	C(11)-P(1)-C(9)	105.8(3)
O(2)-C(1)	1.234(8)	C(17)-P(1)-Pd(1)	112.1(2)
O(3)-C(3)	1.290(8)	C(11)-P(1)-Pd(1)	114.7(2)
O(4)-C(3)	1.238(7)	C(9)-P(1)-Pd(1)	110.3(2)
O(5)-C(5)	1.201(7)	C(23)-P(2)-C(10)	103.9(3)

O(6)-C(5)	1.237(7)	C(23)-P(2)-Pd(1)	114.7(2)
O(7)-C(7)	1.249(7)	C(10)-P(2)-Pd(1)	108.7(2)
O(8)-C(7)	1.267(7)	C(23)-P(2)-Pd(2)	109.7(2)
C(1)-C(2)	1.519(9)	C(10)-P(2)-Pd(2)	124.6(2)
C(3)-C(4)	1.481(9)	Pd(1)-P(2)-Pd(2)	95.74(7)
C(5)-C(6)	1.562(9)	C(43)-P(3)-C(37)	106.8(3)
C(7)-C(8)	1.500(8)	C(43)-P(3)-C(35)	108.3(3)
C(9)-C(10)	1.570(8)	C(37)-P(3)-C(35)	105.5(3)
C(11)-C(12)	1.376(8)	C(43)-P(3)-Pd(3)	111.8(2)
C(11)-C(16)	1.397(8)	C(37)-P(3)-Pd(3)	114.8(2)
C(12)-C(13)	1.392(8)	C(35)-P(3)-Pd(3)	109.3(2)
C(13)-C(14)	1.351(9)	C(49)-P(4)-C(36)	103.4(3)
C(14)-C(15)	1.387(9)	C(49)-P(4)-Pd(4)	110.5(2)
C(15)-C(16)	1.397(8)	C(36)-P(4)-Pd(4)	123.5(2)
C(17)-C(18)	1.404(8)	C(49)-P(4)-Pd(3)	114.0(2)
C(17)-C(22)	1.403(8)	C(36)-P(4)-Pd(3)	109.1(2)
C(18)-C(19)	1.367(9)	Pd(4)-P(4)-Pd(3)	96.70(7)
C(19)-C(20)	1.396(9)	C(1)-O(1)-Pd(1)	123.2(4)
C(20)-C(21)	1.379(9)	C(1)-O(2)-Pd(2)	133.5(4)
C(21)-C(22)	1.379(8)	C(3)-O(3)-Pd(3)	124.4(4)
C(23)-C(24)	1.376(9)	C(3)-O(4)-Pd(4)	134.5(4)
C(23)-C(28)	1.402(8)	C(5)-O(5)-Pd(2)	139.5(4)
C(24)-C(25)	1.390(9)	C(5)-O(6)-Pd(3)	108.1(4)
C(25)-C(26)	1.378(9)	C(7)-O(7)-Pd(4)	139.3(4)
C(26)-C(27)	1.377(9)	C(7)-O(8)-Pd(1)	111.6(4)
C(27)-C(28)	1.365(9)	O(2)-C(1)-O(1)	127.4(6)
C(29)-C(30)	1.370(9)	O(2)-C(1)-C(2)	119.3(6)
C(29)-C(34)	1.399(9)	O(1)-C(1)-C(2)	113.3(6)
C(30)-C(31)	1.419(10)	O(4)-C(3)-O(3)	126.1(6)
C(31)-C(32)	1.383(10)	O(4)-C(3)-C(4)	118.8(6)
C(32)-C(33)	1.384(10)	O(3)-C(3)-C(4)	115.1(6)
C(33)-C(34)	1.350(9)	O(5)-C(5)-O(6)	126.2(7)
C(35)-C(36)	1.536(8)	O(5)-C(5)-C(6)	119.5(6)
C(37)-C(38)	1.388(9)	O(6)-C(5)-C(6)	113.8(6)
C(37)-C(42)	1.402(8)	O(7)-C(7)-O(8)	123.2(5)
C(38)-C(39)	1.378(9)	O(7)-C(7)-C(8)	120.2(6)
C(39)-C(40)	1.392(10)	O(8)-C(7)-C(8)	116.6(6)
C(40)-C(41)	1.362(10)	C(10)-C(9)-P(1)	107.6(4)
C(41)-C(42)	1.385(9)	C(9)-C(10)-P(2)	108.9(4)
C(43)-C(48)	1.386(8)	C(12)-C(11)-C(16)	120.1(6)
C(43)-C(44)	1.380(8)	C(12)-C(11)-P(1)	119.3(5)
C(44)-C(45)	1.385(8)	C(16)-C(11)-P(1)	120.6(5)
C(45)-C(46)	1.376(9)	C(11)-C(12)-C(13)	119.2(6)
C(46)-C(47)	1.386(9)	C(14)-C(13)-C(12)	121.6(6)
C(47)-C(48)	1.341(9)	C(13)-C(14)-C(15)	119.9(6)
C(49)-C(54)	1.357(9)	C(14)-C(15)-C(16)	119.7(6)
C(49)-C(50)	1.394(9)	C(15)-C(16)-C(11)	119.5(6)
C(50)-C(51)	1.390(9)	C(18)-C(17)-C(22)	118.2(6)
C(51)-C(52)	1.380(10)	C(18)-C(17)-P(1)	122.9(5)

C(52)-C(53)	1.365(10)	C(22)-C(17)-P(1)	118.6(4)
C(53)-C(54)	1.387(10)	C(17)-C(18)-C(19)	120.8(6)
C(55)-C(56)	1.389(9)	C(20)-C(19)-C(18)	119.9(6)
C(55)-C(60)	1.381(9)	C(19)-C(20)-C(21)	120.4(6)
C(56)-C(57)	1.403(9)	C(20)-C(21)-C(22)	119.7(6)
C(57)-C(58)	1.375(11)	C(21)-C(22)-C(17)	120.9(6)
C(58)-C(59)	1.367(11)	C(24)-C(23)-C(28)	119.5(6)
C(59)-C(60)	1.382(9)	C(24)-C(23)-P(2)	121.2(5)
		C(28)-C(23)-P(2)	119.2(5)
		C(23)-C(24)-C(25)	119.7(6)
		C(26)-C(25)-C(24)	120.4(6)
		C(27)-C(26)-C(25)	119.9(6)
		C(26)-C(27)-C(28)	120.4(6)
		C(27)-C(28)-C(23)	120.2(6)
		C(30)-C(29)-C(34)	116.5(7)
		C(30)-C(29)-Pd(2)	122.8(6)
		C(34)-C(29)-Pd(2)	120.5(5)
		C(29)-C(30)-C(31)	121.4(7)
		C(32)-C(31)-C(30)	119.2(7)
		C(31)-C(32)-C(33)	119.6(7)
		C(34)-C(33)-C(32)	119.5(8)
		C(33)-C(34)-C(29)	123.6(7)
		C(36)-C(35)-P(3)	108.1(4)
		C(35)-C(36)-P(4)	108.9(4)
		C(38)-C(37)-C(42)	119.6(6)
		C(38)-C(37)-P(3)	118.6(5)
		C(42)-C(37)-P(3)	121.7(5)
		C(37)-C(38)-C(39)	121.2(7)
		C(40)-C(39)-C(38)	118.2(7)
		C(41)-C(40)-C(39)	121.7(7)
		C(42)-C(41)-C(40)	120.4(7)
		C(41)-C(42)-C(37)	118.9(7)
		C(48)-C(43)-C(44)	119.1(6)
		C(48)-C(43)-P(3)	123.6(5)
		C(44)-C(43)-P(3)	117.3(5)
		C(45)-C(44)-C(43)	119.1(6)
		C(44)-C(45)-C(46)	120.8(6)
		C(47)-C(46)-C(45)	119.2(7)
		C(48)-C(47)-C(46)	120.1(6)
		C(47)-C(48)-C(43)	121.7(6)
		C(54)-C(49)-C(50)	117.7(6)
		C(54)-C(49)-P(4)	122.7(5)
		C(50)-C(49)-P(4)	119.6(5)
		C(49)-C(50)-C(51)	121.4(7)
		C(52)-C(51)-C(50)	119.2(7)
		C(53)-C(52)-C(51)	119.5(7)
		C(52)-C(53)-C(54)	120.5(7)
		C(49)-C(54)-C(53)	121.5(7)
		C(56)-C(55)-C(60)	118.2(6)

C(56)-C(55)-Pd(4)	118.9(5)
C(60)-C(55)-Pd(4)	122.9(5)
C(57)-C(56)-C(55)	120.6(7)
C(58)-C(57)-C(56)	119.9(7)
C(59)-C(58)-C(57)	119.3(7)
C(58)-C(59)-C(60)	121.2(7)
C(55)-C(60)-C(59)	120.8(7)

Table 42. Anisotropic displacement parameters ($Å^2$ x 10^4). The anisotropic displacement factor exponent takes the form: $-2\pi^2[h^2a^*2U^{11} + ... + 2 h k a^* b^* U^{12}]$.

	U^{11}	U^{22}	U^{33}	U^{23}	U^{13}	U^{12}
Pd(1)	85(2)	160(2)	123(2)	4(2)	15(2)	-2(2)
Pd(2)	223(3)	230(3)	248(3)	13(2)	29(2)	-10(2)
Pd(3)	111(2)	164(3)	186(3)	-26(2)	39(2)	-17(2)
Pd(4)	162(3)	185(3)	215(3)	-4(2)	28(2)	-12(2)
P(1)	79(8)	159(8)	156(8)	10(7)	11(6)	-14(6)
P(2)	147(8)	276(10)	150(9)	-5(7)	19(7)	-29(7)
P(3)	109(8)	185(9)	240(9)	-54(7)	50(7)	-19(7)
P(4)	121(8)	265(10)	174(9)	-16(8)	34(7)	-33(7)
O(1)	70(20)	340(30)	230(20)	-10(20)	32(18)	28(19)
O(2)	80(20)	350(30)	370(30)	-150(20)	0(20)	-10(20)
O(3)	100(20)	280(30)	280(30)	-10(20)	61(18)	14(19)
O(4)	190(30)	260(30)	400(30)	-90(20)	60(20)	-20(20)
O(5)	180(30)	380(30)	290(30)	120(20)	-30(20)	-70(20)
O(6)	140(20)	220(30)	250(30)	50(20)	9(19)	-61(19)
O(7)	180(20)	150(20)	200(20)	22(19)	3(18)	36(19)
O(8)	170(20)	180(20)	150(20)	14(19)	18(17)	18(18)
C(1)	230(40)	390(40)	190(40)	10(30)	60(30)	80(30)
C(2)	180(40)	690(60)	360(40)	-260(40)	110(30)	30(40)
C(3)	230(40)	260(40)	290(40)	-30(30)	50(30)	0(30)
C(4)	190(40)	390(50)	650(60)	-210(40)	150(40)	-40(30)
C(5)	530(50)	80(30)	240(40)	-40(30)	230(30)	-60(30)
C(6)	530(50)	460(50)	290(40)	0(40)	-80(40)	-40(40)
C(7)	60(30)	270(40)	160(30)	30(30)	50(20)	50(30)
C(8)	250(40)	320(40)	240(40)	-40(30)	20(30)	40(30)
C(9)	170(30)	230(40)	210(30)	0(30)	20(30)	20(30)
C(10)	220(40)	440(50)	130(30)	60(30)	10(30)	60(30)
C(11)	90(30)	180(30)	150(30)	-30(30)	-30(20)	-50(20)
C(12)	110(30)	170(30)	170(30)	-10(30)	20(20)	-40(30)
C(13)	120(30)	220(40)	260(40)	80(30)	-10(30)	-20(30)
C(14)	220(40)	380(40)	200(40)	30(30)	40(30)	-110(30)
C(15)	220(40)	360(40)	250(40)	-110(30)	100(30)	-70(30)
C(16)	160(30)	240(40)	240(40)	-10(30)	10(30)	-70(30)
C(17)	100(30)	180(30)	200(30)	40(30)	20(20)	20(30)
C(18)	120(30)	230(40)	470(50)	90(30)	0(30)	-20(30)
C(19)	280(40)	180(40)	650(60)	30(40)	150(40)	90(30)
C(20)	220(40)	150(30)	540(50)	-10(30)	40(30)	-50(30)
C(21)	200(30)	200(30)	230(40)	-20(30)	20(30)	-30(30)
C(22)	110(30)	220(30)	130(30)	20(30)	30(20)	60(30)

C(23)	130(30)	250(40)	130(30)	50(30)	10(20)	-10(30)
C(24)	240(40)	250(40)	180(30)	10(30)	10(30)	-20(30)
C(25)	230(40)	320(40)	310(40)	110(30)	40(30)	-80(30)
C(26)	210(40)	390(40)	190(40)	120(30)	70(30)	20(30)
C(27)	260(40)	330(40)	190(40)	-40(30)	40(30)	20(30)
C(28)	220(40)	230(40)	200(40)	40(30)	0(30)	-30(30)
C(29)	230(40)	280(40)	450(50)	-60(40)	110(30)	-20(30)
C(30)	300(40)	350(40)	370(50)	-70(40)	60(30)	-140(30)
C(31)	290(40)	440(50)	430(50)	-60(40)	90(40)	-160(40)
C(32)	280(40)	430(50)	560(60)	-40(40)	50(40)	20(40)
C(33)	330(50)	490(50)	450(50)	10(40)	40(40)	-20(40)
C(34)	330(40)	440(50)	270(40)	30(40)	0(30)	160(40)
C(35)	110(30)	290(40)	300(40)	-60(30)	60(30)	-10(30)
C(36)	200(40)	240(40)	280(40)	-40(30)	10(30)	20(30)
C(37)	50(30)	290(40)	190(30)	-70(30)	20(20)	-70(30)
C(38)	170(30)	290(40)	230(40)	0(30)	40(30)	-40(30)
C(39)	210(40)	410(50)	330(40)	70(40)	60(30)	-40(30)
C(40)	290(40)	590(60)	220(40)	0(40)	90(30)	-60(40)
C(41)	250(40)	460(50)	260(40)	-60(40)	90(30)	30(40)
C(42)	170(40)	310(40)	280(40)	-70(30)	50(30)	-40(30)
C(43)	130(30)	180(30)	210(30)	-30(30)	30(30)	-10(30)
C(44)	140(30)	120(30)	380(40)	-30(30)	30(30)	30(30)
C(45)	200(40)	210(40)	430(50)	-20(30)	50(30)	-60(30)
C(46)	240(40)	240(40)	500(50)	-40(40)	120(30)	-10(30)
C(47)	190(40)	270(40)	360(40)	30(30)	100(30)	0(30)
C(48)	90(30)	250(40)	380(40)	-140(30)	-10(30)	60(30)
C(49)	150(30)	260(40)	190(30)	-10(30)	30(30)	-50(30)
C(50)	270(40)	300(40)	220(40)	50(30)	50(30)	-50(30)
C(51)	420(50)	490(50)	240(40)	-70(40)	70(30)	-30(40)
C(52)	340(50)	580(60)	290(40)	130(40)	100(30)	-140(40)
C(53)	460(50)	290(40)	510(50)	60(40)	190(40)	-180(40)
C(54)	440(50)	260(40)	360(40)	-50(40)	90(40)	-50(40)
C(55)	170(30)	180(30)	310(40)	-30(30)	0(30)	-60(30)
C(56)	360(40)	170(40)	310(40)	60(30)	-10(30)	0(30)
C(57)	290(40)	250(40)	460(50)	20(40)	-160(40)	10(30)
C(58)	180(40)	240(40)	840(70)	-80(50)	40(40)	-10(30)
C(59)	280(40)	350(50)	560(60)	-150(40)	220(40)	-90(40)
C(60)	260(40)	250(40)	310(40)	-10(30)	100(30)	-50(30)

A.5m (CCDC 723085)

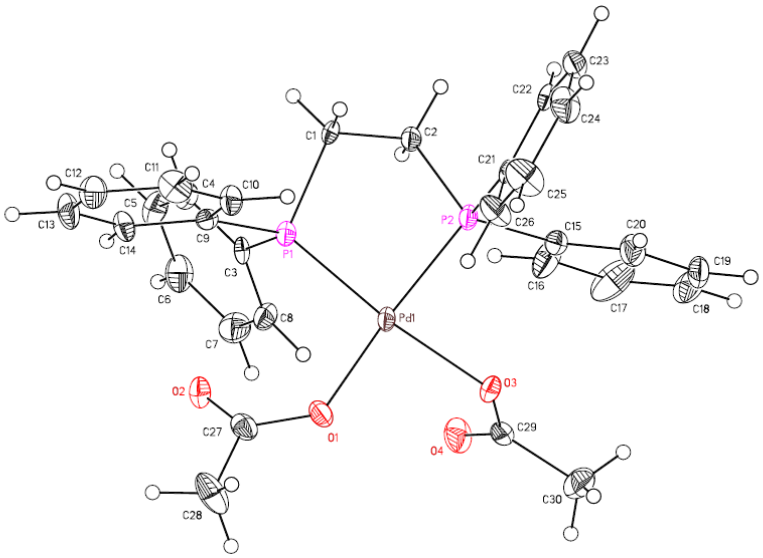

Special Refinement Details

Crystals were mounted on a glass fiber using Paratone oil then placed on the diffractometer under a nitrogen stream at 100K.

The asymmetric unit contains a molecule of acetone at a center of symmetry and refined without restraints at half occupancy.

Refinement of F^2 against ALL reflections. The weighted R-factor (wR) and goodness of fit (S) are based on F^2, conventional R-factors (R) are based on F, with F set to zero for negative F^2. The threshold expression of $F^2 > 2\sigma (F^2)$ is used only for calculating R-factors(gt) etc. and is not relevant to the choice of reflections for refinement. R-factors based on F^2 are statistically about twice as large as those based on F, and R-factors based on ALL data will be even larger.

All esds (except the esd in the dihedral angle between two l.s. planes) are estimated using the full covariance matrix. The cell esds are taken into account individually in the estimation of esds in distances, angles and torsion angles; correlations between esds in cell parameters are only used when they are defined by crystal symmetry. An approximate (isotropic) treatment of cell esds is used for estimating esds involving l.s. planes.

Table 43. Atomic coordinates (x 10^4) and equivalent isotropic displacement parameters (Å^2 x 10^3). U(eq) is defined as the trace of the orthogonalized Uij tensor.

	x	y	z	Ueq
Pd(1)	2933(1)	3374(1)	4057(1)	15(1)
P(1)	4664(1)	2933(1)	5241(1)	16(1)
P(2)	2038(1)	3070(1)	5095(1)	15(1)
O(1)	3651(2)	3830(1)	3109(2)	21(1)
O(2)	5381(2)	3190(1)	3488(2)	24(1)
O(3)	1199(2)	3760(1)	3048(2)	19(1)
O(4)	1243(2)	2743(1)	2308(2)	28(1)
C(1)	4363(3)	2784(2)	6386(2)	17(1)
C(2)	3057(3)	2484(2)	6067(2)	17(1)
C(3)	5037(3)	2070(2)	4931(3)	15(1)
C(4)	5990(3)	1677(2)	5649(3)	21(1)
C(5)	6231(3)	1013(2)	5408(3)	26(1)

C(6)	5541(3)	731(2)	4474(3)	27(1)
C(7)	4595(3)	1116(2)	3763(3)	28(1)
C(8)	4348(3)	1780(2)	3988(3)	20(1)
C(9)	6040(3)	3480(2)	5709(2)	15(1)
C(10)	5921(3)	4139(2)	6044(3)	22(1)
C(11)	6929(3)	4586(2)	6434(3)	26(1)
C(12)	8070(3)	4354(2)	6482(3)	26(1)
C(13)	8196(3)	3705(2)	6150(3)	27(1)
C(14)	7191(3)	3255(2)	5743(2)	21(1)
C(15)	523(3)	2664(2)	4502(3)	18(1)
C(16)	424(3)	1986(2)	4165(3)	33(1)
C(17)	-723(3)	1674(2)	3689(3)	44(1)
C(18)	-1787(3)	2055(3)	3539(3)	38(1)
C(19)	-1703(3)	2728(2)	3849(3)	31(1)
C(20)	-555(3)	3045(2)	4332(3)	26(1)
C(21)	1851(3)	3837(2)	5762(2)	16(1)
C(22)	1531(2)	3779(2)	6597(2)	18(1)
C(23)	1387(3)	4373(2)	7080(3)	25(1)
C(24)	1536(3)	5023(2)	6739(3)	29(1)
C(25)	1864(3)	5081(2)	5925(3)	36(1)
C(26)	2020(3)	4491(2)	5438(3)	28(1)
C(27)	4710(3)	3680(2)	3073(3)	21(1)
C(28)	5056(3)	4192(2)	2421(3)	38(1)
C(29)	728(3)	3292(2)	2361(3)	22(1)
C(30)	-584(3)	3432(2)	1609(3)	37(1)
O(41)	1256(6)	226(3)	4300(5)	63(2)
C(41)	-593(9)	-160(6)	4494(10)	66(4)
C(42)	743(11)	111(6)	4843(10)	57(4)
C(43)	1559(9)	299(8)	5992(7)	95(5)

Table 44. Bond lengths [Å] and angles [°].

Pd(1)-O(1)	2.060(2)	O(1)-Pd(1)-O(3)	86.43(8)
Pd(1)-O(3)	2.107(2)	O(1)-Pd(1)-P(2)	169.86(7)
Pd(1)-P(2)	2.2170(9)	O(3)-Pd(1)-P(2)	87.93(6)
Pd(1)-P(1)	2.2293(9)	O(1)-Pd(1)-P(1)	99.94(6)
P(1)-C(3)	1.814(3)	O(3)-Pd(1)-P(1)	173.55(6)
P(1)-C(9)	1.817(3)	P(2)-Pd(1)-P(1)	85.62(3)
P(1)-C(1)	1.835(3)	C(3)-P(1)-C(9)	110.53(15)
P(2)-C(15)	1.815(3)	C(3)-P(1)-C(1)	103.25(16)
P(2)-C(21)	1.816(4)	C(9)-P(1)-C(1)	102.83(14)
P(2)-C(2)	1.818(3)	C(3)-P(1)-Pd(1)	113.39(11)
O(1)-C(27)	1.300(4)	C(9)-P(1)-Pd(1)	117.94(12)
O(2)-C(27)	1.219(4)	C(1)-P(1)-Pd(1)	107.19(10)
O(3)-C(29)	1.283(4)	C(15)-P(2)-C(21)	106.88(15)
O(4)-C(29)	1.232(4)	C(15)-P(2)-C(2)	108.40(16)
C(1)-C(2)	1.529(4)	C(21)-P(2)-C(2)	106.27(16)
C(3)-C(4)	1.401(4)	C(15)-P(2)-Pd(1)	116.12(11)
C(3)-C(8)	1.384(4)	C(21)-P(2)-Pd(1)	109.27(12)
C(4)-C(5)	1.379(5)	C(2)-P(2)-Pd(1)	109.43(10)

C(5)-C(6)	1.368(5)	C(27)-O(1)-Pd(1)	125.8(2)
C(6)-C(7)	1.384(5)	C(29)-O(3)-Pd(1)	106.4(2)
C(7)-C(8)	1.374(5)	C(2)-C(1)-P(1)	108.8(2)
C(9)-C(10)	1.381(5)	C(1)-C(2)-P(2)	105.7(2)
C(9)-C(14)	1.403(4)	C(4)-C(3)-C(8)	118.9(3)
C(10)-C(11)	1.386(5)	C(4)-C(3)-P(1)	120.9(3)
C(11)-C(12)	1.390(4)	C(8)-C(3)-P(1)	120.1(3)
C(12)-C(13)	1.363(5)	C(5)-C(4)-C(3)	120.0(3)
C(13)-C(14)	1.390(4)	C(4)-C(5)-C(6)	120.6(4)
C(15)-C(16)	1.377(5)	C(7)-C(6)-C(5)	119.7(4)
C(15)-C(20)	1.398(4)	C(8)-C(7)-C(6)	120.4(4)
C(16)-C(17)	1.381(5)	C(7)-C(8)-C(3)	120.4(3)
C(17)-C(18)	1.390(5)	C(10)-C(9)-C(14)	120.0(3)
C(18)-C(19)	1.357(6)	C(10)-C(9)-P(1)	117.3(2)
C(19)-C(20)	1.387(4)	C(14)-C(9)-P(1)	122.7(3)
C(21)-C(26)	1.381(5)	C(11)-C(10)-C(9)	121.2(3)
C(21)-C(22)	1.395(4)	C(10)-C(11)-C(12)	118.4(4)
C(22)-C(23)	1.380(5)	C(13)-C(12)-C(11)	120.9(3)
C(23)-C(24)	1.377(5)	C(12)-C(13)-C(14)	121.4(3)
C(24)-C(25)	1.372(5)	C(13)-C(14)-C(9)	118.1(3)
C(25)-C(26)	1.380(5)	C(16)-C(15)-C(20)	119.4(3)
C(27)-C(28)	1.519(5)	C(16)-C(15)-P(2)	119.9(3)
C(29)-C(30)	1.512(4)	C(20)-C(15)-P(2)	120.7(3)
O(41)-C(42)	1.181(9)	C(17)-C(16)-C(15)	120.8(4)
C(41)-C(42)	1.537(11)	C(16)-C(17)-C(18)	119.3(4)
C(42)-C(43)	1.579(15)	C(19)-C(18)-C(17)	120.4(4)
		C(18)-C(19)-C(20)	120.7(4)
		C(19)-C(20)-C(15)	119.4(4)
		C(26)-C(21)-C(22)	119.0(3)
		C(26)-C(21)-P(2)	119.8(3)
		C(22)-C(21)-P(2)	121.2(3)
		C(23)-C(22)-C(21)	119.6(4)
		C(24)-C(23)-C(22)	120.8(4)
		C(23)-C(24)-C(25)	119.6(4)
		C(24)-C(25)-C(26)	120.2(4)
		C(25)-C(26)-C(21)	120.7(4)
		O(2)-C(27)-O(1)	126.5(3)
		O(2)-C(27)-C(28)	121.3(3)
		O(1)-C(27)-C(28)	112.2(3)
		O(4)-C(29)-O(3)	125.0(3)
		O(4)-C(29)-C(30)	119.7(4)
		O(3)-C(29)-C(30)	115.2(3)
		O(41)-C(42)-C(41)	125.0(13)
		O(41)-C(42)-C(43)	112.8(10)
		C(41)-C(42)-C(43)	122.2(12)

Table 45. Anisotropic displacement parameters ($Å^2$ x 10^4). The anisotropic displacement factor exponent takes the form: $-2\pi^2[h^2a^*2U^{11} + ... + 2\ h\ k\ a^*\ b^*\ U^{12}]$.

	U^{11}	U^{22}	U^{33}	U^{23}	U^{13}	U^{12}

Pd(1)	95(1)	179(2)	172(2)	24(2)	55(1)	32(1)
P(1)	112(5)	187(6)	176(6)	11(5)	56(4)	14(4)
P(2)	100(5)	180(6)	179(6)	14(5)	53(4)	22(4)
O(1)	199(13)	249(17)	226(15)	60(13)	139(11)	49(11)
O(2)	150(13)	320(20)	276(16)	2(14)	99(11)	50(12)
O(3)	118(12)	229(16)	186(15)	21(13)	34(10)	48(11)
O(4)	245(15)	272(18)	332(17)	-92(14)	142(12)	38(12)
C(1)	95(18)	230(20)	160(20)	47(18)	33(14)	70(15)
C(2)	127(18)	210(20)	180(20)	56(18)	70(15)	35(15)
C(3)	80(17)	160(20)	210(20)	-8(18)	73(15)	-10(15)
C(4)	148(18)	260(20)	190(20)	-30(20)	47(14)	-18(18)
C(5)	180(20)	260(30)	310(30)	40(20)	54(17)	50(17)
C(6)	240(20)	200(30)	390(30)	-30(20)	137(19)	28(18)
C(7)	270(20)	290(30)	240(20)	-70(20)	77(18)	-21(19)
C(8)	152(19)	230(30)	210(20)	39(19)	46(15)	42(16)
C(9)	134(17)	190(20)	120(20)	11(18)	45(14)	-15(16)
C(10)	170(20)	260(30)	260(20)	20(20)	100(16)	57(17)
C(11)	330(20)	170(20)	310(30)	-20(20)	157(18)	-37(18)
C(12)	200(20)	290(30)	290(30)	-20(20)	86(17)	-98(18)
C(13)	150(20)	330(30)	360(30)	-70(20)	134(17)	-67(18)
C(14)	175(19)	230(30)	270(20)	-22(19)	134(15)	28(17)
C(15)	143(19)	220(20)	170(20)	-7(18)	57(15)	-19(16)
C(16)	200(20)	330(30)	340(30)	-100(20)	-13(17)	40(18)
C(17)	400(30)	290(30)	390(30)	-60(30)	-83(19)	-70(20)
C(18)	180(20)	580(40)	280(30)	30(20)	-11(18)	-150(20)
C(19)	120(20)	550(30)	250(20)	-80(20)	66(16)	-6(19)
C(20)	200(20)	300(30)	280(20)	-70(20)	103(17)	27(18)
C(21)	40(17)	260(20)	130(20)	-28(18)	6(15)	-13(15)
C(22)	70(17)	240(20)	180(20)	4(18)	16(15)	-1(15)
C(23)	170(20)	390(30)	200(20)	-60(20)	94(16)	-21(18)
C(24)	280(20)	270(30)	360(30)	-110(20)	159(19)	6(19)
C(25)	490(30)	240(30)	450(30)	30(20)	290(20)	30(20)
C(26)	340(20)	270(30)	320(30)	20(20)	237(19)	33(19)
C(27)	210(20)	260(30)	190(20)	-80(20)	106(17)	-65(18)
C(28)	410(20)	340(30)	560(30)	30(20)	370(20)	-50(20)
C(29)	157(19)	370(30)	160(20)	10(20)	82(16)	-40(20)
C(30)	240(20)	590(30)	220(20)	-80(20)	16(16)	50(20)
O(41)	930(50)	510(50)	550(50)	130(40)	420(40)	180(40)
C(41)	700(100)	460(80)	670(100)	350(80)	130(70)	100(70)
C(42)	860(100)	390(70)	780(110)	320(70)	650(90)	190(60)
C(43)	690(80)	1850(170)	180(60)	100(80)	50(50)	270(90)

A.6 (CCDC 724780)

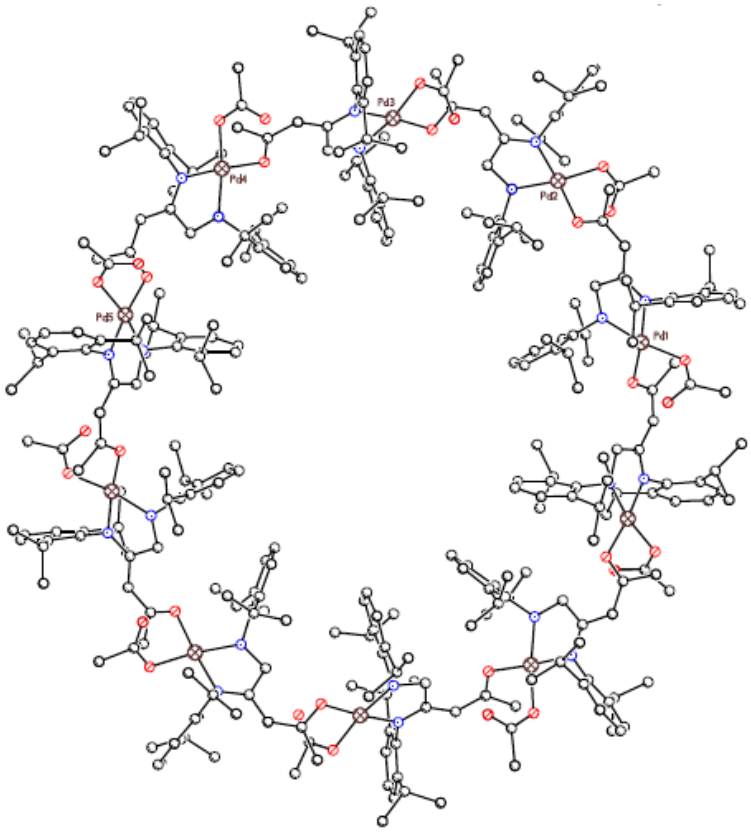

Special Refinement Details

Crystals were mounted on a glass fiber using Paratone oil then placed on the diffractometer under a nitrogen stream at 100K.

All anisotropic displacement parameters were restrained to simulate isotropic behavior and data with 2θ>45º was excluded from the refinement.

Refinement of F^2 against ALL reflections. The weighted R-factor (wR) and goodness of fit (S) are based on F^2, conventional R-factors (R) are based on F, with F set to zero for negative F^2. The threshold expression of $F^2 > 2\sigma (F^2)$ is used only for calculating R-factors(gt) etc. and is not relevant to the choice of reflections for refinement. R-factors based on F^2 are statistically about twice as large as those based on F, and R-factors based on ALL data will be even larger.

All esds (except the esd in the dihedral angle between two l.s. planes) are estimated using the full covariance matrix. The cell esds are taken into account individually in the estimation of esds in distances, angles and torsion angles; correlations between esds in cell parameters are only used when they are defined by crystal symmetry. An approximate (isotropic) treatment of cell esds is used for estimating esds involving l.s. planes.

Table 46. Atomic coordinates (x 10^4) and equivalent isotropic displacement parameters (Å^2 x 10^3). U(eq) is defined as the trace of the orthogonalized Uij tensor.

	x	y	z	Ueq
Pd(1)	-2150(1)	5798(1)	7724(1)	33(1)
Pd(2)	-933(1)	6645(1)	5790(1)	29(1)
Pd(3)	1741(1)	8890(1)	5745(1)	29(1)
Pd(4)	3235(1)	11597(1)	7258(1)	31(1)

Pd(5)	3735(1)	13430(1)	9802(1)	29(1)
O(1)	-3033(6)	6108(3)	8257(3)	38(2)
O(3)	-2257(7)	5151(3)	7815(3)	45(3)
O(4)	-1239(7)	5423(3)	8596(3)	47(3)
O(5)	-651(6)	6396(3)	6348(2)	30(2)
O(7)	-1910(7)	5982(3)	5320(3)	38(2)
O(8)	-3090(6)	6088(3)	5832(3)	39(2)
O(9)	394(6)	8419(3)	5635(2)	29(2)
O(11)	2238(6)	8326(3)	5184(3)	32(2)
O(12)	2509(6)	7831(3)	5600(3)	40(2)
O(13)	3576(6)	10870(3)	7039(3)	40(2)
O(15)	3111(6)	11540(3)	6552(3)	40(2)
O(16)	1612(6)	10950(3)	6215(3)	41(2)
O(17)	2841(6)	13087(3)	9079(2)	28(2)
O(19)	4922(6)	13678(3)	9537(2)	28(2)
O(20)	5542(6)	12929(3)	9181(3)	40(2)
N(1)	-1278(7)	5556(4)	7186(3)	27(3)
N(2)	-2233(7)	6379(4)	7505(3)	32(3)
N(3)	-1152(7)	6936(3)	5284(3)	22(2)
N(4)	155(7)	7298(3)	6187(3)	24(3)
N(5)	3113(7)	9350(3)	5916(3)	27(3)
N(6)	1280(7)	9535(3)	6258(3)	26(3)
N(7)	2858(7)	12300(3)	7508(3)	30(3)
N(8)	3598(7)	11728(3)	8010(3)	27(3)
N(9)	4585(7)	13700(3)	10528(3)	26(3)
N(10)	2493(7)	13345(3)	10130(3)	28(3)
C(1A)	-1104(9)	5838(5)	6944(4)	25(3)
C(2A)	-1515(9)	6343(4)	7133(4)	30(3)
C(3A)	-889(9)	5072(5)	7079(4)	26(3)
C(4A)	187(10)	5029(5)	7255(4)	31(3)
C(5A)	500(10)	4558(5)	7181(4)	37(4)
C(6A)	-228(11)	4117(5)	6948(4)	48(4)
C(7A)	-1311(11)	4149(5)	6759(4)	53(4)
C(8A)	-1678(10)	4615(5)	6811(4)	30(3)
C(9A)	1050(9)	5507(5)	7532(4)	38(4)
C(10A)	2038(9)	5489(5)	7285(4)	52(4)
C(11A)	1416(10)	5590(5)	8097(4)	57(4)
C(12A)	-2828(10)	4639(5)	6596(4)	44(4)
C(13A)	-2985(10)	4575(5)	6042(4)	62(4)
C(14A)	-3656(10)	4275(5)	6646(4)	75(5)
C(15A)	-2105(11)	6870(6)	7876(5)	49(4)
C(16A)	-1178(11)	7092(5)	8234(5)	42(4)
C(17A)	-1033(13)	7614(6)	8599(5)	94(6)
C(18A)	-2028(13)	7868(5)	8502(5)	64(5)
C(19A)	-2958(17)	7606(9)	8164(8)	128(8)
C(20A)	-3019(15)	7133(7)	7884(6)	92(6)
C(21A)	-228(10)	6809(5)	8337(4)	43(4)
C(22A)	888(11)	7017(5)	8330(5)	85(5)
C(23A)	-134(10)	6722(5)	8820(4)	62(4)

C(24A)	-4181(13)	6870(7)	7615(6)	89(6)
C(25A)	-4436(15)	6989(7)	7175(6)	150(8)
C(26A)	-4938(14)	6962(7)	7924(6)	125(7)
C(27A)	-4007(10)	5912(5)	8201(4)	33(3)
C(28A)	-4619(9)	5549(4)	7664(4)	46(4)
C(29A)	-1816(12)	5078(5)	8190(5)	49(4)
C(30A)	-1981(12)	4549(5)	8161(5)	78(5)
C(31A)	-545(8)	5687(5)	6536(4)	27(3)
C(1B)	-637(9)	7386(4)	5403(4)	19(3)
C(2B)	106(8)	7639(4)	5924(4)	24(3)
C(3B)	-1787(9)	6631(4)	4771(4)	27(3)
C(4B)	-1295(10)	6257(4)	4438(4)	30(3)
C(5B)	-1940(11)	5943(4)	3954(4)	42(4)
C(6B)	-2979(10)	5997(5)	3819(4)	43(4)
C(7B)	-3470(10)	6353(5)	4139(4)	45(4)
C(8B)	-2869(10)	6686(5)	4637(4)	37(3)
C(9B)	-132(10)	6203(5)	4589(4)	40(4)
C(10B)	653(10)	6568(5)	4493(4)	51(4)
C(11B)	107(10)	5641(5)	4346(4)	62(4)
C(12B)	-3442(10)	7081(5)	4994(5)	49(4)
C(13B)	-3883(11)	7451(5)	4761(5)	72(5)
C(14B)	-4338(11)	6821(6)	5138(5)	80(5)
C(15B)	111(10)	7553(5)	6726(5)	34(3)
C(16B)	1014(13)	7549(6)	7083(5)	61(5)
C(17B)	990(13)	7805(6)	7585(6)	81(5)
C(18B)	119(14)	8056(6)	7720(5)	79(5)
C(19B)	-770(13)	8051(5)	7381(6)	77(5)
C(20B)	-757(11)	7787(5)	6864(5)	39(4)
C(21B)	1887(16)	7143(9)	6898(7)	115(7)
C(22B)	2750(20)	7491(10)	7016(10)	295(18)
C(23B)	2042(15)	6830(6)	7091(6)	119(7)
C(24B)	-1782(10)	7759(5)	6499(5)	40(4)
C(25B)	-1997(10)	8280(4)	6494(4)	58(4)
C(26B)	-2764(11)	7470(5)	6562(5)	78(5)
C(27B)	-353(9)	5967(5)	6270(4)	20(3)
C(28B)	253(9)	5726(4)	5846(4)	34(3)
C(29B)	-2726(11)	5851(5)	5459(5)	39(4)
C(30B)	-3347(10)	5322(5)	5071(4)	74(5)
C(31B)	-712(9)	7634(4)	5070(4)	27(3)
C(1C)	3189(9)	9821(4)	6249(4)	26(3)
C(2C)	2255(8)	9956(4)	6506(4)	30(3)
C(3C)	4018(9)	9174(4)	5685(4)	28(3)
C(4C)	4856(10)	9028(5)	5927(4)	34(4)
C(5C)	5699(10)	8832(5)	5690(5)	47(4)
C(6C)	5660(10)	8799(5)	5205(5)	48(4)
C(7C)	4842(11)	8941(5)	4962(5)	47(4)
C(8C)	3966(10)	9132(4)	5194(5)	34(3)
C(9C)	4896(10)	9051(5)	6458(5)	51(4)
C(10C)	5881(10)	9432(5)	6842(4)	68(5)

C(11C)	4875(11)	8519(5)	6453(4)	66(5)
C(12C)	3034(11)	9300(5)	4922(4)	54(4)
C(13C)	3327(11)	9827(5)	4919(5)	82(5)
C(14C)	2560(11)	8924(5)	4359(4)	76(5)
C(15C)	723(10)	9487(4)	6637(4)	28(3)
C(16C)	1261(10)	9334(5)	6987(4)	32(3)
C(17C)	701(10)	9315(5)	7335(5)	41(4)
C(18C)	-309(11)	9472(5)	7361(5)	52(4)
C(19C)	-819(10)	9631(5)	7008(5)	46(4)
C(20C)	-298(10)	9639(4)	6636(4)	29(3)
C(21C)	2351(9)	9170(4)	7004(4)	35(3)
C(22C)	3146(9)	9519(5)	7487(4)	51(4)
C(23C)	2282(10)	8618(4)	6916(4)	53(4)
C(24C)	-910(9)	9829(4)	6250(4)	39(4)
C(25C)	-1862(9)	10136(5)	6407(4)	54(4)
C(26C)	-1366(10)	9371(5)	5750(4)	57(4)
C(27C)	-168(9)	8109(4)	5170(4)	23(3)
C(28C)	-212(9)	8289(4)	4743(4)	38(4)
C(29C)	2541(9)	7935(5)	5241(5)	28(3)
C(30C)	2966(9)	7594(5)	4772(4)	55(4)
C(31C)	4142(9)	10192(4)	6386(4)	28(3)
C(1D)	2947(9)	12542(4)	8011(4)	25(3)
C(2D)	3273(9)	12246(4)	8321(4)	35(3)
C(3D)	2580(10)	12543(4)	7185(4)	25(3)
C(4D)	3399(10)	12741(4)	7022(4)	31(3)
C(5D)	3110(10)	12961(4)	6684(4)	41(4)
C(6D)	2027(11)	12995(5)	6508(4)	43(4)
C(7D)	1230(10)	12789(4)	6661(4)	38(4)
C(8D)	1477(10)	12566(4)	7002(4)	33(3)
C(9D)	4572(10)	12720(5)	7212(4)	47(4)
C(10D)	5144(10)	13247(5)	7625(4)	70(5)
C(11D)	5178(10)	12556(5)	6784(5)	76(5)
C(12D)	571(10)	12333(5)	7154(4)	45(4)
C(13D)	-107(10)	12749(5)	7439(4)	71(5)
C(14D)	-182(10)	11904(5)	6711(4)	59(4)
C(15D)	3242(10)	11340(5)	8161(4)	28(3)
C(16D)	3996(11)	11123(5)	8353(4)	37(4)
C(17D)	3635(11)	10765(5)	8511(4)	49(4)
C(18D)	2547(12)	10639(5)	8499(5)	55(4)
C(19D)	1801(11)	10865(5)	8278(4)	50(4)
C(20D)	2117(11)	11210(5)	8105(4)	32(3)
C(21D)	5159(12)	11198(5)	8344(5)	65(5)
C(22D)	5818(12)	11476(6)	8846(5)	114(6)
C(23D)	5639(13)	10763(7)	8068(6)	129(7)
C(24D)	1226(9)	11405(4)	7841(4)	37(4)
C(25D)	475(9)	11689(5)	8198(4)	60(4)
C(26D)	572(10)	10984(4)	7352(4)	55(4)
C(27D)	4262(10)	10700(5)	6744(4)	37(4)
C(28D)	5236(9)	11062(4)	6795(4)	46(4)

C(29D)	2369(11)	11222(5)	6176(5)	40(4)
C(30D)	2514(10)	11180(5)	5656(4)	54(4)
C(31D)	2737(8)	13063(4)	8253(4)	28(3)
C(1E)	4048(9)	13736(5)	10879(4)	32(3)
C(2E)	2871(8)	13498(4)	10691(4)	31(3)
C(3E)	5699(9)	13945(5)	10646(4)	26(3)
C(4E)	6468(10)	13621(5)	10532(4)	33(3)
C(5E)	7501(11)	13866(5)	10599(4)	40(4)
C(6E)	7733(10)	14379(5)	10757(4)	47(4)
C(7E)	6944(10)	14686(5)	10865(4)	41(4)
C(8E)	5893(10)	14467(5)	10820(4)	34(3)
C(9E)	6252(9)	13066(5)	10377(4)	37(4)
C(10E)	6108(9)	12952(4)	10838(4)	51(4)
C(11E)	7086(9)	12770(5)	10108(4)	57(4)
C(12E)	5018(10)	14813(5)	10948(4)	45(4)
C(13E)	5346(10)	15268(5)	11475(4)	59(4)
C(14E)	4667(10)	15004(5)	10540(4)	61(4)
C(15E)	1726(9)	12868(4)	9877(4)	24(3)
C(16E)	2040(10)	12441(5)	9897(4)	36(4)
C(17E)	1241(11)	11994(5)	9699(4)	54(4)
C(18E)	191(11)	12037(5)	9491(4)	52(4)
C(19E)	-90(11)	12463(5)	9433(4)	42(4)
C(20E)	672(10)	12887(5)	9626(4)	34(3)
C(21E)	3195(10)	12386(5)	10084(4)	46(4)
C(22E)	3290(11)	12189(5)	10505(5)	73(5)
C(23E)	3687(10)	12052(5)	9628(4)	64(5)
C(24E)	349(9)	13332(5)	9537(4)	38(4)
C(25E)	-400(9)	13591(5)	9881(4)	62(4)
C(26E)	-179(9)	13211(5)	8979(4)	60(4)
C(27E)	2739(9)	13307(4)	8772(4)	24(3)
C(28E)	2602(9)	13864(4)	8980(4)	39(4)
C(29E)	5595(10)	13403(5)	9300(4)	26(3)
C(30E)	6425(9)	13673(4)	9165(4)	40(4)
C(31E)	-4543(9)	6016(4)	8594(4)	30(3)
O(1F)	8213(7)	3234(3)	4272(3)	57(3)
O(2F)	6725(8)	2978(4)	4442(4)	75(3)
C(1F)	7352(13)	3316(6)	4387(5)	62(5)
C(2F)	6875(11)	3798(5)	4471(5)	75(5)
O(3F)	4007(7)	4196(4)	3308(3)	78(3)
O(4F)	4825(6)	4308(4)	4081(3)	46(3)
C(3F)	4815(11)	4327(5)	3651(5)	49(4)
C(4F)	5854(10)	4553(5)	3600(4)	72(5)
O(5F)	2985(7)	7463(4)	1264(3)	61(3)
O(6F)	4274(7)	7838(3)	1972(3)	47(3)
C(5F)	3315(11)	7746(5)	1765(5)	53(4)
C(6F)	2440(9)	7951(5)	2027(4)	67(5)
O(7F)	9101(7)	5147(4)	9329(3)	53(3)
O(8F)	7869(7)	5639(3)	9638(3)	47(3)
C(7F)	8437(11)	5319(5)	9650(5)	41(4)

C(8F)	8496(9)	5050(5)	10006(4)	51(4)
O(9F)	692(7)	-26(3)	5458(3)	74(3)

Table 47. Bond lengths [Å] and angles [°].

Pd(1)-O(3)	1.985(8)	O(3)-Pd(1)-N(1)	95.0(4)
Pd(1)-N(1)	1.997(9)	O(3)-Pd(1)-N(2)	169.3(3)
Pd(1)-N(2)	2.018(10)	N(1)-Pd(1)-N(2)	81.6(4)
Pd(1)-O(1)	2.020(7)	O(3)-Pd(1)-O(1)	90.8(3)
Pd(2)-N(3)	1.959(9)	N(1)-Pd(1)-O(1)	174.3(4)
Pd(2)-O(5)	2.017(7)	N(2)-Pd(1)-O(1)	92.7(3)
Pd(2)-O(7)	2.025(8)	N(3)-Pd(2)-O(5)	175.9(3)
Pd(2)-N(4)	2.042(9)	N(3)-Pd(2)-O(7)	93.7(3)
Pd(3)-N(5)	1.977(9)	O(5)-Pd(2)-O(7)	90.4(3)
Pd(3)-O(9)	2.007(7)	N(3)-Pd(2)-N(4)	81.7(3)
Pd(3)-O(11)	2.019(7)	O(5)-Pd(2)-N(4)	94.3(3)
Pd(3)-N(6)	2.060(8)	O(7)-Pd(2)-N(4)	172.5(3)
Pd(4)-N(7)	1.977(9)	N(5)-Pd(3)-O(9)	174.6(3)
Pd(4)-O(15)	1.983(7)	N(5)-Pd(3)-O(11)	92.0(3)
Pd(4)-O(13)	2.027(8)	O(9)-Pd(3)-O(11)	89.9(3)
Pd(4)-N(8)	2.037(8)	N(5)-Pd(3)-N(6)	83.0(3)
Pd(5)-N(9)	2.013(8)	O(9)-Pd(3)-N(6)	95.7(3)
Pd(5)-O(19)	2.020(7)	O(11)-Pd(3)-N(6)	171.1(4)
Pd(5)-N(10)	2.025(9)	N(7)-Pd(4)-O(15)	92.8(4)
Pd(5)-O(17)	2.021(7)	N(7)-Pd(4)-O(13)	176.1(4)
O(1)-C(27A)	1.277(13)	O(15)-Pd(4)-O(13)	90.6(3)
O(3)-C(29A)	1.240(13)	N(7)-Pd(4)-N(8)	85.0(4)
O(4)-C(29A)	1.265(14)	O(15)-Pd(4)-N(8)	170.6(4)
O(5)-C(27B)	1.254(12)	O(13)-Pd(4)-N(8)	92.0(3)
O(7)-C(29B)	1.263(13)	N(9)-Pd(5)-O(19)	95.3(3)
O(8)-C(29B)	1.219(12)	N(9)-Pd(5)-N(10)	82.0(3)
O(9)-C(27C)	1.330(11)	O(19)-Pd(5)-N(10)	167.3(3)
O(11)-C(29C)	1.271(12)	N(9)-Pd(5)-O(17)	173.8(4)
O(12)-C(29C)	1.209(12)	O(19)-Pd(5)-O(17)	89.0(3)
O(13)-C(27D)	1.307(12)	N(10)-Pd(5)-O(17)	94.8(3)
O(15)-C(29D)	1.288(14)	C(27A)-O(1)-Pd(1)	121.6(7)
O(16)-C(29D)	1.249(14)	C(29A)-O(3)-Pd(1)	127.7(9)
O(17)-C(27E)	1.282(12)	C(27B)-O(5)-Pd(2)	121.6(7)
O(19)-C(29E)	1.293(12)	C(29B)-O(7)-Pd(2)	118.8(8)
O(20)-C(29E)	1.262(13)	C(27C)-O(9)-Pd(3)	122.1(7)
N(1)-C(1A)	1.305(13)	C(29C)-O(11)-Pd(3)	121.3(8)
N(1)-C(3A)	1.437(13)	C(27D)-O(13)-Pd(4)	121.4(8)
N(2)-C(15A)	1.375(15)	C(29D)-O(15)-Pd(4)	121.9(9)
N(2)-C(2A)	1.511(12)	C(27E)-O(17)-Pd(5)	122.8(7)
N(3)-C(1B)	1.298(13)	C(29E)-O(19)-Pd(5)	125.8(8)
N(3)-C(3B)	1.452(12)	C(1A)-N(1)-C(3A)	123.2(10)
N(4)-C(15B)	1.462(13)	C(1A)-N(1)-Pd(1)	118.8(8)
N(4)-C(2B)	1.467(12)	C(3A)-N(1)-Pd(1)	118.0(8)
N(5)-C(1C)	1.303(12)	C(15A)-N(2)-C(2A)	110.8(11)

N(5)-C(3C)	1.444(13)	C(15A)-N(2)-Pd(1)	118.4(8)
N(6)-C(15C)	1.458(13)	C(2A)-N(2)-Pd(1)	111.6(7)
N(6)-C(2C)	1.525(12)	C(1B)-N(3)-C(3B)	121.0(10)
N(7)-C(1D)	1.335(12)	C(1B)-N(3)-Pd(2)	118.5(7)
N(7)-C(3D)	1.394(13)	C(3B)-N(3)-Pd(2)	120.1(7)
N(8)-C(15D)	1.433(14)	C(15B)-N(4)-C(2B)	113.8(9)
N(8)-C(2D)	1.528(12)	C(15B)-N(4)-Pd(2)	113.5(7)
N(9)-C(1E)	1.300(12)	C(2B)-N(4)-Pd(2)	111.9(6)
N(9)-C(3E)	1.454(13)	C(1C)-N(5)-C(3C)	120.1(10)
N(10)-C(15E)	1.470(13)	C(1C)-N(5)-Pd(3)	118.3(8)
N(10)-C(2E)	1.495(11)	C(3C)-N(5)-Pd(3)	121.6(7)
C(1A)-C(31A)	1.424(13)	C(15C)-N(6)-C(2C)	111.5(8)
C(1A)-C(2A)	1.493(14)	C(15C)-N(6)-Pd(3)	118.8(7)
C(3A)-C(4A)	1.394(14)	C(2C)-N(6)-Pd(3)	109.0(6)
C(3A)-C(8A)	1.445(15)	C(1D)-N(7)-C(3D)	121.5(10)
C(4A)-C(5A)	1.378(14)	C(1D)-N(7)-Pd(4)	116.0(8)
C(4A)-C(9A)	1.538(15)	C(3D)-N(7)-Pd(4)	122.4(7)
C(5A)-C(6A)	1.370(15)	C(15D)-N(8)-C(2D)	112.1(8)
C(6A)-C(7A)	1.403(15)	C(15D)-N(8)-Pd(4)	119.3(7)
C(7A)-C(8A)	1.403(15)	C(2D)-N(8)-Pd(4)	108.5(6)
C(8A)-C(12A)	1.493(14)	C(1E)-N(9)-C(3E)	122.8(9)
C(9A)-C(10A)	1.540(14)	C(1E)-N(9)-Pd(5)	117.6(8)
C(9A)-C(11A)	1.553(13)	C(3E)-N(9)-Pd(5)	118.2(7)
C(12A)-C(14A)	1.505(16)	C(15E)-N(10)-C(2E)	112.7(9)
C(12A)-C(13A)	1.528(13)	C(15E)-N(10)-Pd(5)	118.5(6)
C(15A)-C(16A)	1.349(16)	C(2E)-N(10)-Pd(5)	111.8(6)
C(15A)-C(20A)	1.413(18)	N(1)-C(1A)-C(31A)	123.1(11)
C(16A)-C(17A)	1.434(17)	N(1)-C(1A)-C(2A)	115.1(10)
C(16A)-C(21A)	1.539(16)	C(31A)-C(1A)-C(2A)	121.7(12)
C(17A)-C(18A)	1.528(17)	C(1A)-C(2A)-N(2)	111.7(10)
C(18A)-C(19A)	1.35(2)	C(4A)-C(3A)-N(1)	122.9(11)
C(19A)-C(20A)	1.27(2)	C(4A)-C(3A)-C(8A)	119.4(11)
C(20A)-C(24A)	1.53(2)	N(1)-C(3A)-C(8A)	117.6(10)
C(21A)-C(22A)	1.505(16)	C(5A)-C(4A)-C(3A)	120.7(12)
C(21A)-C(23A)	1.515(14)	C(5A)-C(4A)-C(9A)	118.7(11)
C(24A)-C(26A)	1.393(18)	C(3A)-C(4A)-C(9A)	120.6(11)
C(24A)-C(25A)	1.446(18)	C(6A)-C(5A)-C(4A)	122.0(12)
C(27A)-C(31E)	1.374(13)	C(5A)-C(6A)-C(7A)	118.3(13)
C(27A)-C(28A)	1.524(13)	C(6A)-C(7A)-C(8A)	122.5(13)
C(29A)-C(30A)	1.491(17)	C(7A)-C(8A)-C(3A)	117.0(11)
C(31A)-C(27B)	1.364(14)	C(7A)-C(8A)-C(12A)	121.6(12)
C(1B)-C(31B)	1.410(13)	C(3A)-C(8A)-C(12A)	121.4(11)
C(1B)-C(2B)	1.506(13)	C(4A)-C(9A)-C(10A)	114.5(10)
C(3B)-C(8B)	1.388(14)	C(4A)-C(9A)-C(11A)	108.4(10)
C(3B)-C(4B)	1.395(13)	C(10A)-C(9A)-C(11A)	110.8(10)
C(4B)-C(5B)	1.405(13)	C(8A)-C(12A)-C(14A)	114.3(11)
C(4B)-C(9B)	1.491(14)	C(8A)-C(12A)-C(13A)	111.6(10)
C(5B)-C(6B)	1.336(15)	C(14A)-C(12A)-C(13A)	110.9(10)
C(6B)-C(7B)	1.349(14)	C(16A)-C(15A)-N(2)	122.9(12)

C(7B)-C(8B)	1.423(14)	C(16A)-C(15A)-C(20A)	120.3(14)
C(8B)-C(12B)	1.523(15)	N(2)-C(15A)-C(20A)	116.8(13)
C(9B)-C(10B)	1.543(15)	C(15A)-C(16A)-C(17A)	122.3(14)
C(9B)-C(11B)	1.559(14)	C(15A)-C(16A)-C(21A)	124.9(12)
C(12B)-C(14B)	1.530(16)	C(17A)-C(16A)-C(21A)	112.5(13)
C(12B)-C(13B)	1.554(15)	C(16A)-C(17A)-C(18A)	110.6(13)
C(15B)-C(20B)	1.357(15)	C(19A)-C(18A)-C(17A)	123.0(15)
C(15B)-C(16B)	1.407(16)	C(20A)-C(19A)-C(18A)	120(2)
C(16B)-C(17B)	1.360(16)	C(19A)-C(20A)-C(15A)	122(2)
C(16B)-C(21B)	1.65(2)	C(19A)-C(20A)-C(24A)	113.6(19)
C(17B)-C(18B)	1.378(18)	C(15A)-C(20A)-C(24A)	123.8(16)
C(18B)-C(19B)	1.355(17)	C(22A)-C(21A)-C(23A)	107.5(11)
C(19B)-C(20B)	1.398(15)	C(22A)-C(21A)-C(16A)	117.4(11)
C(20B)-C(24B)	1.501(15)	C(23A)-C(21A)-C(16A)	114.8(10)
C(21B)-C(23B)	1.25(2)	C(26A)-C(24A)-C(25A)	116.4(16)
C(21B)-C(22B)	1.34(3)	C(26A)-C(24A)-C(20A)	115.7(15)
C(24B)-C(26B)	1.533(16)	C(25A)-C(24A)-C(20A)	105.3(16)
C(24B)-C(25B)	1.543(15)	O(1)-C(27A)-C(31E)	124.0(10)
C(27B)-C(28B)	1.520(13)	O(1)-C(27A)-C(28A)	117.9(10)
C(29B)-C(30B)	1.548(16)	C(31E)-C(27A)-C(28A)	118.1(11)
C(31B)-C(27C)	1.389(14)	O(3)-C(29A)-O(4)	124.2(14)
C(1C)-C(31C)	1.444(15)	O(3)-C(29A)-C(30A)	117.9(13)
C(1C)-C(2C)	1.494(13)	O(4)-C(29A)-C(30A)	118.0(13)
C(3C)-C(4C)	1.350(14)	C(27B)-C(31A)-C(1A)	125.1(12)
C(3C)-C(8C)	1.378(14)	N(3)-C(1B)-C(31B)	124.0(10)
C(4C)-C(5C)	1.394(15)	N(3)-C(1B)-C(2B)	116.3(10)
C(4C)-C(9C)	1.517(14)	C(31B)-C(1B)-C(2B)	119.6(11)
C(5C)-C(6C)	1.376(14)	N(4)-C(2B)-C(1B)	111.0(9)
C(6C)-C(7C)	1.325(14)	C(8B)-C(3B)-C(4B)	121.8(11)
C(7C)-C(8C)	1.421(14)	C(8B)-C(3B)-N(3)	120.5(10)
C(8C)-C(12C)	1.514(15)	C(4B)-C(3B)-N(3)	117.5(10)
C(9C)-C(10C)	1.542(15)	C(3B)-C(4B)-C(5B)	116.9(11)
C(9C)-C(11C)	1.527(16)	C(3B)-C(4B)-C(9B)	121.1(10)
C(12C)-C(13C)	1.545(16)	C(5B)-C(4B)-C(9B)	122.0(11)
C(12C)-C(14C)	1.548(14)	C(6B)-C(5B)-C(4B)	121.6(12)
C(15C)-C(16C)	1.361(14)	C(5B)-C(6B)-C(7B)	122.1(12)
C(15C)-C(20C)	1.382(14)	C(6B)-C(7B)-C(8B)	119.5(12)
C(16C)-C(17C)	1.351(14)	C(3B)-C(8B)-C(7B)	117.9(11)
C(16C)-C(21C)	1.477(15)	C(3B)-C(8B)-C(12B)	123.4(11)
C(17C)-C(18C)	1.379(15)	C(7B)-C(8B)-C(12B)	118.7(11)
C(18C)-C(19C)	1.365(15)	C(4B)-C(9B)-C(10B)	112.5(10)
C(19C)-C(20C)	1.375(14)	C(4B)-C(9B)-C(11B)	113.3(11)
C(20C)-C(24C)	1.549(14)	C(10B)-C(9B)-C(11B)	111.3(10)
C(21C)-C(23C)	1.499(14)	C(8B)-C(12B)-C(14B)	110.9(11)
C(21C)-C(22C)	1.505(13)	C(8B)-C(12B)-C(13B)	111.3(10)
C(24C)-C(26C)	1.512(13)	C(14B)-C(12B)-C(13B)	112.0(11)
C(24C)-C(25C)	1.557(13)	C(20B)-C(15B)-C(16B)	122.8(13)
C(27C)-C(28C)	1.527(13)	C(20B)-C(15B)-N(4)	120.5(11)
C(29C)-C(30C)	1.541(14)	C(16B)-C(15B)-N(4)	116.7(12)

C(31C)-C(27D)	1.400(14)	C(17B)-C(16B)-C(15B)	116.5(15)
C(1D)-C(31D)	1.445(14)	C(17B)-C(16B)-C(21B)	121.8(15)
C(1D)-C(2D)	1.494(13)	C(15B)-C(16B)-C(21B)	120.1(13)
C(3D)-C(4D)	1.395(15)	C(16B)-C(17B)-C(18B)	120.2(15)
C(3D)-C(8D)	1.415(14)	C(19B)-C(18B)-C(17B)	124.0(15)
C(4D)-C(5D)	1.378(14)	C(18B)-C(19B)-C(20B)	116.3(15)
C(4D)-C(9D)	1.499(15)	C(15B)-C(20B)-C(19B)	120.2(13)
C(5D)-C(6D)	1.395(15)	C(15B)-C(20B)-C(24B)	124.6(11)
C(6D)-C(7D)	1.366(15)	C(19B)-C(20B)-C(24B)	115.0(13)
C(7D)-C(8D)	1.388(14)	C(23B)-C(21B)-C(22B)	114(2)
C(8D)-C(12D)	1.510(16)	C(23B)-C(21B)-C(16B)	119.4(19)
C(9D)-C(11D)	1.511(14)	C(22B)-C(21B)-C(16B)	97(2)
C(9D)-C(10D)	1.544(15)	C(20B)-C(24B)-C(26B)	112.0(11)
C(12D)-C(14D)	1.505(14)	C(20B)-C(24B)-C(25B)	113.8(11)
C(12D)-C(13D)	1.560(15)	C(26B)-C(24B)-C(25B)	113.2(11)
C(15D)-C(16D)	1.329(15)	O(5)-C(27B)-C(31A)	124.7(11)
C(15D)-C(20D)	1.410(15)	O(5)-C(27B)-C(28B)	119.5(11)
C(16D)-C(17D)	1.373(16)	C(31A)-C(27B)-C(28B)	115.9(11)
C(16D)-C(21D)	1.477(17)	O(8)-C(29B)-O(7)	129.3(12)
C(17D)-C(18D)	1.390(16)	O(8)-C(29B)-C(30B)	118.5(12)
C(18D)-C(19D)	1.385(15)	O(7)-C(29B)-C(30B)	112.2(11)
C(19D)-C(20D)	1.349(15)	C(27C)-C(31B)-C(1B)	126.8(11)
C(20D)-C(24D)	1.512(14)	N(5)-C(1C)-C(31C)	122.4(11)
C(21D)-C(23D)	1.428(17)	N(5)-C(1C)-C(2C)	116.4(11)
C(21D)-C(22D)	1.431(16)	C(31C)-C(1C)-C(2C)	121.1(10)
C(24D)-C(26D)	1.511(13)	C(1C)-C(2C)-N(6)	112.4(9)
C(24D)-C(25D)	1.553(13)	C(4C)-C(3C)-C(8C)	121.0(11)
C(27D)-C(28D)	1.512(15)	C(4C)-C(3C)-N(5)	121.2(11)
C(29D)-C(30D)	1.523(14)	C(8C)-C(3C)-N(5)	117.6(11)
C(31D)-C(27E)	1.395(13)	C(3C)-C(4C)-C(5C)	121.0(12)
C(1E)-C(31E)#1	1.418(13)	C(3C)-C(4C)-C(9C)	121.4(11)
C(1E)-C(2E)	1.507(14)	C(5C)-C(4C)-C(9C)	117.6(12)
C(3E)-C(8E)	1.373(15)	C(6C)-C(5C)-C(4C)	118.1(12)
C(3E)-C(4E)	1.375(14)	C(7C)-C(6C)-C(5C)	121.7(13)
C(4E)-C(5E)	1.388(16)	C(6C)-C(7C)-C(8C)	120.9(13)
C(4E)-C(9E)	1.470(16)	C(3C)-C(8C)-C(7C)	117.4(11)
C(5E)-C(6E)	1.355(16)	C(3C)-C(8C)-C(12C)	121.4(11)
C(6E)-C(7E)	1.365(15)	C(7C)-C(8C)-C(12C)	121.2(12)
C(7E)-C(8E)	1.397(15)	C(4C)-C(9C)-C(10C)	110.4(11)
C(8E)-C(12E)	1.524(15)	C(4C)-C(9C)-C(11C)	111.1(11)
C(9E)-C(11E)	1.521(13)	C(10C)-C(9C)-C(11C)	112.9(11)
C(9E)-C(10E)	1.545(14)	C(8C)-C(12C)-C(13C)	113.5(11)
C(12E)-C(14E)	1.508(14)	C(8C)-C(12C)-C(14C)	114.8(11)
C(12E)-C(13E)	1.538(14)	C(13C)-C(12C)-C(14C)	106.5(10)
C(15E)-C(16E)	1.330(15)	C(16C)-C(15C)-C(20C)	124.5(12)
C(15E)-C(20E)	1.415(14)	C(16C)-C(15C)-N(6)	118.6(11)
C(16E)-C(17E)	1.437(16)	C(20C)-C(15C)-N(6)	116.7(11)
C(16E)-C(21E)	1.505(15)	C(17C)-C(16C)-C(15C)	114.9(12)
C(17E)-C(18E)	1.390(15)	C(17C)-C(16C)-C(21C)	118.7(12)

C(18E)-C(19E)	1.361(15)
C(19E)-C(20E)	1.363(15)
C(20E)-C(24E)	1.472(15)
C(21E)-C(22E)	1.539(14)
C(21E)-C(23E)	1.555(13)
C(24E)-C(25E)	1.509(13)
C(24E)-C(26E)	1.538(13)
C(27E)-C(28E)	1.503(14)
C(29E)-C(30E)	1.467(15)
C(31E)-C(1E)#1	1.418(13)
O(1F)-C(1F)	1.201(14)
O(2F)-C(1F)	1.296(16)
C(1F)-C(2F)	1.491(17)
O(3F)-C(3F)	1.218(13)
O(4F)-C(3F)	1.277(13)
C(3F)-C(4F)	1.487(16)
O(5F)-C(5F)	1.334(13)
O(6F)-C(5F)	1.216(13)
C(5F)-C(6F)	1.472(14)
O(7F)-C(7F)	1.334(13)
O(8F)-C(7F)	1.205(13)
C(7F)-C(8F)	1.521(15)

C(15C)-C(16C)-C(21C)	126.3(12)
C(16C)-C(17C)-C(18C)	123.4(13)
C(19C)-C(18C)-C(17C)	120.0(13)
C(18C)-C(19C)-C(20C)	118.7(13)
C(19C)-C(20C)-C(15C)	118.4(12)
C(19C)-C(20C)-C(24C)	116.4(11)
C(15C)-C(20C)-C(24C)	125.2(11)
C(16C)-C(21C)-C(23C)	110.7(11)
C(16C)-C(21C)-C(22C)	111.6(10)
C(23C)-C(21C)-C(22C)	113.3(10)
C(26C)-C(24C)-C(20C)	108.7(10)
C(26C)-C(24C)-C(25C)	107.7(10)
C(20C)-C(24C)-C(25C)	116.7(10)
O(9)-C(27C)-C(31B)	121.7(10)
O(9)-C(27C)-C(28C)	118.1(10)
C(31B)-C(27C)-C(28C)	120.1(10)
O(12)-C(29C)-O(11)	126.9(12)
O(12)-C(29C)-C(30C)	123.2(11)
O(11)-C(29C)-C(30C)	109.9(11)
C(27D)-C(31C)-C(1C)	124.4(11)
N(7)-C(1D)-C(31D)	122.4(11)
N(7)-C(1D)-C(2D)	116.8(10)
C(31D)-C(1D)-C(2D)	120.8(10)
C(1D)-C(2D)-N(8)	113.2(9)
N(7)-C(3D)-C(4D)	119.2(11)
N(7)-C(3D)-C(8D)	120.6(12)
C(4D)-C(3D)-C(8D)	120.1(12)
C(5D)-C(4D)-C(3D)	118.7(12)
C(5D)-C(4D)-C(9D)	120.6(12)
C(3D)-C(4D)-C(9D)	120.7(12)
C(4D)-C(5D)-C(6D)	122.0(13)
C(7D)-C(6D)-C(5D)	118.8(12)
C(6D)-C(7D)-C(8D)	121.6(12)
C(7D)-C(8D)-C(3D)	118.8(12)
C(7D)-C(8D)-C(12D)	119.9(12)
C(3D)-C(8D)-C(12D)	121.2(12)
C(4D)-C(9D)-C(11D)	111.5(10)
C(4D)-C(9D)-C(10D)	111.0(11)
C(11D)-C(9D)-C(10D)	108.5(12)
C(8D)-C(12D)-C(14D)	113.6(10)
C(8D)-C(12D)-C(13D)	110.7(10)
C(14D)-C(12D)-C(13D)	109.1(10)
C(16D)-C(15D)-C(20D)	123.1(13)
C(16D)-C(15D)-N(8)	117.9(12)
C(20D)-C(15D)-N(8)	118.9(11)
C(15D)-C(16D)-C(17D)	116.8(13)
C(15D)-C(16D)-C(21D)	123.7(13)
C(17D)-C(16D)-C(21D)	119.1(13)
C(16D)-C(17D)-C(18D)	123.5(14)

C(17D)-C(18D)-C(19D)	116.6(14)
C(20D)-C(19D)-C(18D)	121.7(14)
C(19D)-C(20D)-C(15D)	118.0(13)
C(19D)-C(20D)-C(24D)	116.8(13)
C(15D)-C(20D)-C(24D)	125.1(12)
C(23D)-C(21D)-C(22D)	110.0(13)
C(23D)-C(21D)-C(16D)	118.4(14)
C(22D)-C(21D)-C(16D)	111.7(13)
C(20D)-C(24D)-C(26D)	111.9(10)
C(20D)-C(24D)-C(25D)	112.4(10)
C(26D)-C(24D)-C(25D)	111.1(10)
O(13)-C(27D)-C(31C)	122.5(12)
O(13)-C(27D)-C(28D)	119.1(10)
C(31C)-C(27D)-C(28D)	118.4(11)
O(16)-C(29D)-O(15)	125.2(12)
O(16)-C(29D)-C(30D)	121.0(12)
O(15)-C(29D)-C(30D)	113.8(12)
C(27E)-C(31D)-C(1D)	123.1(11)
N(9)-C(1E)-C(31E)#1	121.8(11)
N(9)-C(1E)-C(2E)	115.9(10)
C(31E)#1-C(1E)-C(2E)	122.2(10)
N(10)-C(2E)-C(1E)	111.8(9)
C(8E)-C(3E)-C(4E)	125.2(12)
C(8E)-C(3E)-N(9)	118.7(11)
C(4E)-C(3E)-N(9)	115.8(11)
C(3E)-C(4E)-C(5E)	114.1(12)
C(3E)-C(4E)-C(9E)	124.0(12)
C(5E)-C(4E)-C(9E)	121.9(12)
C(6E)-C(5E)-C(4E)	123.3(13)
C(5E)-C(6E)-C(7E)	120.7(13)
C(6E)-C(7E)-C(8E)	119.1(13)
C(3E)-C(8E)-C(7E)	117.5(12)
C(3E)-C(8E)-C(12E)	123.6(12)
C(7E)-C(8E)-C(12E)	118.9(12)
C(4E)-C(9E)-C(11E)	113.8(11)
C(4E)-C(9E)-C(10E)	110.4(10)
C(11E)-C(9E)-C(10E)	112.0(10)
C(14E)-C(12E)-C(8E)	111.3(10)
C(14E)-C(12E)-C(13E)	109.9(11)
C(8E)-C(12E)-C(13E)	113.8(10)
C(16E)-C(15E)-C(20E)	122.9(12)
C(16E)-C(15E)-N(10)	119.3(11)
C(20E)-C(15E)-N(10)	117.8(11)
C(15E)-C(16E)-C(17E)	118.3(12)
C(15E)-C(16E)-C(21E)	124.3(13)
C(17E)-C(16E)-C(21E)	117.3(12)
C(18E)-C(17E)-C(16E)	117.1(13)
C(19E)-C(18E)-C(17E)	123.6(14)
C(20E)-C(19E)-C(18E)	118.6(13)

C(19E)-C(20E)-C(15E)	119.0(12)
C(19E)-C(20E)-C(24E)	116.9(12)
C(15E)-C(20E)-C(24E)	124.0(12)
C(16E)-C(21E)-C(22E)	111.8(11)
C(16E)-C(21E)-C(23E)	110.5(9)
C(22E)-C(21E)-C(23E)	113.0(11)
C(20E)-C(24E)-C(25E)	109.9(11)
C(20E)-C(24E)-C(26E)	114.5(10)
C(25E)-C(24E)-C(26E)	110.0(10)
O(17)-C(27E)-C(31D)	124.4(11)
O(17)-C(27E)-C(28E)	118.3(10)
C(31D)-C(27E)-C(28E)	117.2(11)
O(20)-C(29E)-O(19)	122.8(12)
O(20)-C(29E)-C(30E)	121.1(11)
O(19)-C(29E)-C(30E)	116.1(11)
C(27A)-C(31E)-C(1E)#1	125.3(11)
O(1F)-C(1F)-O(2F)	122.0(15)
O(1F)-C(1F)-C(2F)	125.2(17)
O(2F)-C(1F)-C(2F)	112.8(13)
O(3F)-C(3F)-O(4F)	123.6(13)
O(3F)-C(3F)-C(4F)	120.5(13)
O(4F)-C(3F)-C(4F)	115.7(12)
O(6F)-C(5F)-O(5F)	121.1(12)
O(6F)-C(5F)-C(6F)	124.2(12)
O(5F)-C(5F)-C(6F)	114.7(12)
O(8F)-C(7F)-O(7F)	122.6(13)
O(8F)-C(7F)-C(8F)	126.8(13)
O(7F)-C(7F)-C(8F)	110.6(12)

Symmetry transformations used to generate equivalent atoms: #1 -x,-y+2,-z+2

Table 48. Anisotropic displacement parameters ($Å^2$ x 10^4). The anisotropic displacement factor exponent takes the form: $-2\pi^2[h^2a^*2U^{11} + ... + 2 h k a^* b^* U^{12}]$.

	U^{11}	U^{22}	U^{33}	U^{23}	U^{13}	U^{12}
Pd(1)	256(6)	463(7)	180(6)	70(5)	20(5)	-40(6)
Pd(2)	299(6)	207(6)	287(6)	42(5)	62(5)	-15(5)
Pd(3)	281(6)	193(6)	292(6)	13(5)	60(5)	-16(5)
Pd(4)	326(7)	242(6)	244(6)	-12(5)	82(5)	-41(6)
Pd(5)	238(6)	327(7)	197(6)	4(5)	30(5)	-9(6)
O(1)	250(50)	510(50)	290(40)	90(40)	70(40)	-50(40)
O(3)	550(60)	570(60)	220(50)	190(40)	80(40)	-50(50)
O(4)	530(50)	470(50)	380(50)	180(40)	60(40)	10(50)
O(5)	320(50)	160(40)	340(50)	0(40)	140(40)	10(40)
O(7)	450(50)	270(50)	350(50)	60(40)	120(40)	-70(40)
O(8)	380(50)	440(50)	260(50)	30(40)	130(40)	-30(40)
O(9)	330(50)	190(40)	260(40)	-10(40)	120(40)	-40(40)
O(11)	290(50)	250(50)	370(50)	60(40)	90(40)	30(40)
O(12)	370(50)	460(50)	450(50)	240(40)	130(40)	80(40)
O(13)	320(50)	330(50)	440(50)	50(40)	110(40)	-60(40)

O(15)	440(50)	330(50)	430(50)	180(40)	100(40)	-60(40)
O(16)	410(50)	420(50)	320(50)	130(40)	20(40)	10(50)
O(17)	330(50)	300(50)	140(40)	20(40)	10(40)	-10(40)
O(19)	280(50)	330(50)	120(40)	0(40)	0(40)	-40(40)
O(20)	300(50)	380(50)	350(50)	30(40)	10(40)	-20(50)
N(1)	170(50)	360(60)	200(50)	70(50)	-50(40)	-10(50)
N(2)	350(60)	420(60)	120(50)	20(50)	100(40)	120(50)
N(3)	200(50)	110(50)	230(50)	-60(40)	80(40)	-50(50)
N(4)	260(50)	220(50)	190(50)	90(40)	-10(40)	-60(50)
N(5)	290(50)	130(50)	370(50)	40(40)	160(50)	-20(50)
N(6)	230(40)	190(40)	300(40)	20(30)	90(30)	-50(30)
N(7)	370(60)	240(50)	280(50)	100(50)	30(50)	-10(50)
N(8)	350(60)	200(50)	240(50)	80(40)	80(40)	20(50)
N(9)	320(60)	370(60)	120(50)	90(40)	100(40)	40(50)
N(10)	260(50)	360(60)	120(50)	0(40)	40(40)	-70(50)
C(1A)	210(60)	320(70)	250(60)	190(60)	-40(50)	-40(60)
C(2A)	270(60)	350(70)	250(60)	120(50)	-40(50)	80(60)
C(3A)	300(70)	360(70)	100(60)	100(50)	0(50)	20(60)
C(4A)	370(70)	310(70)	250(60)	90(50)	60(50)	110(60)
C(5A)	430(70)	450(70)	260(60)	160(60)	120(50)	90(60)
C(6A)	570(80)	450(70)	450(70)	150(60)	250(60)	40(70)
C(7A)	620(80)	430(80)	460(70)	70(60)	240(60)	-90(70)
C(8A)	330(70)	370(70)	210(60)	120(50)	120(50)	20(60)
C(9A)	350(70)	400(70)	340(70)	90(50)	40(50)	130(60)
C(10A)	490(70)	510(80)	500(70)	140(60)	100(60)	90(70)
C(11A)	570(80)	580(80)	440(70)	160(60)	-70(60)	90(70)
C(12A)	500(70)	370(70)	360(70)	50(60)	110(60)	-70(60)
C(13A)	540(80)	810(80)	400(70)	140(60)	90(60)	70(70)
C(14A)	670(80)	800(90)	600(80)	100(70)	250(70)	-190(70)
C(15A)	380(70)	620(80)	570(80)	350(60)	50(60)	200(70)
C(16A)	580(80)	210(70)	520(70)	70(60)	380(60)	130(60)
C(17A)	960(90)	1110(100)	870(90)	460(70)	460(70)	-160(80)
C(18A)	880(90)	350(70)	750(80)	150(60)	520(70)	230(70)
C(19A)	1240(110)	1360(110)	1260(110)	580(80)	310(80)	-20(90)
C(20A)	950(90)	860(90)	820(90)	120(70)	420(80)	150(80)
C(21A)	420(70)	400(70)	370(70)	90(60)	110(60)	-210(60)
C(22A)	750(90)	760(90)	880(80)	160(70)	250(70)	-20(80)
C(23A)	630(80)	620(80)	460(70)	120(60)	40(60)	0(70)
C(24A)	840(90)	1130(100)	720(90)	410(70)	100(70)	290(80)
C(25A)	1480(120)	1650(120)	1600(110)	840(90)	500(90)	230(90)
C(26A)	1210(110)	1270(110)	1260(100)	560(80)	160(80)	270(90)
C(27A)	310(70)	380(70)	250(60)	90(50)	40(60)	-10(60)
C(28A)	350(70)	600(80)	310(60)	90(60)	70(50)	-110(60)
C(29A)	570(80)	460(80)	430(70)	140(60)	160(60)	0(70)
C(30A)	970(90)	710(90)	620(80)	290(70)	100(70)	0(80)
C(31A)	210(60)	330(70)	220(60)	50(50)	70(50)	10(60)
C(1B)	180(60)	190(60)	230(60)	110(50)	90(50)	50(50)
C(2B)	160(60)	260(60)	240(60)	60(50)	30(50)	10(50)
C(3B)	300(60)	220(60)	290(60)	80(50)	100(50)	90(60)

C(4B)	410(70)	250(60)	320(60)	200(50)	60(60)	20(60)
C(5B)	560(80)	230(70)	390(70)	60(50)	100(60)	0(60)
C(6B)	490(70)	300(70)	380(70)	60(60)	20(60)	-50(60)
C(7B)	410(70)	460(70)	430(70)	160(60)	20(60)	-20(60)
C(8B)	340(70)	330(70)	390(70)	120(60)	60(60)	-30(60)
C(9B)	440(70)	310(70)	390(70)	60(50)	140(60)	80(60)
C(10B)	550(80)	490(70)	510(70)	180(60)	170(60)	160(70)
C(11B)	610(80)	600(80)	670(80)	200(60)	280(60)	170(70)
C(12B)	380(70)	500(80)	440(70)	100(60)	20(60)	-40(70)
C(13B)	670(80)	560(80)	870(80)	230(70)	170(70)	140(70)
C(14B)	640(80)	950(90)	780(80)	280(70)	260(70)	110(80)
C(15B)	350(70)	350(70)	380(70)	250(60)	-40(60)	-30(60)
C(16B)	740(80)	690(80)	460(70)	310(70)	140(70)	-40(70)
C(17B)	830(90)	940(90)	620(80)	410(70)	-70(70)	-90(80)
C(18B)	1080(100)	650(90)	510(80)	160(70)	50(70)	-80(80)
C(19B)	930(90)	690(90)	780(80)	370(70)	190(70)	250(70)
C(20B)	550(70)	290(70)	280(70)	80(50)	100(60)	20(60)
C(21B)	1020(110)	1590(120)	910(100)	680(80)	10(80)	110(90)
C(22B)	3100(200)	2700(200)	3300(200)	1580(120)	450(100)	350(100)
C(23B)	1010(110)	970(100)	1410(110)	340(80)	200(80)	10(90)
C(24B)	490(70)	320(70)	490(70)	200(60)	260(60)	150(60)
C(25B)	590(80)	490(80)	610(70)	130(60)	230(60)	170(70)
C(26B)	810(90)	770(90)	780(80)	250(70)	350(70)	140(80)
C(27B)	210(60)	220(60)	130(60)	40(50)	-20(50)	-30(60)
C(28B)	410(70)	260(70)	350(60)	120(50)	130(50)	30(60)
C(29B)	420(70)	290(70)	400(70)	120(60)	70(60)	-60(60)
C(30B)	690(80)	660(80)	690(80)	80(60)	280(70)	-110(70)
C(31B)	210(60)	200(60)	270(60)	-20(50)	50(50)	0(60)
C(1C)	230(60)	300(70)	210(60)	70(50)	20(50)	0(60)
C(2C)	280(60)	230(60)	330(60)	70(50)	90(50)	-10(60)
C(3C)	280(70)	270(70)	260(60)	50(50)	110(50)	30(60)
C(4C)	290(70)	380(70)	350(70)	140(60)	70(60)	80(60)
C(5C)	510(70)	470(80)	520(70)	230(60)	260(60)	60(60)
C(6C)	440(70)	470(70)	570(80)	230(60)	140(60)	210(60)
C(7C)	530(70)	440(70)	420(70)	100(60)	280(60)	-10(60)
C(8C)	300(70)	270(70)	440(70)	120(60)	50(60)	110(60)
C(9C)	350(70)	560(80)	620(80)	210(60)	150(60)	90(70)
C(10C)	650(80)	770(90)	650(80)	270(70)	240(60)	180(70)
C(11C)	620(80)	730(80)	700(80)	400(70)	100(60)	30(70)
C(12C)	620(80)	560(80)	450(70)	160(60)	270(60)	10(70)
C(13C)	920(90)	680(80)	710(80)	230(70)	-40(70)	160(80)
C(14C)	770(90)	730(80)	790(80)	370(70)	100(70)	-60(70)
C(15C)	320(70)	200(60)	240(60)	40(50)	30(60)	0(60)
C(16C)	310(70)	360(70)	310(70)	140(60)	130(60)	-20(60)
C(17C)	350(70)	360(70)	450(70)	160(60)	-30(60)	0(60)
C(18C)	480(80)	560(80)	460(70)	100(60)	280(60)	-90(70)
C(19C)	410(70)	410(70)	530(70)	210(60)	10(60)	-10(60)
C(20C)	330(70)	230(60)	280(60)	90(50)	100(60)	-100(60)
C(21C)	280(70)	340(70)	340(60)	100(50)	-60(50)	60(60)

C(22C)	340(70)	600(80)	440(70)	70(60)	60(60)	40(60)
C(23C)	440(70)	470(70)	560(70)	180(60)	-80(60)	40(70)
C(24C)	330(70)	380(70)	360(70)	80(60)	40(60)	20(60)
C(25C)	500(70)	550(80)	520(70)	180(60)	90(60)	130(70)
C(26C)	620(80)	570(80)	450(70)	140(60)	50(60)	200(70)
C(27C)	230(60)	290(70)	240(60)	150(50)	120(50)	120(60)
C(28C)	340(70)	340(70)	360(60)	30(50)	120(50)	60(60)
C(29C)	210(60)	200(70)	380(70)	70(60)	50(60)	50(60)
C(30C)	520(70)	460(70)	670(80)	200(60)	200(60)	110(70)
C(31C)	220(60)	240(60)	310(60)	30(50)	120(50)	20(60)
C(1D)	220(60)	250(60)	280(60)	140(50)	-20(50)	30(60)
C(2D)	200(60)	360(70)	320(60)	0(50)	30(50)	-70(60)
C(3D)	340(70)	270(60)	80(60)	50(50)	10(50)	-20(60)
C(4D)	360(70)	280(70)	310(70)	150(50)	60(60)	20(60)
C(5D)	450(70)	350(70)	370(70)	100(60)	60(60)	-30(60)
C(6D)	550(80)	380(70)	310(70)	120(60)	40(60)	10(70)
C(7D)	370(70)	410(70)	280(60)	90(60)	0(60)	70(60)
C(8D)	370(70)	300(70)	280(60)	70(50)	80(60)	60(60)
C(9D)	440(70)	490(80)	460(70)	200(60)	110(60)	10(70)
C(10D)	550(80)	790(90)	630(80)	170(70)	100(60)	50(70)
C(11D)	670(80)	790(90)	850(80)	340(70)	230(70)	80(70)
C(12D)	450(70)	510(70)	390(70)	230(60)	0(60)	20(70)
C(13D)	620(80)	860(90)	620(80)	280(70)	120(60)	50(70)
C(14D)	500(80)	560(80)	640(70)	220(60)	90(60)	-20(70)
C(15D)	280(70)	250(70)	240(60)	30(50)	30(50)	0(60)
C(16D)	400(70)	320(70)	420(70)	220(60)	30(60)	-30(60)
C(17D)	460(80)	480(80)	440(70)	120(60)	-10(60)	190(70)
C(18D)	710(80)	490(80)	500(70)	210(60)	230(70)	20(70)
C(19D)	490(80)	490(80)	510(70)	170(60)	190(60)	60(70)
C(20D)	470(70)	220(60)	340(70)	150(50)	160(60)	70(60)
C(21D)	680(80)	530(80)	730(80)	360(70)	-140(70)	130(70)
C(22D)	950(100)	1240(100)	1010(90)	200(70)	340(80)	170(80)
C(23D)	1040(100)	1470(110)	1110(100)	230(80)	300(80)	170(90)
C(24D)	320(70)	310(70)	380(70)	50(50)	80(60)	-80(60)
C(25D)	510(80)	610(80)	650(70)	190(60)	210(60)	90(70)
C(26D)	500(70)	460(70)	560(70)	120(60)	80(60)	-80(70)
C(27D)	310(70)	320(70)	410(70)	90(60)	100(60)	-60(60)
C(28D)	350(70)	400(70)	510(70)	20(60)	240(60)	-80(60)
C(29D)	490(80)	380(70)	430(70)	220(60)	190(60)	130(60)
C(30D)	610(80)	630(80)	460(70)	280(60)	120(60)	220(70)
C(31D)	280(60)	260(60)	220(60)	30(50)	10(50)	-40(60)
C(1E)	290(70)	360(70)	310(70)	140(60)	80(60)	20(60)
C(2E)	300(60)	310(70)	280(60)	90(50)	70(50)	30(60)
C(3E)	160(60)	280(70)	250(60)	40(50)	40(50)	-70(60)
C(4E)	210(60)	470(70)	300(60)	150(60)	50(50)	40(60)
C(5E)	430(70)	480(70)	310(60)	180(60)	80(60)	80(70)
C(6E)	300(70)	680(80)	380(70)	170(60)	100(60)	-20(70)
C(7E)	400(70)	470(70)	280(60)	90(60)	80(60)	-10(60)
C(8E)	270(70)	490(70)	220(60)	120(60)	70(50)	20(60)

C(9E)	240(60)	430(70)	350(70)	70(60)	50(50)	80(60)
C(10E)	480(70)	500(70)	510(70)	210(60)	30(60)	70(60)
C(11E)	410(70)	580(80)	570(70)	70(60)	100(60)	80(70)
C(12E)	440(70)	410(70)	390(70)	80(60)	50(60)	-30(60)
C(13E)	620(80)	460(80)	620(70)	100(60)	250(60)	-30(70)
C(14E)	610(80)	510(80)	670(80)	230(60)	100(60)	40(70)
C(15E)	270(70)	190(60)	230(60)	60(50)	60(50)	20(60)
C(16E)	330(70)	380(70)	290(60)	60(60)	100(50)	-10(60)
C(17E)	610(80)	480(80)	520(70)	190(60)	150(60)	110(70)
C(18E)	430(80)	570(80)	460(70)	120(60)	140(60)	-120(70)
C(19E)	440(70)	380(70)	390(70)	120(60)	110(60)	-20(70)
C(20E)	340(70)	270(70)	340(70)	40(50)	120(50)	-50(60)
C(21E)	550(80)	490(70)	330(70)	130(60)	190(60)	60(60)
C(22E)	690(80)	710(80)	810(80)	360(70)	70(70)	80(70)
C(23E)	490(70)	630(80)	630(80)	70(60)	160(60)	80(70)
C(24E)	260(70)	520(70)	240(60)	40(60)	60(50)	-20(60)
C(25E)	480(70)	670(80)	590(70)	100(60)	190(60)	120(70)
C(26E)	460(70)	640(80)	540(70)	100(60)	70(60)	30(70)
C(27E)	180(60)	260(70)	190(60)	40(50)	20(50)	-20(50)
C(28E)	360(70)	380(70)	320(60)	40(50)	100(50)	0(60)
C(29E)	250(60)	270(70)	210(60)	30(50)	70(50)	-20(60)
C(30E)	330(70)	480(70)	380(70)	150(60)	120(50)	40(60)
C(31E)	250(60)	390(70)	210(60)	50(50)	80(50)	-10(60)
O(1F)	490(60)	550(60)	740(60)	310(50)	240(50)	130(50)
O(2F)	630(60)	700(70)	1150(70)	500(60)	410(50)	240(60)
C(1F)	550(80)	540(80)	760(80)	250(70)	220(70)	50(70)
C(2F)	700(80)	710(80)	1020(90)	450(70)	320(70)	240(70)
O(3F)	450(60)	1300(80)	520(60)	370(50)	50(50)	-40(60)
O(4F)	320(50)	680(60)	330(50)	210(40)	-10(40)	-110(50)
C(3F)	400(70)	720(80)	350(70)	240(60)	100(60)	-10(70)
C(4F)	680(80)	930(90)	570(80)	370(70)	80(60)	-60(70)
O(5F)	360(50)	710(60)	560(50)	50(50)	130(40)	60(50)
O(6F)	370(50)	520(60)	420(50)	70(40)	110(40)	20(50)
C(5F)	330(70)	570(80)	520(80)	40(60)	110(60)	50(70)
C(6F)	390(70)	740(80)	570(70)	-90(60)	230(60)	10(70)
O(7F)	550(60)	560(60)	450(50)	200(50)	-10(50)	200(50)
O(8F)	430(50)	420(50)	450(50)	100(40)	10(40)	130(50)
C(7F)	390(70)	390(70)	340(70)	60(60)	30(60)	30(60)
C(8F)	590(80)	580(80)	380(70)	220(60)	90(60)	160(70)
O(9F)	680(60)	670(60)	640(60)	70(50)	130(50)	-130(50)

Table 49. Hydrogen bonds [Å and °].

D-H...A	d(D-H)	d(H...A)	d(D...A)	<(DHA)
O(2F)-H(2F)...O(12)#2	0.84	1.71	2.538(12)	168.9
O(4F)-H(4F)...O(8)#3	0.84	1.69	2.509(11)	165.2
O(5F)-H(5F)...O(20)#4	0.84	2.13	2.517(11)	107.7
O(7F)-H(7F)...O(4)#5	0.84	1.71	2.548(11)	171.7
O(9F)-H(9F2)...O(9F)#6	0.87	2.12	2.991(16)	179.4

O(9F)-H(9F1)...O(16)#7	0.87	1.94	2.812(11)	179.1

Symmetry transformations used to generate equivalent atoms: #1 -x,-y+2,-z+2, #2 -x+1,-y+1,-z+1, #3 -x,-y+1,-z+1, #4 -x+1,-y+2,-z+1, #5 x+1,y,z, #6 -x,-y,-z+1, #7 x,y-1,z

B.1a (CCDC 736628)

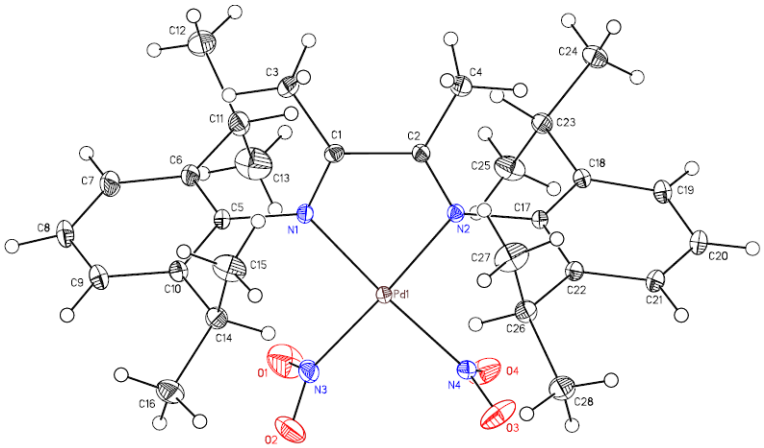

Special Refinement Details

Crystals were mounted on a glass fiber using Paratone oil then placed on the diffractometer under a nitrogen stream at 100K.

Refinement of F^2 against ALL reflections. The weighted R-factor (wR) and goodness of fit (S) are based on F^2, conventional R-factors (R) are based on F, with F set to zero for negative F^2. The threshold expression of $F^2 > 2\sigma(F^2)$ is used only for calculating R-factors(gt) etc. and is not relevant to the choice of reflections for refinement. R-factors based on F^2 are statistically about twice as large as those based on F, and R-factors based on ALL data will be even larger.

All esds (except the esd in the dihedral angle between two l.s. planes) are estimated using the full covariance matrix. The cell esds are taken into account individually in the estimation of esds in distances, angles and torsion angles; correlations between esds in cell parameters are only used when they are defined by crystal symmetry. An approximate (isotropic) treatment of cell esds is used for estimating esds involving l.s. planes.

Table 50. Atomic coordinates (x 10^4) and equivalent isotropic displacement parameters (Å^2 x 10^3). U(eq) is defined as the trace of the orthogonalized Uij tensor.

	x	y	z	Ueq
Pd(1)	4941(1)	1146(1)	7464(1)	9(1)
O(1)	7026(1)	256(1)	6694(1)	36(1)
O(2)	4374(1)	-1276(1)	6418(1)	27(1)
O(3)	3156(1)	-1876(1)	8129(1)	28(1)
O(4)	5860(1)	-824(1)	8293(1)	26(1)
N(1)	5285(1)	3170(1)	6929(1)	10(1)
N(2)	4367(1)	2517(1)	8153(1)	9(1)
N(3)	5535(1)	-102(1)	6756(1)	17(1)
N(4)	4600(1)	-766(1)	8042(1)	13(1)
C(1)	5005(1)	4288(1)	7244(1)	11(1)
C(2)	4481(1)	3911(1)	7950(1)	10(1)
C(3)	5180(1)	5868(1)	6957(1)	16(1)
C(4)	4162(1)	5126(1)	8363(1)	16(1)
C(5)	5897(1)	3424(1)	6257(1)	11(1)
C(6)	7615(1)	4528(1)	6188(1)	14(1)
C(7)	8170(1)	4712(1)	5530(1)	19(1)
C(8)	7065(1)	3819(1)	4981(1)	21(1)

C(9)	5375(1)	2720(1)	5070(1)	18(1)
C(10)	4752(1)	2487(1)	5712(1)	13(1)
C(11)	8870(1)	5446(1)	6785(1)	16(1)
C(12)	9999(1)	7305(1)	6670(1)	27(1)
C(13)	9967(2)	4592(2)	6941(1)	33(1)
C(14)	2906(1)	1292(1)	5822(1)	15(1)
C(15)	1866(1)	2233(1)	5918(1)	24(1)
C(16)	2074(1)	-69(1)	5248(1)	22(1)
C(17)	3944(1)	2018(1)	8833(1)	10(1)
C(18)	5213(1)	2742(1)	9360(1)	12(1)
C(19)	4789(1)	2110(1)	9999(1)	16(1)
C(20)	3172(1)	850(1)	10103(1)	18(1)
C(21)	1937(1)	189(1)	9574(1)	16(1)
C(22)	2294(1)	746(1)	8922(1)	12(1)
C(23)	6987(1)	4115(1)	9240(1)	13(1)
C(24)	7856(1)	5302(1)	9863(1)	20(1)
C(25)	8094(1)	3359(1)	8988(1)	22(1)
C(26)	961(1)	63(1)	8337(1)	15(1)
C(27)	154(1)	1215(1)	8223(1)	25(1)
C(28)	-428(1)	-1728(1)	8424(1)	21(1)

Table 51. Bond lengths [Å] and angles [°].

Pd(1)-N(4)	2.0107(7)	N(4)-Pd(1)-N(3)	84.86(3)
Pd(1)-N(3)	2.0111(8)	N(4)-Pd(1)-N(1)	176.52(3)
Pd(1)-N(1)	2.0441(7)	N(3)-Pd(1)-N(1)	98.52(3)
Pd(1)-N(2)	2.0502(7)	N(4)-Pd(1)-N(2)	98.10(3)
O(1)-N(3)	1.2277(11)	N(3)-Pd(1)-N(2)	177.04(3)
O(2)-N(3)	1.2324(11)	N(1)-Pd(1)-N(2)	78.52(3)
O(3)-N(4)	1.2332(10)	C(1)-N(1)-C(5)	120.80(7)
O(4)-N(4)	1.2338(10)	C(1)-N(1)-Pd(1)	115.71(5)
N(1)-C(1)	1.2964(10)	C(5)-N(1)-Pd(1)	123.39(5)
N(1)-C(5)	1.4437(10)	C(2)-N(2)-C(17)	121.57(7)
N(2)-C(2)	1.2920(10)	C(2)-N(2)-Pd(1)	115.54(5)
N(2)-C(17)	1.4424(10)	C(17)-N(2)-Pd(1)	122.82(5)
C(1)-C(2)	1.4925(11)	O(1)-N(3)-O(2)	121.51(8)
C(1)-C(3)	1.4926(12)	O(1)-N(3)-Pd(1)	119.73(7)
C(2)-C(4)	1.4874(12)	O(2)-N(3)-Pd(1)	118.65(7)
C(3)-H(3A)	1.030(16)	O(3)-N(4)-O(4)	120.97(8)
C(3)-H(3B)	0.942(15)	O(3)-N(4)-Pd(1)	120.25(6)
C(3)-H(3C)	0.979(13)	O(4)-N(4)-Pd(1)	118.76(6)
C(4)-H(4A)	1.018(17)	N(1)-C(1)-C(2)	114.99(7)
C(4)-H(4B)	0.965(16)	N(1)-C(1)-C(3)	125.30(8)
C(4)-H(4C)	0.929(15)	C(2)-C(1)-C(3)	119.71(7)
C(5)-C(6)	1.4022(11)	N(2)-C(2)-C(4)	125.21(7)
C(5)-C(10)	1.4044(11)	N(2)-C(2)-C(1)	115.24(7)
C(6)-C(7)	1.4008(12)	C(4)-C(2)-C(1)	119.54(7)
C(6)-C(11)	1.5182(12)	C(1)-C(3)-H(3A)	111.8(9)
C(7)-C(8)	1.3861(14)	C(1)-C(3)-H(3B)	107.7(10)

C(7)-H(7)	0.966(14)	H(3A)-C(3)-H(3B)	115.9(13)
C(8)-C(9)	1.3890(14)	C(1)-C(3)-H(3C)	109.8(9)
C(8)-H(8)	0.953(15)	H(3A)-C(3)-H(3C)	112.9(12)
C(9)-C(10)	1.3935(12)	H(3B)-C(3)-H(3C)	97.8(12)
C(9)-H(9)	0.980(13)	C(2)-C(4)-H(4A)	114.7(9)
C(10)-C(14)	1.5210(12)	C(2)-C(4)-H(4B)	112.3(9)
C(11)-C(13)	1.5297(16)	H(4A)-C(4)-H(4B)	102.3(13)
C(11)-C(12)	1.5323(14)	C(2)-C(4)-H(4C)	112.7(9)
C(11)-H(11)	0.977(14)	H(4A)-C(4)-H(4C)	105.6(13)
C(12)-H(12A)	0.999(18)	H(4B)-C(4)-H(4C)	108.4(14)
C(12)-H(12B)	0.916(16)	C(6)-C(5)-C(10)	123.58(7)
C(12)-H(12C)	0.981(16)	C(6)-C(5)-N(1)	118.39(7)
C(13)-H(13A)	0.87(2)	C(10)-C(5)-N(1)	117.96(7)
C(13)-H(13B)	0.949(18)	C(7)-C(6)-C(5)	116.72(8)
C(13)-H(13C)	1.04(2)	C(7)-C(6)-C(11)	120.03(7)
C(14)-C(16)	1.5321(13)	C(5)-C(6)-C(11)	123.21(7)
C(14)-C(15)	1.5350(14)	C(8)-C(7)-C(6)	121.03(8)
C(14)-H(14)	0.974(15)	C(8)-C(7)-H(7)	120.5(9)
C(15)-H(15A)	0.965(14)	C(6)-C(7)-H(7)	118.5(9)
C(15)-H(15B)	0.944(17)	C(7)-C(8)-C(9)	120.69(8)
C(15)-H(15C)	0.909(17)	C(7)-C(8)-H(8)	124.9(9)
C(16)-H(16A)	0.987(18)	C(9)-C(8)-H(8)	114.1(9)
C(16)-H(16B)	0.995(16)	C(8)-C(9)-C(10)	120.81(8)
C(16)-H(16C)	0.961(16)	C(8)-C(9)-H(9)	119.5(8)
C(17)-C(18)	1.4041(11)	C(10)-C(9)-H(9)	119.5(8)
C(17)-C(22)	1.4057(10)	C(9)-C(10)-C(5)	117.15(7)
C(18)-C(19)	1.3988(12)	C(9)-C(10)-C(14)	121.73(7)
C(18)-C(23)	1.5227(11)	C(5)-C(10)-C(14)	121.10(7)
C(19)-C(20)	1.3888(13)	C(6)-C(11)-C(13)	110.31(8)
C(19)-H(19)	0.891(14)	C(6)-C(11)-C(12)	112.53(8)
C(20)-C(21)	1.3862(13)	C(13)-C(11)-C(12)	110.08(9)
C(20)-H(20)	0.932(16)	C(6)-C(11)-H(11)	112.3(8)
C(21)-C(22)	1.3971(12)	C(13)-C(11)-H(11)	105.1(9)
C(21)-H(21)	1.000(13)	C(12)-C(11)-H(11)	106.2(8)
C(22)-C(26)	1.5158(12)	C(11)-C(12)-H(12A)	108.6(10)
C(23)-C(24)	1.5298(12)	C(11)-C(12)-H(12B)	110.1(10)
C(23)-C(25)	1.5290(13)	H(12A)-C(12)-H(12B)	106.3(13)
C(23)-H(23)	0.995(16)	C(11)-C(12)-H(12C)	111.4(9)
C(24)-H(24A)	0.952(15)	H(12A)-C(12)-H(12C)	115.5(15)
C(24)-H(24B)	0.959(13)	H(12B)-C(12)-H(12C)	104.7(13)
C(24)-H(24C)	0.942(16)	C(11)-C(13)-H(13A)	110.6(13)
C(25)-H(25A)	0.969(16)	C(11)-C(13)-H(13B)	111.0(10)
C(25)-H(25B)	0.905(16)	H(13A)-C(13)-H(13B)	110.5(18)
C(25)-H(25C)	1.002(17)	C(11)-C(13)-H(13C)	114.1(11)
C(26)-C(27)	1.5325(14)	H(13A)-C(13)-H(13C)	106.3(17)
C(26)-C(28)	1.5320(12)	H(13B)-C(13)-H(13C)	104.1(14)
C(26)-H(26)	0.976(13)	C(10)-C(14)-C(16)	112.28(8)
C(27)-H(27A)	0.913(17)	C(10)-C(14)-C(15)	111.69(8)
C(27)-H(27B)	0.898(16)	C(16)-C(14)-C(15)	110.15(8)

C(27)-H(27C)	0.965(19)
C(28)-H(28A)	1.029(14)
C(28)-H(28B)	0.937(16)
C(28)-H(28C)	0.984(14)

C(10)-C(14)-H(14)	107.3(8)
C(16)-C(14)-H(14)	108.9(8)
C(15)-C(14)-H(14)	106.3(8)
C(14)-C(15)-H(15A)	111.1(8)
C(14)-C(15)-H(15B)	113.1(11)
H(15A)-C(15)-H(15B)	109.4(13)
C(14)-C(15)-H(15C)	112.4(9)
H(15A)-C(15)-H(15C)	105.4(12)
H(15B)-C(15)-H(15C)	105.0(14)
C(14)-C(16)-H(16A)	107.5(9)
C(14)-C(16)-H(16B)	108.4(9)
H(16A)-C(16)-H(16B)	106.3(13)
C(14)-C(16)-H(16C)	111.9(9)
H(16A)-C(16)-H(16C)	111.0(14)
H(16B)-C(16)-H(16C)	111.4(13)
C(18)-C(17)-C(22)	123.52(7)
C(18)-C(17)-N(2)	118.89(6)
C(22)-C(17)-N(2)	117.47(7)
C(19)-C(18)-C(17)	116.87(7)
C(19)-C(18)-C(23)	121.35(7)
C(17)-C(18)-C(23)	121.76(7)
C(20)-C(19)-C(18)	120.99(8)
C(20)-C(19)-H(19)	118.5(9)
C(18)-C(19)-H(19)	120.5(9)
C(19)-C(20)-C(21)	120.62(8)
C(19)-C(20)-H(20)	117.8(9)
C(21)-C(20)-H(20)	121.6(9)
C(20)-C(21)-C(22)	121.03(8)
C(20)-C(21)-H(21)	120.9(8)
C(22)-C(21)-H(21)	118.0(8)
C(21)-C(22)-C(17)	116.94(7)
C(21)-C(22)-C(26)	122.09(7)
C(17)-C(22)-C(26)	120.94(7)
C(18)-C(23)-C(24)	113.03(7)
C(18)-C(23)-C(25)	110.81(7)
C(24)-C(23)-C(25)	110.51(8)
C(18)-C(23)-H(23)	112.3(8)
C(24)-C(23)-H(23)	103.5(8)
C(25)-C(23)-H(23)	106.3(8)
C(23)-C(24)-H(24A)	111.2(10)
C(23)-C(24)-H(24B)	112.5(8)
H(24A)-C(24)-H(24B)	105.8(12)
C(23)-C(24)-H(24C)	109.6(9)
H(24A)-C(24)-H(24C)	110.8(13)
H(24B)-C(24)-H(24C)	106.9(12)
C(23)-C(25)-H(25A)	107.7(8)
C(23)-C(25)-H(25B)	107.9(10)
H(25A)-C(25)-H(25B)	107.1(13)
C(23)-C(25)-H(25C)	111.2(9)

H(25A)-C(25)-H(25C)	108.3(13)
H(25B)-C(25)-H(25C)	114.3(13)
C(22)-C(26)-C(27)	111.02(8)
C(22)-C(26)-C(28)	113.17(8)
C(27)-C(26)-C(28)	109.68(8)
C(22)-C(26)-H(26)	107.5(8)
C(27)-C(26)-H(26)	108.3(8)
C(28)-C(26)-H(26)	107.0(8)
C(26)-C(27)-H(27A)	112.4(11)
C(26)-C(27)-H(27B)	112.8(10)
H(27A)-C(27)-H(27B)	107.8(14)
C(26)-C(27)-H(27C)	112.7(11)
H(27A)-C(27)-H(27C)	102.9(15)
H(27B)-C(27)-H(27C)	107.7(16)
C(26)-C(28)-H(28A)	110.7(8)
C(26)-C(28)-H(28B)	109.4(10)
H(28A)-C(28)-H(28B)	106.1(12)
C(26)-C(28)-H(28C)	112.6(8)
H(28A)-C(28)-H(28C)	109.3(12)
H(28B)-C(28)-H(28C)	108.4(12)

Table 52. Anisotropic displacement parameters ($Å^2$ x 10^4). The anisotropic displacement factor exponent takes the form: $-2\pi^2[h^2a^*2U^{11} + ... + 2 h k a^* b^* U^{12}]$.

	U^{11}	U^{22}	U^{33}	U^{23}	U^{13}	U^{12}
Pd(1)	107(1)	89(1)	75(1)	6(1)	11(1)	48(1)
O(1)	277(4)	388(5)	436(6)	-65(4)	133(4)	170(4)
O(2)	373(4)	259(4)	204(4)	-99(3)	-64(3)	171(3)
O(3)	190(3)	189(3)	483(5)	160(3)	133(3)	94(3)
O(4)	233(3)	185(3)	314(4)	58(3)	-115(3)	73(3)
N(1)	103(2)	107(2)	83(3)	14(2)	8(2)	42(2)
N(2)	87(2)	99(2)	87(3)	5(2)	8(2)	36(2)
N(3)	257(3)	168(3)	126(3)	15(2)	37(3)	138(3)
N(4)	184(3)	110(3)	112(3)	6(2)	13(2)	74(2)
C(1)	99(3)	98(3)	118(3)	10(2)	-2(2)	40(2)
C(2)	103(3)	101(3)	95(3)	1(2)	4(2)	43(2)
C(3)	204(3)	129(3)	154(4)	40(3)	24(3)	87(3)
C(4)	226(4)	141(3)	152(4)	6(3)	40(3)	108(3)
C(5)	133(3)	117(3)	83(3)	14(2)	17(2)	53(2)
C(6)	135(3)	137(3)	115(3)	12(2)	29(2)	46(3)
C(7)	185(3)	196(4)	150(4)	18(3)	72(3)	55(3)
C(8)	257(4)	229(4)	106(4)	19(3)	62(3)	88(3)
C(9)	225(4)	197(4)	100(3)	-4(3)	6(3)	89(3)
C(10)	153(3)	135(3)	102(3)	7(2)	0(2)	64(3)
C(11)	127(3)	180(4)	144(4)	0(3)	22(3)	34(3)
C(12)	243(4)	191(4)	249(5)	-9(4)	27(4)	-13(4)
C(13)	291(5)	341(6)	357(6)	-42(5)	-120(5)	169(5)
C(14)	146(3)	148(3)	132(3)	-2(3)	-23(2)	50(3)
C(15)	175(4)	244(4)	300(5)	-57(4)	-55(3)	103(3)

C(16)	220(4)	189(4)	202(4)	-47(3)	-50(3)	56(3)
C(17)	117(3)	99(3)	82(3)	10(2)	18(2)	49(2)
C(18)	134(3)	113(3)	91(3)	3(2)	4(2)	52(2)
C(19)	203(3)	164(3)	93(3)	11(2)	0(3)	78(3)
C(20)	236(4)	169(4)	110(3)	38(3)	47(3)	77(3)
C(21)	174(3)	139(3)	132(3)	29(3)	57(3)	45(3)
C(22)	121(3)	113(3)	112(3)	10(2)	29(2)	46(2)
C(23)	128(3)	130(3)	119(3)	-7(2)	-18(2)	42(3)
C(24)	204(4)	167(4)	163(4)	-43(3)	-34(3)	39(3)
C(25)	140(3)	207(4)	279(5)	-55(4)	9(3)	63(3)
C(26)	107(3)	151(3)	151(3)	3(3)	14(2)	36(3)
C(27)	150(4)	235(4)	365(6)	46(4)	-20(4)	86(3)
C(28)	143(3)	171(4)	220(4)	-5(3)	28(3)	1(3)

Table 53. Hydrogen coordinates (x 10^4) and isotropic displacement parameters (Å^2 x 10^3).

	x	y	z	Uiso
H(3A)	5507(18)	5954(18)	6463(8)	28(4)
H(3B)	5913(19)	6768(19)	7259(8)	31(4)
H(3C)	4144(17)	5965(17)	7016(7)	21(3)
H(4A)	3809(19)	4780(20)	8838(9)	34(4)
H(4B)	3220(19)	5260(19)	8175(8)	30(4)
H(4C)	5105(18)	6178(19)	8420(8)	29(4)
H(7)	9342(17)	5485(17)	5466(8)	23(3)
H(8)	7390(18)	3798(19)	4531(8)	28(4)
H(9)	4632(16)	2039(16)	4681(7)	16(3)
H(11)	8306(17)	5414(17)	7200(8)	23(3)
H(12A)	10800(20)	7390(20)	6316(10)	44(5)
H(12B)	10661(18)	7841(19)	7055(9)	28(4)
H(12C)	9320(18)	7885(19)	6584(8)	28(4)
H(13A)	9330(20)	3530(30)	7010(11)	61(6)
H(13B)	10740(20)	5140(20)	7321(10)	44(5)
H(13C)	10740(20)	4630(20)	6556(11)	50(5)
H(14)	2885(16)	759(17)	6243(7)	20(3)
H(15A)	2382(16)	3103(17)	6275(8)	22(3)
H(15B)	730(20)	1520(20)	6007(9)	41(4)
H(15C)	1805(18)	2764(18)	5543(8)	26(4)
H(16A)	1957(19)	480(20)	4841(9)	35(4)
H(16B)	900(20)	-850(20)	5365(9)	35(4)
H(16C)	2721(19)	-652(19)	5166(8)	30(4)
H(19)	5558(16)	2502(17)	10348(7)	19(3)
H(20)	2942(17)	491(18)	10541(8)	24(3)
H(21)	753(16)	-673(16)	9652(7)	19(3)
H(23)	6974(17)	4875(17)	8889(8)	23(3)
H(24A)	7199(19)	5818(19)	10012(8)	30(4)
H(24B)	8941(16)	6206(17)	9774(7)	19(3)
H(24C)	8048(17)	4709(18)	10210(8)	22(3)
H(25A)	8270(17)	2753(18)	9352(8)	23(3)
H(25B)	9120(20)	4210(20)	8911(8)	32(4)
H(25C)	7519(19)	2550(20)	8590(9)	35(4)

H(26)	1529(16)	27(16)	7931(7)	17(3)
H(27A)	-300(20)	1390(20)	8603(9)	33(4)
H(27B)	-667(19)	820(20)	7888(9)	33(4)
H(27C)	970(20)	2340(20)	8122(10)	47(5)
H(28A)	91(17)	-2521(17)	8499(8)	21(3)
H(28B)	-1128(18)	-2137(18)	8025(8)	26(4)
H(28C)	-1140(17)	-1794(17)	8799(8)	24(3)

B.1b (CCDC 736629)

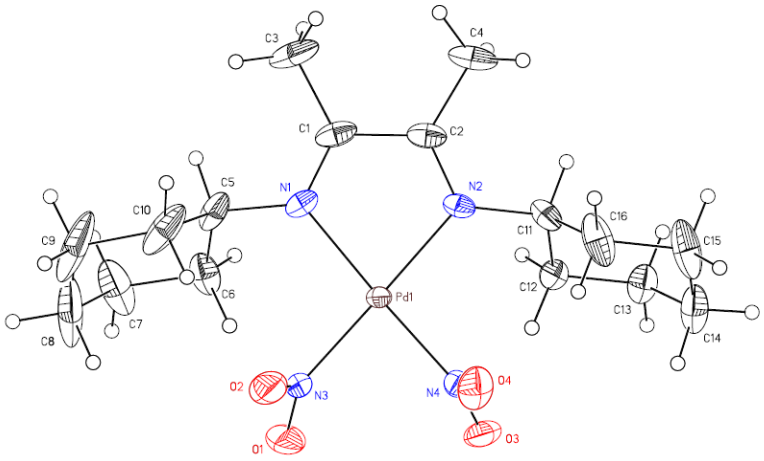

Special Refinement Details

Crystals were mounted on a glass fiber using Paratone oil then placed on the diffractometer under a nitrogen stream at 100K.

One molecule of acetone sits on a center of symmetry and therefore has the occupancy fixed at one-half. No restraints were applied.

Refinement of F^2 against ALL reflections. The weighted R-factor (wR) and goodness of fit (S) are based on F^2, conventional R-factors (R) are based on F, with F set to zero for negative F^2. The threshold expression of $F^2 > 2\sigma(F^2)$ is used only for calculating R-factors(gt) etc. and is not relevant to the choice of reflections for refinement. R-factors based on F^2 are statistically about twice as large as those based on F, and R-factors based on ALL data will be even larger.

All esds (except the esd in the dihedral angle between two l.s. planes) are estimated using the full covariance matrix. The cell esds are taken into account individually in the estimation of esds in distances, angles and torsion angles; correlations between esds in cell parameters are only used when they are defined by crystal symmetry. An approximate (isotropic) treatment of cell esds is used for estimating esds involving l.s. planes.

Table 54. Atomic coordinates (x 10^4) and equivalent isotropic displacement parameters (Å^2 x 10^3). U(eq) is defined as the trace of the orthogonalized Uij tensor.

	x	y	z	Ueq	Occ
Pd(1)	576(1)	1684(1)	5365(1)	17(1)	1
O(1)	-485(1)	3014(1)	6077(1)	66(1)	1
O(2)	-981(1)	1503(1)	6199(1)	61(1)	1
O(3)	-872(1)	2942(1)	4788(1)	38(1)	1
O(4)	-1473(1)	1453(1)	4850(1)	41(1)	1
N(1)	1903(1)	1154(1)	5786(1)	23(1)	1
N(2)	1560(1)	1184(1)	4759(1)	21(1)	1
N(3)	-407(1)	2121(1)	5967(1)	38(1)	1
N(4)	-755(1)	2078(1)	4938(1)	24(1)	1
C(1)	2512(1)	570(1)	5508(1)	28(1)	1
C(2)	2334(1)	613(1)	4917(1)	26(1)	1
C(3)	3422(1)	-67(1)	5719(1)	45(1)	1
C(4)	3123(1)	91(1)	4550(1)	39(1)	1
C(5)	2166(1)	1377(1)	6354(1)	32(1)	1
C(6)	2147(1)	2498(1)	6435(1)	34(1)	1

C(7)	2354(2)	2769(2)	7017(1)	63(1)	1
C(8)	1514(2)	2242(3)	7369(1)	99(1)	1
C(9)	1599(2)	1136(3)	7311(1)	101(1)	1
C(10)	1404(1)	811(2)	6727(1)	55(1)	1
C(11)	1487(1)	1476(1)	4189(1)	27(1)	1
C(12)	1497(1)	2605(1)	4156(1)	23(1)	1
C(13)	1465(1)	2939(1)	3574(1)	33(1)	1
C(14)	485(1)	2504(2)	3283(1)	44(1)	1
C(15)	493(2)	1385(2)	3317(1)	56(1)	1
C(16)	506(2)	1029(2)	3899(1)	45(1)	1
O(30)	10810(4)	5273(3)	7132(2)	98(2)	0.5
C(31)	10029(5)	4872(4)	7323(2)	38(1)	0.5
C(32)	9951(6)	4719(4)	7908(2)	46(1)	0.5
C(33)	9111(5)	4508(3)	6993(2)	67(2)	0.5

Table 55. Bond lengths [Å] and angles [°].

Pd(1)-N(3)	2.0129(14)	N(3)-Pd(1)-N(4)	80.82(5)
Pd(1)-N(4)	2.0140(12)	N(3)-Pd(1)-N(2)	177.80(6)
Pd(1)-N(2)	2.0458(11)	N(4)-Pd(1)-N(2)	99.51(5)
Pd(1)-N(1)	2.0576(12)	N(3)-Pd(1)-N(1)	100.70(5)
O(1)-N(3)	1.235(2)	N(4)-Pd(1)-N(1)	174.99(5)
O(2)-N(3)	1.231(2)	N(2)-Pd(1)-N(1)	78.78(5)
O(3)-N(4)	1.2277(17)	C(1)-N(1)-C(5)	121.07(13)
O(4)-N(4)	1.2334(16)	C(1)-N(1)-Pd(1)	112.83(11)
N(1)-C(1)	1.284(2)	C(5)-N(1)-Pd(1)	126.09(10)
N(1)-C(5)	1.487(2)	C(2)-N(2)-C(11)	119.97(13)
N(2)-C(2)	1.2796(18)	C(2)-N(2)-Pd(1)	113.64(11)
N(2)-C(11)	1.481(2)	C(11)-N(2)-Pd(1)	126.25(9)
C(1)-C(2)	1.497(2)	O(2)-N(3)-O(1)	120.53(16)
C(1)-C(3)	1.498(2)	O(2)-N(3)-Pd(1)	119.60(14)
C(2)-C(4)	1.504(2)	O(1)-N(3)-Pd(1)	119.69(14)
C(5)-C(6)	1.520(2)	O(3)-N(4)-O(4)	120.41(13)
C(5)-C(10)	1.521(2)	O(3)-N(4)-Pd(1)	120.27(11)
C(6)-C(7)	1.521(2)	O(4)-N(4)-Pd(1)	119.24(11)
C(7)-C(8)	1.526(3)	N(1)-C(1)-C(2)	115.38(13)
C(8)-C(9)	1.497(5)	N(1)-C(1)-C(3)	125.91(17)
C(9)-C(10)	1.543(4)	C(2)-C(1)-C(3)	118.50(15)
C(11)-C(12)	1.519(2)	N(2)-C(2)-C(1)	115.74(13)
C(11)-C(16)	1.523(2)	N(2)-C(2)-C(4)	124.30(16)
C(12)-C(13)	1.525(2)	C(1)-C(2)-C(4)	119.61(14)
C(13)-C(14)	1.516(2)	N(1)-C(5)-C(6)	108.91(12)
C(14)-C(15)	1.505(3)	N(1)-C(5)-C(10)	110.74(14)
C(15)-C(16)	1.533(3)	C(6)-C(5)-C(10)	113.88(16)
O(30)-C(31)	1.194(6)	C(5)-C(6)-C(7)	111.27(17)
C(31)-C(33)	1.472(7)	C(6)-C(7)-C(8)	109.30(16)
C(31)-C(32)	1.483(7)	C(9)-C(8)-C(7)	111.0(2)
		C(8)-C(9)-C(10)	111.19(19)
		C(5)-C(10)-C(9)	110.20(17)
		N(2)-C(11)-C(12)	108.39(12)

N(2)-C(11)-C(16)	113.71(13)
C(12)-C(11)-C(16)	112.00(14)
C(11)-C(12)-C(13)	110.23(13)
C(14)-C(13)-C(12)	111.45(13)
C(15)-C(14)-C(13)	110.68(16)
C(14)-C(15)-C(16)	111.47(16)
C(11)-C(16)-C(15)	109.73(14)
O(30)-C(31)-C(33)	122.2(5)
O(30)-C(31)-C(32)	120.5(5)
C(33)-C(31)-C(32)	117.3(4)

Table 56. Anisotropic displacement parameters ($Å^2$ x 10^4). The anisotropic displacement factor exponent takes the form: $-2\pi^2[h^2a^*2U^{11} + ... + 2 h k a^* b^* U^{12}]$.

	U^{11}	U^{22}	U^{33}	U^{23}	U^{13}	U^{12}
Pd(1)	157(1)	175(1)	188(1)	-16(1)	-9(1)	39(1)
O(1)	801(12)	685(11)	483(9)	-317(8)	-200(7)	496(8)
O(2)	462(8)	993(13)	378(8)	268(8)	195(6)	399(8)
O(3)	334(6)	395(7)	408(7)	90(6)	17(5)	182(6)
O(4)	256(6)	598(9)	369(7)	11(6)	-56(5)	-118(5)
N(1)	189(6)	192(6)	312(7)	68(5)	-44(5)	-1(5)
N(2)	211(6)	152(6)	279(7)	-12(5)	60(5)	11(5)
N(3)	354(8)	584(11)	198(7)	-28(7)	-40(6)	288(7)
N(4)	203(6)	346(8)	186(6)	9(6)	19(4)	57(5)
C(1)	175(7)	161(7)	506(10)	113(7)	8(6)	-3(6)
C(2)	199(7)	136(7)	435(10)	-14(6)	64(6)	-13(5)
C(3)	275(8)	357(10)	727(14)	236(10)	5(8)	122(8)
C(4)	291(8)	217(8)	658(12)	-69(8)	146(8)	61(7)
C(5)	195(7)	465(10)	288(9)	179(7)	-65(6)	-69(7)
C(6)	264(8)	502(11)	251(8)	-58(7)	53(6)	-157(7)
C(7)	258(9)	1290(20)	352(11)	-297(12)	54(7)	-242(11)
C(8)	323(12)	2470(40)	170(10)	74(17)	-2(8)	-203(18)
C(9)	242(10)	2320(40)	476(15)	840(20)	-55(9)	-146(17)
C(10)	261(9)	807(16)	593(13)	523(12)	-99(8)	-133(9)
C(11)	342(9)	207(8)	249(8)	-41(6)	105(6)	-17(6)
C(12)	210(7)	237(8)	247(8)	0(6)	-24(5)	-36(6)
C(13)	323(9)	409(10)	270(9)	57(7)	-32(6)	-70(7)
C(14)	416(10)	673(15)	223(9)	37(9)	-53(7)	-151(9)
C(15)	719(15)	711(16)	241(10)	-149(10)	19(9)	-344(11)
C(16)	635(13)	442(12)	284(9)	-138(8)	62(8)	-302(9)
O(30)	1190(30)	710(30)	1040(30)	140(20)	700(30)	-260(20)
C(31)	620(30)	172(19)	340(30)	-8(16)	160(40)	3(19)
C(32)	730(40)	360(30)	290(30)	20(20)	-150(30)	-60(30)
C(33)	1380(50)	360(30)	280(20)	-52(18)	-110(30)	230(30)

B.2a (CCDC 736631)

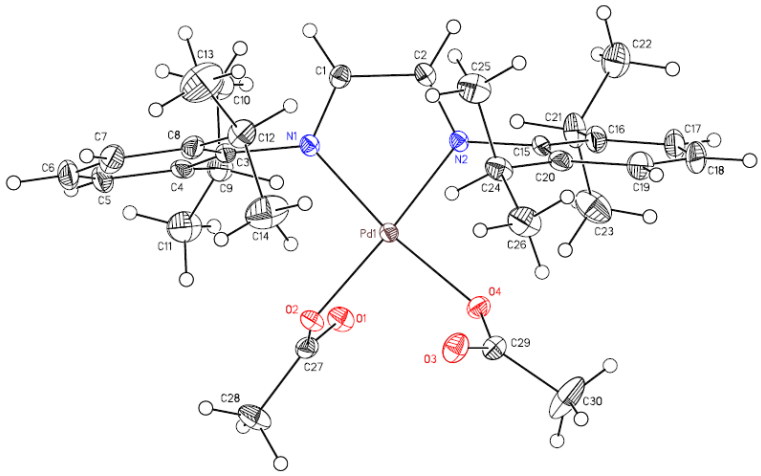

Special Refinement Details

Crystals were mounted on a glass fiber using Paratone oil then placed on the diffractometer under a nitrogen stream at 100K.

The crystal contains dichloromethane, two molecules in the asymmetric unit. One of those is disordered with both orientations sharing one of the chlorine sites. No restraints were used.

Refinement of F^2 against ALL reflections. The weighted R-factor (wR) and goodness of fit (S) are based on F^2, conventional R-factors (R) are based on F, with F set to zero for negative F^2. The threshold expression of $F^2 > 2\sigma(F^2)$ is used only for calculating R-factors(gt) etc. and is not relevant to the choice of reflections for refinement. R-factors based on F^2 are statistically about twice as large as those based on F, and R-factors based on ALL data will be even larger.

All esds (except the esd in the dihedral angle between two l.s. planes) are estimated using the full covariance matrix. The cell esds are taken into account individually in the estimation of esds in distances, angles and torsion angles; correlations between esds in cell parameters are only used when they are defined by crystal symmetry. An approximate (isotropic) treatment of cell esds is used for estimating esds involving l.s. planes.

Table 57. Atomic coordinates (x 10^4) and equivalent isotropic displacement parameters (Å^2 x 10^3). U(eq) is defined as the trace of the orthogonalized Uij tensor.

	x	y	z	Ueq	Occ
Pd(1)	6833(1)	1473(1)	1378(1)	12(1)	1
O(1)	6045(1)	1815(1)	473(1)	19(1)	1
O(2)	6842(1)	2548(1)	769(1)	15(1)	1
O(3)	6878(1)	3440(1)	2049(1)	22(1)	1
O(4)	6237(1)	2267(1)	1789(1)	17(1)	1
N(1)	7370(1)	467(1)	1013(1)	12(1)	1
N(2)	6893(1)	396(1)	1975(1)	12(1)	1
C(1)	7438(1)	-388(1)	1285(1)	15(1)	1
C(2)	7164(1)	-426(1)	1833(1)	15(1)	1
C(3)	7706(1)	659(1)	522(1)	16(1)	1
C(4)	7469(1)	517(1)	-5(1)	19(1)	1
C(5)	7804(1)	754(1)	-461(1)	27(1)	1
C(6)	8341(1)	1122(1)	-394(1)	31(1)	1
C(7)	8566(1)	1248(1)	129(1)	28(1)	1

C(8)	8255(1)	1021(1)	607(1)	20(1)	1
C(9)	6891(1)	43(1)	-73(1)	22(1)	1
C(10)	6938(1)	-1153(1)	-117(1)	29(1)	1
C(11)	6566(1)	476(2)	-572(1)	34(1)	1
C(12)	8490(1)	1208(1)	1186(1)	23(1)	1
C(13)	9114(1)	950(2)	1239(1)	49(1)	1
C(14)	8368(1)	2324(2)	1361(1)	40(1)	1
C(15)	6663(1)	492(1)	2531(1)	15(1)	1
C(16)	6143(1)	45(1)	2645(1)	20(1)	1
C(17)	5936(1)	172(1)	3185(1)	26(1)	1
C(18)	6232(1)	722(1)	3578(1)	27(1)	1
C(19)	6740(1)	1177(1)	3449(1)	24(1)	1
C(20)	6969(1)	1084(1)	2917(1)	18(1)	1
C(21)	5790(1)	-511(1)	2213(1)	24(1)	1
C(22)	5613(1)	-1604(1)	2408(1)	29(1)	1
C(23)	5278(1)	165(2)	2069(1)	34(1)	1
C(24)	7533(1)	1575(1)	2771(1)	20(1)	1
C(25)	8011(1)	789(1)	2842(1)	28(1)	1
C(26)	7657(1)	2568(1)	3103(1)	29(1)	1
C(27)	6408(1)	2496(1)	443(1)	16(1)	1
C(28)	6384(1)	3345(1)	13(1)	25(1)	1
C(29)	6402(1)	3086(1)	2058(1)	19(1)	1
C(30)	5946(1)	3592(2)	2402(1)	43(1)	1
C(60)	4975(1)	2371(2)	1115(1)	36(1)	1
Cl(1)	4948(1)	3589(1)	771(1)	46(1)	1
Cl(2)	4316(1)	1803(1)	1169(1)	60(1)	1
C(61A)	5007(1)	3445(3)	4589(1)	32(1)	0.804(4)
Cl(3A)	4543(1)	4484(1)	4437(1)	34(1)	0.804(4)
C(61B)	5196(5)	3783(11)	4453(6)	37(3)	0.196(4)
Cl(3B)	4507(1)	3842(6)	4583(2)	56(2)	0.196(4)
Cl(4)	5326(1)	2924(1)	3964(1)	45(1)	1

Table 58. Bond lengths [Å] and angles [°].

Pd(1)-N(2)	1.9950(12)	N(2)-Pd(1)-O(4)	92.70(4)
Pd(1)-O(4)	2.0071(9)	N(2)-Pd(1)-O(2)	175.22(4)
Pd(1)-O(2)	2.0086(9)	O(4)-Pd(1)-O(2)	91.09(4)
Pd(1)-N(1)	2.0170(11)	N(2)-Pd(1)-N(1)	79.98(5)
O(1)-C(27)	1.2302(17)	O(4)-Pd(1)-N(1)	170.75(4)
O(2)-C(27)	1.3005(16)	O(2)-Pd(1)-N(1)	96.51(4)
O(3)-C(29)	1.2218(17)	C(27)-O(2)-Pd(1)	113.24(9)
O(4)-C(29)	1.2926(18)	C(29)-O(4)-Pd(1)	116.18(9)
N(1)-C(1)	1.2850(18)	C(1)-N(1)-C(3)	119.33(12)
N(1)-C(3)	1.4469(17)	C(1)-N(1)-Pd(1)	113.68(10)
N(2)-C(2)	1.2794(18)	C(3)-N(1)-Pd(1)	126.75(9)
N(2)-C(15)	1.4495(17)	C(2)-N(2)-C(15)	120.52(12)
C(1)-C(2)	1.4700(19)	C(2)-N(2)-Pd(1)	114.30(10)
C(3)-C(4)	1.398(2)	C(15)-N(2)-Pd(1)	125.18(9)
C(3)-C(8)	1.403(2)	N(1)-C(1)-C(2)	115.32(13)
C(4)-C(5)	1.389(2)	N(2)-C(2)-C(1)	115.90(13)

C(4)-C(9)	1.514(2)	C(4)-C(3)-C(8)	123.58(14)
C(5)-C(6)	1.374(2)	C(4)-C(3)-N(1)	119.39(13)
C(6)-C(7)	1.376(2)	C(8)-C(3)-N(1)	116.98(13)
C(7)-C(8)	1.398(2)	C(5)-C(4)-C(3)	116.89(15)
C(8)-C(12)	1.519(2)	C(5)-C(4)-C(9)	121.66(14)
C(9)-C(11)	1.529(2)	C(3)-C(4)-C(9)	121.28(13)
C(9)-C(10)	1.538(2)	C(6)-C(5)-C(4)	121.23(16)
C(12)-C(14)	1.516(2)	C(5)-C(6)-C(7)	120.76(15)
C(12)-C(13)	1.530(2)	C(6)-C(7)-C(8)	121.21(15)
C(15)-C(16)	1.394(2)	C(7)-C(8)-C(3)	116.32(15)
C(15)-C(20)	1.400(2)	C(7)-C(8)-C(12)	121.61(14)
C(16)-C(17)	1.398(2)	C(3)-C(8)-C(12)	122.01(13)
C(16)-C(21)	1.512(2)	C(4)-C(9)-C(11)	113.66(14)
C(17)-C(18)	1.374(2)	C(4)-C(9)-C(10)	109.86(13)
C(18)-C(19)	1.378(2)	C(11)-C(9)-C(10)	110.10(13)
C(19)-C(20)	1.396(2)	C(14)-C(12)-C(8)	109.24(14)
C(20)-C(24)	1.525(2)	C(14)-C(12)-C(13)	111.55(15)
C(21)-C(22)	1.533(2)	C(8)-C(12)-C(13)	113.67(14)
C(21)-C(23)	1.537(2)	C(16)-C(15)-C(20)	123.87(13)
C(24)-C(26)	1.530(2)	C(16)-C(15)-N(2)	118.83(13)
C(24)-C(25)	1.531(2)	C(20)-C(15)-N(2)	117.21(12)
C(27)-C(28)	1.501(2)	C(15)-C(16)-C(17)	116.61(14)
C(29)-C(30)	1.511(2)	C(15)-C(16)-C(21)	123.72(13)
C(60)-Cl(2)	1.7372(17)	C(17)-C(16)-C(21)	119.60(14)
C(60)-Cl(1)	1.766(2)	C(18)-C(17)-C(16)	121.03(15)
C(61A)-Cl(3A)	1.768(3)	C(17)-C(18)-C(19)	120.94(15)
C(61A)-Cl(4)	1.810(3)	C(18)-C(19)-C(20)	120.95(16)
C(61B)-Cl(4)	1.638(12)	C(19)-C(20)-C(15)	116.53(14)
C(61B)-Cl(3B)	1.672(13)	C(19)-C(20)-C(24)	121.40(14)
		C(15)-C(20)-C(24)	122.04(13)
		C(16)-C(21)-C(22)	111.90(13)
		C(16)-C(21)-C(23)	109.39(14)
		C(22)-C(21)-C(23)	111.32(13)
		C(20)-C(24)-C(26)	113.11(13)
		C(20)-C(24)-C(25)	111.15(13)
		C(26)-C(24)-C(25)	110.10(13)
		O(1)-C(27)-O(2)	124.21(14)
		O(1)-C(27)-C(28)	121.73(13)
		O(2)-C(27)-C(28)	114.07(13)
		O(3)-C(29)-O(4)	125.00(14)
		O(3)-C(29)-C(30)	121.31(14)
		O(4)-C(29)-C(30)	113.69(13)
		Cl(2)-C(60)-Cl(1)	111.70(10)
		Cl(3A)-C(61A)-Cl(4)	111.70(17)
		Cl(4)-C(61B)-Cl(3B)	110.5(8)
		C(61B)-Cl(4)-C(61A)	22.9(5)

Table 59. Anisotropic displacement parameters ($Å^2$ x 10^4). The anisotropic displacement factor exponent takes the form: $-2p^2[h^2a^*2U^{11} + ... + 2 h k a^* b^* U^{12}]$.

	U^{11}	U^{22}	U^{33}	U^{23}	U^{13}	U^{12}
Pd(1)	136(1)	108(1)	101(1)	3(1)	4(1)	4(1)
O(1)	217(5)	180(6)	184(5)	4(5)	-23(4)	-16(4)
O(2)	181(4)	130(5)	146(5)	35(4)	-16(4)	-6(4)
O(3)	185(5)	225(6)	257(5)	-68(5)	34(4)	-31(5)
O(4)	168(5)	145(6)	188(5)	-15(5)	21(4)	15(4)
N(1)	155(5)	119(6)	95(5)	-11(5)	-2(5)	-16(4)
N(2)	139(5)	126(6)	92(5)	0(5)	-12(4)	-12(5)
C(1)	157(6)	140(8)	155(8)	-26(6)	3(5)	-2(5)
C(2)	170(7)	140(8)	127(7)	19(6)	-2(5)	-14(6)
C(3)	230(7)	91(8)	147(7)	-1(6)	56(6)	15(6)
C(4)	334(8)	102(8)	143(7)	-2(6)	38(6)	41(6)
C(5)	483(10)	163(9)	161(8)	8(7)	100(8)	26(7)
C(6)	495(11)	168(9)	272(9)	11(8)	231(8)	-25(7)
C(7)	318(9)	141(9)	371(10)	-32(8)	170(8)	-56(6)
C(8)	227(8)	121(8)	247(8)	-22(7)	83(6)	-4(6)
C(9)	294(8)	218(9)	136(7)	-29(7)	-20(7)	28(7)
C(10)	348(10)	219(10)	304(9)	-47(8)	-43(7)	-35(7)
C(11)	498(11)	343(11)	176(8)	-48(8)	-89(8)	95(9)
C(12)	188(7)	207(9)	285(8)	-37(7)	19(6)	-41(6)
C(13)	302(10)	571(15)	583(15)	-115(12)	-59(10)	90(9)
C(14)	459(10)	353(12)	397(11)	-154(10)	-144(10)	46(9)
C(15)	206(7)	149(8)	94(6)	22(6)	22(5)	36(6)
C(16)	215(7)	235(9)	137(7)	18(7)	18(6)	6(6)
C(17)	248(8)	348(11)	177(8)	21(8)	71(7)	5(7)
C(18)	373(9)	332(11)	111(7)	-10(7)	58(7)	62(7)
C(19)	357(9)	238(9)	129(7)	-30(7)	-14(6)	27(7)
C(20)	246(8)	155(8)	137(7)	12(6)	-15(6)	40(6)
C(21)	208(7)	333(11)	175(8)	-1(7)	34(6)	-67(7)
C(22)	246(8)	314(11)	306(10)	-21(8)	39(7)	-20(7)
C(23)	309(9)	359(12)	357(11)	103(9)	-97(8)	-82(8)
C(24)	264(7)	178(9)	147(7)	-1(7)	-48(6)	-19(6)
C(25)	284(9)	263(11)	283(9)	-8(8)	-75(7)	-15(7)
C(26)	401(10)	230(10)	232(9)	-23(8)	-69(8)	-46(7)
C(27)	228(7)	135(8)	125(7)	-20(6)	3(6)	37(6)
C(28)	362(9)	176(9)	205(8)	48(7)	-84(7)	-29(7)
C(29)	218(7)	157(8)	201(8)	-23(7)	32(6)	26(6)
C(30)	272(8)	399(13)	612(13)	-282(11)	176(9)	-31(9)
C(60)	267(8)	424(13)	379(10)	-16(10)	32(9)	35(8)
Cl(1)	421(2)	334(3)	621(3)	-58(3)	81(2)	27(2)
Cl(2)	315(2)	546(4)	935(5)	144(4)	-177(3)	-100(2)
C(61A)	324(16)	318(18)	307(15)	51(13)	-66(11)	-27(12)
Cl(3A)	306(3)	406(7)	316(4)	9(3)	-39(2)	81(3)
C(61B)	400(80)	300(80)	410(80)	-70(60)	-80(60)	80(50)
Cl(3B)	286(13)	690(50)	710(30)	-180(30)	32(14)	-12(15)
Cl(4)	508(3)	428(3)	419(3)	-99(2)	-183(2)	114(2)

B.3a (CCDC 736630)

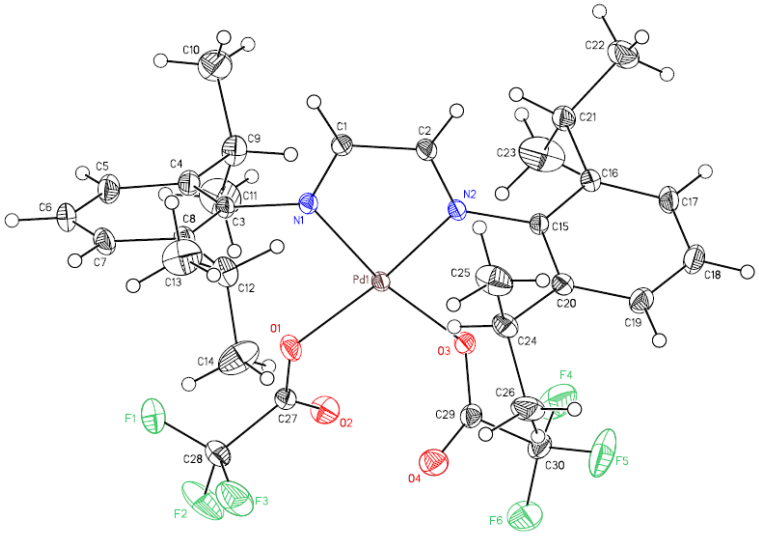

Special Refinement Details

Crystals were mounted on a glass fiber using Paratone oil then placed on the diffractometer under a nitrogen stream at 100K.

Refinement of F^2 against ALL reflections. The weighted R-factor (wR) and goodness of fit (S) are based on F^2, conventional R-factors (R) are based on F, with F set to zero for negative F^2. The threshold expression of $F^2 > 2\sigma(F^2)$ is used only for calculating R-factors(gt) etc. and is not relevant to the choice of reflections for refinement. R-factors based on F^2 are statistically about twice as large as those based on F, and R-factors based on ALL data will be even larger.

All esds (except the esd in the dihedral angle between two l.s. planes) are estimated using the full covariance matrix. The cell esds are taken into account individually in the estimation of esds in distances, angles and torsion angles; correlations between esds in cell parameters are only used when they are defined by crystal symmetry. An approximate (isotropic) treatment of cell esds is used for estimating esds involving l.s. planes.

Table 60. Atomic coordinates (x 10^4) and equivalent isotropic displacement parameters ($Å^2$ x 10^3). U(eq) is defined as the trace of the orthogonalized Uij tensor.

	x	y	z	Ueq
Pd(1)	2368(1)	7592(1)	3015(1)	13(1)
F(1)	4608(1)	5670(1)	1697(1)	44(1)
F(2)	3924(1)	5786(1)	564(1)	47(1)
F(3)	4516(1)	7111(1)	1105(1)	42(1)
F(4)	89(1)	8295(1)	1146(1)	45(1)
F(5)	644(1)	9816(1)	1124(1)	48(1)
F(6)	1056(1)	8729(1)	266(1)	36(1)
O(1)	3226(1)	6793(1)	2326(1)	21(1)
O(2)	2340(1)	6376(1)	1252(1)	23(1)
O(3)	1471(1)	8152(1)	2190(1)	18(1)
O(4)	2531(1)	8713(1)	1314(1)	24(1)
N(1)	3043(1)	7012(1)	3953(1)	13(1)
N(2)	1751(1)	8416(1)	3842(1)	13(1)
C(1)	2742(1)	7356(1)	4606(1)	16(1)

C(2)	2023(1)	8172(1)	4542(1)	16(1)
C(3)	3778(1)	6241(1)	3939(1)	14(1)
C(4)	3501(1)	5218(1)	3868(1)	18(1)
C(5)	4229(1)	4494(1)	3839(1)	23(1)
C(6)	5184(1)	4773(1)	3880(1)	24(1)
C(7)	5427(1)	5791(1)	3942(1)	21(1)
C(8)	4742(1)	6557(1)	3961(1)	16(1)
C(9)	2454(1)	4896(1)	3831(1)	23(1)
C(10)	2210(1)	4278(2)	4557(1)	34(1)
C(11)	2214(2)	4300(2)	3081(1)	42(1)
C(12)	5024(1)	7676(1)	3954(1)	22(1)
C(13)	5921(1)	7896(2)	4446(1)	37(1)
C(14)	5154(2)	8037(1)	3118(1)	37(1)
C(15)	1099(1)	9253(1)	3698(1)	13(1)
C(16)	130(1)	9149(1)	3866(1)	15(1)
C(17)	-465(1)	9971(1)	3677(1)	20(1)
C(18)	-112(1)	10848(1)	3336(1)	23(1)
C(19)	858(1)	10931(1)	3189(1)	21(1)
C(20)	1485(1)	10134(1)	3360(1)	16(1)
C(21)	-282(1)	8173(1)	4193(1)	20(1)
C(22)	-1154(1)	8356(1)	4692(1)	30(1)
C(23)	-517(2)	7439(1)	3530(1)	45(1)
C(24)	2556(1)	10239(1)	3248(1)	20(1)
C(25)	3039(1)	10626(2)	4002(1)	33(1)
C(26)	2806(1)	10929(1)	2564(1)	29(1)
C(27)	3084(1)	6486(1)	1633(1)	16(1)
C(28)	4040(1)	6249(1)	1248(1)	22(1)
C(29)	1735(1)	8540(1)	1550(1)	17(1)
C(30)	866(1)	8844(1)	1021(1)	20(1)

Table 61. Bond lengths [Å] and angles [°].

Pd(1)-N(1)	1.9935(11)	N(1)-Pd(1)-N(2)	80.75(4)
Pd(1)-N(2)	1.9958(10)	N(1)-Pd(1)-O(1)	89.82(4)
Pd(1)-O(1)	2.0024(9)	N(2)-Pd(1)-O(1)	168.28(4)
Pd(1)-O(3)	2.0051(10)	N(1)-Pd(1)-O(3)	169.43(4)
F(1)-C(28)	1.3282(19)	N(2)-Pd(1)-O(3)	91.64(4)
F(2)-C(28)	1.3255(17)	O(1)-Pd(1)-O(3)	98.56(4)
F(3)-C(28)	1.3372(18)	C(27)-O(1)-Pd(1)	129.67(9)
F(4)-C(30)	1.3252(19)	C(29)-O(3)-Pd(1)	124.35(9)
F(5)-C(30)	1.3248(18)	C(1)-N(1)-C(3)	120.66(11)
F(6)-C(30)	1.3364(17)	C(1)-N(1)-Pd(1)	114.03(9)
O(1)-C(27)	1.2644(16)	C(3)-N(1)-Pd(1)	125.26(8)
O(2)-C(27)	1.2220(17)	C(2)-N(2)-C(15)	121.19(10)
O(3)-C(29)	1.2710(16)	C(2)-N(2)-Pd(1)	113.77(8)
O(4)-C(29)	1.2162(17)	C(15)-N(2)-Pd(1)	124.95(8)
N(1)-C(1)	1.2880(15)	N(1)-C(1)-C(2)	115.38(11)
N(1)-C(3)	1.4425(16)	N(2)-C(2)-C(1)	115.83(10)
N(2)-C(2)	1.2881(16)	C(4)-C(3)-C(8)	123.17(12)
N(2)-C(15)	1.4433(15)	C(4)-C(3)-N(1)	118.48(11)

C(1)-C(2)	1.4705(18)
C(3)-C(4)	1.4006(18)
C(3)-C(8)	1.4085(19)
C(4)-C(5)	1.3944(19)
C(4)-C(9)	1.523(2)
C(5)-C(6)	1.385(2)
C(6)-C(7)	1.382(2)
C(7)-C(8)	1.3897(18)
C(8)-C(12)	1.5195(19)
C(9)-C(10)	1.531(2)
C(9)-C(11)	1.533(2)
C(12)-C(13)	1.522(2)
C(12)-C(14)	1.524(2)
C(15)-C(16)	1.3996(18)
C(15)-C(20)	1.4061(17)
C(16)-C(17)	1.3943(18)
C(16)-C(21)	1.5170(18)
C(17)-C(18)	1.386(2)
C(18)-C(19)	1.391(2)
C(19)-C(20)	1.3902(19)
C(20)-C(24)	1.5213(19)
C(21)-C(23)	1.518(2)
C(21)-C(22)	1.526(2)
C(24)-C(26)	1.528(2)
C(24)-C(25)	1.529(2)
C(27)-C(28)	1.5379(19)
C(29)-C(30)	1.5493(19)

C(8)-C(3)-N(1)	118.28(11)
C(5)-C(4)-C(3)	117.07(13)
C(5)-C(4)-C(9)	120.67(13)
C(3)-C(4)-C(9)	122.26(12)
C(6)-C(5)-C(4)	121.44(14)
C(7)-C(6)-C(5)	119.64(13)
C(6)-C(7)-C(8)	122.16(13)
C(7)-C(8)-C(3)	116.47(12)
C(7)-C(8)-C(12)	121.23(12)
C(3)-C(8)-C(12)	122.17(12)
C(4)-C(9)-C(10)	110.31(13)
C(4)-C(9)-C(11)	111.49(13)
C(10)-C(9)-C(11)	111.29(15)
C(8)-C(12)-C(13)	112.90(14)
C(8)-C(12)-C(14)	110.26(12)
C(13)-C(12)-C(14)	110.18(14)
C(16)-C(15)-C(20)	123.23(12)
C(16)-C(15)-N(2)	120.07(11)
C(20)-C(15)-N(2)	116.66(11)
C(17)-C(16)-C(15)	116.85(12)
C(17)-C(16)-C(21)	120.58(12)
C(15)-C(16)-C(21)	122.48(12)
C(18)-C(17)-C(16)	121.56(13)
C(17)-C(18)-C(19)	120.02(13)
C(20)-C(19)-C(18)	121.01(13)
C(19)-C(20)-C(15)	117.32(12)
C(19)-C(20)-C(24)	121.46(12)
C(15)-C(20)-C(24)	121.05(12)
C(16)-C(21)-C(23)	109.64(13)
C(16)-C(21)-C(22)	112.99(12)
C(23)-C(21)-C(22)	111.00(15)
C(20)-C(24)-C(26)	113.36(13)
C(20)-C(24)-C(25)	109.75(11)
C(26)-C(24)-C(25)	110.29(13)
O(2)-C(27)-O(1)	130.53(13)
O(2)-C(27)-C(28)	119.01(12)
O(1)-C(27)-C(28)	110.45(12)
F(2)-C(28)-F(1)	107.90(14)
F(2)-C(28)-F(3)	105.99(13)
F(1)-C(28)-F(3)	107.30(14)
F(2)-C(28)-C(27)	112.55(13)
F(1)-C(28)-C(27)	112.35(12)
F(3)-C(28)-C(27)	110.41(12)
O(4)-C(29)-O(3)	130.62(13)
O(4)-C(29)-C(30)	117.88(12)
O(3)-C(29)-C(30)	111.49(12)
F(5)-C(30)-F(4)	107.76(14)
F(5)-C(30)-F(6)	106.90(12)
F(4)-C(30)-F(6)	106.25(13)

F(5)-C(30)-C(29)	110.65(12)
F(4)-C(30)-C(29)	113.53(11)
F(6)-C(30)-C(29)	111.42(12)

Table 62. Anisotropic displacement parameters ($Å^2$ x 10^4). The anisotropic displacement factor exponent takes the form: $-2\pi^2[h^2a^*2U^{11} + ... + 2 h k a^* b^* U^{12}]$.

	U^{11}	U^{22}	U^{33}	U^{23}	U^{13}	U^{12}
Pd(1)	119(1)	172(1)	93(1)	-9(1)	-3(1)	40(1)
F(1)	327(6)	513(7)	478(7)	125(5)	112(5)	236(5)
F(2)	397(7)	672(9)	339(6)	-301(6)	121(5)	-7(6)
F(3)	347(6)	354(6)	561(7)	-12(5)	222(5)	-80(5)
F(4)	234(5)	623(8)	474(7)	252(6)	-128(5)	-83(5)
F(5)	641(9)	293(6)	490(7)	-79(5)	-233(6)	251(6)
F(6)	373(6)	547(7)	169(5)	-2(4)	-62(4)	62(5)
O(1)	200(5)	296(5)	137(4)	-46(3)	-7(3)	108(4)
O(2)	205(5)	281(5)	198(5)	-27(3)	-35(4)	-24(4)
O(3)	164(4)	264(5)	121(4)	9(3)	-8(3)	73(4)
O(4)	201(5)	272(5)	242(5)	32(4)	10(4)	-28(4)
N(1)	118(4)	157(4)	123(4)	0(3)	-6(3)	23(3)
N(2)	114(4)	144(4)	128(4)	-8(3)	13(3)	25(3)
C(1)	153(5)	197(5)	120(5)	3(3)	-8(4)	34(4)
C(2)	158(5)	184(5)	127(5)	-12(3)	6(4)	37(4)
C(3)	123(5)	171(5)	134(5)	2(3)	-4(4)	36(4)
C(4)	164(6)	169(5)	212(6)	15(4)	8(4)	20(4)
C(5)	230(7)	171(6)	296(7)	18(4)	25(5)	54(5)
C(6)	201(7)	247(7)	266(7)	21(5)	28(5)	106(5)
C(7)	129(6)	281(7)	219(6)	-11(4)	5(4)	49(5)
C(8)	131(5)	199(5)	166(5)	-15(4)	-6(4)	23(4)
C(9)	186(6)	179(6)	317(7)	9(5)	-10(5)	-13(5)
C(10)	240(8)	389(9)	407(10)	108(7)	37(7)	-59(7)
C(11)	350(11)	507(12)	384(11)	-99(8)	-33(8)	-126(9)
C(12)	168(6)	215(6)	266(7)	-55(5)	-5(5)	-16(5)
C(13)	320(9)	423(10)	350(9)	-24(7)	-100(7)	-133(8)
C(14)	539(12)	251(8)	324(9)	47(6)	-107(8)	-119(8)
C(15)	131(5)	143(5)	125(5)	-3(3)	-2(4)	27(4)
C(16)	134(5)	162(5)	160(5)	2(3)	11(4)	20(4)
C(17)	134(5)	204(6)	250(6)	21(4)	9(4)	46(5)
C(18)	207(7)	194(6)	293(7)	53(5)	-12(5)	56(5)
C(19)	212(6)	174(6)	252(7)	56(4)	17(5)	8(5)
C(20)	141(5)	178(5)	161(5)	9(4)	19(4)	5(4)
C(21)	163(6)	178(6)	253(6)	31(4)	43(5)	2(5)
C(22)	263(8)	295(8)	352(9)	31(6)	126(6)	-28(6)
C(23)	671(15)	258(9)	442(11)	-130(7)	182(10)	-178(9)
C(24)	160(6)	221(6)	217(6)	0(4)	41(4)	-21(5)
C(25)	188(7)	518(11)	284(8)	-37(7)	2(6)	-98(7)
C(26)	285(8)	305(8)	280(8)	50(5)	102(6)	-66(6)
C(27)	164(6)	173(5)	137(5)	0(3)	9(4)	25(4)
C(28)	211(7)	238(6)	205(6)	-38(4)	43(5)	23(5)
C(29)	190(6)	166(5)	145(5)	-12(3)	-19(4)	32(4)

C(30)	219(6)	210(6)	168(6)	19(4)	-37(4)	37(5)

B.4 (CCDC 727271)

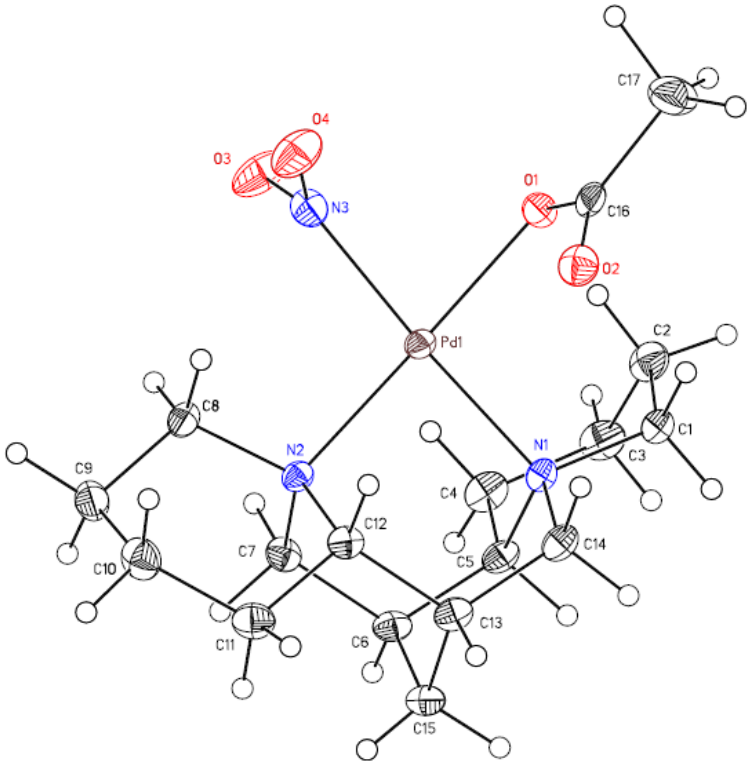

Special Refinement Details

Crystals were mounted on a glass fiber using Paratone oil then placed on the diffractometer under a nitrogen stream at 100K.

Refinement of F^2 against ALL reflections. The weighted R-factor (wR) and goodness of fit (S) are based on F^2, conventional R-factors (R) are based on F, with F set to zero for negative F^2. The threshold expression of $F^2 > 2\sigma(F^2)$ is used only for calculating R-factors(gt) etc. and is not relevant to the choice of reflections for refinement. R-factors based on F^2 are statistically about twice as large as those based on F, and R-factors based on ALL data will be even larger.

All esds (except the esd in the dihedral angle between two l.s. planes) are estimated using the full covariance matrix. The cell esds are taken into account individually in the estimation of esds in distances, angles and torsion angles; correlations between esds in cell parameters are only used when they are defined by crystal symmetry. An approximate (isotropic) treatment of cell esds is used for estimating esds involving l.s. planes.

Table 63. Atomic coordinates (x 10^4) and equivalent isotropic displacement parameters (Å^2 x 10^3). U(eq) is defined as the trace of the orthogonalized Uij tensor.

	x	y	z	Ueq
Pd(1)	652(1)	7259(1)	8526(1)	13(1)
O(1)	656(2)	9091(1)	8291(1)	18(1)
O(2)	1210(1)	9293(1)	9467(1)	21(1)
O(3)	-2260(1)	7272(1)	7872(1)	31(1)
O(4)	-2382(1)	8023(1)	8936(1)	30(1)
N(1)	3033(1)	7054(1)	8458(1)	13(1)
N(2)	554(2)	5471(1)	8936(1)	13(1)

N(3)	-1638(1)	7532(1)	8457(1)	19(1)
C(1)	3797(2)	8163(2)	8148(1)	17(1)
C(2)	3346(2)	8372(2)	7363(1)	21(1)
C(3)	3735(2)	7275(2)	6898(1)	22(1)
C(4)	2992(2)	6147(2)	7221(1)	20(1)
C(5)	3502(2)	5976(2)	7998(1)	16(1)
C(6)	2994(2)	4761(2)	8332(1)	15(1)
C(7)	1269(2)	4590(1)	8415(1)	16(1)
C(8)	-1097(2)	5158(2)	9069(1)	16(1)
C(9)	-1369(2)	4002(2)	9506(1)	21(1)
C(10)	-569(3)	4116(2)	10232(1)	22(1)
C(11)	1112(2)	4380(2)	10121(1)	20(1)
C(12)	1421(2)	5508(2)	9649(1)	15(1)
C(13)	3145(2)	5666(2)	9535(1)	16(1)
C(14)	3617(2)	6884(2)	9214(1)	16(1)
C(15)	3786(2)	4637(2)	9064(1)	18(1)
C(16)	894(2)	9717(2)	8872(1)	17(1)
C(17)	775(3)	11087(2)	8766(1)	31(1)

Table 64. Bond lengths [Å] and angles [°].

Pd(1)-N(3)	2.0193(13)	N(3)-Pd(1)-O(1)	81.00(5)
Pd(1)-O(1)	2.0527(10)	N(3)-Pd(1)-N(1)	172.51(5)
Pd(1)-N(1)	2.0870(12)	O(1)-Pd(1)-N(1)	95.19(5)
Pd(1)-N(2)	2.1009(12)	N(3)-Pd(1)-N(2)	96.93(5)
O(1)-C(16)	1.2922(19)	O(1)-Pd(1)-N(2)	170.79(4)
O(2)-C(16)	1.226(2)	N(1)-Pd(1)-N(2)	87.83(5)
O(3)-N(3)	1.2442(17)	C(16)-O(1)-Pd(1)	109.97(10)
O(4)-N(3)	1.2214(16)	C(1)-N(1)-C(14)	107.88(12)
N(1)-C(1)	1.499(2)	C(1)-N(1)-C(5)	107.31(12)
N(1)-C(14)	1.5001(19)	C(14)-N(1)-C(5)	109.64(12)
N(1)-C(5)	1.511(2)	C(1)-N(1)-Pd(1)	112.12(10)
N(2)-C(7)	1.499(2)	C(14)-N(1)-Pd(1)	107.04(9)
N(2)-C(8)	1.498(2)	C(5)-N(1)-Pd(1)	112.75(9)
N(2)-C(12)	1.520(2)	C(7)-N(2)-C(8)	110.85(12)
C(1)-C(2)	1.522(2)	C(7)-N(2)-C(12)	111.70(13)
C(1)-H(1A)	0.946(15)	C(8)-N(2)-C(12)	109.87(12)
C(1)-H(1B)	0.989(15)	C(7)-N(2)-Pd(1)	110.49(9)
C(2)-C(3)	1.516(3)	C(8)-N(2)-Pd(1)	108.16(10)
C(2)-H(2A)	0.972(17)	C(12)-N(2)-Pd(1)	105.59(9)
C(2)-H(2B)	0.958(16)	O(4)-N(3)-O(3)	120.08(13)
C(3)-C(4)	1.518(3)	O(4)-N(3)-Pd(1)	122.85(11)
C(3)-H(3A)	0.893(17)	O(3)-N(3)-Pd(1)	116.79(10)
C(3)-H(3B)	0.989(16)	N(1)-C(1)-C(2)	111.88(14)
C(4)-C(5)	1.517(2)	N(1)-C(1)-H(1A)	107.6(10)
C(4)-H(4A)	0.925(17)	C(2)-C(1)-H(1A)	112.6(9)
C(4)-H(4B)	0.944(18)	N(1)-C(1)-H(1B)	108.6(9)
C(5)-C(6)	1.532(2)	C(2)-C(1)-H(1B)	109.5(9)
C(5)-H(5)	1.024(16)	H(1A)-C(1)-H(1B)	106.4(13)
C(6)-C(7)	1.520(2)	C(3)-C(2)-C(1)	111.42(15)

C(6)-C(15)	1.527(2)
C(6)-H(6)	0.872(18)
C(7)-H(7A)	1.018(17)
C(7)-H(7B)	0.983(16)
C(8)-C(9)	1.521(2)
C(8)-H(8A)	0.920(17)
C(8)-H(8B)	0.935(17)
C(9)-C(10)	1.518(3)
C(9)-H(9A)	1.037(15)
C(9)-H(9B)	0.900(17)
C(10)-C(11)	1.505(3)
C(10)-H(10A)	0.958(17)
C(10)-H(10B)	0.942(17)
C(11)-C(12)	1.535(2)
C(11)-H(11A)	0.89(2)
C(11)-H(11B)	0.84(2)
C(12)-C(13)	1.525(2)
C(12)-H(12)	0.956(15)
C(13)-C(14)	1.517(2)
C(13)-C(15)	1.529(2)
C(13)-H(13)	0.894(16)
C(14)-H(14A)	0.993(13)
C(14)-H(14B)	0.936(15)
C(15)-H(15A)	1.017(15)
C(15)-H(15B)	0.896(18)
C(16)-C(17)	1.517(2)
C(17)-H(17A)	1.15(3)
C(17)-H(17B)	1.06(2)
C(17)-H(17C)	0.96(2)

C(3)-C(2)-H(2A)	110.1(10)
C(1)-C(2)-H(2A)	108.3(10)
C(3)-C(2)-H(2B)	111.2(10)
C(1)-C(2)-H(2B)	106.6(10)
H(2A)-C(2)-H(2B)	109.1(14)
C(2)-C(3)-C(4)	109.06(13)
C(2)-C(3)-H(3A)	110.2(13)
C(4)-C(3)-H(3A)	106.6(13)
C(2)-C(3)-H(3B)	110.2(10)
C(4)-C(3)-H(3B)	109.8(10)
H(3A)-C(3)-H(3B)	110.8(14)
C(3)-C(4)-C(5)	110.45(15)
C(3)-C(4)-H(4A)	113.3(10)
C(5)-C(4)-H(4A)	108.5(11)
C(3)-C(4)-H(4B)	109.1(10)
C(5)-C(4)-H(4B)	111.4(10)
H(4A)-C(4)-H(4B)	104.0(15)
N(1)-C(5)-C(4)	110.98(14)
N(1)-C(5)-C(6)	111.94(13)
C(4)-C(5)-C(6)	113.86(14)
N(1)-C(5)-H(5)	105.9(9)
C(4)-C(5)-H(5)	106.4(9)
C(6)-C(5)-H(5)	107.2(9)
C(7)-C(6)-C(5)	115.63(14)
C(7)-C(6)-C(15)	110.14(14)
C(5)-C(6)-C(15)	107.73(14)
C(7)-C(6)-H(6)	105.4(12)
C(5)-C(6)-H(6)	108.5(12)
C(15)-C(6)-H(6)	109.3(12)
N(2)-C(7)-C(6)	113.33(13)
N(2)-C(7)-H(7A)	106.9(9)
C(6)-C(7)-H(7A)	115.4(10)
N(2)-C(7)-H(7B)	111.0(10)
C(6)-C(7)-H(7B)	105.9(9)
H(7A)-C(7)-H(7B)	104.1(13)
N(2)-C(8)-C(9)	115.28(13)
N(2)-C(8)-H(8A)	109.3(10)
C(9)-C(8)-H(8A)	110.0(10)
N(2)-C(8)-H(8B)	106.8(10)
C(9)-C(8)-H(8B)	110.0(10)
H(8A)-C(8)-H(8B)	104.8(14)
C(8)-C(9)-C(10)	109.36(14)
C(8)-C(9)-H(9A)	108.9(9)
C(10)-C(9)-H(9A)	112.4(9)
C(8)-C(9)-H(9B)	111.2(10)
C(10)-C(9)-H(9B)	112.0(10)
H(9A)-C(9)-H(9B)	102.9(13)
C(11)-C(10)-C(9)	109.90(14)
C(11)-C(10)-H(10A)	114.5(10)
C(9)-C(10)-H(10A)	107.0(10)

C(11)-C(10)-H(10B)	109.9(12)
C(9)-C(10)-H(10B)	109.9(11)
H(10A)-C(10)-H(10B)	105.4(14)
C(10)-C(11)-C(12)	113.75(15)
C(10)-C(11)-H(11A)	113.3(14)
C(12)-C(11)-H(11A)	113.4(13)
C(10)-C(11)-H(11B)	114.5(14)
C(12)-C(11)-H(11B)	101.7(14)
H(11A)-C(11)-H(11B)	98.8(18)
N(2)-C(12)-C(13)	111.71(13)
N(2)-C(12)-C(11)	112.63(13)
C(13)-C(12)-C(11)	110.01(14)
N(2)-C(12)-H(12)	106.6(9)
C(13)-C(12)-H(12)	108.3(10)
C(11)-C(12)-H(12)	107.4(9)
C(14)-C(13)-C(15)	109.00(14)
C(14)-C(13)-C(12)	114.84(14)
C(15)-C(13)-C(12)	110.80(14)
C(14)-C(13)-H(13)	105.1(12)
C(15)-C(13)-H(13)	107.5(11)
C(12)-C(13)-H(13)	109.2(11)
N(1)-C(14)-C(13)	112.50(13)
N(1)-C(14)-H(14A)	108.1(8)
C(13)-C(14)-H(14A)	109.7(8)
N(1)-C(14)-H(14B)	105.2(9)
C(13)-C(14)-H(14B)	112.9(9)
H(14A)-C(14)-H(14B)	108.2(12)
C(13)-C(15)-C(6)	106.01(14)
C(13)-C(15)-H(15A)	107.0(10)
C(6)-C(15)-H(15A)	111.5(9)
C(13)-C(15)-H(15B)	113.9(11)
C(6)-C(15)-H(15B)	109.4(11)
H(15A)-C(15)-H(15B)	109.0(15)
O(2)-C(16)-O(1)	125.69(15)
O(2)-C(16)-C(17)	120.37(15)
O(1)-C(16)-C(17)	113.94(15)
C(16)-C(17)-H(17A)	106.0(13)
C(16)-C(17)-H(17B)	109.2(13)
H(17A)-C(17)-H(17B)	104.9(18)
C(16)-C(17)-H(17C)	113.3(14)
H(17A)-C(17)-H(17C)	113.2(19)
H(17B)-C(17)-H(17C)	109.8(18)

Table 65. Anisotropic displacement parameters ($Å^2$ x 10^4). The anisotropic displacement factor exponent takes the form: $-2\pi^2[h^2a^*2U^{11} + ... + 2 h k a^* b^* U^{12}]$.

	U^{11}	U^{22}	U^{33}	U^{23}	U^{13}	U^{12}
Pd(1)	111(1)	136(1)	134(1)	-11(1)	1(1)	12(1)
O(1)	174(6)	152(5)	202(5)	8(4)	13(5)	1(6)
O(2)	202(6)	228(6)	209(6)	-26(5)	29(5)	4(5)

O(3)	210(6)	483(8)	222(6)	-100(7)	-93(5)	71(7)
O(4)	205(6)	415(9)	273(7)	-108(6)	26(5)	45(6)
N(1)	119(6)	159(6)	109(6)	-8(5)	-2(5)	-8(5)
N(2)	116(7)	140(6)	127(6)	-17(4)	-3(6)	7(6)
N(3)	209(7)	171(8)	191(7)	2(6)	20(6)	-2(5)
C(1)	128(8)	175(8)	212(9)	5(6)	9(6)	-2(6)
C(2)	171(9)	269(10)	193(9)	56(7)	34(7)	-2(8)
C(3)	212(8)	307(9)	157(7)	50(8)	23(6)	33(9)
C(4)	200(10)	278(10)	132(8)	-16(7)	-6(7)	18(8)
C(5)	123(9)	204(9)	141(8)	-27(6)	5(6)	28(7)
C(6)	164(8)	153(7)	136(7)	-47(6)	4(6)	49(6)
C(7)	186(8)	140(7)	144(8)	-30(6)	-9(6)	3(6)
C(8)	124(8)	177(8)	175(8)	-18(6)	0(6)	-9(6)
C(9)	199(9)	165(8)	250(9)	-8(7)	36(7)	-24(7)
C(10)	248(10)	222(8)	201(8)	45(7)	45(9)	-17(9)
C(11)	225(10)	218(9)	160(8)	27(7)	-12(7)	29(7)
C(12)	165(9)	155(8)	130(7)	-26(6)	-15(6)	18(6)
C(13)	165(8)	201(8)	108(7)	-5(6)	-27(6)	22(7)
C(14)	139(9)	228(8)	125(7)	-17(6)	-21(6)	0(7)
C(15)	172(9)	171(8)	192(8)	17(7)	-6(7)	45(7)
C(16)	94(9)	175(8)	250(8)	-16(6)	29(7)	-8(6)
C(17)	349(12)	193(9)	376(10)	-51(7)	-122(10)	51(9)

Table 66. Hydrogen coordinates (x 10^4) and isotropic displacement parameters (Å^2 x 10^3).

	x	y	z	Uiso
H(1A)	4870(18)	8067(15)	8208(8)	9(4)
H(1B)	3499(17)	8882(14)	8439(9)	8(4)
H(2A)	2250(20)	8534(16)	7344(9)	18(5)
H(2B)	3890(18)	9084(15)	7205(9)	14(4)
H(3A)	4750(20)	7143(18)	6901(9)	21(5)
H(3B)	3358(18)	7400(15)	6399(9)	26(5)
H(4A)	3210(19)	5439(16)	6968(9)	11(4)
H(4B)	1910(20)	6221(15)	7187(9)	16(5)
H(5)	4679(18)	5979(14)	7992(8)	5(4)
H(6)	3300(20)	4169(17)	8049(9)	20(5)
H(7A)	650(20)	4642(14)	7949(9)	16(4)
H(7B)	1125(17)	3743(15)	8577(10)	18(4)
H(8A)	-1605(18)	5109(14)	8634(9)	14(4)
H(8B)	-1538(19)	5828(16)	9303(9)	16(5)
H(9A)	-2542(18)	3864(15)	9558(8)	7(4)
H(9B)	-1060(18)	3335(16)	9262(9)	17(5)
H(10A)	-1111(19)	4726(15)	10501(9)	16(5)
H(10B)	-690(20)	3387(15)	10497(9)	23(4)
H(11A)	1650(20)	3730(20)	9988(10)	36(6)
H(11B)	1590(20)	4557(17)	10501(11)	28(6)
H(12)	1047(18)	6205(14)	9907(8)	7(4)
H(13)	3620(20)	5628(16)	9962(9)	17(5)
H(14A)	4756(16)	6945(13)	9202(7)	-6(3)
H(14B)	3234(16)	7551(14)	9473(8)	9(4)
H(15A)	4939(18)	4776(16)	9024(8)	10(4)

H(15B)	3617(19)	3888(16)	9242(9)	15(5)
H(17A)	-520(30)	11320(20)	8797(13)	91(9)
H(17B)	1100(30)	11310(20)	8231(13)	66(8)
H(17C)	1390(30)	11550(20)	9104(12)	52(7)